SPECIATION AND SEPARATION OF FISSION PRODUCT RHODIUM

By

N. M. Patel B.Sc, M.Sc., G.R.S.C.

A Doctoral Thesis
submitted in partial fulfilment of the requirement
for the award of Doctor of Philosophy of the
Loughborough University of Technology

April 1985

Supervisors: Dr. J.R. Thornback B.Sc., D.I.C., Ph.D., C.Chem., M.R.S.C.
Dr. J.H. Miles B.Sc., Ph.D., (AERE Harwell).

Department of Nuclear Chemistry

The author certifies that the work contained in this thesis is his original work, and that it has not been submitted, in full, or in part, to this or any other institution for a higher award.

To Sumi, for her unfailing encouragment and support.

ACKNOWLEDGEMENTS

I would like to take this opportunity in thanking Dr. J.R. Thornback for his everhelpful comments and guidance during the course of this work. My thanks are also due to Dr. J.H. Miles and Dr. R.P. Bush for their many valuable discussions and assistance during my stay at AERE Harwell.

For their friendship and encouragement, special thanks are due to Dr. P. Warwick, Miss G.F.E. Morgan and Miss J. Newman, who did much of the proof reading, and to colleagues in the Department of Chemistry, in particular Mr. A. Majid and Miss J. Cain.

Acknowledgement is also made to the assistance of the following:-

To Dr. B.E. Mann and the SERC High Field NMR service at Sheffield University for producing the ^{103}Rh NMR spectra.

To Mr. I. Longden for assisting with the studies on the organo-phosphine sulphides.

To the SERC for the provision of a research grant for this work.

To AERE Harwell, for the provision of equipment, materials and financial assistance.

CONTENTS

ABSTRACT

The rhodium speciation in nitric acid has been identified, primarily by the use of ^{103}Rh Nuclear Magnetic Resonance Spectroscopy. The results have indicated that the rhodium species in stored high level waste (HLW) will range from the hexaaquo ion, $\{Rh(H_2O)_6\}^{3+}$ to complexes of the general formula $\{Rh(H_2O)_{6-n}(NO_2)_n\}^{(3-n)+}$, depending on the nitrite ion concentration.

The solvent extraction of these complexes by dinonylnaphthalene sulphonic acid and various organo-phosphine sulphides has been investigated, and an integrated scheme for recovering rhodium from HLW is proposed.

ABBREVIATIONS

MIBK	Methyl isobutyl ketone
DIBK	Diisobutyl ketone
HD	Dinonylnaphthalene sulphonic acid
HDEHP	Diethylhexylphosphoric acid
HDEHDTP	Diethylhexyldithiophosphoric acid
TBPS	Tributylphosphine sulphide
THPS	Trihexylphosphorothioictriamide
TOPO	Trioctylphosphine oxide
TPPS	Triphenylphosphine sulphide
TBDPDS	Tetrabutyldiphosphine disulphide
HTTA	Theonyltrifluoro acetone
2-HTTA	2-Thiotheonyltrifluoro acetone
TOA	Trioctylamine
DOS	Dioctyl sulphide
TBP	Tributyl phosphate
DBP	Dibutylphosphate
MBP	Monobutylphosphate
DAMP	Di-isoamylmethylphosphonate
ε	Molar absorptivity ($mol^{-1}.cm^{-1}$)
δ	Chemical shift (Parts per million)
γ	Magnetogyric ratio ($rad.T^{-1}.s^{-1}$)
E	Electrode potential (V)
$E_{\frac{1}{2}}$	Half-wave potential (V)
i	Instantaneous current (μA)

i_d	Diffusion current (μA)
SCE	Standard Calomel Electrode
α	Interfacial surface tension (Nm^{-1})
AOM	Angular overlap model
SPE	Structural preference energy
NMR	Nuclear magnetic resonance
AAS	Atomic absorption spectroscopy
CAGR	Commercial advanced gas cooled reactor
LWR	Light water reactor
ORNL	Oak ridge national laboratory.

LIST OF FIGURES

LIST OF TABLES

CHAPTER ONE

INTRODUCTION

1.1. GENERALITIES

1.1.1. Discovery, Occurrence and Isolation

Rhodium was discovered by William Hyde Wollaston (1766-1828) at about the same time (1803) as Smithson Tennant's discovery of osmium and iridium (1). The new element was named rhodium (Greek rhodos - a rose) "from the rose colour of a dilute solution of the salts containing it (2)". Wollaston succeeded in making a button of the pure metal by treating a neutralised solution of the crude platinum concentrate with ammonium chloride and mercuric cyanide to remove platinum and palladium. Acidification of the filtrate, after evaporation and alcohol washing, gave the red-rose salt $Na_3(RhCl_6)$, which was then reduced with hydrogen.

The abundance of the Platinum Group Metals (Os,Ru,Rh,Ir) is between 10^{-7}—10^{-6}% of the earths crust, rhodium having been assessed at 0.0004 ppm (3). Rhodium occurs native with other platinum metals in river sands of the Urals and in North and South America. The largest source of rhodium however is to be found in the gold bearing mines of South Africa. Small quantities of rhodium (1 troy ounce per 28 ton of ore) are also to be found in the copper-nickel sulphide ores of the Sudbury-Ontario region in Canada. The large tonnages of nickel processed make the recovery of rhodium commercially feasible (4).

The refining of the platinum metals was first described in detail by Johnson and Atkinson (5). Although many improvements have been made, the process, until recently, has remained basically unchanged (6, 7). After aqua regia treatment, the insoluble portion (Rh, Ir, Ru and Ag) of the platinum metals concentrates is smelted with lead carbonate and treated with nitric acid to remove silver, as the nitrate, Figure 1.1.1. The insoluble residue is subjected to a bisulphate fusion, and the resulting mass treated with water. The rhodium sulphate solution so obtained is treated with sodium hydroxide to precipitate hydrated rhodium (III) sesquioxide. After dissolution in hydrochloric acid, the rhodium solution is treated with sodium nitrite, which reacts to form sodium hexanitritorhodate (III), solutions of which are stable over a wide pH range (6).

$$Na_3(RhCl_6) + 6NaNO_2 \rightarrow Na_3\{Rh(NO_2)_6\} + 6NaCl \quad \text{.....1.1}$$

Under these conditions, it is possible to separate the base metals hydrolytically without the formation of rhodium (III) sesquioxide. After the base metals have been filtered off, the rhodium (III) complex is precipitated by the addition of ammonium chloride. The sparingly soluble, creamy white precipitate of ammonium hexanitritorhodate (III) is of reasonably high purity, but further purification can be carried out by passing a solution of the ammonium hexanitritorhodate (III), in hydrochloric acid, through a cation exchange resin, which removes lead, bismuth, copper, iron and tellurium. The final purified rhodium (III) solution is treated with formic acid, to precipitate rhodium black, which is then ignited in a muffle furnace

Figure 1.1.1. Refining of the Platinum Group Metals Rh, Ir and Ru Rich (6, 7).

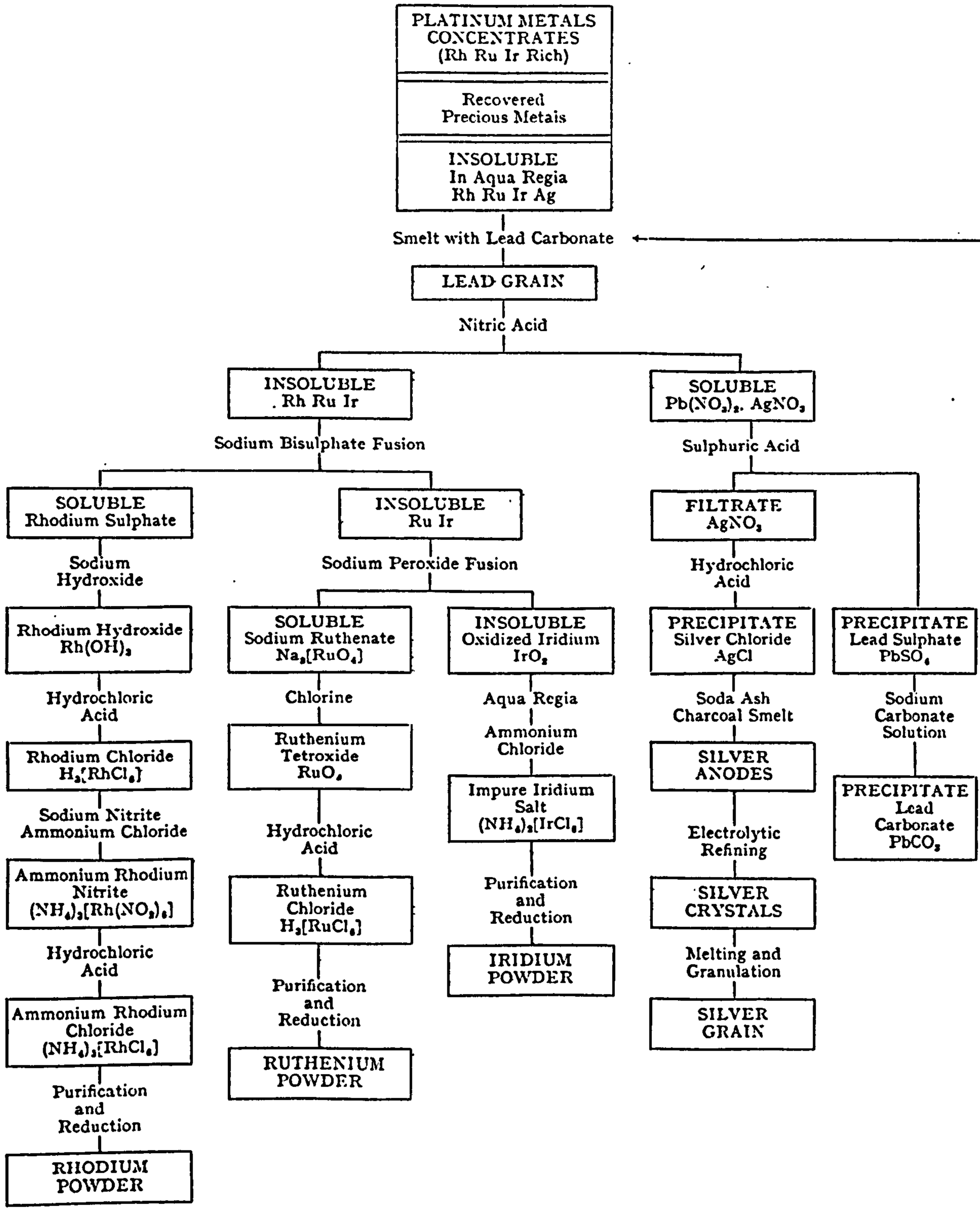

and reduced under hydrogen to give rhodium powder, assaying greater than 99.9% rhodium (6-8).

Recently, both Johnson Matthey plc and Inco plc have developed processing plants employing liquid-liquid extractions to refine the PGM concentrates. The Johnson Matthey plc "SOLVEX" process (9, 10) is outlined in Figure 1.1.2. The first solvent extraction cycle (SX-1), employs methyl isobutyl ketone (MIBK) to extract gold, present as $(AuCl_4)^{2-}$, from a 1M aqueous hydrochloric acid feed. Under these conditions, iron, tellurium and platinum, which are the major contaminants, are not extracted. After a scrub stage (SX-2), to remove co-extracted impurities, the loaded gold organic phase is contacted with an aqueous phase of oxalic acid which reduces Au(II) directly to Au(0). The third solvent extraction cycle (SX-3) employs β-hydroxy oximes (e.g. LIX 65N or LIX 70) to recover palladium. The basic extraction reaction is:

$$(PdCl_4)^{2-} + \overline{2(RH)} = \overline{(PdR_2)} + 4Cl^- + 2H^+ \quad \text{.....1.2.}$$

where the bars denote the organic phase. The kinetics of the oxime system are too slow for continuous mixer-settler operation, requiring the use of modifiers for realistic operation. Palladium is recovered from the organic phase by stripping with 10-12 M HCl (11).

Solvent extraction is not employed for ruthenium and osmium recovery, although the extraction of ruthenium via the nitrosyl complex $(RuNOCl_5)^{2-}$, has been reported (9, 10). The preferred method is the conventional distillation of ruthenium and osmium as their tetraoxides, as this gives the desired product in both high yield and purity.

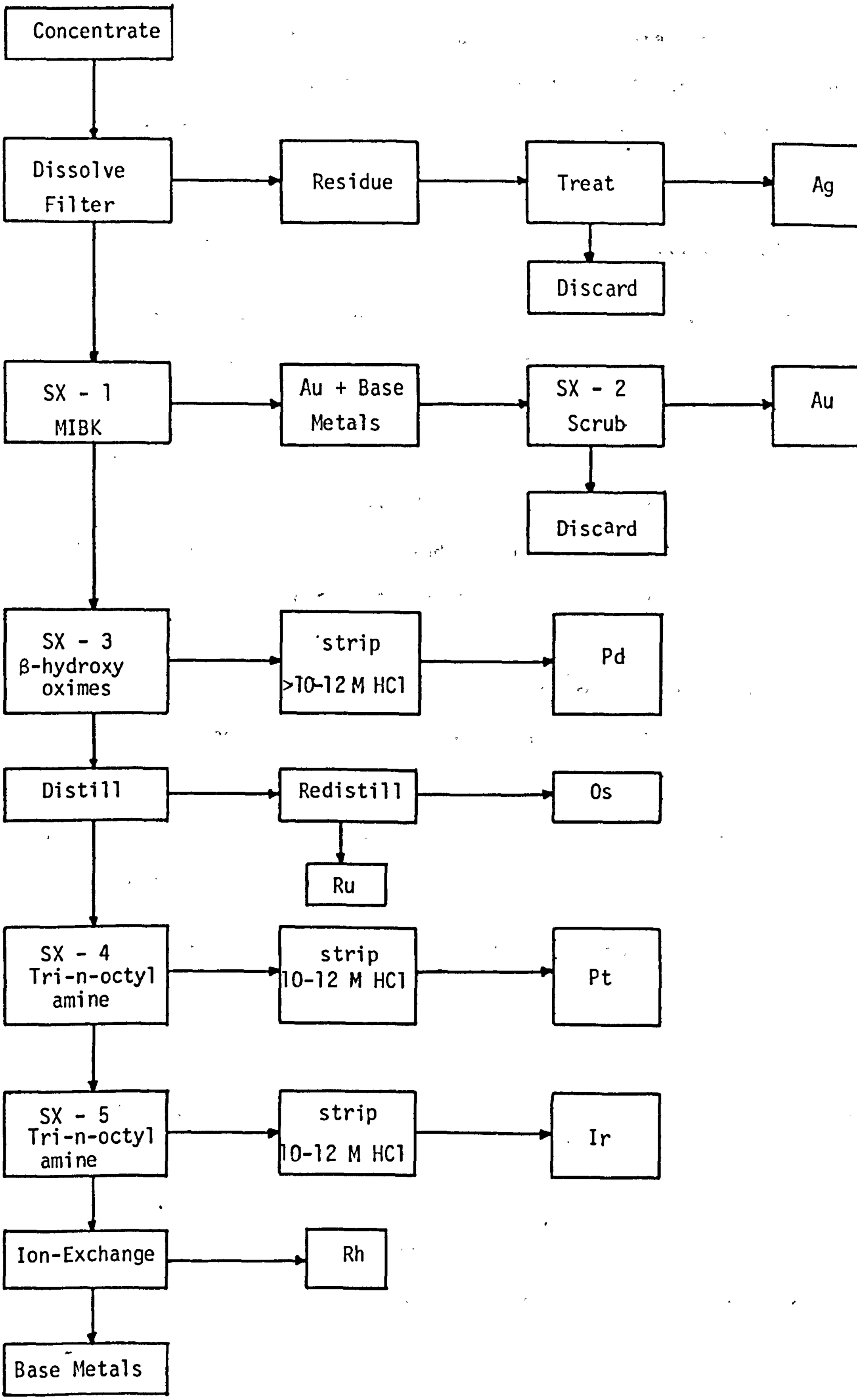

Figure 1.1.2 Johnson Matthey plc "SOLVEX" process (9-11)

In the absence of gold and palladium, platinum is recovered in the fourth solvent extraction cycle (SX-4) by extraction with tri-n-octylamine. Iridium, which is present as $(IrCl_6)^{3-}$ is not extracted. The general extraction reaction is represented as:

$$\overline{2R_3NHCl} + (PtCl_6)^{2-} = \overline{(R_3NH)_2PtCl_6} + 2Cl^- \quad \text{.....1.3.}$$

The equilibrium lies well to the right, and so stripping is difficult unless strong acid or alkali is used. In the SOLVEX process, a 10-12M HCl strip is used (11).

Having removed gold, platinum, palladium and ruthenium, the iridium is oxidised to the +4 state $(IrCl_6)^{2-}$, and the aqueous feed adjusted to approximately 4M HCl before extraction with tri-n-octylamine (SX-5).

Finally, the raffinate containing the rhodium and residual base metals, mainly nickel and sodium chloride, is treated in a variety of ways, such as:-

(a) cation exchange of base metals followed by conventional precipitation refining of rhodium;

(b) hydrolysis of rhodium and some base metals to remove excess chloride, followed by redissolution and removal of rhodium by anion exchange; or

(c) conventional rhodium refining including removal of base metals by hydrolysis.

The Inco plc solvent extraction process is illustrated in Figure 1.1.3. (12). After removal of silver, ruthenium and osmium by the conventional

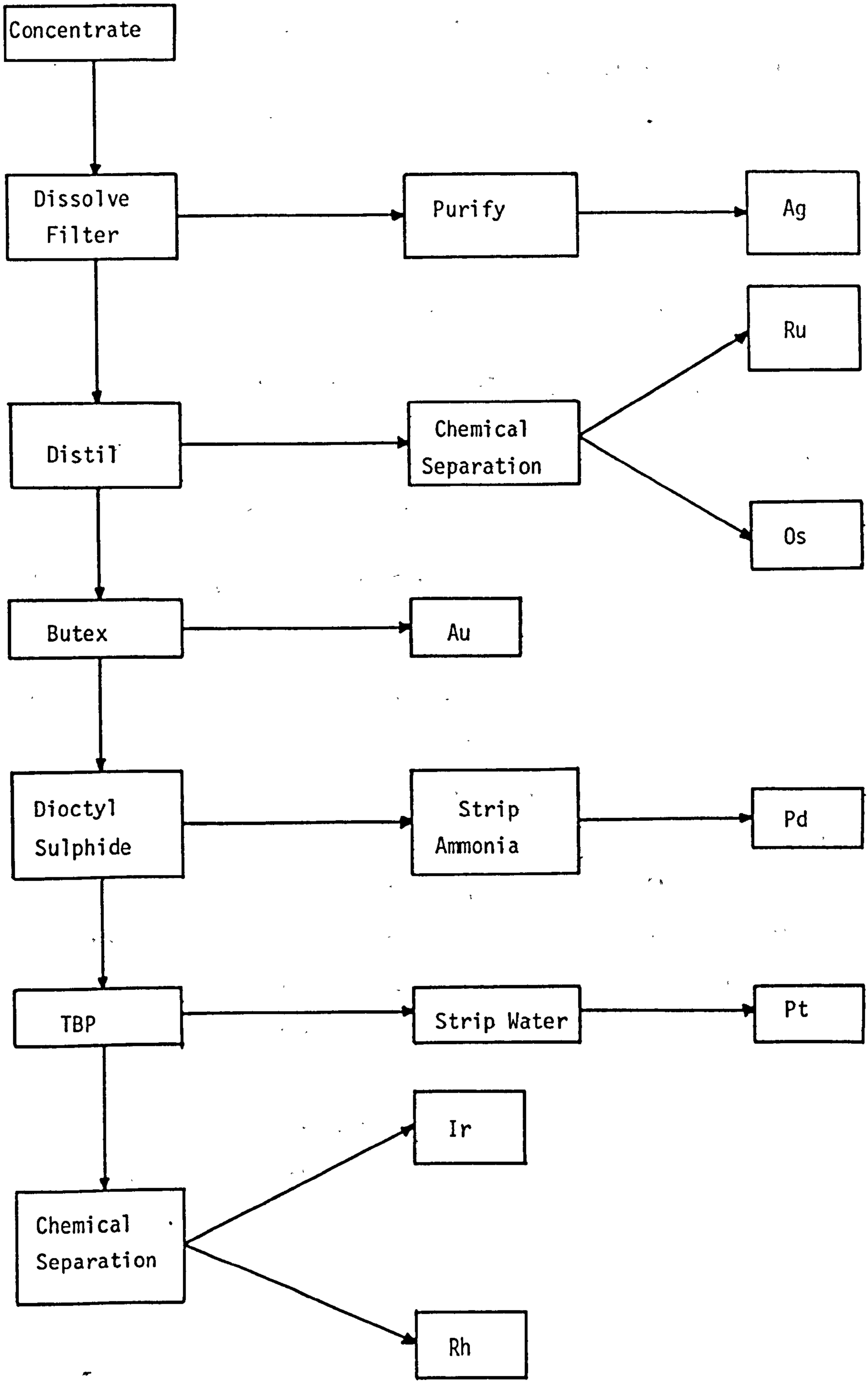

Figure 1.1.3. Inco plc solvent extraction process (12).

techniques, solvent extraction using Butex (diethyleneglycol dibutyl ether) is employed to recover gold from a 3-4M hydrochloric acid feed. The gold is recovered from the organic phase by direct reduction with aqueous oxalic acid.

In the second solvent extraction cycle, palladium is recovered by extraction with di-n-octyl sulphide (DOS) in an aliphatic hydrocarbon diluent (Esso Isopar M). The extraction reaction being:

$$(PdCl_4)^{2-} + \overline{2R_2S} = \overline{PdCl_2(R_2S)_2} + 2Cl^- \quad \text{.....1.4.}$$

After scrubbing, the palladium is recovered from the organic phase by stripping with aqueous ammonia to give palladium in the form $Pd(NH_3)_4^{2+}$:

$$\overline{PdCl_2(R_2S)_2} + 4NH_3 = \overline{2R_2S} + \{Pd(NH_3)_4\}^{2+} + 2Cl^- \quad \text{.....1.5.}$$

The palladium is recovered from the strip liquor as the salt $Pd(NH_3)_2Cl_2$ by neutralisation with hydrochloric acid.

Platinum is recovered in the final solvent extraction cycle by extraction with 60% $^{v}/v$ TBP in Isopar M. The distribution coefficient for platinum goes through a maximum (D_{Pt}=5) between 5-6M HCl and approaches zero at acid concentrations less than 1M HCl. Platinum is thus recovered in a multi-stage counter-current process involving extraction and scrubbing with 5M HCl, and stripping with water.

Conventional chemical separation is used to recover rhodium and iridium from the raffinate after platinum extraction.

1.1.2. Complex Formation/Ligand Exchange Rates

The most marked difference between PGM's and the light transition metals is in the ligand exchange rates. Inertness to substitution for transition metal complexes varies:

3rd row > 2nd row > 1st row

For comparable complexes, the extent of this variation is indicated in Table 1.1.1. The actual rate varies with electron configuration, but the relative comparison holds (11).

The effect of d electrons on the rate of substitution of inner sphere water molecules by other ligands on both transition metal and non-transition metal ions falls over a wide range of values. Figure 1.1.4. shows a tabulation of these constants by periodic group for a large number of ions, and in Figure 1.1.5., the constants have been plotted against the number of d electrons for the di- and trivalent ions for the first row transition metals.

The metal ions can be placed in four distinct classes depending on their substitution rates (13,14):

Class I. Exchange of water is essentially diffusion controlled ($K \geqslant 10^8$ sec^{-1}). The ions are of Periodic Groups IA and IIA (except Be^{2+} and Mg^{2+}) and IIB (except Zn^{2+}) in addition to Cr^{2+} and Cu^{2+}.

Class II. K is in the range 10^4 to 10^8 sec^{-1}, and this class includes most first row transition metal ions in the divalent state (except V^{2+}, Cr^{2+}, Cu^{2+}), Mg^{2+} and the rare earths.

Table 1.1.1. Variation of substitution kinetics with position in the periodic table (11)

Metal	Row	Complex	Reaction	Rate K (s^{-1})
Co(III)(d^6)	1st	$Co(NH_3)_5Br^{2+}$	Acid hydrolysis	6.3×10^{-6}
Rh(III)(d^6)	2nd	$Rh(NH_3)_5Br^{2+}$	Acid hydrolysis	$\sim 1 \times 10^{-8}$
Ir(III)(d^6)	3rd	$Ir(NH_3)_5Br^{2+}$	Acid hydrolysis	$\sim 2 \times 10^{-10}$
Ni(III)(d^8)	1st	trans$\{Ni(PEt_3)_2$(o-tolyl)Cl$\}$	With pyridine	3.3×10^{1}
Pd(II)(d^8)	2nd	trans$\{Pd(PEt_3)_2$(o-tolyl)Cl$\}$	With pyridine	5.8×10^{-1}
Pt(II)(d^8)	3rd	trans$\{Pt(PEt_3)_2$(o-tolyl)Cl$\}$	With pyridine	6.7×10^{-6}

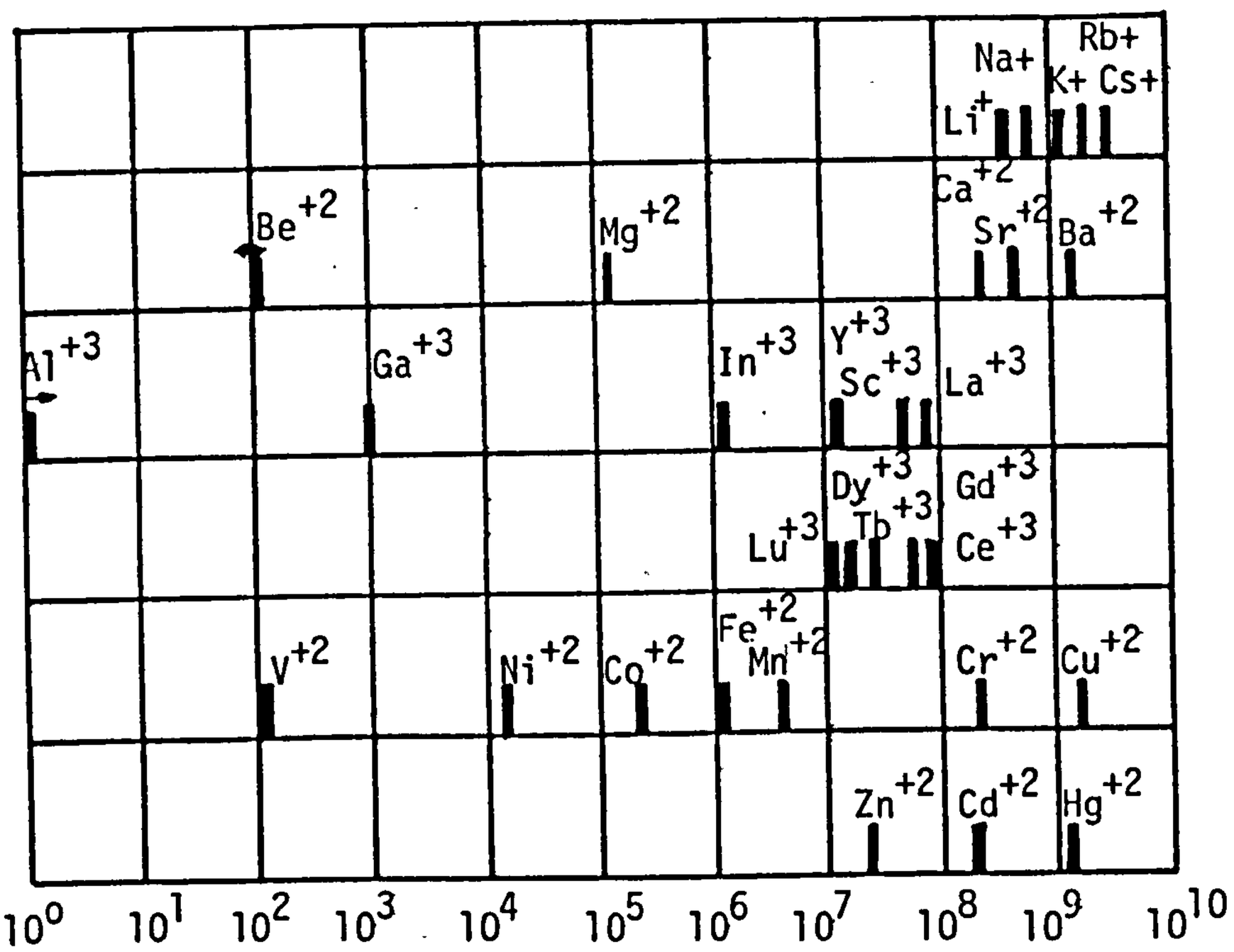

Figure 1.1.4. Characteristic rate constants (sec^{-1}) for the substitution of inner sphere water molecules in a number of metal ions (14).

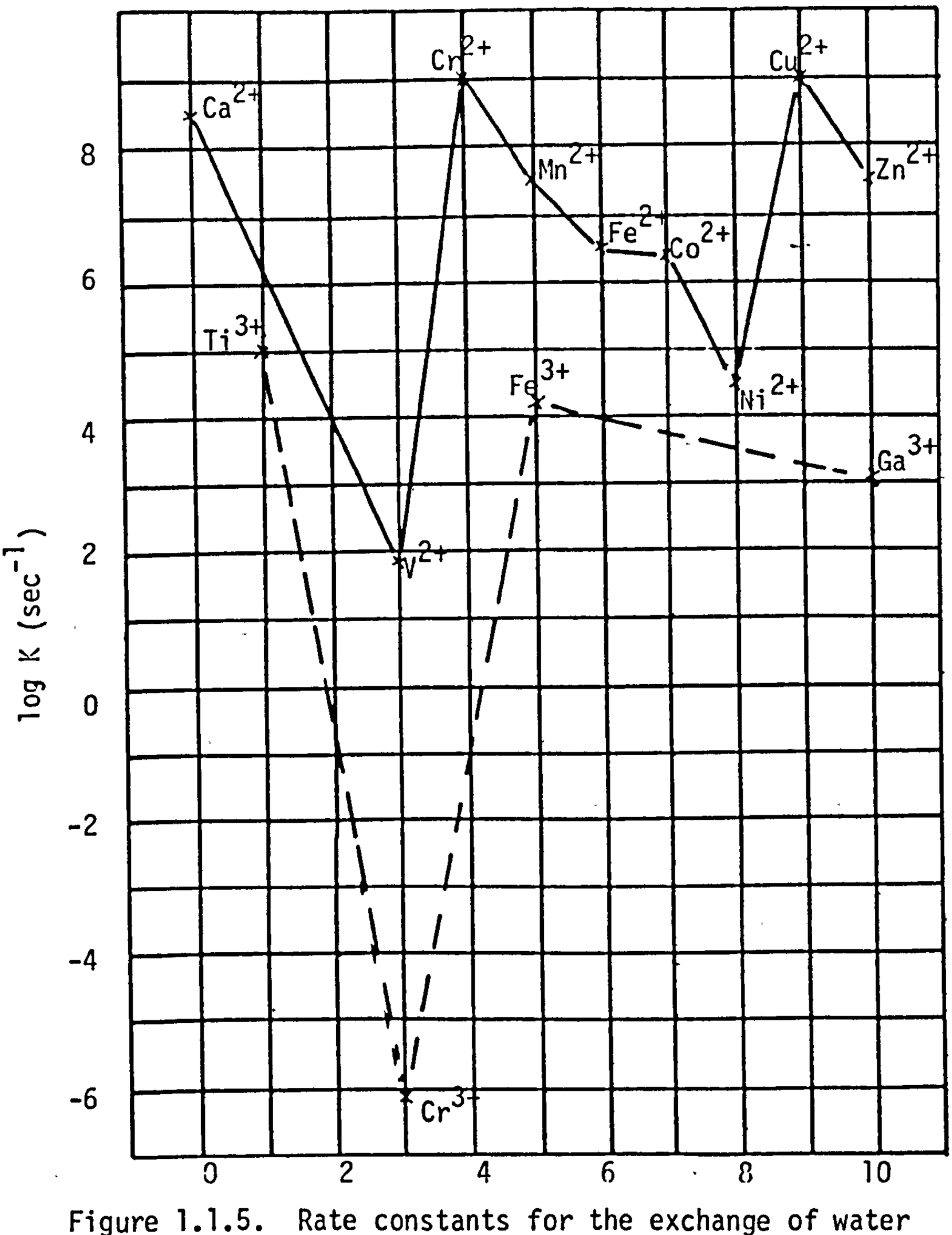

Figure 1.1.5. Rate constants for the exchange of water molecules in the first coordination sphere of $\{M(H_2O)_6\}^{n+}$ in aqueous solution (14).

Class III K lies roughly between 1 and 10^{-4} sec^{-1}. Be^{2+}, Al^{3+}, V^{2+} and some 3+ ions of the first row transition metals are the elements in this group.

Class IV Rate constants are in the range 10^{-3} to 10^{-6} sec^{-1}, and this includes Cr^{3+}, Co^{3+}, Rh^{3+}, Ir^{3+} and Pt^{2+}.

The reasons for this ordering are rather complex, but it is clear for Group IA ions that decreasing ionic size slows the substitution rate. This is probably controlled by the change in effective charge with the size of the ion. Groups IIA and IIB follow the same general trend, although Be^{2+} is an exception because of hydrolysis reactions.

Outside of these elements no correlation between rate and ion size is observed since Cr^{2+}, Ni^{2+} and Cu^{2+} have almost identical ionic radii. However, Cr^{2+} and Cu^{2+} substitute more rapidly than Ni^{2+}. To explain this,one must consider the effect of d electrons on the structure of the complexes. Cu^{2+} (d^9) and Cr^{2+} (d^4) are subject to large Jahn-Teller distortions resulting in weaker and longer axial bonds, thus exchange is rapid. The overall effect of d electrons on the rate of substitution of $\{M(H_2O)_6\}^{n+}$ is shown in Figure 1.1.5. It can be seen that, in general, the substitution rate decreases with increasing charge (14).

Rh^{3+}, which together with Rh^{+} is the most common oxidation state of rhodium, falls into Class IV along with Co^{3+}, Ir^{3+}, Pt^{2+} and Cr^{3+}. In this class rate constants range from 10^{-3} to 10^{-6} sec^{-1}.

To explain the differences in rate, one must consider the d orbital energies. A significant proportion of the activation energy required

d Electron Configuration		Reaction by Dissociative Activation	
		sp Intermediate	tbp Intermediate
		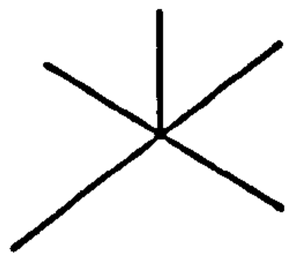	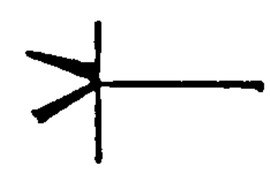
		C_{4v}	D_{3h}
d^0		inert	inert
d^1		inert	inert
d^2		inert	inert
d^3		inert	inert
d^4	low spin	inert	inert
	high spin	labile	labile
d^5	low spin	inert	inert
	high spin	labile	labile
d^6	low spin	inert	inert
	high spin	labile	labile
d^7	low spin	labile	inert
	high spin	labile	labile
d^8		labile	inert
d^9		labile	labile
d^{10}		labile	labile

Table 1.1.2. Predictions of inertness and lability for octahedral transition metal complexes (14)

for the substitution goes into changing the d orbital energy from the ground state of the complex to the transition state (14). For the exchange of water, a dissociative mechanism via a five co-ordinate intermediate is thought to apply. The structure of this intermediate may be a square based pyramid or a trigonal bipyramid. Using the angular overlap model (AOM) one can reach the results which are shown in Table 1.1.2. These are obtained by proposing that the structural preference energy (SPE) of the octahedrons (i.e. the difference between the d orbital energy of the octahedron and its transition state) is less than a specific value then a labile complex will result, and above that value the complex will be inert to substitution. Rh^{3+} being a low spin d^6 ion is thus shown to be inert to substitution.

1.2. RHODIUM SPECIATION IN ACIDIC MEDIA

1.2.1. Aqueous Chemistry

The visible spectra of rhodium (III) complexes display two bands towards the blue end of the spectrum, although in most cases only the first spin allowed ligand field band ($^1A_{1g} \rightarrow {}^1T_{1g}$) is observed. The second band $^1A_{1g} \rightarrow {}^1T_{2g}$ is often obscured by charge-transfer transitions Figure 1.2.1. These bands are responsible for the yellow, red or red-brown colours of rhodium (III) compounds. The results of Jørgenson's electronic absorption measurements on rhodium (III) complexes are presented in Table 1.2.1. (15).

The yellow hexaaquo ion of rhodium, $\{Rh(H_2O)_6\}^{3+}$ is obtained by dissolution of rhodium (III) sesquioxide ($Rh_2O_3 . 5H_2O$) in cold mineral

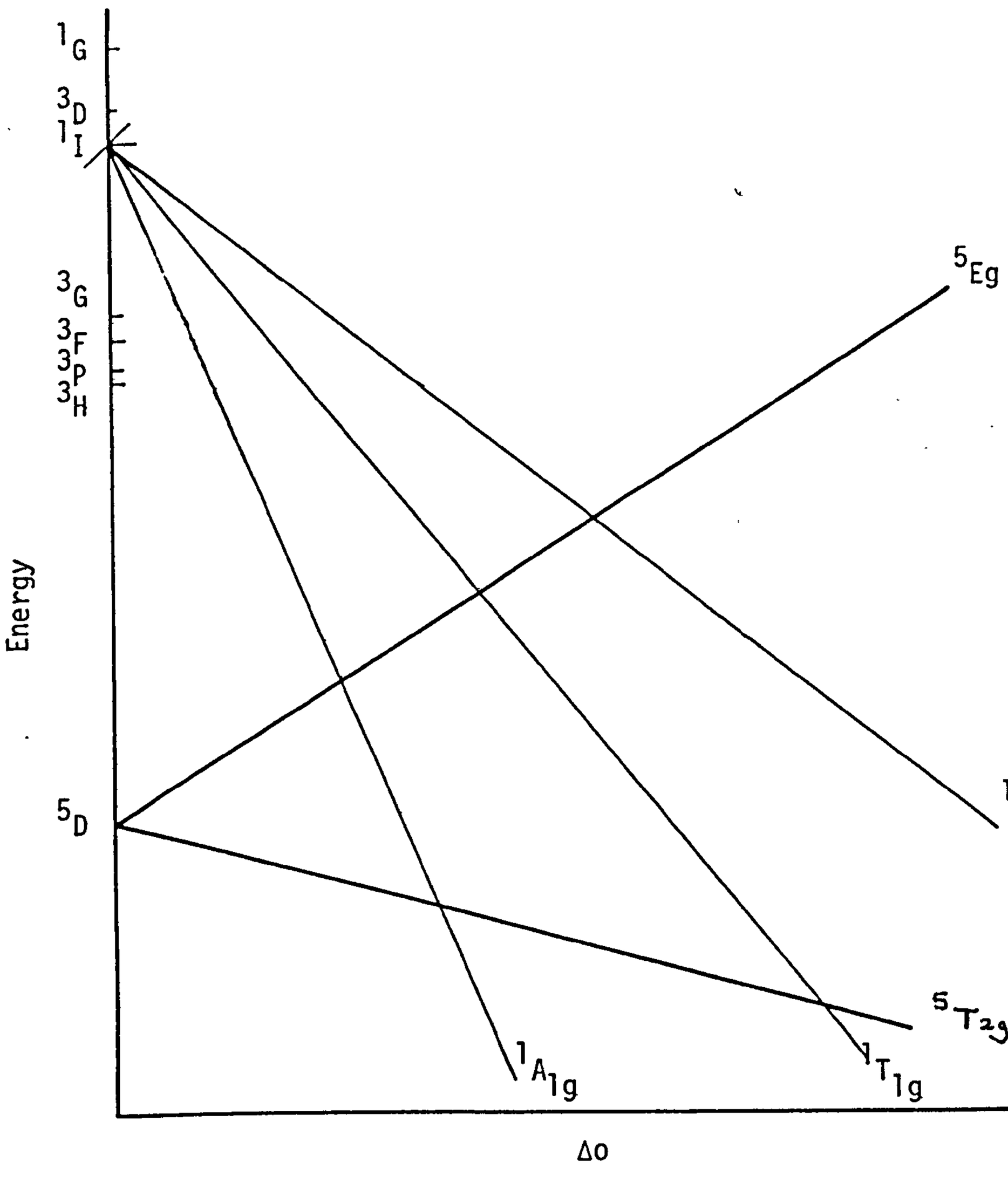

Figure 1.2.1. Simplified energy level diagram for a d^6 ion in an octahedral field (14).

Table 1.2.1. Absorption bands of rhodium (III) complexes (15)

COMPLEX	WAVE LENGTH (nm)	WAVE NUMBER (cm^{-1})	MOLAR ABSORBTIVITY (ε)
$\{RhBr_6\}^{3-}$	553	18100	190
	450	22200	180
$\{RhCl_6\}^{3-}$	680	14700	3
	518	19300	102
	412	24300	82
$\{Rh(C_2O_4)_3\}^{3-}$	520	19200	8
	398	25100	290
	333	30000	-
$\{Rh(H_2O)_6\}^{3+}$	393	25500	47
	305	32800	55
$\{Rh(NH_3)_5I\}^{2+}$	416	24100	270
	388	25800	230
	278	36000	3200
$\{Rh(NH_3)_5Br\}^{2+}$	424	23600	25
	359	27800	122
$\{Rh(NH_3)_5Cl\}^{2+}$	349	28700	100
	277	36100	103
$\{Rh(NH_3)_5OH\}^{2+}$	321	31200	124
	278	36000	108
$\{Rh(NH_3)_5H_2O\}^{3+}$	316	31600	105
	263	38100	89
$\{Rh(NH_3)_6\}^{3+}$	306	32700	135
	256	39100	100
$\{Rhen_3\}^{3+}$	301	33200	210
	253	39600	190
$\{Rh(NH_3)_5NO_2\}^{2+}$	296	33800	330
	246	40600	1030

acids, or as the perchlorate by repeated evaporations of perchloric acid solutions of rhodium trichloride (16, 17). The crystalline deliquesent perchlorate is isomorphous with other salts containing octahedral cations, e.g. $\{Co(NH_3)_6\}(ClO_4)_3$. Kinetic studies of the exchange reaction between Rh_{aq}^{3+} and ^{18}O-labelled solvent water, confirm the hydration number as 5.9 ± 0.4 (18). The ion is acidic, pKa ∿ 3.3, giving $\{Rh(H_2O)_5OH\}^{2+}$ in solutions less than 0.1M in acid.

Rhodium trichloride, "$RhCl_3.nH_2O$ (n = 3 or 4)" is the usual starting material for the preparation of many rhodium complexes. In chloride solutions, the rhodium species present range from the hexaaquo ion to hexachlororhodate (III) ion $(RhCl_6)^{3-}$. All the intermediate species of the general formula $\{Rh(H_2O)_{6-n}Cl_n\}^{(3-n)+}$ have been identified (19, 20) and their interconversions studied (21).

The kinetics of the exchange and substitution reaction between $(RhCl_6)^{3-}$ and $(RhH_2OCl_5)^{2-}$ in aqueous acid solutions have also been investigated (22).

The action of sulphuric acid on rhodium (III) sesquioxide gives rhodium (III) sulphate. Vacuum evaporation of such solutions at 0^oC gives the yellow sulphate of formula $Rh_2(SO_4)_3.12H_2O$, while evaporation at 100^oC gives the red sulphate, formula $Rh_2(SO_4)_3.6H_2O$ (1, 23). The rhodium speciation in aqueous solutions containing sulphate ions is uncertain. Lederer (24) found a weak cationic and a single anionic band when solutions of rhodium (III) in 0.2M sulphuric acid were subjected to paper electrophoresis. Under similar

conditions, Shukla (25) reports two anionic bands from 0.5M sulphuric acid, but from 1M sulphuric acid only one anionic band was observed. No cationic bands were observed.

"Rhodium (III) nitrate" can be prepared in an analogous manner to rhodium (III) sulphate. Dissolution of rhodium (III) sesquioxide in concentrated nitric acid, yields a red mass upon evaporation which has been suggested to be the hydrate rhodium (III) nitrate, $Rh(NO_3)_3.2H_2O$ (26).

Anhydrous "rhodium (III) nitrate" can be obtained by treating rhodium (III) iodide with boiling concentrated nitric acid. Evaporation of the resulting solution and drying to constant mass gives a compound of empirical formula $Rh(NO_3)_3$ (27-29). The anhydrous nitrate can also be prepared by the reaction of dinitrogen pentoxide with rhodium (III) bromide (27).

Potassium hexanitratorhodate (III) has been prepared by boiling potassium hexanitritorhodate (III) with concentrated nitric acid for a prolonged period (27, 28). The resulting syrupy mass when dried to constant weight gave $K_3Rh(NO_3)_6$ as a brown product. The compound is non-hygroscopic and air-stable, soluble in water, methanol and nitric acid. The infra-red spectrum of potassium hexanitratorhodate (III) contains all the bands characteristic of unidentate coordinated nitrato-groups (27,30-33), Table 1.2.2.

The speciation of rhodium in aqueous nitrate media is still uncertain. Shubochkin et.al. (27) showed that potassium hexanitratorhodate (III)

Table 1.2.2. IR vibrations of the nitrato group (30-33)

Type	$V_2(A_1)$	$V_6(B_2)$	$V_1(A_1)$	$V_4(B_1)$	$V_3(A_1)$	$V_5(B_1)$
Assignment	NO Stretch	Out of Plane Rock	NO_2 symm. stretch	NO_2 asymm. stretch	NO_2 bend symm.	NO_2 bend asymm. (out of plane rock)
Frequency (cm^{-1})	1034-970	800-781	1290-1253	1531-1481	~739	~713
Found for $K_3\{Rh(NO_3)_6\}$ (26)	970	770, 795	1280	1510	735	720

Figure 1.2.2. Rhodium speciation in acidic media (16,24,35,36)

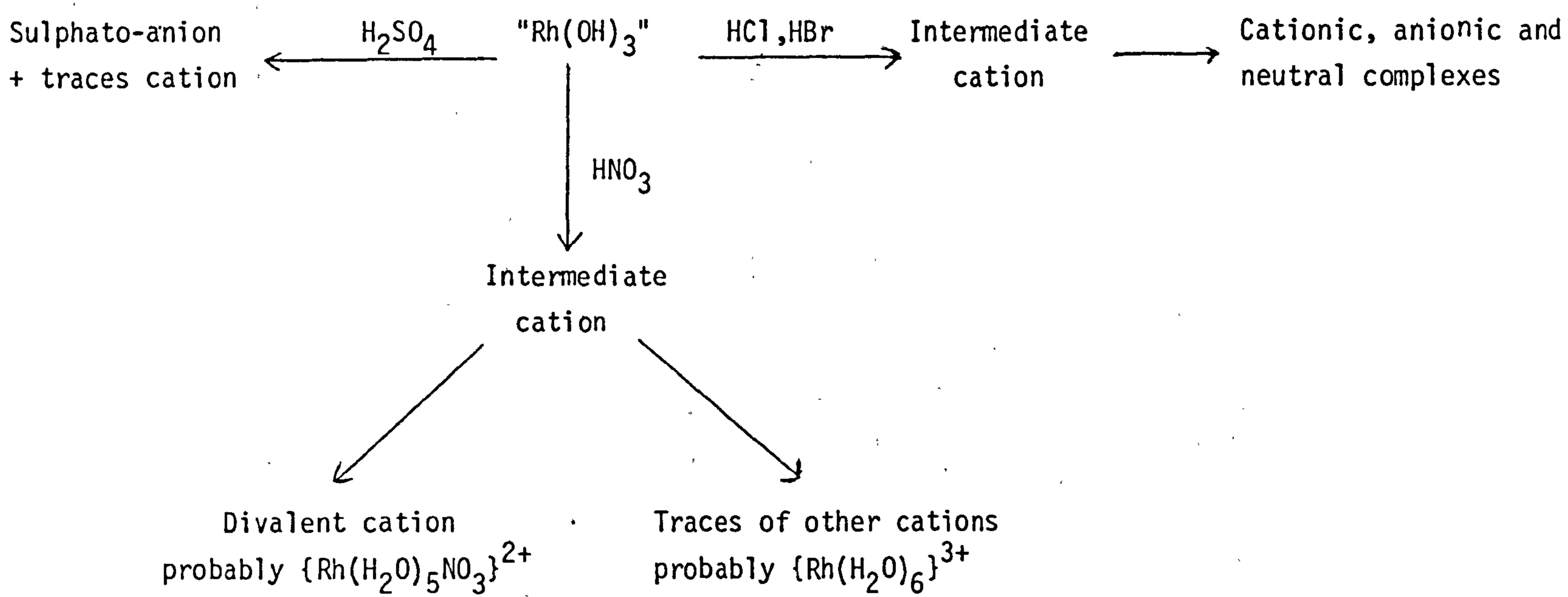

in water underwent extensive hydrolysis. This result is not unexpected since previous work has shown that hydrolysis of rhodium (III) complexes in solutions less than 0.1M acid is quite marked (15, 34). Lederer and coworkers (16, 24, 35, 36) investigated the speciation of rhodium (III) in acidic media by electrophoresis, ion-exchange chromatography and absorption spectroscopy. Their results are summarised in Figure 1.2.2.

Shukla (25) measured the absorption spectra of rhodium containing solutions, which were 1M in nitric acid, and found λ_{max} to be 400nm. Since Jørgensen (15) had shown that the hexaaquo ion, $\{Rh(H_2O)_6\}^{3+}$ had characteristic absorptions at λ_{max} 310nm and 400nm, Shukla concluded that this was indeed the major cation present in nitric acid. The absorption at 310nm could not be measured since the nitrate ion also absorbs in this region (30, 37). However, the molar absorptivity at 400 nm was not recorded, and Shukla made no mention of the discrepency between his absorption measurements and the earlier studies in nitrate media, which showed the divalent species $\{Rh(H_2O)_5NO_3\}^{2+}$ as the major cation.

1.2.2. ^{103}Rh Nuclear Magnetic Resonance (NMR) Spectroscopy

It is only in recent years that the importance of NMR as a tool for studying rhodium chemistry has been realised. This interest is a consequence of improved techniques and the availability of more powerful spectrometers. The properties of ^{103}Rh are listed in Table 1.2.3. (38).

Table 1.2.3. Properties of ^{103}Rh (38)

Natural abundance N/%	100
Magnetic moment	-0.1522 μ/μ_N
Magnetogyric ratio	-0.8420 $\gamma/10^7 radT^{-1}S^{-1}$
NMR frequency	3.172310 MHz
Relative receptivity (relative to ^1H)	3.12×10^{-5}
Nuclear spin	$\frac{1}{2}$

The favourable properties of ^{103}Rh are that it is 100% abundant and has a nuclear spin of $\frac{1}{2}$. However, the magnetogyric ratio (and hence resonance frequency) is very low cf. $\gamma_{^1H} = 26.751 \times 10^7$ rad $T^{-1}S^{-1}$. The practical consequences of this are that solutions of rhodium for NMR spectroscopy have to contain at least 25 mg/ml Rh, and the spectra recorded over several hours.

NMR spectroscopic studies of ^{103}Rh have been concerned mainly with determining the stereochemistry of various rhodium complexes, and on compiling a library of ^{103}Rh chemical shifts (38). In aqueous acidic media, all the rhodium chloro and chloro-bromo species have been identified (39, 40). The ^{103}Rh chemical shifts for these complexes are displayed in Tables 1.2.4. and 1.2.5.

1.2.3. Electrochemistry: Polarographic Characteristics

Problems associated with the polarography of the platinum group metals are often due to the spontaneous oxidation of the electrode by the metal complex, production of catalytic hydrogen waves, and high reduction potentials very near to those of the supporting

Table 1.2.4. ^{103}Rh chemical shifts for $\{Rh(H_2O)_{6-n}Cl_n\}^{(3-n)+}$ in hydrochloric acid (39)

SPECIES	$\delta(^{103}Rh)$/ppm
$\{Rh(H_2O)_6\}^{3+}$	9992
$\{Rh(H_2O)_5Cl\}^{2+}$	9479
cis-$\{Rh(H_2O)_4Cl_2\}^{+}$	8794
Trans-$\{Rh(H_2O)_4Cl_2\}^{+}$	9115
fac-$Rh(H_2O)_3Cl_3$	8545
mer-$Rh(H_2O)_3Cl_3$	8858
cis-$\{Rh(H_2O)_2Cl_4\}^{-}$	8295
trans-$\{Rh(H_2O)_2Cl_4\}^{-}$	8605
$\{Rh(H_2O)Cl_5\}^{2-}$	8233
$\{RhCl_6\}^{3-}$	7975

Table 1.2.5. ^{103}Rh chemical shifts for $\{RhCl_{6-n}Br_n\}^{3-}$ in mixtures of hydrochloric and hydrobromic acids (40)

SPECIES	$\delta(^{103}Rh)$/ppm
$\{RhCl_6\}^{3-}$	7985
$\{RhCl_5Br\}^{3-}$	7848
$cis\{RhCl_4Br_2\}^{3-}$	7707
$trans\text{-}\{RhCl_4Br_2\}^{3-}$	7712
$fac\text{-}\{RhCl_3Br_3\}^{3-}$	7556
$mer\text{-}\{RhCl_3Br_3\}^{3-}$	7561
$cis\text{-}\{RhCl_2Br_4\}^{3-}$	7403
$trans\text{-}\{RhCl_2Br_4\}^{3-}$	7409
$\{RhClBr_5\}^{3-}$	7243
$\{RhBr_6\}^{3-}$	7077

electrolyte. As a result, the literature on the polarography of the platinum group metals contains a great deal of contradictory data (41).

Rhodium (III) complexes generally give rise to two or more polarographic waves, for which the total limiting current is proportional to the rhodium (III) concentration (42-46). From plots of E against log $i/(i_d-i)$ (see section 2.6.1.), and by comparison of the polarograms of rhodium (III) complexes to those of the equivalent cobalt complexes, Willis (47) calculated the number of electrons transferred during reduction as one or two. However, later studies using coulometry and electrolysis at controlled potential, gave a value of three, indicating reduction to rhodium metal (42).

Van Loon and Page (42) studied the reduction of the rhodium (III) hexaaquo ion in 0.13M $HClO_4$ + $NaClO_4$ at a dropping mercury electrode. Two polarographic waves were observed, the first of which was irreversible and diffusion controlled with $E_{\frac{1}{2}}$ = -0.38 V. The second wave, at a more negative potential ($E_{\frac{1}{2}}$ = -0.72 V) occurred with a pronounced maximum, the usual suppressors, methyl red, gelatin and Triton X-100, having little effect. Studies of this second wave proved difficult since it was close to the discharge of the supporting electrolyte.

In his polarographic studies of the rhodium (III) chloro complexes, Scarano (48) makes brief mention of a "rhodium nitrate" compound which, when placed in potassium nitrate as supporting electrolyte shows two polarographic waves, while in nitric acid is decomposed by mercury showing only one wave.

For the reduction of rhodium (III) chloro complexes (heat stabilised) in 1M KNO_3, Cozzi and Pantani (43) report a single irreversible wave with $E_{\frac{1}{2}}$ = -0.012 V.

The polarographic data for rhodium (III) complexes in acidic media is summarised in Table 1.2.6.

1.3. ANALYTICAL CHEMISTRY

1.3.1. Atomic Absorption Spectroscopy and Colorimetric Methods

Progress in the analytical chemistry of rhodium is closely linked to the separation procedures used in its isolation from the rest of the noble metals. The most frequently used methods of separation involve ion-exchange accompanied by liquid-liquid extraction. Separation methods based on partition chromatography are of less importance (8, 51-53).

Having isolated rhodium, macro quantities of the element can be determined gravimetrically using such reagents as thiobarbituric acid (54,55), 2-mercaptobenzoxazole (56), thioacetanilide (57) or hydrogen sulphide (58). For microgram quantities, great reliance is placed on colorimetric methods (52, 53, 59) and, more recently, on atomic absorption spectroscopy (AAS) as routine methods. Solutions of rhodium which also contain the other platinum metals, notably platinum, iridium and palladium are unsuitable for direct measurement because of mutual interferences (60-64). Base metals and sodium salts also seriously effect the analysis (65). Hence the use of AAS for analysing rhodium must be linked with separation and pre-concentration schemes if any of the above interferants are present (66,67).

Table 1.2.6. Polarographic characteristics of rhodium (III) complexes in acidic media

MEDIUM	$E_{\frac{1}{2}}$ (VsSCE)	REMARKS	REFS
0.5M $HClO_4$	-0.39	n = 2	41
1M $HClO_4$	+0.035	n = 3	43
0.5M $HClO_4$	-0.39	n = 2	49
0.13M ($HClO_4$+$KClO_4$) pH1.5-2.7	-0.38	n = 3, irreversible, 2 waves	42
6M HCl	-0.28	n = 3, irreversible, 2 waves	42, 43
0.1M HCl+NaCl pH1.3-3.8	-0.07	irreversible	43
4M(HBr + NaBr)	-0.366	reversible	50

All the colorimetric methods developed for rhodium also suffer, to varying degrees from interferants such as the platinum group metals and base metals. The development of these methods has therefore, often been accompanied by elaborate separation schemes (68, 69).

The most popular of the colorimetric methods for rhodium is the tin(II) chloride procedure (52). Developed in 2M hydrochloric acid, the red complex of rhodium with tin(II) chloride forms quickly (within five minutes on boiling), is stable for at least 24 hours, and gives reproducible results (70-75). It is the most studied procedure for rhodium analysis, and has been adapted for use with samples containing fission products (76, 77), uranium (78) and plutonium (79).

1.3.2. Radioanalytical Methods

Despite the fact that neutron activation of rhodium produces only very short lived radionuclides, thus requiring fast radiochemical separations, or separation prior to irradiation, Steele and Meinke (80) were able to determine rhodium by thermal neutron activation using the reaction $^{103}Rh\ (n,\gamma)\ ^{104}Rh + ^{104m}Rh$. ^{104}Rh ($t_{\frac{1}{2}}$ = 44 sec.) was used for a non-destructive method, while the equilibrated species of ^{104}Rh and ^{104m}Rh, with an effective half-life of 4.4 minutes, was used for a destructive procedure. A 42 second irradiation at a thermal neutron flux of 10^{12} n $cm^{-2}sec^{-1}$ was required for the non-destructive method, followed by gamma scintillation counting of the 0.56 MeV photopeak of ^{104}Rh.

Miller (81) used ^{104m}Rh for a destructive method which required heating the irradiated sample with sodium peroxide, dissolving the product in hydrochloric acid, treating with sodium hydroxide, adding rhodium (III) chloride carrier, tartaric acid and pyridine, and filtering into a separating funnel. After rinsing with hydrochloric acid and neutralising with base, an aliquot of the pyridine-rhodium layer is taken for gamma-ray counting.

Detailed radiochemical procedures for rhodium are collected in a monograph by Armstrong and Choppin (82).

1.4. THE REPROCESSING OF NUCLEAR FUEL

The burn-up of ^{235}U in a nuclear reactor gives rise to a variety of radioactive products, many of which act as fission poisons by absorbing the neutrons required to propagate the chain reaction. These fission products are the chief source of radiation from spent fuel, and comprise isotopes of elements ranging in atomic number from 30 (zinc) to 66 (dysprosium), with mass numbers from 76-161. Because of the slightly asymmetric nature of fission, yields of fission products are greatest in the mass ranges 90-100 and 133-144, as shown in Figure 1.4.1. (83, 84).

The reprocessing of spent fuel is necessary in order to recover both uranium and plutonium, and to concentrate the fission products for eventual disposal. A typical fuel cycle is shown in Figure 1.4.2. (85). After initial studies, the solvent extraction process was

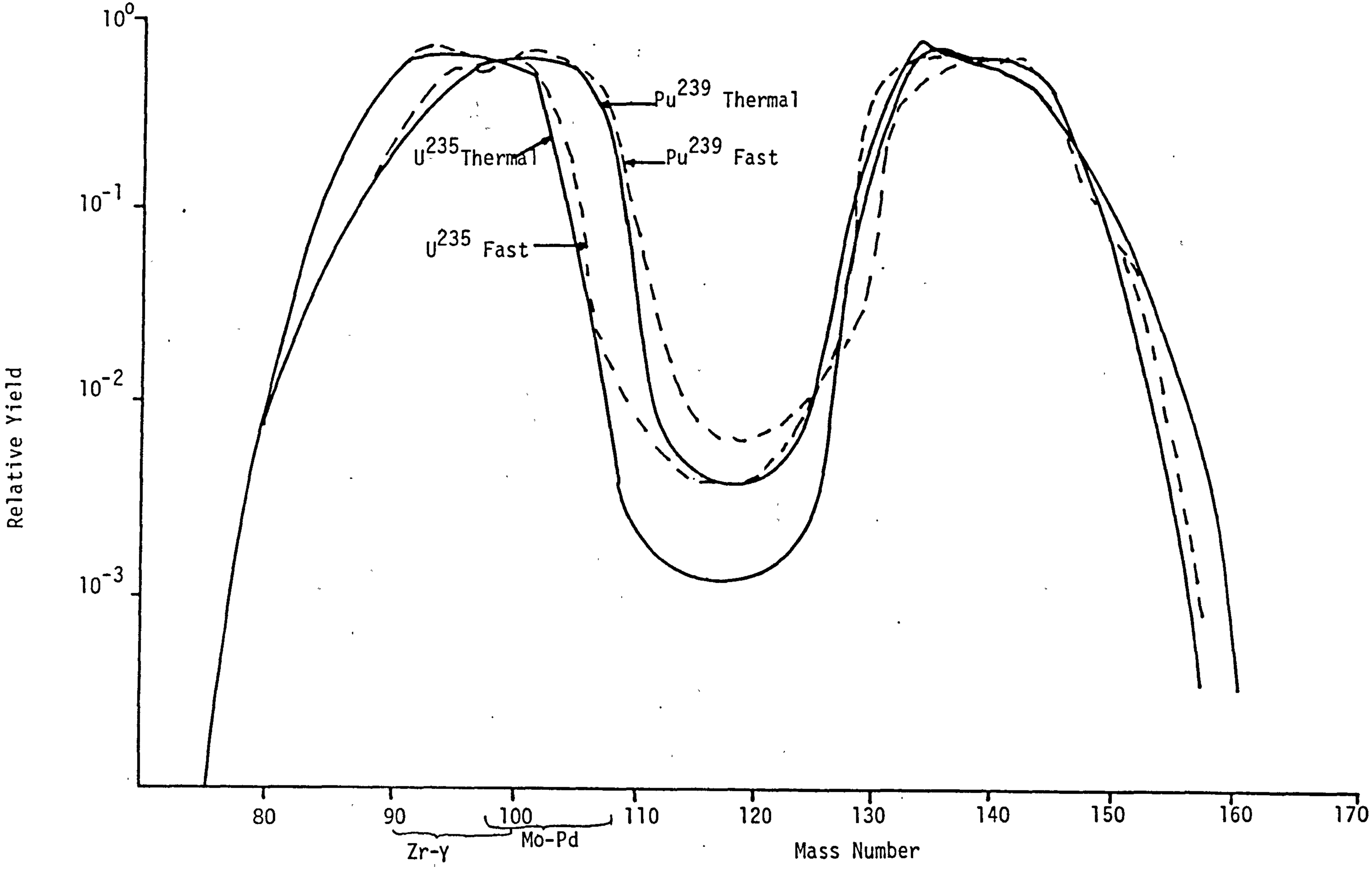

Figure 1.4.1. Fission yield spectra of ^{235}U and ^{239}Pu

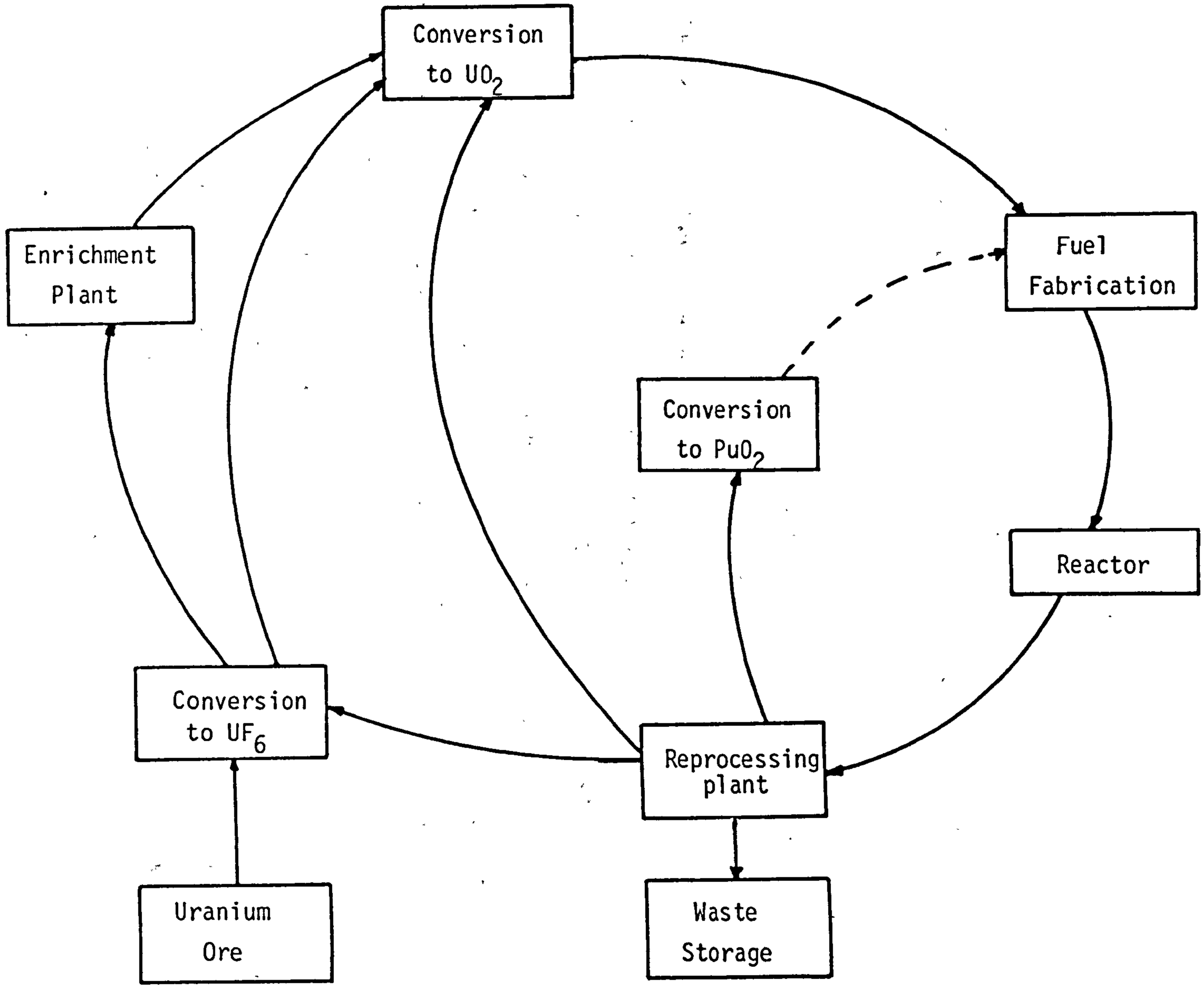

Figure 1.4.2. Nuclear fuel cycle (85)

chosen for reprocessing spent fuel because of its greater efficiency, and because it generated smaller volumes of waste streams than the alternatives (86-88).

The first step in the treatment of spent fuel is to store it for several months in water-filled pools. During this period, the radioactivity and evolution of heat decreases by a factor of about 10,000. The major contributors to fission product activity after a cooling period of 50 days are given in Table 1.4.1.

After cooling, the irradiated fuel is decanned, and the uranium rods, 6M nitric acid and oxygen are fed continuously to a dissolver to produce a uranyl nitrate solution approximately 3M in nitric acid, Figure 1.4.3. In this dissolution, gaseous fission products, such as krypton and xenon . are evolved from the solution. These radioactive gases are passed through a gas treatment plant, before being discharged to the air. After filtration and acidity adjustment, the aqueous solution of the irradiated fuel is fed into the first cycle of the separation process.

Virtually all the major reprocessing plants now employ the Purex process, Figure 1.4.4., to partition uranium and plutonium from the rest of the fission products. A 30% $^{v}/v$ solution of tributyl phosphate (TBP) in kerosene is used as the solvent. The distribution of uranium, plutonium and some fission products between TBP and nitric acid is shown in Figure 1.4.5. The distribution ratios of strontium (II) and caesium (I) for all nitric acid concentrations is much less than 0.01 (89).

Table 1.4.1. The Major Contributors to Fission Product Activity After A 50 Day Cooling Period (84)

Nuclide	Half-life	Cumulative fission yield (%)			
		^{235}U (thermal neutrons)	^{239}Pu	^{238}U (fission spectrum neutrons)	^{239}Pu
^{3}H	12.3 y	0.009	-	-	-
^{85}Kr	10.76y	0.271	0.12	0.153	0.145
^{89}Sr	50.6 d	4.76	1.73	3.3	1.8
^{90}Sr	28.8 y	5.83	2.2	3.2	2.11
^{90}Y	64.4 h	5.83	2.2	3.2	2.11
^{91}Y	58.8 d	5.9	2.6	4.6	2.6
^{95}Zr	65 d	6.2	5.2	5.8	5.3
^{95}Nb	35 d	6.41	5.2	5.8	5.3
^{103}Ru	39.6 d	3.0	5.0	5.8	5.85
^{106}Ru	367 d	0.399	4.4	2.8	4.7
^{106}Rh	30 s	0.399	4.4	2.8	4.7
^{129m}Te	34 d	0.35	1.7	0.24	0.45
^{131}I	8.05d	2.91	3.69	3.2	3.4
^{137}Cs	30.0 y	6.20	6.56	6.3	6.5
^{137m}Ba	153 s	5.80	6.2	5.9	6.1
^{140}Ba	12.8 d	6.30	5.33	6.0	5.1
^{140}La	40.2 h	6.34	5.51	6.0	5.1
^{141}Ce	32.4 d	6.1	5.75	5.5	4.2
^{143}Pr	13.6 d	5.91	4.52	4.3	4.41
^{144}Ce	285 d	5.40	3.79	4.3	3.53
^{144}Pr	17.3 min	5.40	3.79	4.3	3.53
^{147}Nb	11.1 d	2.19	1.87	2.9	2.0
^{147}Pm	2.62 y	2.19	1.87	2.9	2.0

Figure 1.4.3. Continuous dissolution and conditioning of irradiated fuel (86)

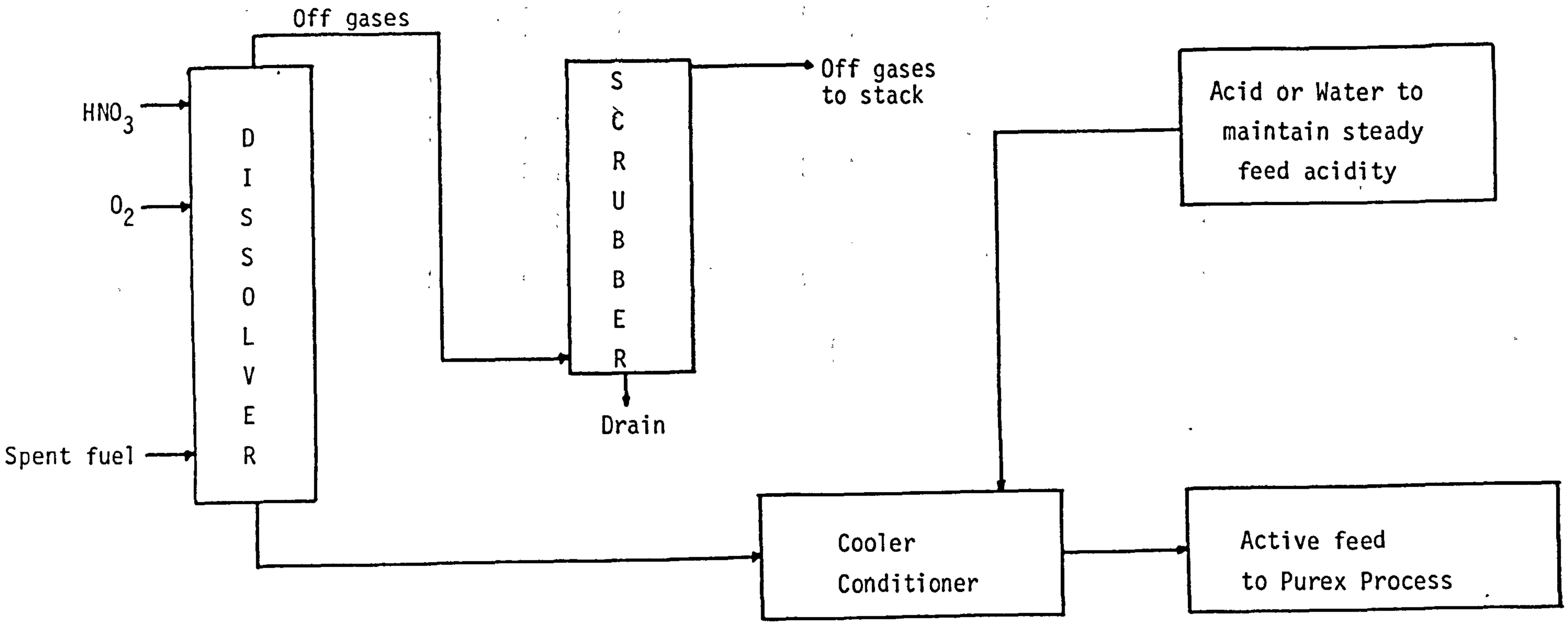

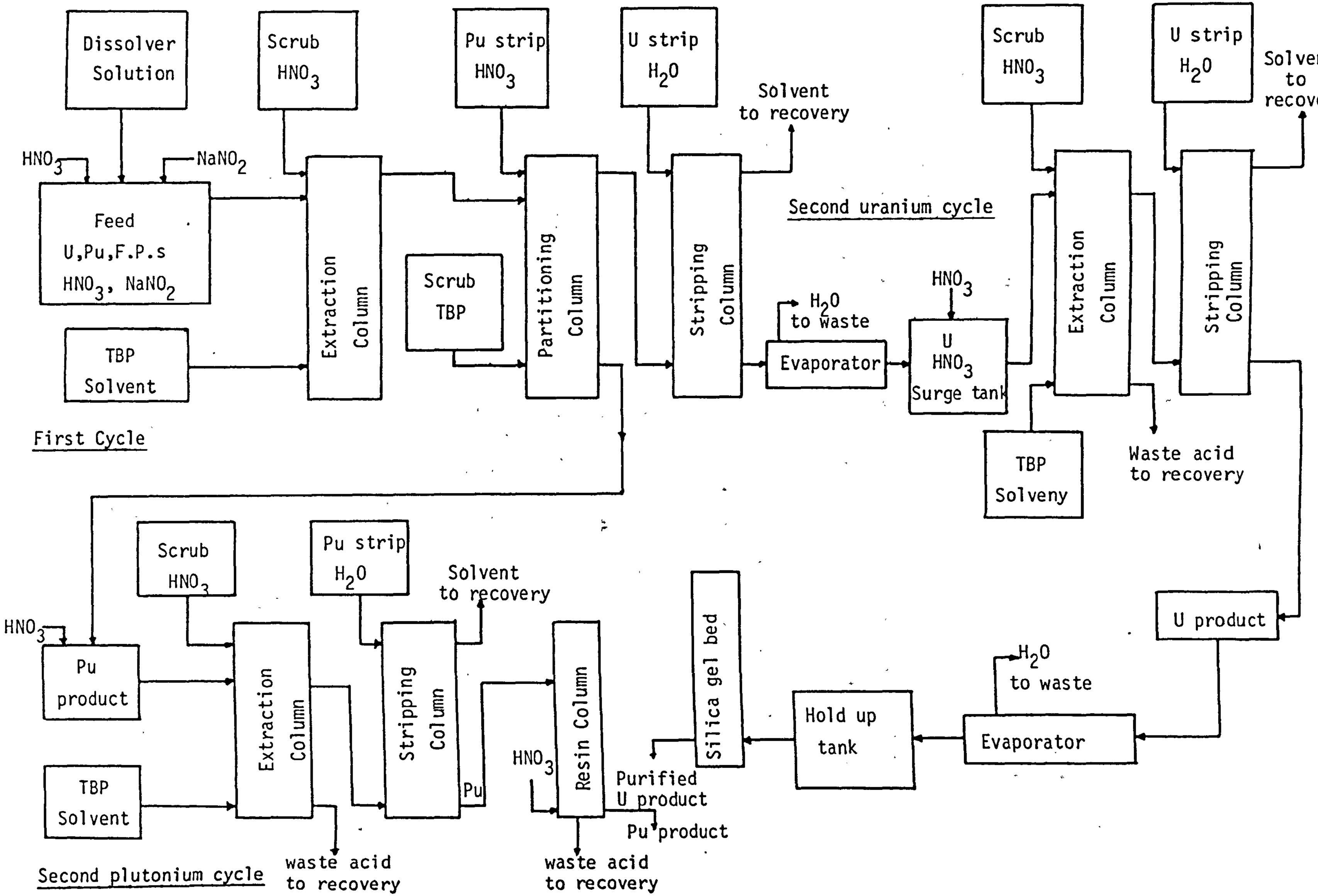

Figure 1.1.1 : Flow sheet of the extraction of uranium & plutonium (PUREX)

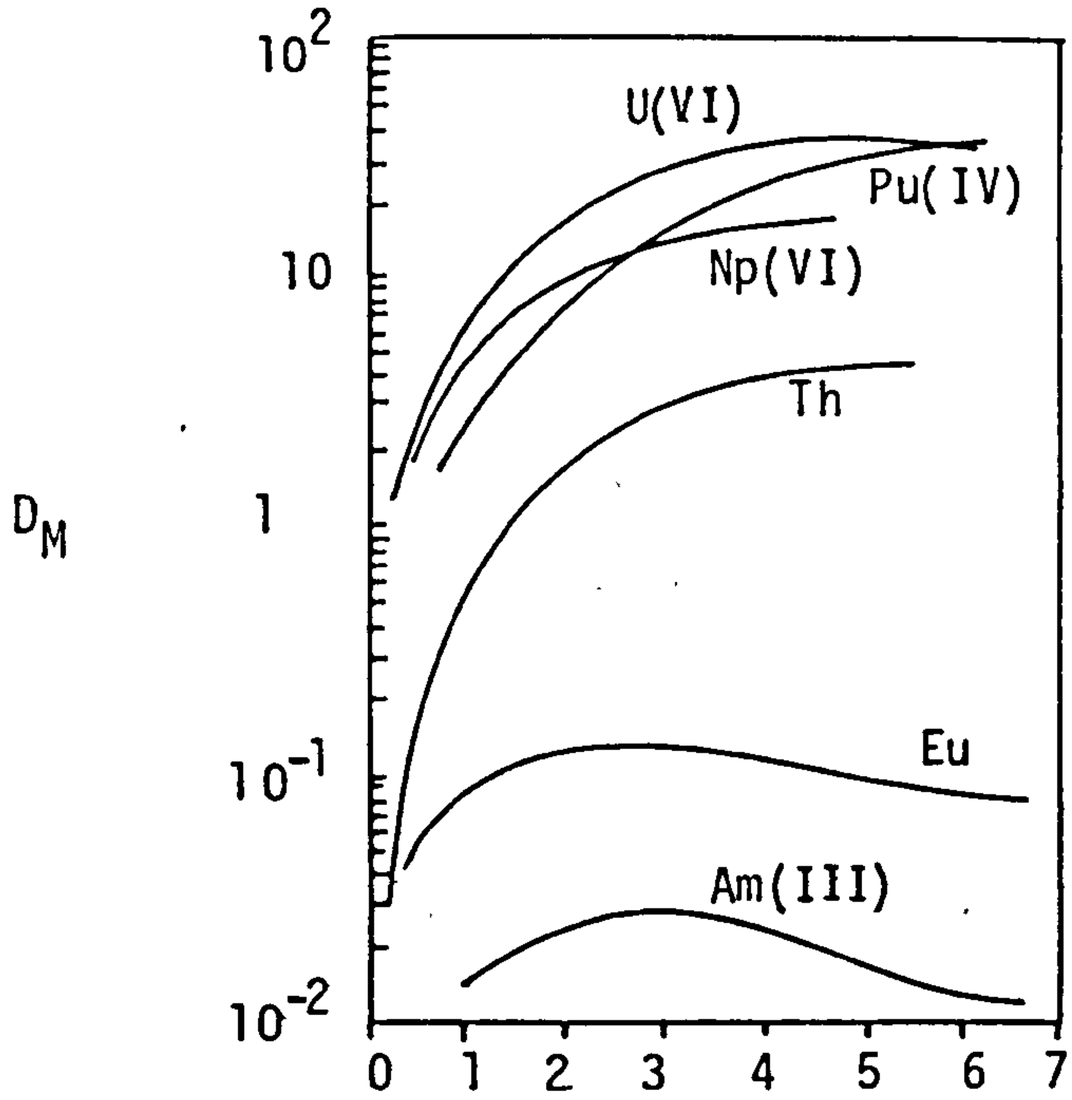

Figure 1.4.5. Distribution of actinide species and Eu(III) between 30 vol.% TBP in kerosene and aqueous HNO_3. (89)

In the first cycle of the Purex process, more than 99.5% of uranium (VI) and plutonium (IV) are co-extracted in the organic phase, leaving approximately 99% of the fission products in the aqueous phase (90). The organic phase is then passed into the partitioning column, where uranium and plutonium are separated from one another. This is accomplished by reducing plutonium (IV) to the +3 state by contacting the organic phase with an aqueous phase containing ferrous sulphamate, or other suitable reducing agents (91, 92). Uranium, which as U(VI) remains in the organic phase, is stripped with water in a third column.

Further uranium and plutonium purification is achieved in the second uranium and plutonium extraction cycles, after which the product streams can be directly handled.

1.4.1. Fission Product Rhodium

One of the products of ^{235}U fission is rhodium. Figures 1.4.6. and 1.4.7. show the relevant parts of the ^{235}U fission chains that give rise to the stable isotopes of ruthenium, rhodium, palladium and silver (93).

The rhodium is present mainly as the stable isotope ^{103}Rh. It also contains small amounts of ^{102}Rh ($t_{\frac{1}{2}}$ = 2.9y), but after 25 years this will have decayed to a harmless level, Table 1.4.2., and so allow fission product rhodium to be used in place of natural rhodium for many of its applications (94).

The projected range of availability of rhodium, palladium, ruthenium and technetium from nuclear fuels (USA), as given by Deonigi et.al. (95), is shown in Table 1.4.3. This shows that in 1980 the production of fission product rhodium was approximately equal to the U.S. annual demand.

1.4.2. Concentration and Storage of Highly Active Liquid Waste

The aqueous waste from the Purex process, which now contains all the fission products and residual uranium and plutonium, is steam stripped to remove organic volatiles and then evaporated (100 fold) under vacuum. The maximum acidity in the evaporator is approximately

Figure 1.4.6. ^{235}U fission chains: Mass numbers 98-104

Mass No.	Atomic No. 42	43	44	45	46
98	Stable Mo 5.9[a]				
99	67h Mo 6.1	~10% → 6.04h Tc ~0.6; ~90% → 2.12×10^5y Tc 6.1		→ Stable Ru	
100	Stable Mo 6.5[a]	15.8s Tc	→ Stable Ru		
101	14.6m Mo 5.0	→ 14.0m Tc 5.0	→ Stable Ru		
102	12m Mo 4.2	→ <25s Tc 4.2	→ Stable Ru		
103			41d Ru 2.9	>95% → 54m Rh 2.9; <5% → Stable Rh	
104			Stable Ru 1.8[a]	4.4m Rh → 42s Rh	→ Stable Pd

Figure 1.4.7. ^{235}U fission chains: Mass numbers 105-110

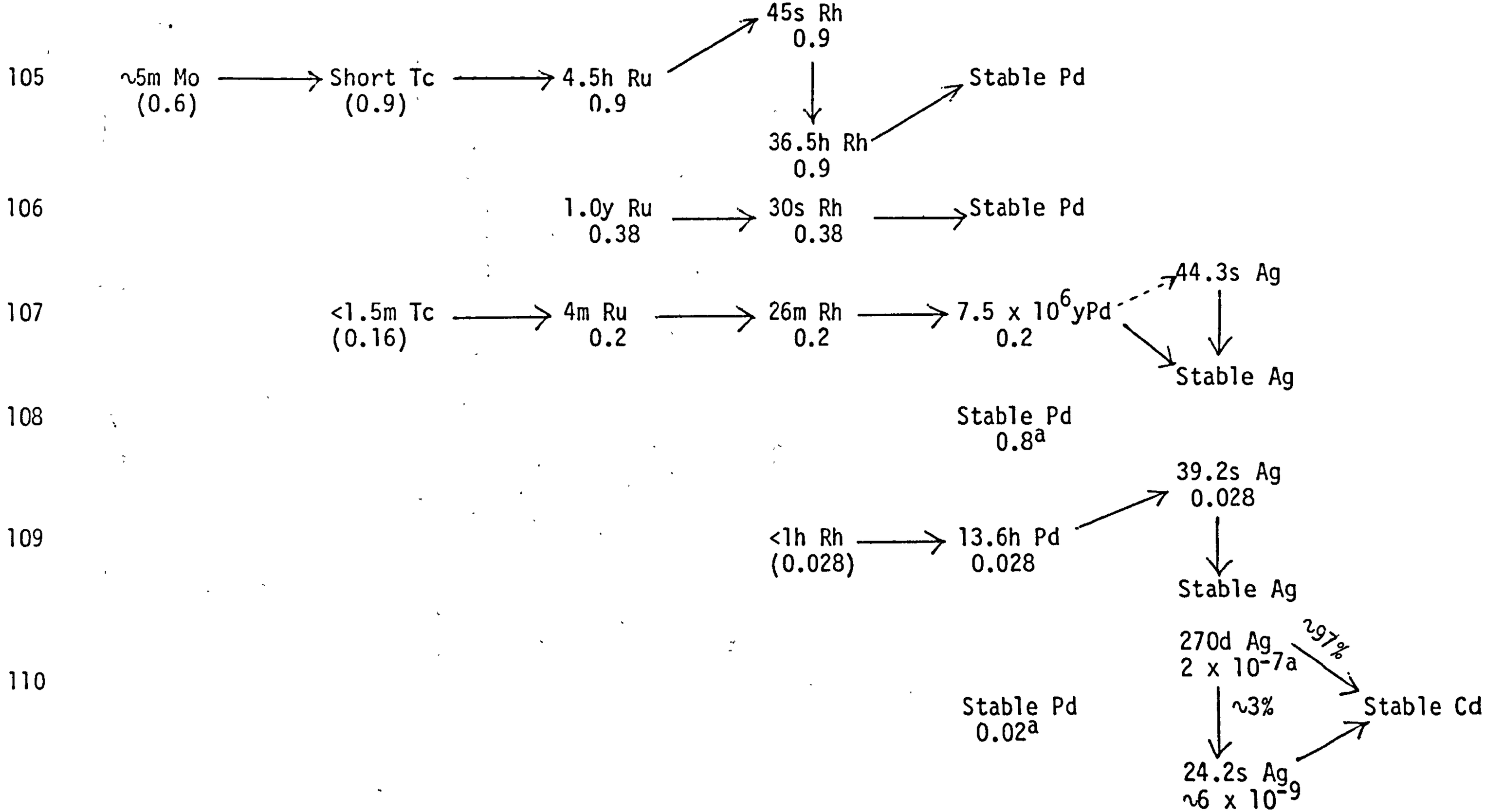

Table 1.4.2. Activity of Rhodium Isotopes (94)

	After Discharge	After 25 years
102m Rh	290μCi/g	1.7μCi/g
102 Rh	1900μCi/g	-
106 Ru	400μCi/g	12μCi/g

Table 1.4.3. Annual Availability of Fission Products Pd, Ru, Rh and Tc in (000) troy oz/yr (95)

	Pd	Rh	Ru	Tc
1970	0.77	0.51	2-3	0.93
1975	22-23	13-14	61-67	25-27
1980	55-75	30-42	145-201	57-70
1985	115-170	64-95	302-450	119-178
1990	214-328	110-176	524-801	204-311

9M, and under these conditions there is no significant formation of volatile RuO_4 (86). Finally, the active waste from the evaporator is transferred to underground stainless steel tanks for storage, prior to permanent disposal probably by incorporation into glass blocks, Figure 1.4.8.

Table 1.4.4. shows the typical composition of high level liquid waste derived from CAGR, LWR and Magnox fuels.

1.4.3. Radiolysis of the Aqueous and Organic Phases

Radiolysis of TBP gives rise to dibutyl phosphate (DBP, $(BuO)_2$ POOH), monobutyl phosphate (MBP, $BuOPO(OH)_2$ and butyl alcohol (97)). DBP and MBP form strong complexes with many of the fission products, and a synergistic effect between the diluent and degradation products has been noted (98). As the amount of DBP and MBP in the organic phase increases, the decontamination efficiency decreases, and losses of fissile material to the aqueous waste streams increases (84). It is therefore necessary to remove these degradation products, e.g. by successive washings with sodium carbonate, sodium hydroxide and dilute acid (99), before re-cycling the solvent.

The overall effect of radiation on nitric acid is to reduce nitrate ion to nitrite, and to liberate hydrogen and oxygen (100-102). Reduction in the hydrogen yield as the nitrate concentration is increased, is qualitatively explained by the reaction of nitrate ions with diffusing hydrogen atoms (30).

$$NO_3^- + H^\bullet \rightarrow NO_2 + OH^- \quad \text{.....1.6}$$

Figure 1.4.8. Concentration and Storage of Highly Active Liquid Waste (86)

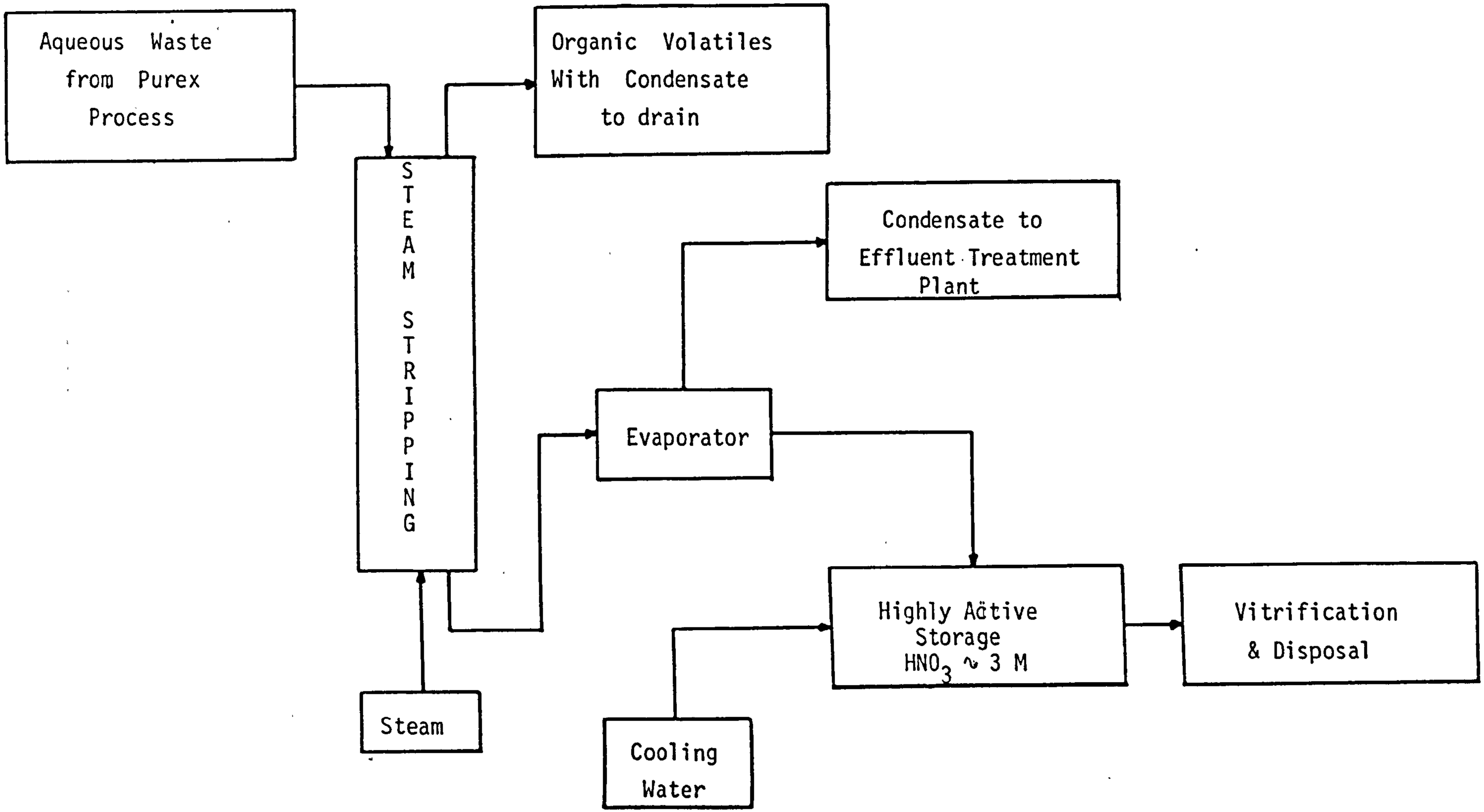

Table 1.4.4. Composition of high level liquid waste (96)

Type of fuel	CAGR	LWR	Magnox
Irradiation	20,000 MWd/te	22,000 MWd/te	3500 MWd/te
Element	g/te U	g/te U	g/te U
Ge	0.21	0.33	0.03
As	0.06	0.07	0.01
Se	26.68	29.35	4.68
Rb	217.79	239.37	39.40
Sr	626.79	689.44	110.30
Y	320.53	325.48	55.10
Zr	2407.78	2646.90	430.50
Mo	2141.00	2310.30	385.00
Tc	542.78	597.06	82.60
Ru	1180.99	1299.30	210.00
Rh	359.14	395.10	63.00
Pd	548.67	603.60	87.50
Ag	48.52	53.23	7.00
Cd	22.70	24.86	3.96
In	1.91	2.19	0.34
Sn	15.76	17.34	2.76
Sb	12.31	13.53	1.55
Te	298.27	328.10	50.80
Cs	1697.82	1867.70	299.30
Ba	729.40	802.30	140.00
La	796.10	875.60	152.30
Ce	1583.10	1741.60	329.90
Pr	742.80	817.20	146.10
Nd	2864.90	3151.50	500.50
Pm	206.00	226.60	40.90
Sm	625.70	668.10	87.50
Eu	31.67	34.82	5.90
Gd	24.98	27.50	3.85
Tb	0.63	0.68	0.11
Fe	1500.00	1500.00	600.00
Ni	330.00	330.00	90.00
Cr	330.00	330.00	120.00
U	2500.00	2500.00	15.00

1.4.4. Solvent Extraction Equipment

It is essential for reprocessing equipment to be highly reliable, have a high stage efficiency, short contact times, small liquid inventory, and be easy to decontaminate and service (103). In effect this means simple design and few, if any, moving parts. The simplest counter-current solvent extraction equipment is the packed column. This is simply a vertical column, filled with metal or ceramic rings that obstruct the flow of liquid through the column. The mixing in such columns is not vigorous, and the flow rates are low, hence a very tall column is required for efficient extraction.

The height of the column can be reduced if the column is "pulsed", so that the phases are drawn back and forth through perforated plates as they pass through the column. This provides good mixing, but phase separation is still poor.

An alternative to the columns is the mixer-settler. In this, the organic and aqueous phases are repeatedly mixed and separated in banks of from 12 to 24 horizontal stages, each consisting of a square mixing chamber at one end and a long settling tank at the other. Mixer-settlers provide good mixing and phase separation (~98%), but have rather large hold-ups.

Clean phase separation can be achieved using centrifugal contactors, which also provide good mixing and have very small hold-ups. Also

the organic/aqueous phase contact time can be made much shorter than in columns or mixer-settlers, with the advantage that damage due to radiolysis is minimised.

Schematic diagrams of the four types of contactors are shown in Figures 1.4.9. - 1.4.11. (104).

1.5. SEPARATION METHODS FOR RHODIUM

A large majority of the separation schemes reported for rhodium, have been developed with the aim of separating rhodium from iridium, prior to chemical analysis. These two elements are usually isolated simultaneously, and their separation from one another presents one of the most difficult aspects of platinum metal analysis. The preferred methods usually involve ion exchange and/or liquid-liquid extraction. Although numerous partition chromatographic methods have been reported, these procedures have not found wide applications in the analytical chemistry of the platinum group metals (105-111).

1.5.1. Ion Exchange

In hydrochloric acid solutions (>1M), rhodium forms stable anionic complexes which are not retained on strong acid cation exchangers, such as Dowex 50-X8. Cation exchangers have therefore been used to separate rhodium, together with platinum, palladium and iridium, from large amounts of metals such as copper, iron, nickel, lead, cobalt, rare earths, beryllium and sodium, which are strongly retained from dilute hydrochloric acid (109).

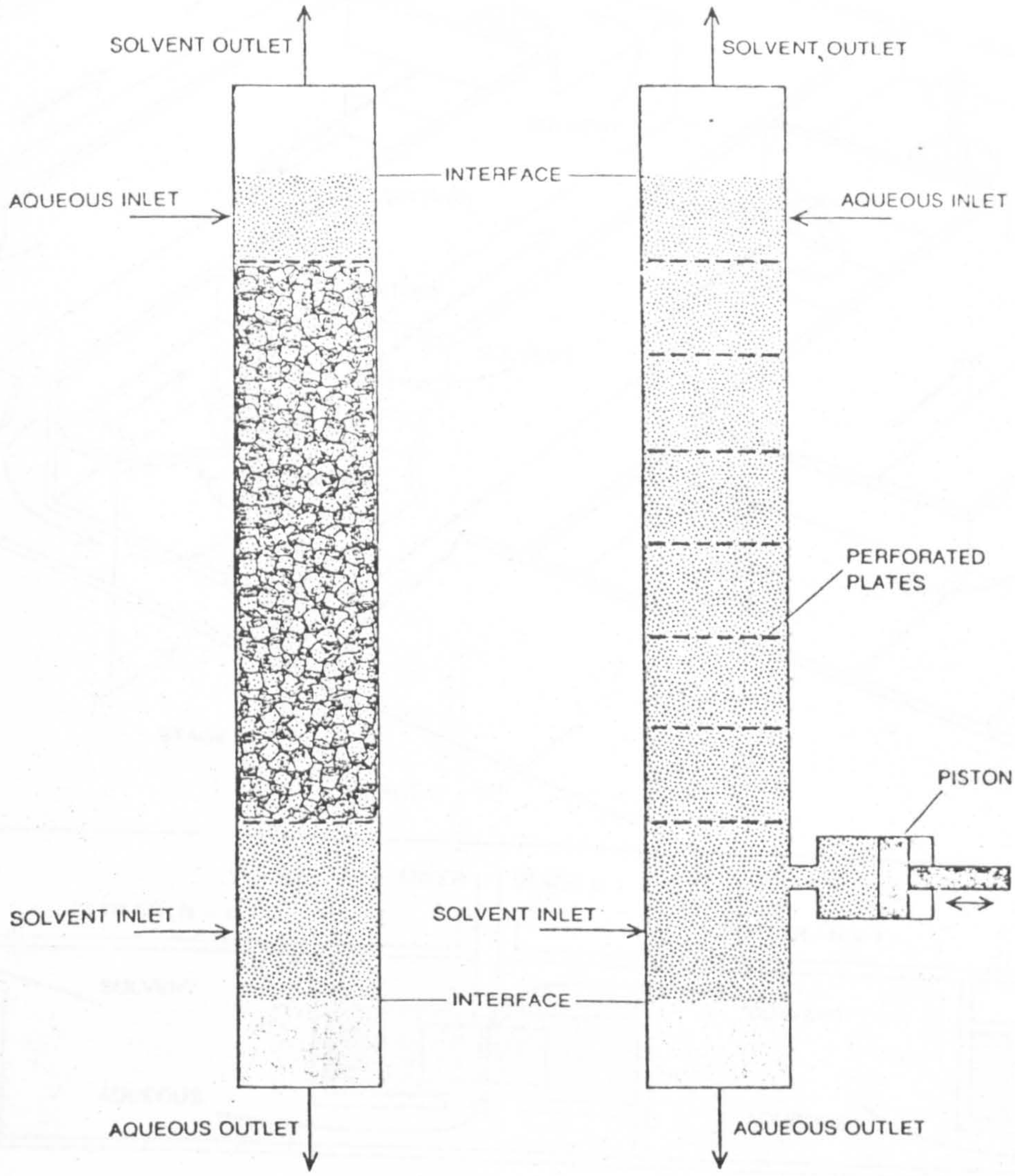

Figure 1.4.9. Packed and pulsed columns (104)

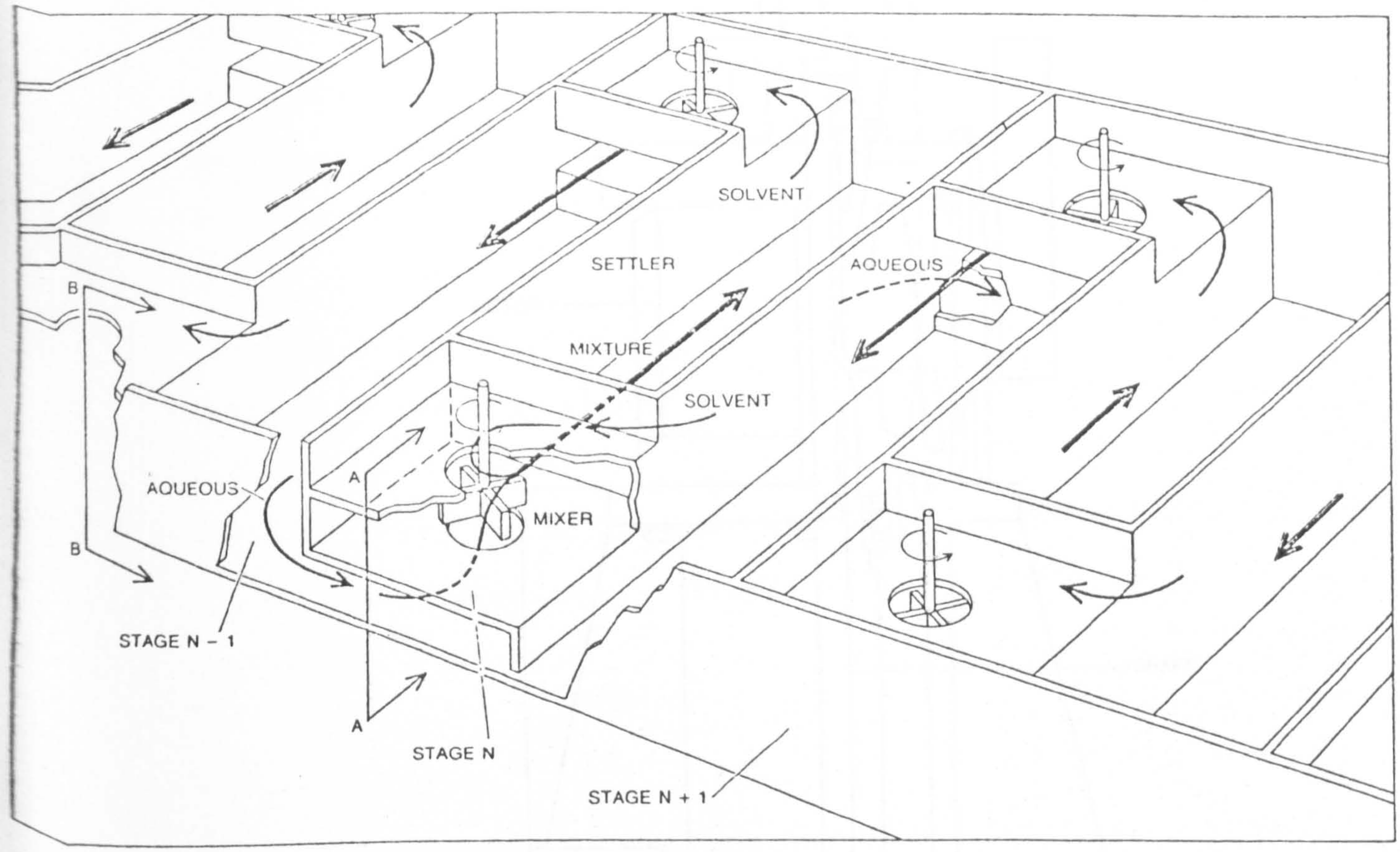

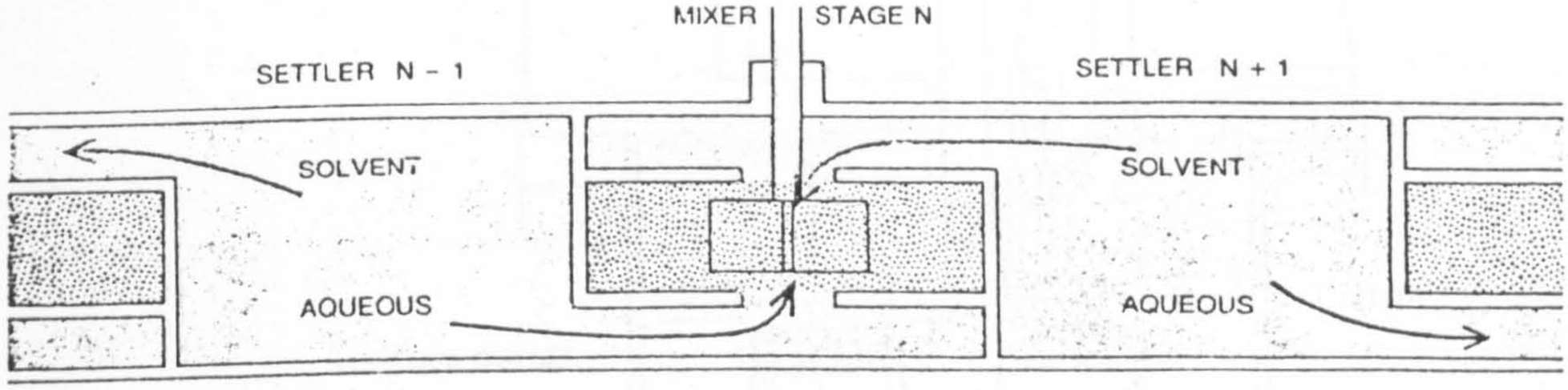

SECTION B–B

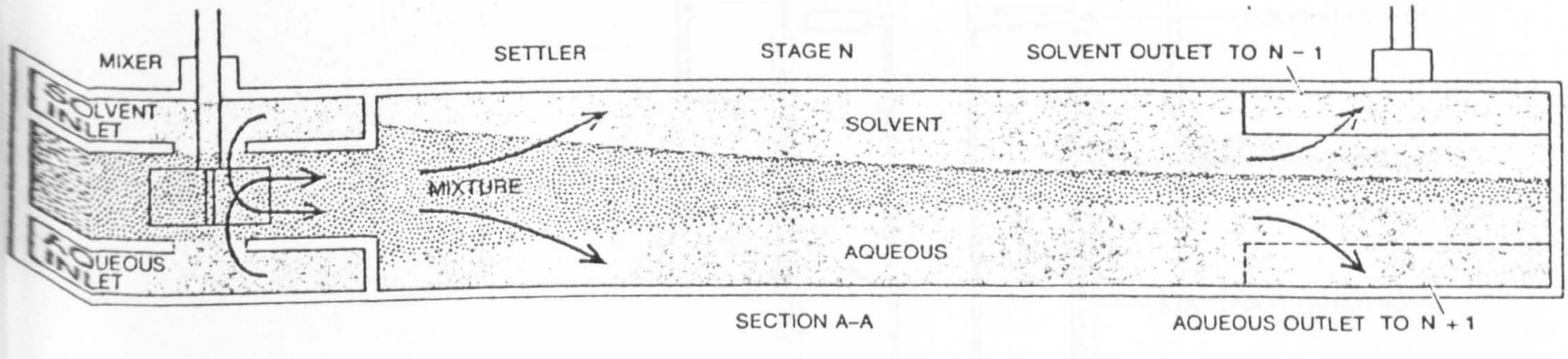

SECTION A–A

Figure 1.4.10. Mixer Settlers (104)

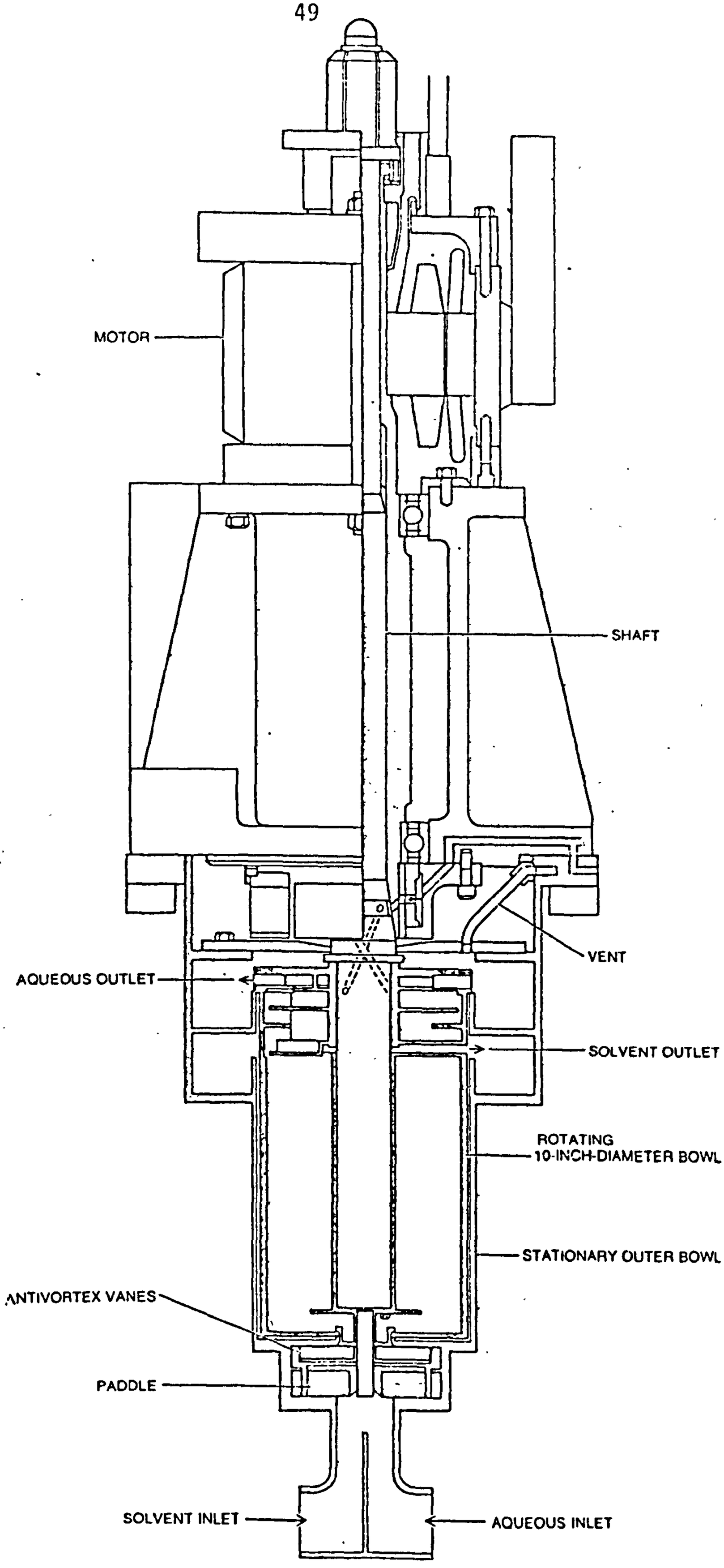

Figure 1.4.11. Centrifugal Contactor (104)

In dilute nitric, sulphuric and perchloric acids, cationic complexes are formed and these are retained on Dowex 50-X8 (16, 24, 35, 36). The absorption is relatively high from 0.1M acid ($D_{Rh(III)}$ = 80-100), but decreases rapidly with increasing acid concentration (76, 112, 113).

The anionic complexes of rhodium in hydrochloric acid are strongly retained on base anion exchange resins. However, with acid solutions greater than 6M, rhodium (III) and iridium (III) are easily eluted from the column. Hence, these two elements can be separated from the rest of the platinum group metals, which are retained on the resin (109).

1.5.2. Solvent Extraction

In solvent extraction processes the chemical form in which the element to be extracted exists in the aqueous phase is of great importance. From a practical point of view, the most important aqueous medium for rhodium is one which contains chloride ions (from the hydrochloric acid processing of platinum metal ores), and nitrate ions (as found in highly active liquid waste). In the former case the rhodium speciation is well known, and much of the solvent extraction work has been carried out from this media. By comparison, relatively little work has been done on the solvent extraction of rhodium from nitrate media.

The various extraction systems can be classified into four basic types, Table 1.5.1., depending on the type of extractant used (13, 114).

Table 1.5.1. Extractant Types

Extractant Type	Mechanism	State of Metal
Chelating agents e.g. Hydroxyoximes	Compound formation e.g. $M^{n+} + \overline{n(HR)} = \overline{(MR_n)} + nH^+$	Cationic
Acids, e.g. phosphoric and carboxylic	Compound formation	Cationic
Neutral donors e.g. TBP, ethers	Solvation, e.g. $MX_n + \overline{mS} = \overline{(MX_n mS)}$	Neutral Compound
Amines and Alkyl - ammonium salts e.g. Alamine 336	Ion-pair formation e.g. $\overline{(A^+X^-)} + M^- = \overline{(A^+M^-)} + X^-$	Anionic

5.2.1. Chelating Agents/Acids Table 1.5.2.

All the extractants listed in Table 1.5.2. have been used to isolate rhodium from the rest of the platinum metals prior to analysis. The exception is dinonylnaphthalene sulphonic acid, a liquid cation exchanger, which was suggested as an extractant for the rhodium (III) cationic species formed in dilute hydrochloric acid (123).

In all cases, strong heating is required to form the extractable complexes. In the case of 2-mercapto-4,5-dimethylthiazole, prior reduction of Rh(III) to Rh(II) by chromous or titanous ions, enables the extractable species to form at room temperature (120).

5.2.2. Neutral Donors. Table 1.5.3.

Rhodium is not extracted from hydrochloric acid by solvents such as diethyl ether, methyl isobutyl ketone (MIBK) or ethyl acetate. However, in the presence of stannous chloride, it is possible to form extractable platinum metal group complexes, and so isolate them from iron, copper and many other metal ions (109).

Extraction of rhodium in hydrochloric acid by TBP is negligible (127, 128, 130-132). Diheptyl and dioctyl sulphoxides, however show good extraction from 5M HCl (129), probably according to:

$$3H^+ + RhCl_6^{3-} + \overline{mR_2SO} = \overline{H_3RhCl_6.mR_2SO} \quad \text{.....1.7.}$$

These results, taken together with those of chelating agents, show that rhodium (III) forms extractable complexes with reagents containing

sulphur, rather than oxygen or nitrogen donors. This is in keeping with the classification of Arhland, Chatt and Davies (147), who class rhodium as a soft or class b acceptor (11, 148).

1.5.2.3. Amines/Quarternary Ammonium Salts - Table 1.5.4.

Lunichkina and Renard (146) have reported the extraction of rhodium (III), by di-isoamyl methylphosphonate (DAMP) and tri-n-octylamine (TOA), from nitrate solutions. Distribution ratios are low (<0.2) in the region 0.1-1M HNO_3. However, by employing aluminium and ammonium nitrates (1-2M), as salting-out agents, the distribution ratio can be increased to ~1.4 at 0.8M HNO_3. Ignoring the co-extraction of water, the authors proposed the following extraction mechanism:

$$Rh^{3+} + 3NO_3^- + \overline{n(DAMP)} = \overline{Rh(NO_3)_3.(DAMP)_n} \quad \text{.....1.8.}$$

and $$Rh^{3+} + 3NO_3^- + \overline{n(TOA.HNO_3)} = \overline{Rh(NO_3)_3.(TOA.HNO_3)_n} \quad \text{.....1.9.}$$

where n = 2-3.

Extraction by aliphatic amines is negligible from 1-12M HCl. At acid concentration less than 0.05M HCl, 100% extraction can be achieved, and a process employing a primary amine in kerosene diluent has been described (103). The addition of stannous chloride to the aqueous phase ensures quantitative extraction of rhodium by tri-n-octylamine (75). Octylaniline in di-isobutyl ketone (DIBK) shows more than 80% extraction of rhodium from 2-12M HCl (144).

Pohlandt (144) also reports 20% maximum extraction of rhodium by octylaniline/DIBK from 2-14M HNO_3. The rhodium solutions were prepared by dissolving rhodium (III) trichloride in nitric acid. It

Table 1.5.2. Chelating Agents/Acids

	Aqueous phase	Organic phase	Remarks	Ref.
1.	pH8 (chloride)	Diethyl dithiocarbonate /4-methyl-2-pentanone	Quantitative	115
2.	pH5.1 (chloride)	1-(2-Pyridylazo)-2-naphthol/$CHCl_3$	Quantitative	116
3.	Acetic acid-sodium acetate buffer	2-Thenoyltrifluoroacetone /Benzene	Quantitative	117
4.	pH 4-6.4	Oxime/propanol,chloroform or benzene	Quantitative	70,118
5.	3-9M HCl	2-mercapto-4,5-dimethyl-thiazole/$CHCl_3$	Quantitative	119,120
6.	Dilute HCl	2-mercapto benzimidazole/ butanol	Quantitative	109
7.	4-6M HCl	2-mercaptobenzothiazole/ $CHCl_3$	Quantitative	121
8.	1-2M HCl, $SnCl_2$	Diphenylthiourea/$CHCl_3$	Quantitative	122
9.	0.1M HCl	Dinonylnaphthalene-sulphonic acid/heptane	D_{Rh} = 50	123
10.	pH 8-11	Sodium diethyl dithio-carbonate/$CHCl_3$	Quantitative	124
11.	pH 5-8	8-hydroxy-2,4-di-methyl quinazoline	Quantitative	126

Table 1.5.3. Neutral Donors

	Aqueous phase	Organic phase	Remarks	Ref.
1.	Alkaline	Pyridine	Quantitative	80
2.	12 M HCl	TBP/benzene	1% extracted	126
3.	3-7M HCl	1:1 TBP/hexane	Not extracted	127,128
4.	0.1-8M HCl	Diheptylsulphoxide/ Trichloroethane	60% at 5.7M HCl	129
5.	0.1-8M HCl	Dioctylsulphoxide/ Trichloroethane	70% at 5M HCl	129
6.	0.1-8M HCl	Di-p-tolylsulphoxide Diheptylsulphide, Di-octyl sulphide	Not extracted	129
7.	5-9M HCl/NaCl	TBP	D_{Rh} = 0.03	130,131
8.	HCl	TBP	<3% extracted	132
9.	$SnBr_2/HClO_4$-HBr	Isopentyl alcohol	Quantitative	133
10.	3-4M HCl	Pyridine-thiocyanate/ MIBK	Quantitative	134,135
11.	Br^-/HBr	Amyl acetate, MIBK or TBP	$^{max}D_{Rh}$ = 2	136
12.	HCl	Thiocyanate/TBP	$^{max}D_{Rh}$ = 0.19	137
13.	Iodide complexes	TBP	Not extracted	127
14.	HCl or HNO_3	TOPO	Not extracted	138
15.	HCl	HDEHP	Not extracted	138
16.	HCl, H_2SO_4 or HNO_3	Quarternary ammonium salts/MIBK	Not extracted	139

Table 1.5.4. Amines/Quarternary Ammonium Salts

	Aqueous phase	Organic phase	Remarks.	Ref.
1.	6M HCl	Trioctylamine/benzene	Not extracted	140
2.	0.1-0.5M H_2SO_4	Aliphatic amines/decane	89% max.	141
3.	0.1-9M HCl	Dioctylacetamide/$CHCl_3$	D_{Rh} = 2.7 at 0.1M HCl	142
4.	0.1-12M HCl	Trioctylammonium chloride/benzene	D_{Rh} = 3 at 0.1M HCl	143
5.	7-12M HCl/$SnCl_2$	Trioctylamine/benzene	Quantitative	75
6.	$RhCl_3/H_2SO_4$	Octylaniline/DIBK	20% at 1M H_2SO_4	144
7.	$RhCl_3$/HCl	Octylaniline/DIBK	>80% from 2-12M HCl	144
8.	$RhCl_3/HNO_3$	Octylaniline/DIBK	<20% from 2-14M HNO_3	144
9.	1-8M HCl	Tetraoctylammonium chloride/dichloroethane and nitrobenzone	$^{max}D_{Rh}$ = 6	145
10.	HCl	Tri-isobutylamine/$CHCl_3$	Not extracted	138
11.	HCl	Primary amine/isononyl alcohol-kerosene	100% at 0.05M HCl	103
12.	0.1-1M HNO_3/ 1.7M $Al(NO_3)_3$-1M NH_4NO_3	Di-isoamyl methylphosphonate or tri-n-octyl amine	$^{Rh}D_{max}$ = 1.4 at 0.7M HNO_3	146

is quite likely that the chloride complexes of rhodium (III) would still be present in solutions prepared in this manner.

Like the rhodium (III) chloride complexes, rhodium (III) sulphate complexes are also extracted by aliphatic amines from dilute acid solutions (141). Orlov et.al. (141) suggested the following general extraction reaction, (R = alkyl NH_2):

$$Rh_2O(SO_4)_7^{10-} + \overline{m(RH)_2SO_4} = \overline{(RH)_{10}\ Rh_2O(SO_4)_7 . n(RH)_2SO_4} + 5SO_4^{2-} \quad ....1.10.$$

1.3.3. Isolation of Rhodium From Fission Products

The typical composition of dissolver solids from a reprocessing plant is not well defined, but the principal constituents are apparently ruthenium, rhodium and silica (149, 150).

Others have shown that the dissolution of mixed-oxide fuels in 6.5M HNO_3, gives rise to solids which have the same compositions as the metallic inclusions. These metallic inclusions are composed of Mo-Ru-Tc-Rh-Pd alloy with composition nearly proportional to their fission yields (151, 152).

Oak Ridge National Laboratory (ORNL) data however, indicate that a large fraction (40-80%) of ruthenium, and probably rhodium, remains with the solids, while the bulk of palladium and technetium are dissolved (153).

Smith and McDuffie (154) report a typical solids composition of 10-20% molybdenum, 2-20% technetium, 30-50% ruthenium, 2-10% rhodium and about 10% palladium for fast reactor fuel elements. Separation of

ruthenium/rhodium and palladium is accomplished by liquid-liquid partition, between immisible liquid metals. The residues from the dissolution step are treated with molten magnesium, in which ruthenium, rhodium and palladium are expected to be soluble. The magnesium solution is then contacted with molten uranium-chromium eutectic at 950^{o}C to extract the ruthenium. After allowing the uranium eutectic-ruthenium phase to freeze, it is stored for a period of time to allow $^{106}Ru \rightarrow {}^{106}Pd$, and $^{103}Ru \rightarrow {}^{103}Rh$ decays to occur. The ^{106}Pd and ^{103}Rh so formed are re-extracted with molten magnesium, and recovered by conventional methods.

For treating Purex waste, Moore (155) suggested contacting the acidic waste with a series of carbon beds, each of which had absorbed on it a different chelating agent, specific for the metals to be recovered. After removal of palladium and technetium on carbon beds absorbed with dimethylglyoxime (DMG) and diacetyl dithiol (DAD) the rhodium and ruthenium are removed by phenyl thiourea (PTU) on the final carbon bed. The flowsheet for this process is shown in Figure 1.5.1.

Panesko (156-158) showed that anion exchangers will absorb rhodium from neutral aqueous nitrate solutions. Elution of this absorbed rhodium with 10M nitric acid formed a precipitate which would not dissolve in acid or base, and could only be solubilised after fusion with sodium bisulphate. The precipitate was thought to be Rh_2O_3, and the final process that he described is shown in Figure 1.5.2.

Figure 1.5.1. Recovery of fission product Tc, Pd, Rh and Ru (155)

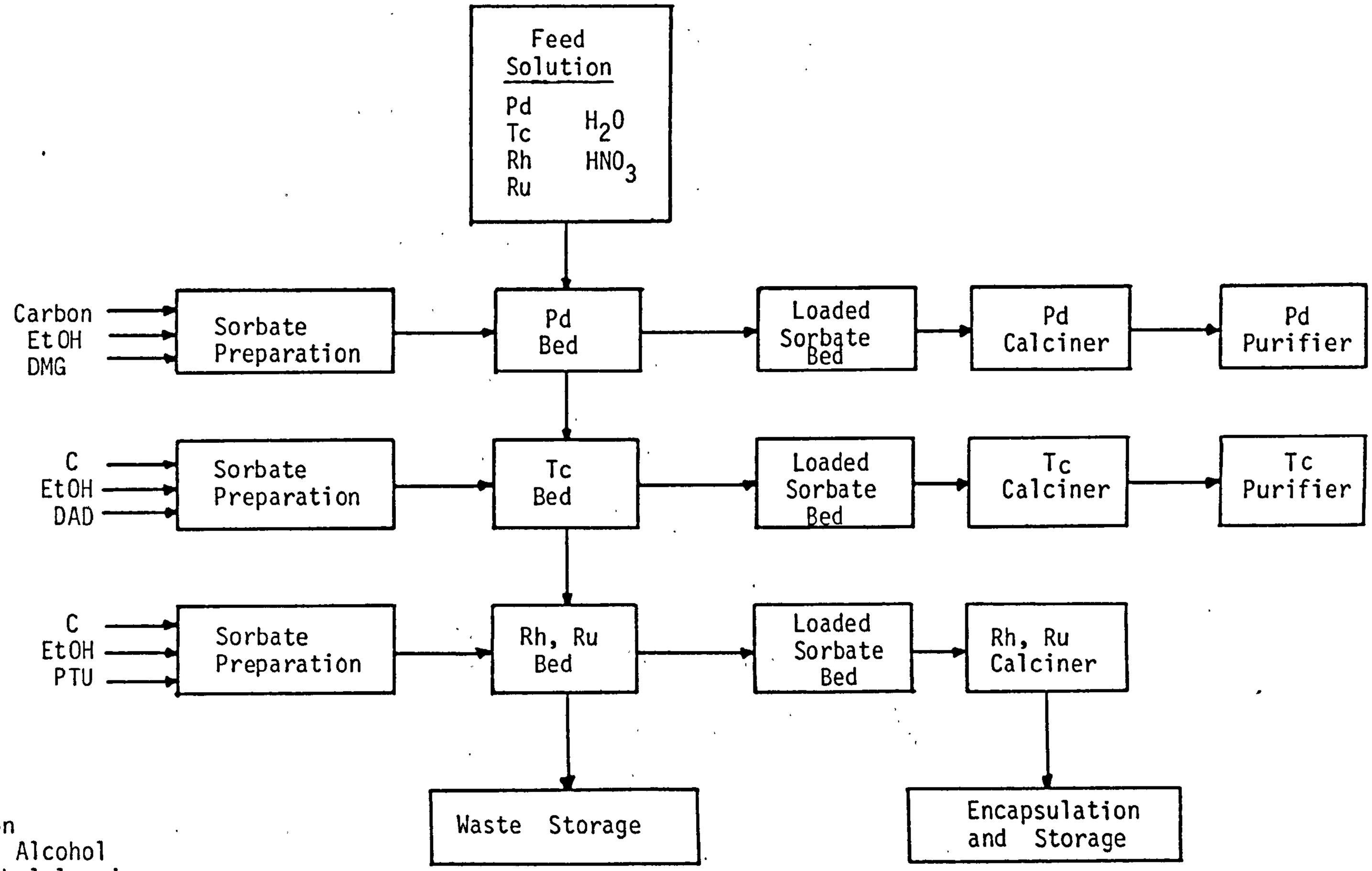

Legend:

C = Carbon
EtOH = Ethyl Alcohol
DMG = Dimethylglyoxime
DAD = Diacetyldithiol
PTU = Phenylthiourea

Figure 1.5.2. Process for Rhodium Purification (156-158)

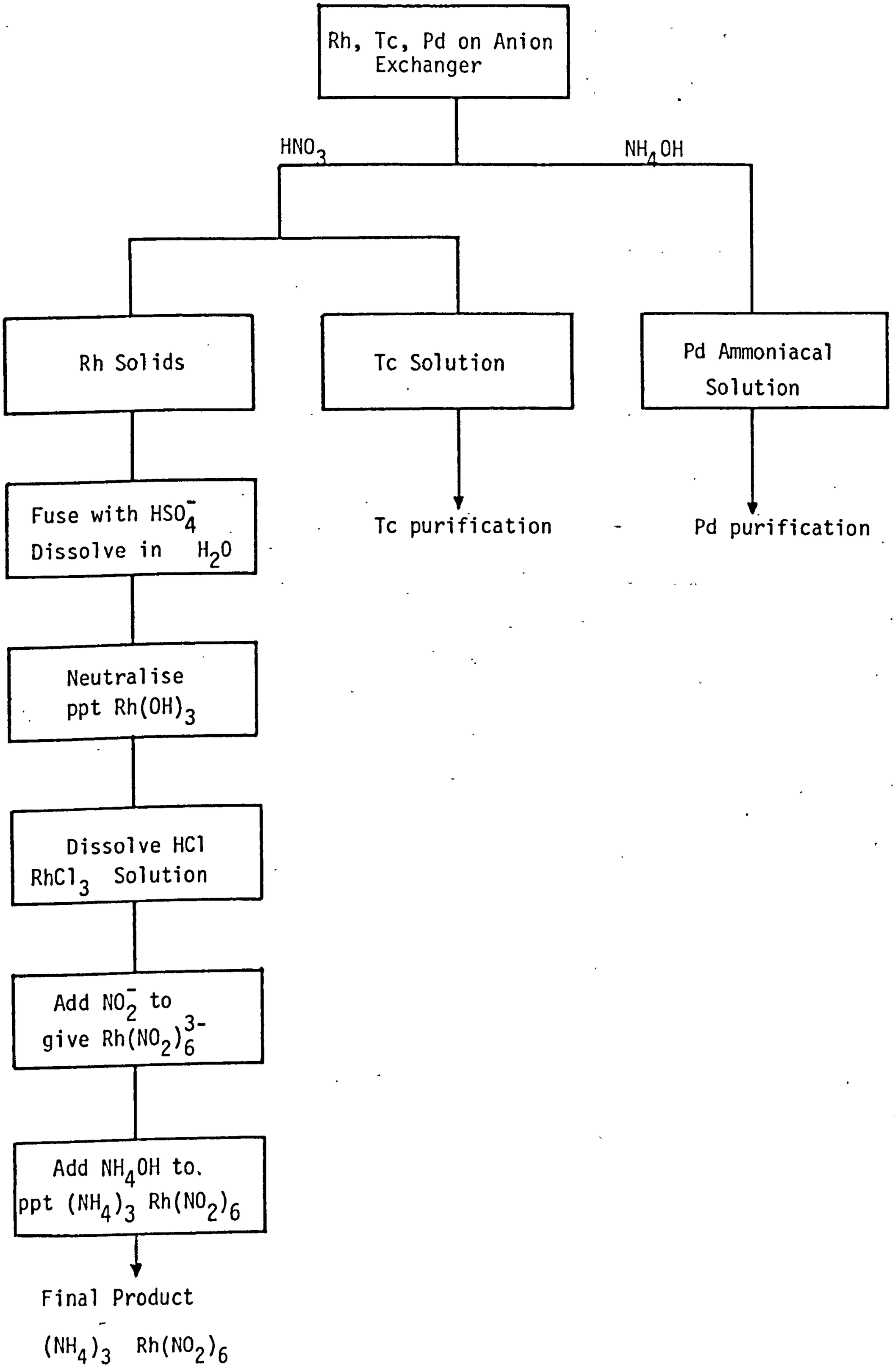

Figure 1.5.3. Process for Rhodium Recovery (153)

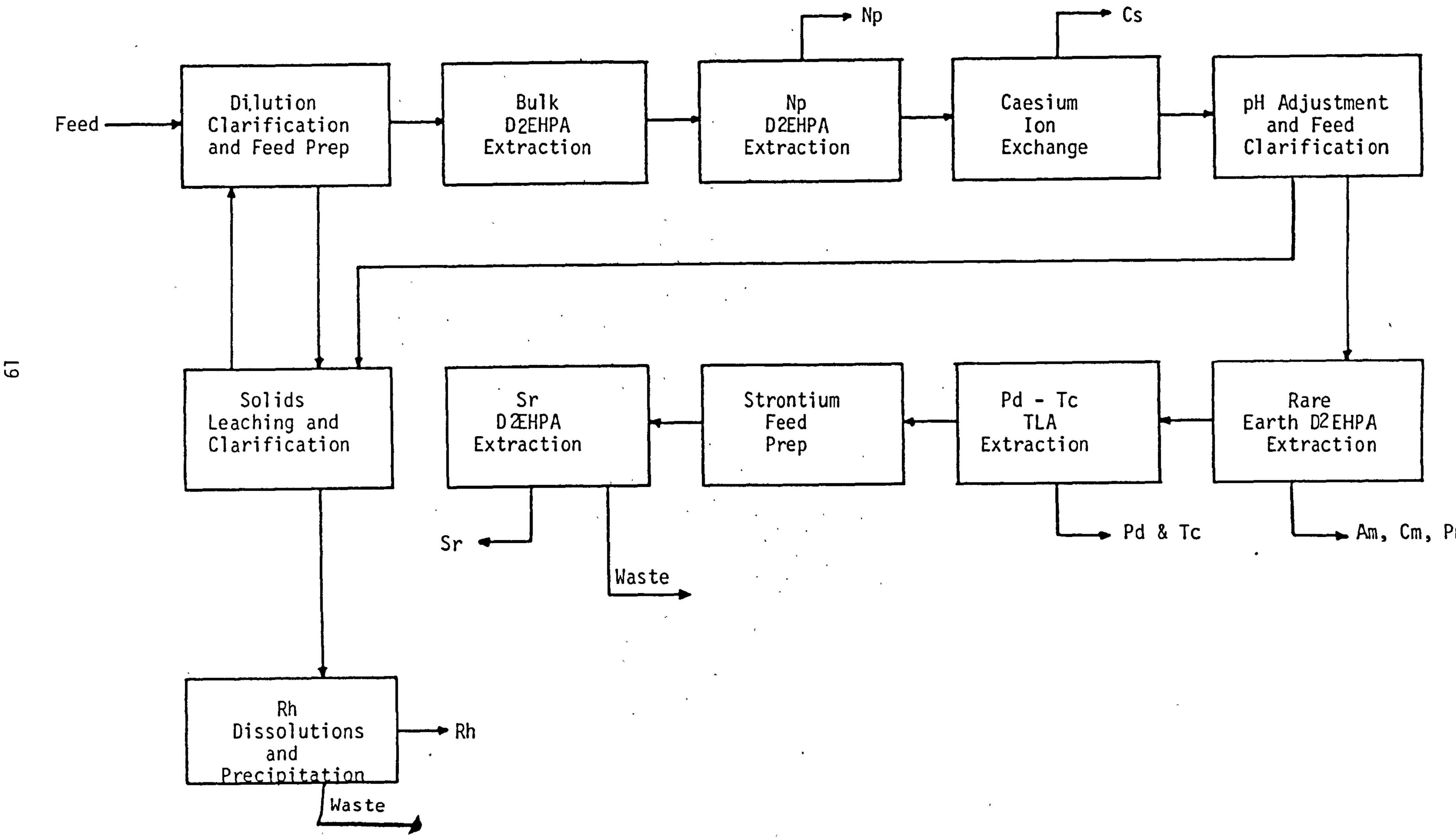

Exxon (153) concluded that the best method of rhodium purification from fission product waste was essentially to extract all the other elements, until pure rhodium was left, Figure 1.5.3.

1.6. THE AIMS OF THIS RESEARCH

The above review has shown that the rhodium speciation in nitric acid is not clearly defined. The continuing importance of rhodium as a precious metal, taken together with the fact that in high level waste the rhodium is present mainly in the inactive form, are sufficient reasons for further studies on its recovery.

It is the aim of this research to:

a) Identify the rhodium speciation in nitric acid, and

b) To investigate the recovery of rhodium by solvent extraction processes.

CHAPTER TWO

RHODIUM SPECIATION IN NITRIC ACID

2.1. FOREWORD

There are conflicting reports in the literature on the rhodium speciation in nitric acid (16, 24, 25, 35, 36). Previous studies were carried out in dilute nitric acid solution (0.1 - 1 M HNO_3), with the major species believed to be the hexaaquo ion, $\{Rh(H_2O)_6\}^{3+}$ or the pentaaquonitrato rhodium (III) ion, $\{Rh(H_2O)_5NO_3\}^{2+}$ (25, 36). Shubochkin et.al. (27) prepared potassium hexanitratorhodate (III), $K_3\{Rh(NO_3)_6\}$, and showed it to contain unidentate coordinated nitrato-groups. They did not, however, show whether or not nitric acid solutions of $K_3\{Rh(NO_3)_6\}$ contained nitratorhodium (III) species of the type $\{Rh(H_2O)_{6-n}(NO_3)_n\}^{(3-n)+}$.

In this chapter, results using such techniques as electrophoresis, electronic absorption measurements, ion-exchange chromatography, ^{103}Rh nuclear magnetic resonance (NMR) spectroscopy and polarography are presented, and their implications to rhodium speciation in nitric acid discussed.

2.2. ELECTROPHORESIS

In electrophoresis, separation depends on the differences in the electrical properties of the components in a mixture. A sample of the solution under investigation is placed at the centre of a strip of filter paper which has been previously moistened with a suitable electrolyte. The ends of the filter paper are then connected to a

high voltage DC source for a predetermined period of time. Any substance that bears an electrical charge will migrate along the paper, the direction and rate being governed by the sign and magnitude of the charge on the ion and the mobility of the ion. The technique is especially useful in separating ionic compounds (159).

Solutions of rhodium in nitric acid were prepared by two methods:

(a) Rhodium (III) sesquioxide, $Rh_2O_3.5H_2O$ was dissolved in the minimum quantity of concentrated nitric acid, evaporated to dryness and the residue dissolved in the required strength acid. The solution was then boiled for ten minutes, cooled and made up to a standard volume before being used (section 5.5.2.).

(b) Commercially available "rhodium (III) nitrate" (Fluka $Rh(NO_3)_3.2H_2O$) was dissolved in the required strength acid without heating.

Solutions of rhodium in nitric acid concentrations of 0.1, 0.5 and 1M, when subjected to electrophoresis (electrolyte 0.1M HNO_3/0.02M $NaNO_3$, see section 5.6.2.) produced a single,well defined,cationic band. No anionic bands were observed and no second cationic band, as observed previously by Lederer (24), was found. The electrophoretograms are illustrated in Figure 2.2.1a. There were no significant differences in the distance moved by rhodium bands produced from commercially available "rhodium (III) nitrate" and those produced from rhodium (III) sesquioxide.

To determine whether the cationic bands could be further resolved, these rhodium solutions were spotted closer to the anode and the electrophoretogram

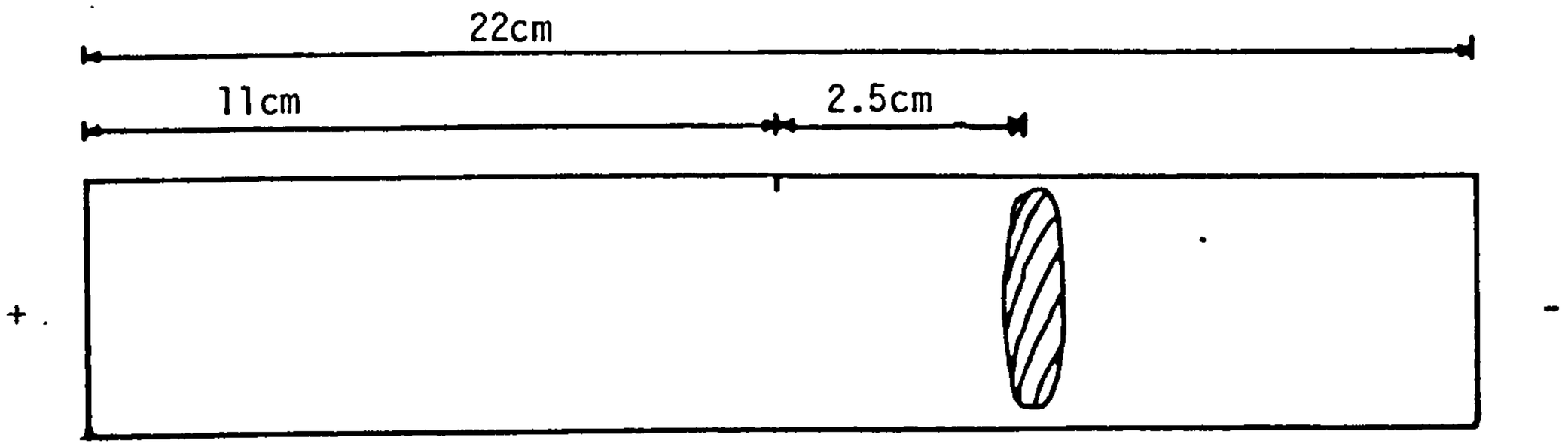

Figure 2.2.1a. Electrophoretogram of rhodium (III) sesquioxide in 0.1M HNO_3.
Electrolyte - 0.1M HNO_3/0.02M $NaNO_3$.
Potential 200±10V, Current 60mA, Time 1hr.

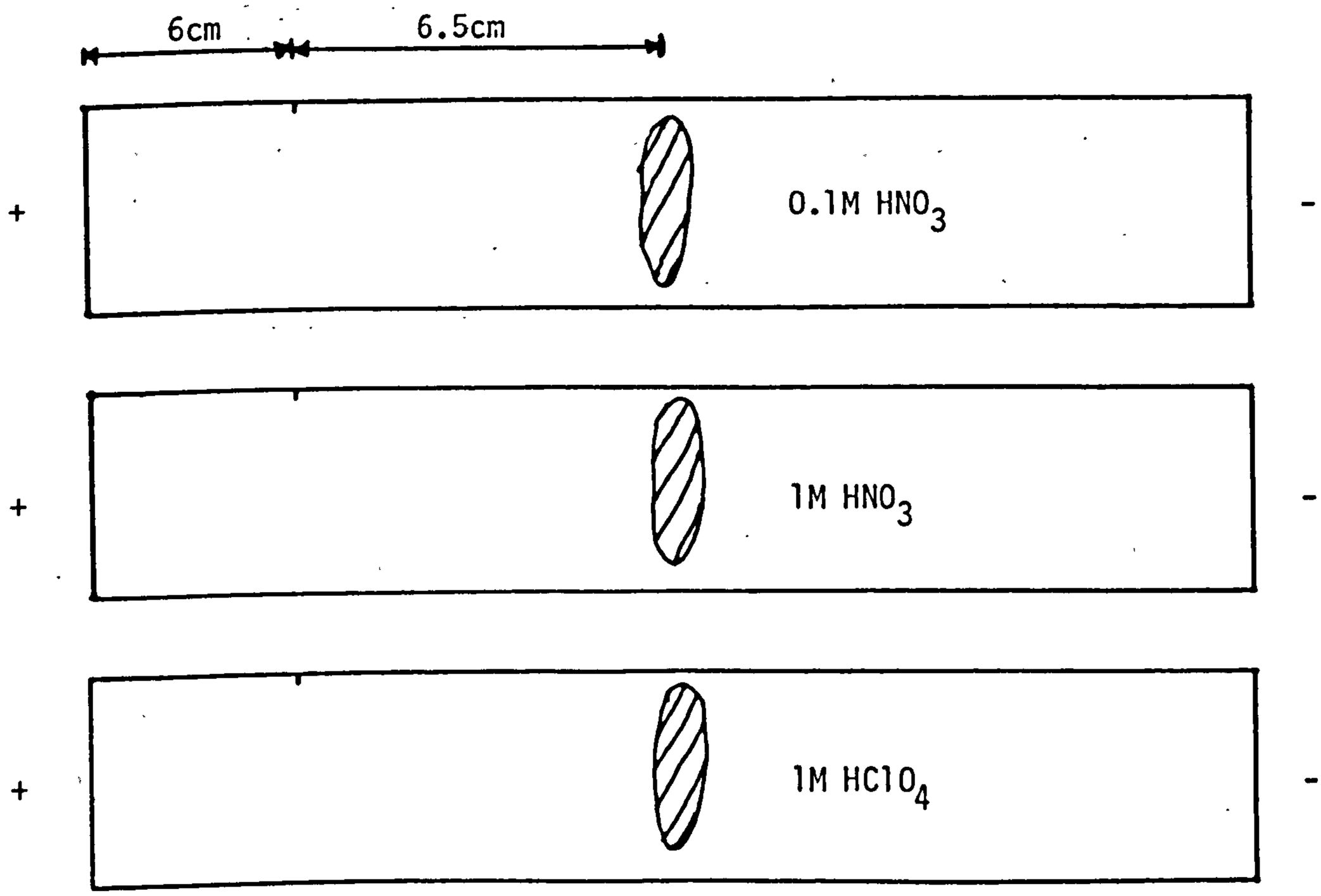

Figure 2.2.1b. Electrophoretogram of rhodium (III) sesquioxide in nitric and perchloric acids.
Electrolyte - 0.1M HNO_3/0.9 $NaNO_3$.
Potential 250±10V, Current 60mA, Time 2hrs.

running time was increased from 1 hour to 2 hours, using 0.1M HNO_3/0.9M $NaNO_3$ as electrolyte. Again only a single cationic band was observed, Figure 2.2.1b.

Solutions of rhodium (III)sesquioxide in 1 to 10M nitric acid prepared by method (a), also gave a single cationic band. There was no observable difference in electrophoresis between freshly prepared rhodium (III) containing solutions, and those which had been aged for 3 weeks and 84 weeks.

A solution of the hexaaquo rhodium (III) ion, $\{Rh(H_2O)_6\}^{3+}$ was prepared by dissolving rhodium (III) sesquioxide in concentrated perchloric acid (section 5.5.1.). Electrophoresis of this solution, run at the same time as those of rhodium containing solutions prepared by method (a), gave a single cationic band. In all cases, the cationic band moved the same distance towards the cathode, Figure 2.2.1b.

These results indicate that in 0.1-10M nitric acid there is a single cationic species, which is probably the aquated rhodium (III) cation, $\{Rh(H_2O)_6\}^{3+}$.

Lederer (24) prepared his rhodium solutions, using rhodium (III) sesquioxide which had been precipitated only once from an aqueous chloride solution. Under these conditions it is possible that some chloride ions would be entrained with the rhodium (III) sesquioxide precipitate, and if these were not thoroughly washed off, would give rise to traces of various rhodium (III) chloro complexes in aqueous solution, which could be separated from $\{Rh(H_2O)_6\}^{3+}$ by electrophoresis.

2.3. ELECTRONIC ABSORPTION MEASUREMENTS

The absorption spectrum of the hexaaquo rhodium (III) ion has previously been reported by a number of workers (15, 17, 20, 25, 34). This cation is readily prepared by dissolving rhodium (III) sesquioxide in perchloric acid (section 5.5.1.). The electronic absorption spectra of solutions of this cation have two absorption bands. The first ($^1A_{1g} \rightarrow {}^1T_{1g}$, see Figure 1.2.1.) at 400nm (ε 47-62) and the second ($^1A_{1g} \rightarrow {}^1T_{2g}$) at 310nm (ε = 55 - 69). The absorption spectrum of the hexaaquo rhodium (III) ion is reproduced in Figure 2.3.1., and shows the characteristic bands at 400nm (ε = 65) and 315nm (ε = 68).

The electronic absorption spectra of solutions of rhodium (III) sesquioxide in nitric acid (section 5.5.2.), shows a single band at 400nm. The molar absorptivity of this band varied from 80-90, depending on the nitric acid concentration, Figure 2.3.1. This variation is a consequence of the increase in base line, due to the absorbance by increasing concentrations of nitric acid. The second band, which should appear at 310nm for the hexaaquo rhodium (III) ion is obscured by the band due to the absorbance of nitric acid, which has maxima at 303nm and 194nm (30, 37).

Potassium hexanitratorhodate (III), $K_3\{Rh(NO_3)_6\}$ was prepared according to the method of Shubochkin et.al. (27, 28) (section 3.5.2.). A freshly prepared solution of this compound in nitric acid should contain significant quantities of rhodium (III) nitrate species of the type $\{Rh(H_2O)_{6-n}(NO_3)_n\}^{(3-n)+}$, if they exist. The electronic absorption spectrum of such a solution would be expected to show absorption bands due to the nitrate complexes in addition to the hexaaquo rhodium (III)

Figure 2.3.1. Electronic Absorptions of Rhodium (III) Sesquioxide in nitric and perchloric acids.

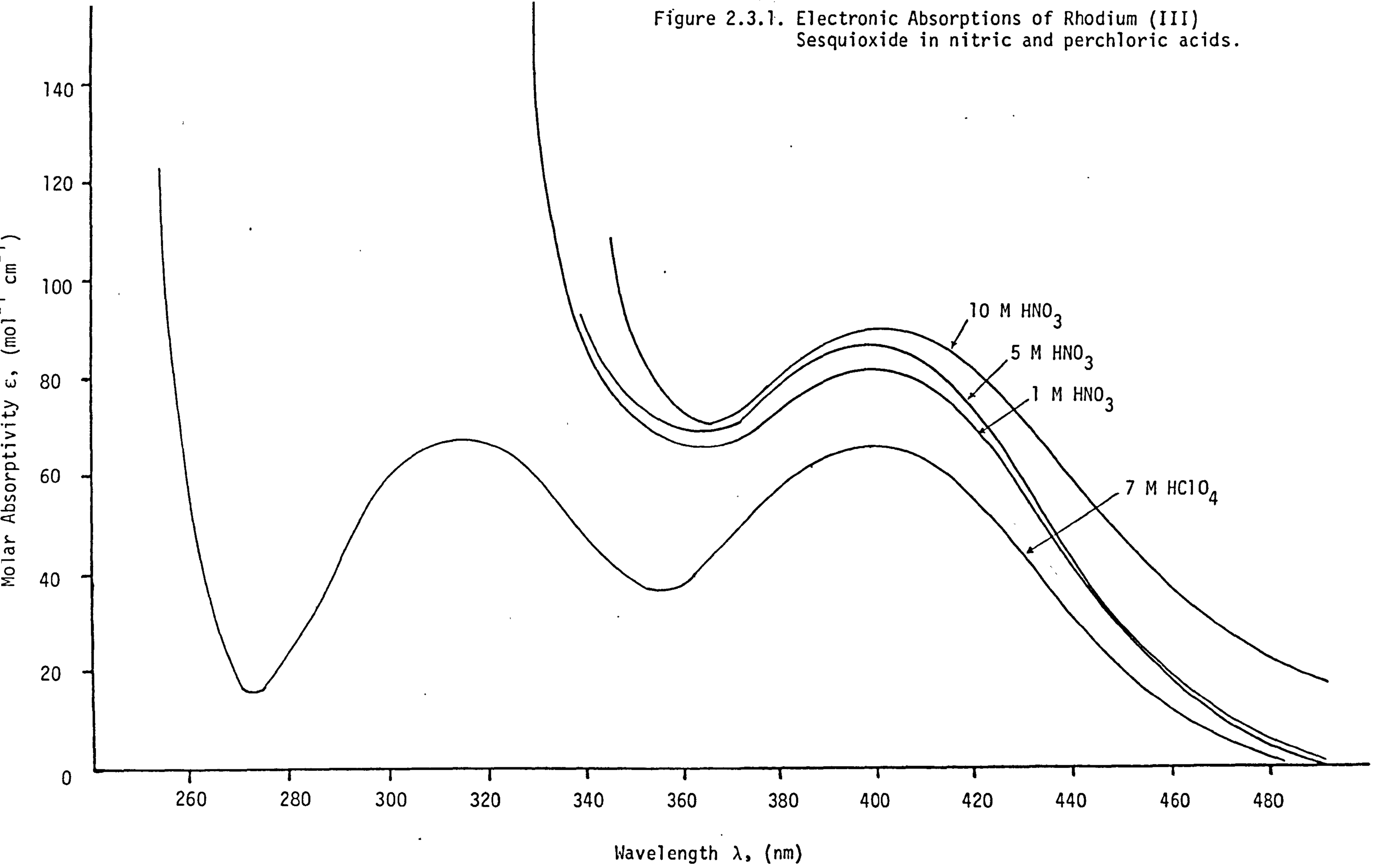

Figure 2.3.2. Electronic absorption of $K_3\{Rh(NO_3)_6\}$
in 0.1M nitric acid.

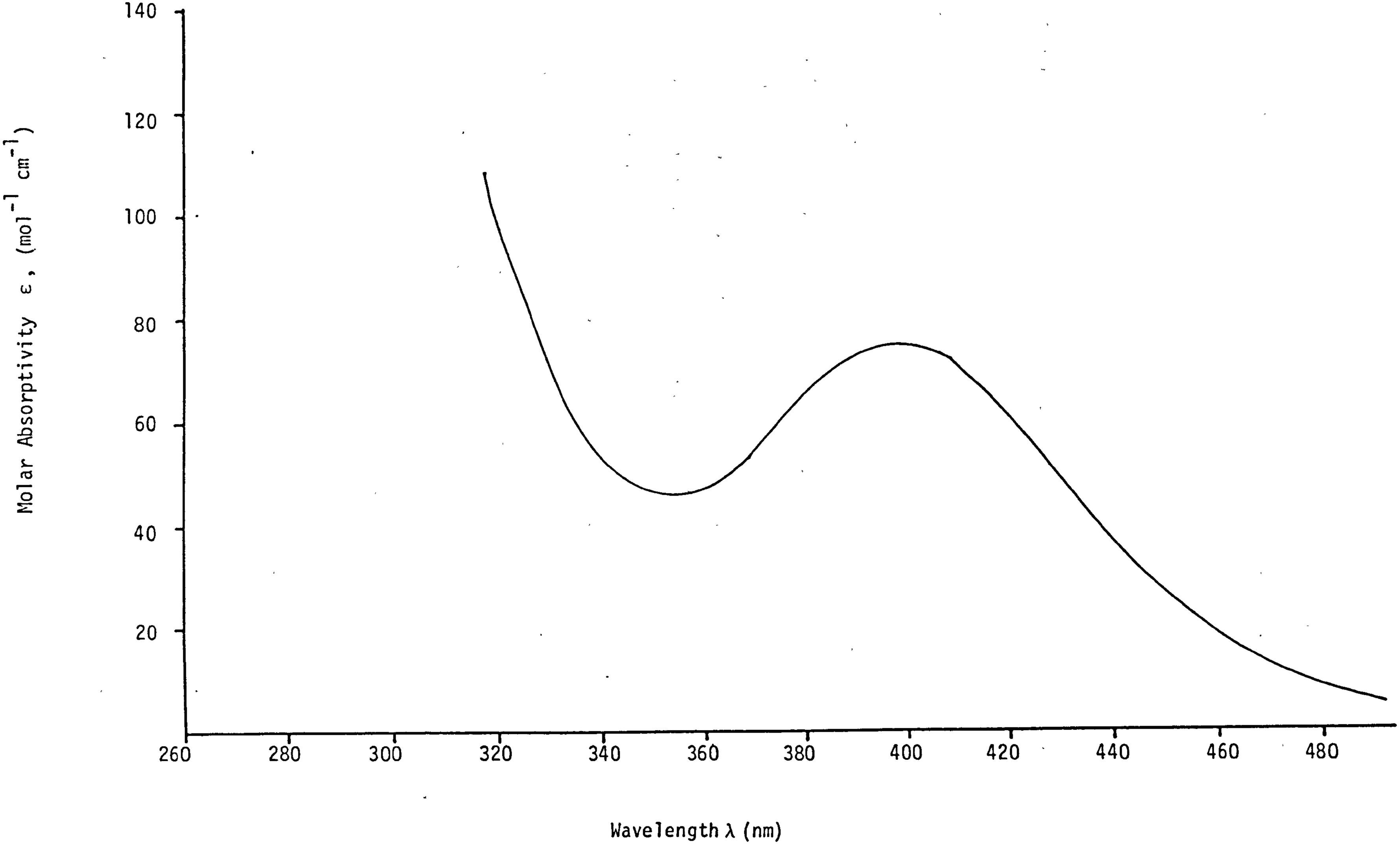

band at 400nm. In fact, as Figure 2.3.2. shows, only a single absorption band with λ_{max} = 400nm is observed, indicating the presence of one species in solution, i.e. $\{Rh(H_2O)_6\}^{3+}$.

2.4. ION EXCHANGE EXPERIMENTS

2.4.1. Determination of Charge per Metal Atom

Aqueous solutions in which metal ions form several complexes, and which do not equilibrate rapidly are particularly suitable for investigations using an ion exchange method developed by Connick and Cady (160). The method is based on the fixed exchange capacity of the cation resin, Dowex 50W - X8, in its hydrogen form, measured in equivalents of charge. The various rhodium complex species are absorbed onto the resin and then eluted with another metal ion whose charge is known. In this work a solution of the thorium ion (+4) in its perchlorate form is used. During the course of elution, the various rhodium complex species are separated into distinct bands. These bands are eluted from the column, collected, and analysed for rhodium and free hydrogen ion concentration. Since the value of the charge exchanged on the resin must be the same, it follows that:

$$x\{Rh^{x+}\}_z + \{H^+\}_z = \{H^+\}_y + 4\{Th^{4+}\}_y \quad \ldots\ldots\ldots\ldots\ldots\ldots\ldots\ldots 2.1.$$

where x is the unknown charge, and y and z represent the elutriant and eluate concentration respectively. The charge per metal atom x is given by:

$$x = \frac{\{H^+\}_y + 4\{Th^{4+}\}_y - \{H^+\}_z}{\{Rh^{x+}\}_z} \quad \ldots\ldots\ldots\ldots\ldots\ldots\ldots\ldots 2.2.$$

The rhodium solutions for loading onto the resin were prepared in the following manner:-

Solution A:- Rhodium (III) sesquioxide was dissolved in 2mls. of concentrated nitric acid and evaporated on a hot plate to dryness. The residue was then dissolved and diluted to the required concentration in 0.1m nitric acid.

Solution B:- Rhodium (III) sesquioxide was refluxed for three hours with 2M nitric acid. The resulting solution was diluted to give an acid concentration of 0.5M before being loaded onto the resin.

Solution C:- Rhodium (III) sesquioxide was dissolved directly in 0.1m nitric acid without heating. The solution was then loaded onto the resin.

In a typical experiment, 3-5 gm of Dowex 50 W-X8 resin in the hydrogen form was stirredwith 200 mls of a 0.006M rhodium solution prepared by the above methods. The mixture was then added as a slurry to the ion exchange column, which contained enough unloaded resin to provide a 3cm high bed. Sufficient additional resin was added to the top of the column to give a layer 2cm in height. This extra resin served to prevent mixing of the resin in the centre section of the column as the initial eluting solution was added. Experimental details are given in section 5.6.3.

In each of the above, elution of the adsorbed rhodium with a 0.02M solution of thorium (IV) nitrate in 0.1M nitric acid produced a single orange/yellow band. Two-ml fractions were collected as the rhodium containing band eluted from the column. The fractions were analysed

Table 2.4.1. Charge per rhodium(III) atom in solution

Expt.	Elutriant Compn. (M) Th^{4+}	Elutriant Compn. (M) H^+	Eluent Sol^n. Compn. (M) H^+	Eluent Sol^n. Compn. (M) Rh^{x+}	Charge per Rh atom
A6	0.0210	0.180	0.210	0.0204	2.7
A7	0.0210	0.180	0.200	0.0223	2.9
A8	0.0210	0.180	0.200	0.0214	3.0
A9	0.0210	0.180	0.200	0.0223	2.9
A10	0.0210	0.180	0.210	0.0204	2.7
B5	0.0208	0.1057	0.135	0.0167	3.2
B6	0.0208	0.1057	0.135	0.0175	3.1
B7	0.0208	0.1057	0.133	0.0181	3.1
B8	0.0208	0.1057	0.133	0.0186	3.0
B9	0.0208	0.1057	0.132	0.0178	3.2
C3	0.0210	0.1057	0.126	0.0209	3.0
C4	0.0210	0.1057	0.124	0.0233	2.8
C5	0.0210	0.1057	0.116	0.0243	3.0
C6	0.0210	0.1057	0.116	0.0227	3.3

for rhodium and hydrogen ion content and the charge per metal atom, x, determined by applying equation 2.2. The results, Table 2.4.1., show the charge per metal atom in each case to be three.

The electronic absorption spectrum of fraction B9 (2mls diluted to 50ml with 1M HNO_3) produced a single absorption band with λ_{max} 398-402nm and ε = 66, which compares very favourably with the values found for the first absorption band of the hexaaquo rhodium (III) ion, $\{Rh(H_2O)_6\}^{3+}$.

2.4.2. Determination of Charge per Species

The charge per species is determined from the dependence of the equilibrium distribution of the unknown ion on the concentration of the known exchangeable ion in the resin and aqueous phases, in this case the hydrogen ion (160). The equilibration reaction is represented by:

$$M^{x+} + x\overline{H^{+}} = \overline{M^{x+}} + xH^{+} \qquad \text{..... 2.3.}$$

$$\text{and } K = \frac{\{\overline{M^{x+}}\}\ \{H^{+}\}^{x}}{\{M^{x+}\}\ \{\overline{H^{+}}\}^{x}} \qquad \text{..... 2.4.}$$

where K is the equilibrium constant expressed in molar concentrations, and the bar signifies the resin phase. The distribution of M, given by $\{\overline{M^{x+}}\}/\{M^{x+}\}$, varies as the x power of the hydrogen ion distribution, $\{\overline{H^{+}}\}/\{H^{+}\}$. Hence equilibration at two different hydrogen ion concentrations and substitution into equation 2.4 permits the simultaneous solution of the two unknowns x and K, if their values are the same for the two experiments. The equilibrium constant,

K, will vary because of activity coefficient changes, but in practice this can be minimised in two ways (160). Firstly, the mole fractions of rhodium and hydrogen ion in the resin are kept at very nearly the same absolute value in the two experiments, so that the activity coefficients in the resin phase will not vary appreciably. Secondly, changes in the aqueous activity coefficients are minimised by maintaining the aqueous nitric acid concentration in the region 0.2-1M.

The quadratic form of equation 2.4 is:

$$\log K_1 = \log \frac{\{\overline{M^{X+}}\}_1}{\{M^{X+}\}_1} + x \log \frac{\{H^+\}_1}{\{\overline{H^+}\}_1} \qquad \ldots\ldots\ldots\ldots\ldots\ldots 2.5.$$

and for the second equilibration:

$$\log K_2 = \log \frac{\{\overline{M^{X+}}\}_2}{\{M^{X+}\}_2} + x \log \frac{\{H^+\}_2}{\{\overline{H^+}\}_2} \qquad \ldots\ldots\ldots\ldots\ldots\ldots 2.6.$$

hence x, from

$$x = \frac{\log \frac{\{\overline{M^{X+}}\}_1}{\{M^{X+}\}_1} - \log \frac{\{\overline{M^{X+}}\}_2}{\{M^{X+}\}_2}}{\log \frac{\{H^+\}_1}{\{\overline{H^+}\}_1} - \log \frac{\{H^+\}_2}{\{\overline{H^+}\}_2}} \qquad \ldots\ldots\ldots\ldots\ldots\ldots 2.7.$$

In a typical experiment, a fraction of the eluate containing the pure complex species, whose charge per rhodium atom had been found, was diluted with a known volume of standardised nitric acid. The resulting solution was equilibrated (6hrs) with a weighed quantity of Dowex 50 W-X8 (H^+) resin. A sample of the solution was then removed for rhodium analysis, and the remaining solution was diluted with water to a known exact volume, and the equilibration repeated. From a

Table 2.4.2. Charge per rhodium (III) species in solution

Fraction No.	Total Mg Rh	$\{H^+\}M$	V(ml)	wt. resin (gm)	Capacity of resin (meq/gm)	mg Rh_{eq}	Charge
A8	0.4400	1.057	60.2	2.8189	1.98	0.3793	2.8
	0.3770	0.630	100.2	2.8189	1.98	0.2355	
A9	0.4600	1.057	60.2	2.9162	1.98	0.4029	2.6
	0.3930	0.600	100.2	2.9162	1.98	0.2605	

knowledge of the resin capacity (section 5.6.3.1.), the rhodium content in the initial and equilibrated solutions, and the initial hydrogen ion concentration of each solution, the charge per complex species was calculated from equation 2.7. Experimental details are given in section 5.6.3.2.

The results of the charge per species determinations are given in Table 2.4.2. The rhodium fractions analysed were those obtained from Solution A in the charge per metal atom determinations. The first column in Table 2.2. gives the total quantity of rhodium present during the equilibration. The second column is the aqueous concentration of hydrogen ion before equilibration. In the third, fourth and fifth columns are the aqueous phase volume, the weight of resin (air dried, hydrogen ion form) and the total capacity of the resin respectively. The sixth column contains the aqueous rhodium concentration after equilibration. In the last column is the calculated value of the charge per species, x. The values lie fairly close to +3 and so the rhodium species in dilute nitric acid can be formulated as the hexaaquo ion, $\{Rh(H_2O)_6\}^{3+}$.

2.5. ^{103}Rh NUCLEAR MAGNETIC RESONANCE SPECTROSCOPY

The properties of ^{103}Rh relevant to NMR spectroscopy are listed in Table 1.1.5. Solutions of rhodium (III) nitrates and perchlorates were prepared as outlined in Section 5.5.3. The solutions were equilibrated at room temperature for one week before recording the ^{103}Rh NMR specta. Resonance signals were measured at 12.6MHz using a Bruker WH-400 NMR spectrometer, a service provided by Sheffield

University on behalf of the Science and Engineering Research Council (SERC). The chemical shifts are referenced to -3.16 MHz via the ^{2}H lock, and use the IUPAC recommended sign convention of high frequency being positive (39). Values of the chemical shift are given in parts per million (ppm).

2.5.1. Rhodium (III) Nitrates and Perchlorates

A convenient starting point for this study is the spectrum obtained for rhodium (III) sesquioxide (0.6 M) in perchloric acid (1.25 M), Figure 2.5.1. Previous work on the speciation of rhodium in perchloric acid has identified only a single cationic speies in solution, i.e. the hexaaquo ion $\{Rh(H_2O)_6\}^{3+}$, with no trace of other species (16, 17). As Figure 2.5.1. shows, two resonance signals are observed, the major at δ9899 (intensity 10.0), and the minor at δ9478 (intensity 1.7). Ligand substitution (e.g. of water by perchlorate) will reduce the electron density around the central metal ion and cause the resonance signals to appear at lower frequencies. The signal at δ9899 must therefore be due to the hexaaquo ion, $\{Rh(H_2O)_6\}^{3+}$ and the signal at δ9478 to the pentaaquorhodium (III) perchlorate, $\{Rh(H_2O)_5ClO_4\}^{2+}$. The intensities of the resonances cannot be taken as an indication of the relative concentrations of the various species in solution. The magnetogyric ratio for ^{103}Rh, ($-0.8420\ \gamma/10^{7}$ rad.T^{-1} S^{-1}) gives a negative value for the nuclear overhauser effect (NOE) and a consequent diminution in peak intensities (see Appendix I).

The above resonances for the hexaaquorhodium (III) ion and the pentaaquo rhodium (III) perchlorate do not compare very favourably with those

Figure 2.5.1. ^{103}Rh NMR spectrum of rhodium (III) sesquioxide (0.6M) in perchloric acid (1.25M)

δppm	Intensity
9899	45.1
9478	7.0

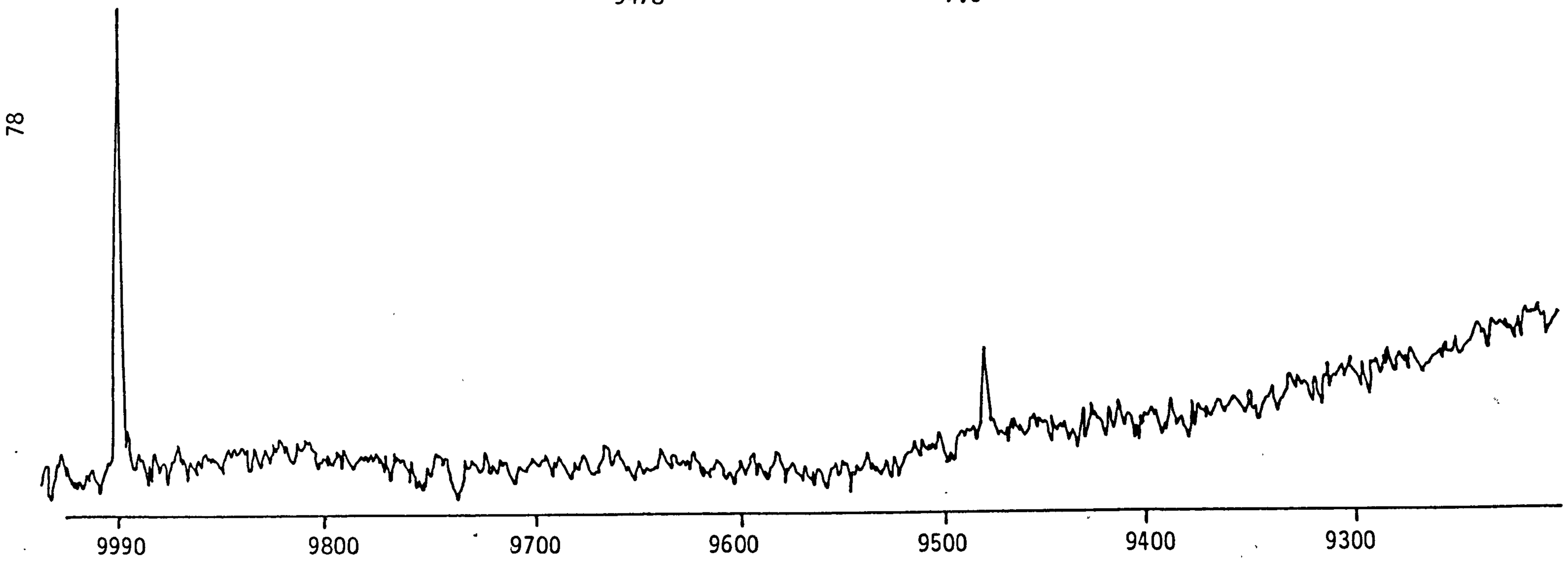

Figure 2.5.2. ^{103}Rh NMR spectrum of rhodium (III) sesquioxide (0.64M) in nitric acid (0.6M)

δppm	Intensity
9906	3.8
9902	9.1
9484	2.2

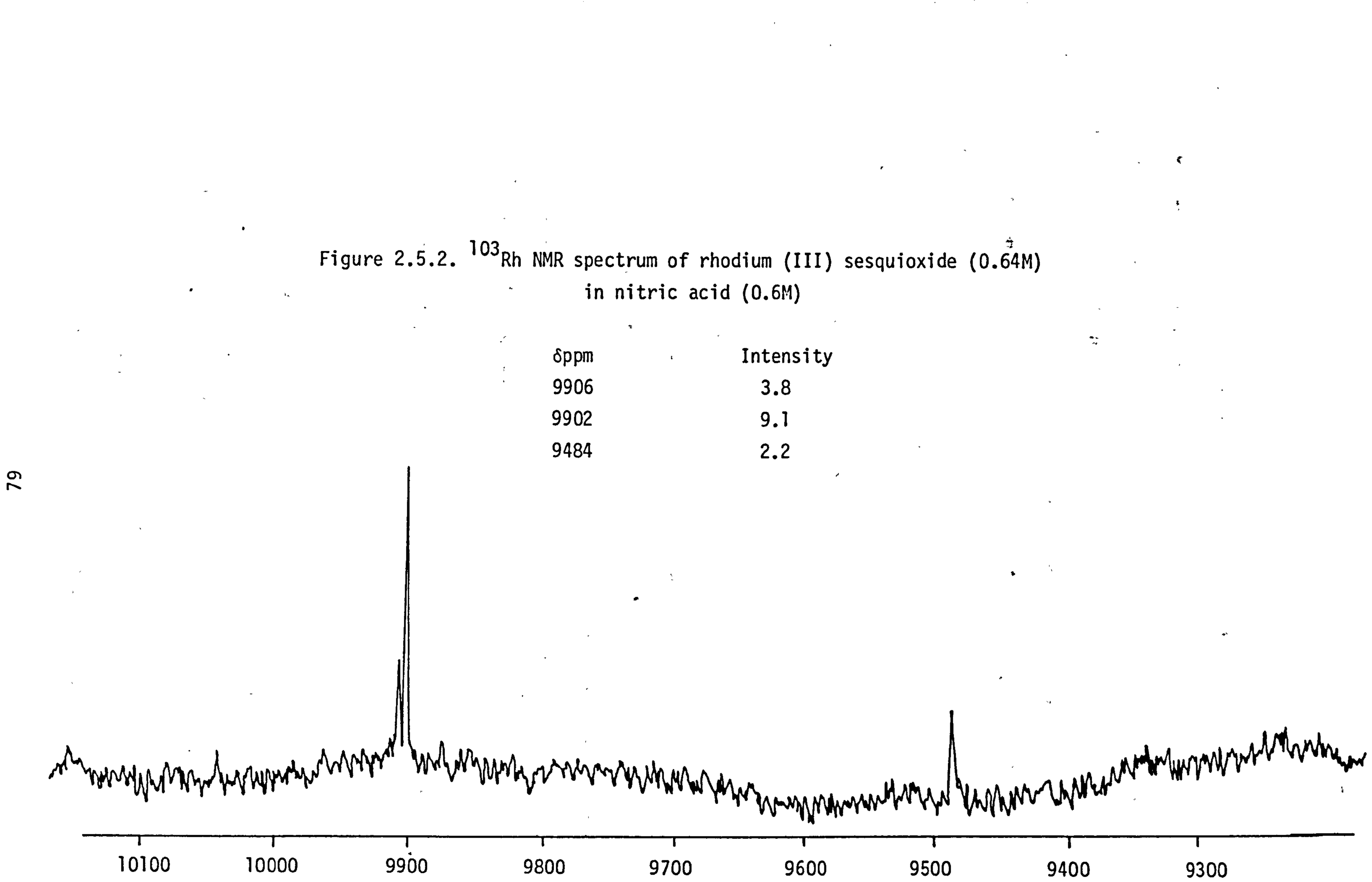

observed by Mann and Spencer (39). For rhodium (III) sesquioxide in perchloric acid, the authors report one resonance at δ9992 which they assigned to $\{Rh(H_2O)_6\}^{3+}$. On addition of a half equivalent of lithium chloride, three resonances at δ9991, δ9819 and δ9479 were observed. The second of these, δ9819 was assigned to $\{Rh(H_2O)_5ClO_4\}^{2+}$. It appears unusual however to observe the resonance for $\{Rh(H_2O)_5ClO_4\}^{2+}$ in the presence of chloride ions but not in their absence.

The spectrum obtained from rhodium (III) sesquioxide (0.64M) in 0.6M nitric acid is reproduced in Figure 2.5.2. The major resonance, at δ9902 (intensity 9.1), is again assigned to the ion $\{Rh(H_2O)_6\}^{3+}$. A minor resonance at δ9484 (intensity 2.2), is also observed. It is interesting to note that the intensity and frequency of this resonance are almost identical to that observed for $\{Rh(H_2O)_5ClO_4\}^{2+}$. In this case, since there are no perchlorate ions present in solution, the peak is assigned to the pentaaquo-nitrato rhodium (III) ion, $\{Rh(H_2O)_5NO_3\}^{2+}$.

On increasing the nitric acid concentration to 2, 5 and 8 molar, the spectra reproduced in Figures 2.5.3. - 2.5.5. respectively, were observed. The resonance at δ9484 attributed to $\{Rh(H_2O)_5NO_3\}^{2+}$ in 0.6M nitric acid is not observed at 2, 5 and 8 Molar nitric acid. Instead additional resonances very close to the hexaaquorhodium (III) resonance (some of which are to higher frequencies) are observed. The aquo ion, $\{Rh(H_2O)_6\}^{3+}$ can be regarded, in aqueous solution, as being composed of the central metal ion surrounded by six water molecules arranged in an octahedral field, representing the first coordination sphere. Beyond this is the second ordered coordination sphere followed

Figure 2.5.3. ^{103}Rh NMR spectrum of rhodium (III) sesquioxide (0.64M) in nitric acid (2M)

δppm	Intensity
10202	6.3
9898	26.6
9891	10.2
9887	6.0
9813	2.4

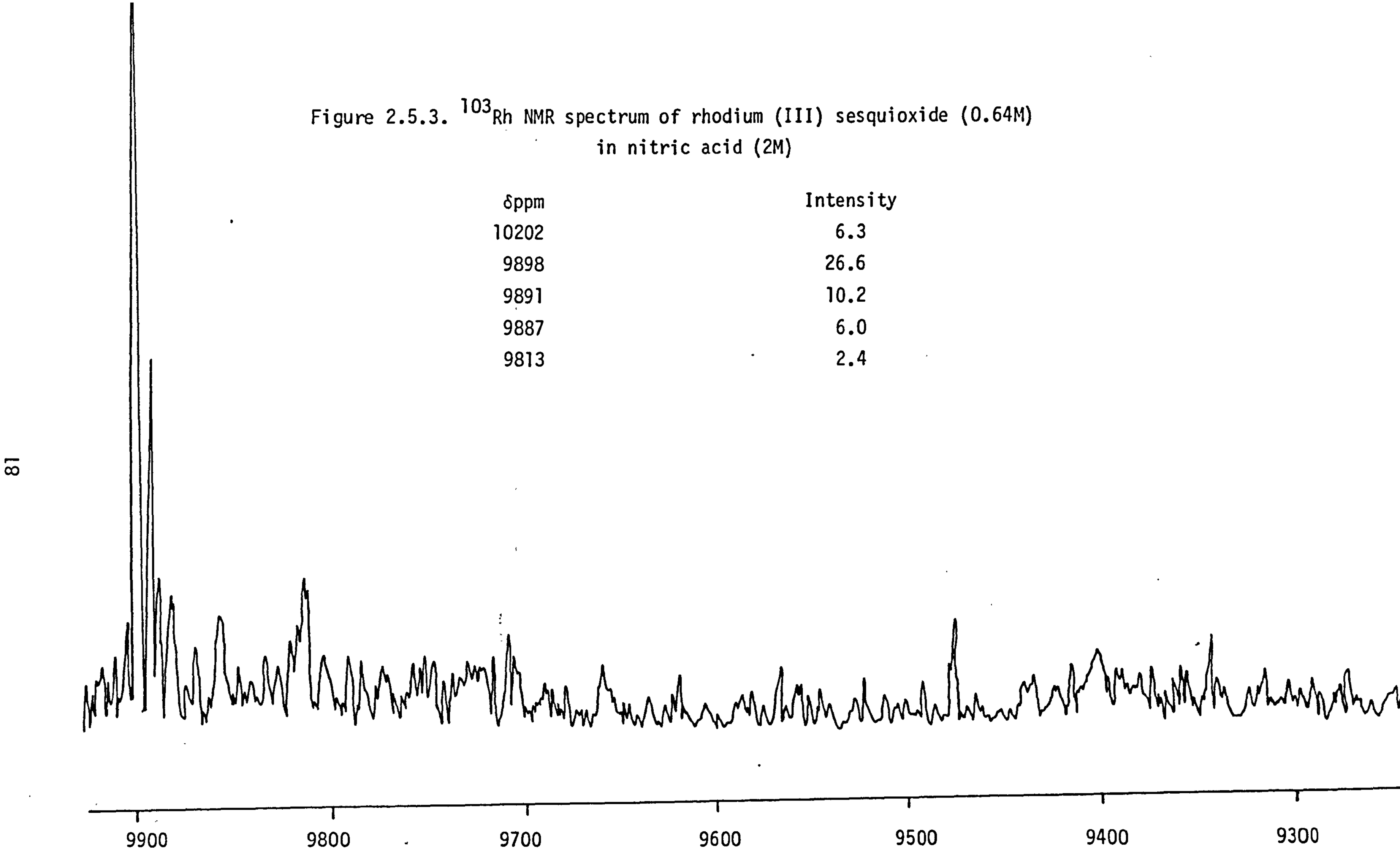

Figure 2.5.4. ^{103}Rh NMR spectrum of rhodium (III) sesquioxide (0.64M) in nitric acid (5M)

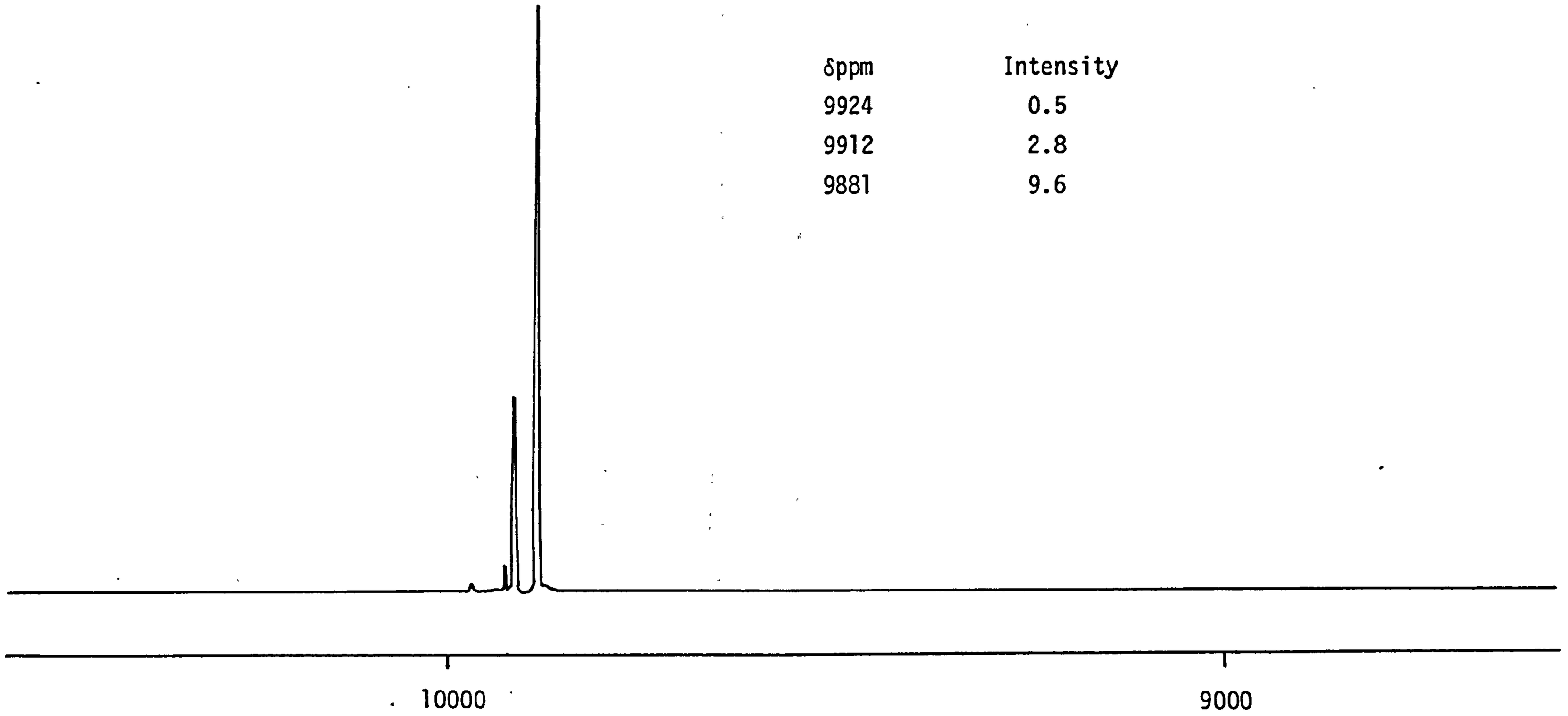

Figure 2.5.5. ^{103}Rh NMR spectrum of rhodium (III) sesquioxide (0.64M) in nitric acid (8M)

δppm	Intensity
9954	3.4
9911	2.5
9904	15.5
9874	7.1

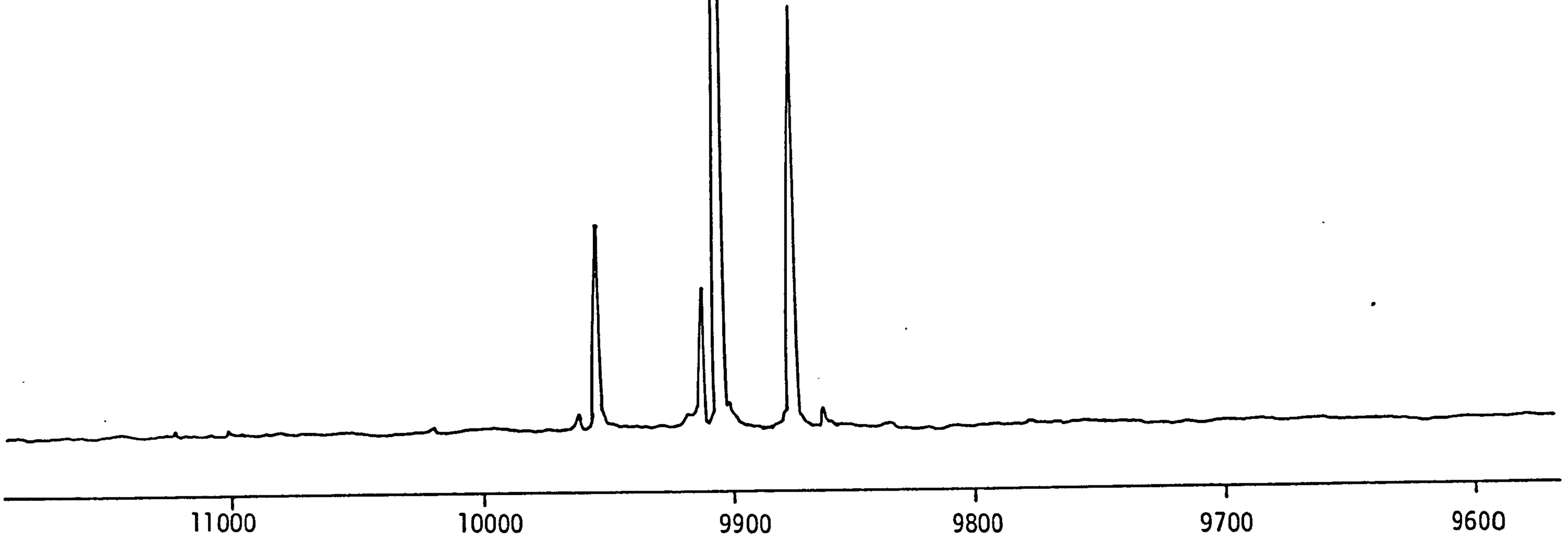

Figure 2.5.6. ^{103}Rh NMR spectrum of rhodium (III) sesquioxide (0.64M) in perchloric acid (3.5M)

δppm	Intensity
9986	1.4
9909	1.1
9906	8.2
9815	1.7

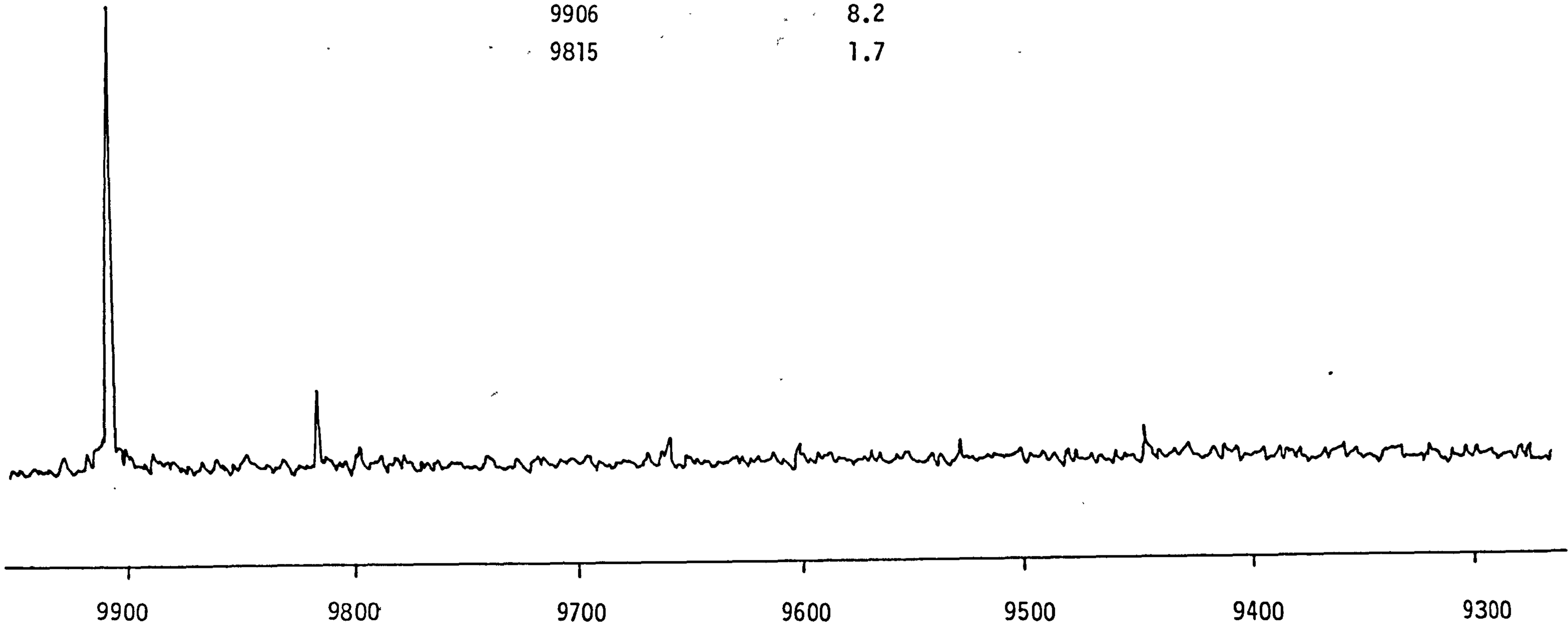

Table 2.5.1. ^{103}Rh NMR spectra in nitric and perchloric acids

{Rh} = 0.64M, 50% D_2O

Figure	Acid	δppm	Intensity
2.5.1.	1.25M $HClO_4$	9899	45.1
		9478	7.0
2.5.6.	3.5M $HClO_4$	9986	1.4
		9909	1.1
		9906	8.2
		9815	1.7
2.5.2.	0.6M HNO_3	9902	9.1
		9484	2.2
2.5.3.	2M HNO_3	10202	6.3
		9898	26.6
		9891	10.2
		9887	6.0
		9813	2.4
2.5.4.	5M HNO_3	9924	0.5
		9912	2.8
		9881	9.6
2.5.5.	8M HNO_3	9954	3.4
		9911	2.5
		9904	15.5
		9874	7.1

by a disordered third sphere, and finally the bulk solvent (161). At the higher nitric acid concentrations, invasion of the second coordination sphere would occur. The result of this would be to reduce the effective concentration of $\{Rh(H_2O)_5NO_3\}^{2+}$ to a level where it is not observable by NMR spectroscopy, and also to produce a more complex NMR spectrum. It is worth comparing the rhodium spectra obtained at the higher nitric acid concentrations to that obtained for rhodium in 3.5M perchloric acid, Figure 2.5.6. Again, the resonance at δ9478 attributed to $\{Rh(H_2O)_5ClO_4\}^{2+}$ in 1.25M perchloric acid is not observed at 3.5M perchloric acid, but additional resonances either side of the hexaaquo resonance are obtained.

The NMR spectra for rhodium in nitric and perchloric acids are summarised in Table 2.5.1.

2.5.2. Rhodium (III) Nitrites

In the presence of nitrite ions, a series of rhodium (III) complexes of the type $\{Rh(H_2O)_{6-n}(NO_2)_n\}^{(3-n)+}$ exist and may be identified by ^{103}Rh NMR spectroscopy. Figure 2.5.7. shows the resonances obtained for rhodium (III) sesquioxide, (0.64M Rh), in 2M nitric acid and 1M sodium nitrite. Only two resonances are observed, at δ8591 and δ7454. If several rhodium species do exist in solution, it may well be that a higher concentration of rhodium is required for further resonances to be observed. For this reason the concentration of rhodium in solution was increased from 0.64M to 1.70M. However, at this higher rhodium concentration, increasing the nitrite concentration beyond 1M precipitated a creamy white solid (21.8%Rh, cf. 23% for $Na_3\{Rh(NO_2)_6\}$) to

Figure 2.5.7. ^{103}Rh NMR spectrum of rhodium (III) sesquioxide (0.64M) in nitric acid (2M) and sodium nitrite (1M)

δppm	Intensity
8591	2.7
7454	10.6

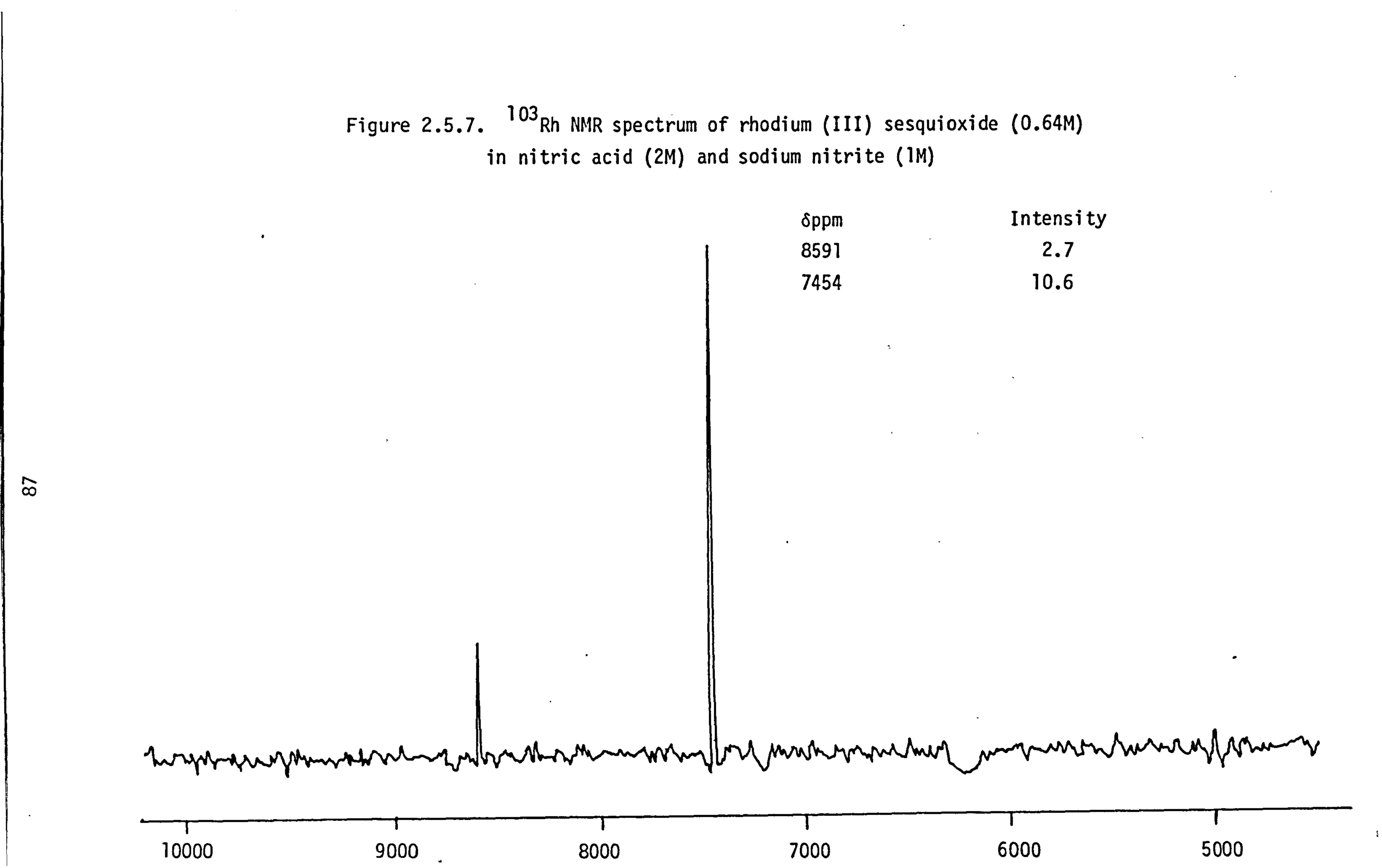

keep all species in solution it was necessary to use a higher nitric acid concentration.

Figure 2.5.8. shows the resonances obtained for rhodium (III) sesquioxide (1.72M) in 5M nitric acid and 0.98M sodium nitrite. In addition to the resonances at δ8583 and δ7441 (both observed at 2M HNO_3), further resonances at δ9887, δ9460 and δ8101 are observed.

On increasing the sodium nitrite concentration to 2.7M, Figure 2.5.9., three new resonances at δ7040, δ6945 and δ6607 appeared. The resonances at δ8574 and δ8094 decreased in intensity relative to the resonance at δ7436.

A further increase in the concentration of sodium nitrite, to 3.97M, Figure 2.5.10., increased the intensities of the resonances at δ8577, δ8079, δ7041 and δ6934. The resonance at δ9455 could also be observed.

Finally at 5.2M sodium nitrite, Figure 2.5.11., the resonances at δ9457, δ8578 and δ8097 are not observed, but additional resonances at δ6606, δ6432, δ6211 and δ6008 are found. The weakest resonance is at δ6432 (intensity = 2.7) and appears with a cluster of smaller resonances. Attempts to increase the nitrite concentration beyond 5.2M resulted in the precipitation of a creamy white solid.

For convenience, the intensities of the resonances obtained in Figures 2.5.8.-2.5.11., are given in Table 2.5.2., and the relative intensities are displayed in Figure 2.5.12. The chemical shifts in Table 2.5.2., are the average values taken from all the spectra obtained. In fact,

Figure 2.5.8. ^{103}Rh NMR spectrum of rhodium (III) sesquioxide (1.72M) in nitric acid (5M) and sodium nitrite (0.98M)

δppm	Intensity
9888	10.5
9459	22.3
8583	14.7
8101	8.6
7442	3.3

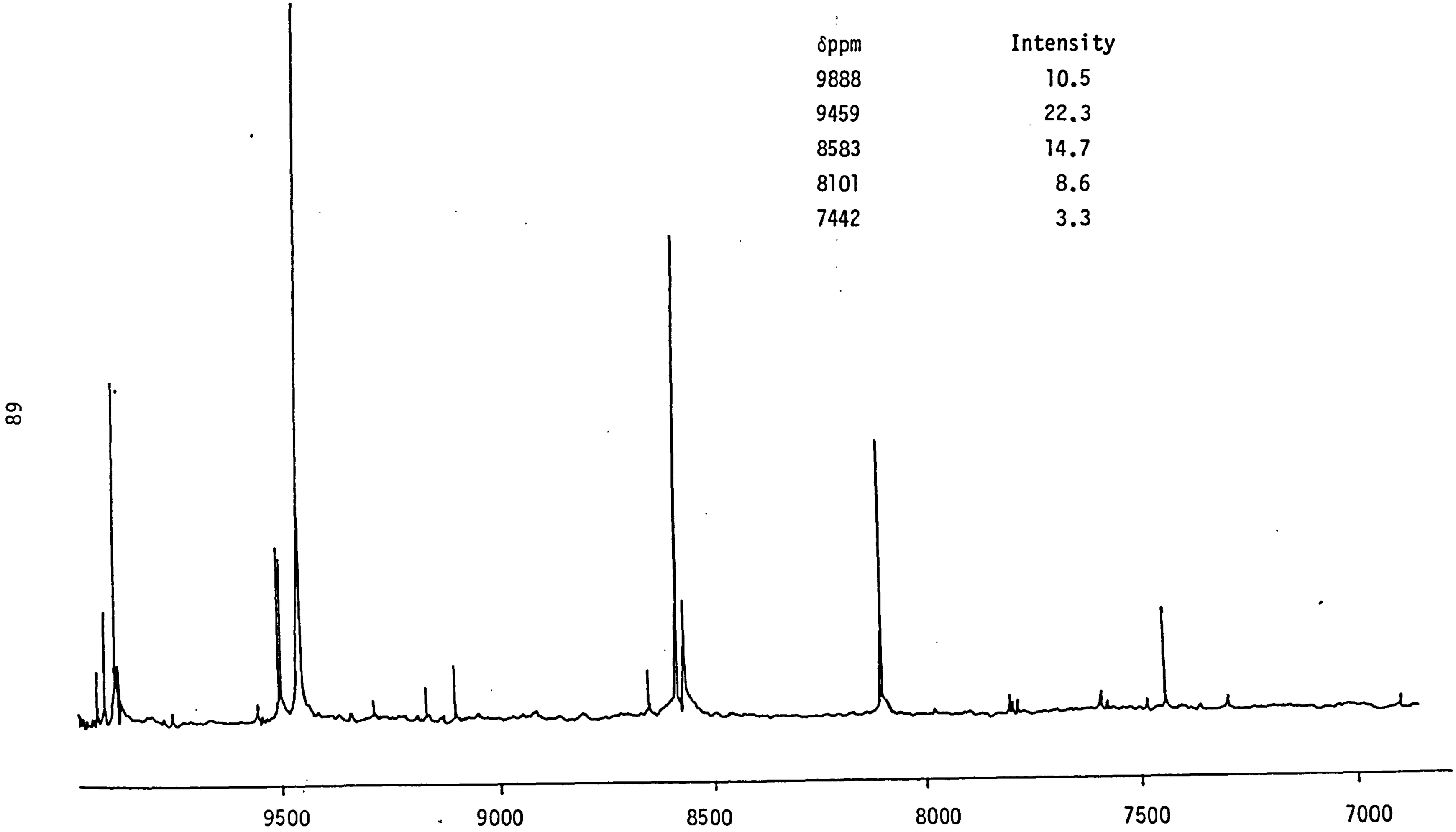

Figure 2.5.9. ^{103}Rh NMR spectrum of rhodium (III) sesquioxide (1.69M) in nitric acid (5M) and sodium nitrite (2.70M)

δppm	Intensity
8574	2.9
8094	2.8
7436	22.9
7040	1.5
6945	1.6
6607	1.9

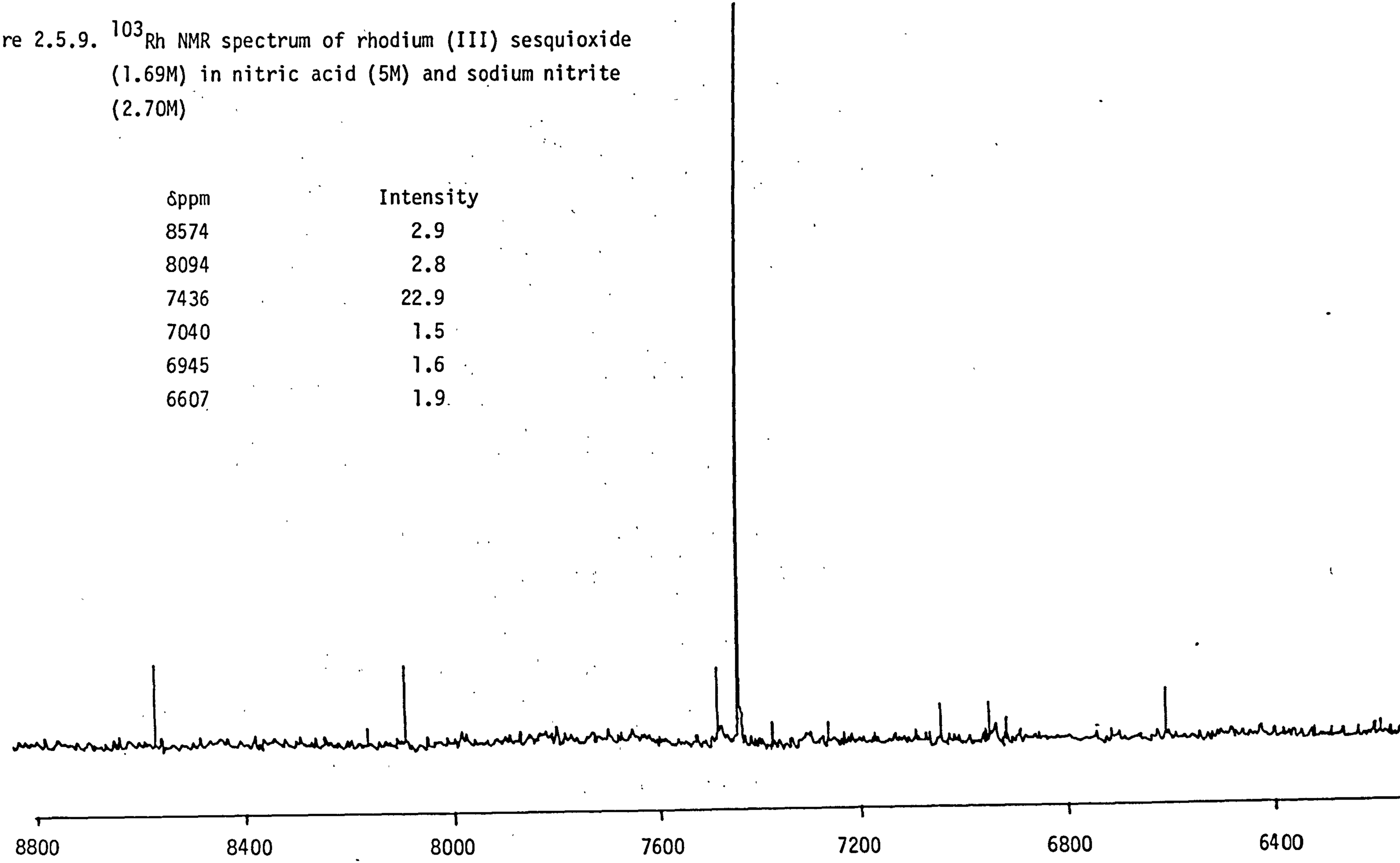

Figure 2.5.10. ^{103}Rh NMR spectrum of rhodium (III) sesquioxide (1.69M) in nitric acid (5M) and sodium nitrite (3.97M).

δppm	Intensity
9455	1.4
8578	5.3
8097	11.9
7480	3.6
7438	22.8
7375	1.8
7359	2.2
7262	1.7
7042	3.1
6935	2.1

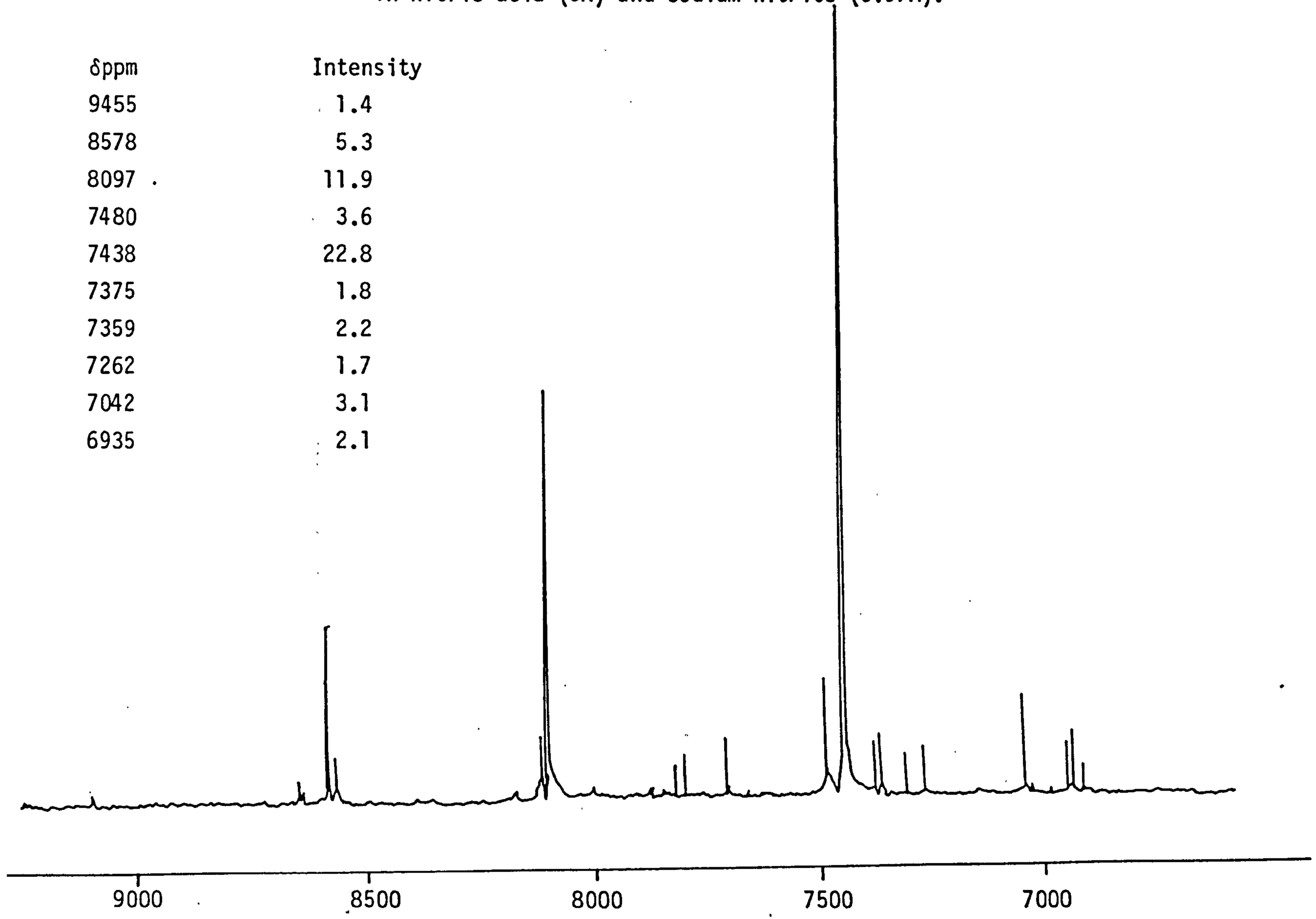

Figure 2.5.11. ^{103}Rh NMR spectrum of rhodium (III) sesquioxide (1.69M) in nitric acid (5M) and sodium nitrite (5.20M)

δppm	Intensity
7432	21.3
7257	3.9
7031	7.8
6930	27.4
6866	0.8
6712	1.0
6604	6.9
6587	1.8
6439	2.1
6432	2.7
6421	0.6
6415	1.2
6211	3.0
6007	11.1
5993	0.9

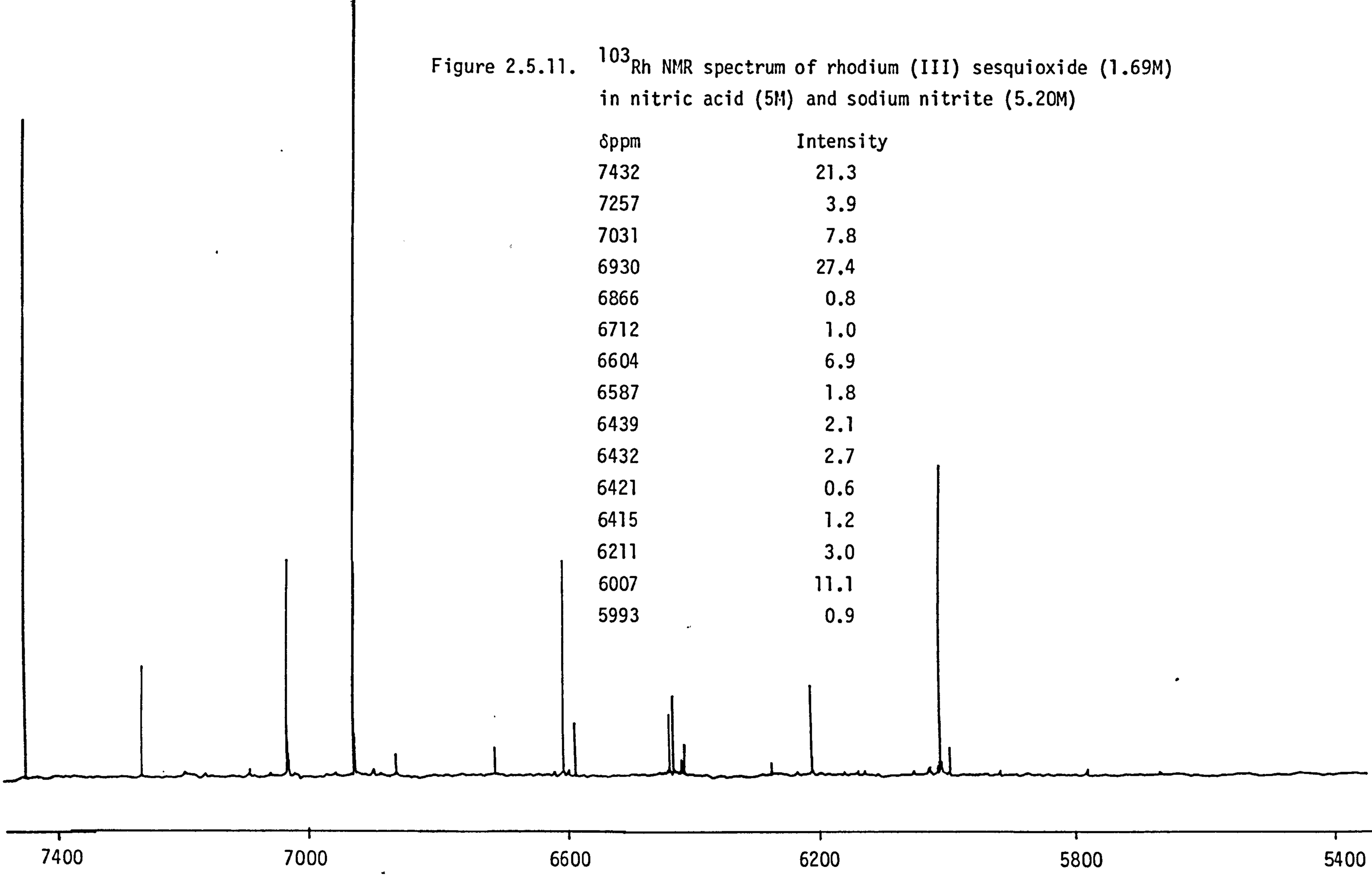

					Chemical Shift δppm											
Figure	(Rh)M	(HNO_3)M	($NaNO_2$)M	NO_2^-/Rh	9888	9457	8578	8097	7437	7260	7038	6937	6606	6432	6211	6008
2.5.8.	1.72	5	0.98	0.6	10.5	22.3	14.7	8.6	3.3							
2.5.9.	1.69	5	2.70	1.6			2.9	2.8	22.9		1.5	1.6	1.9			
2.5.10.	1.69	5	3.97	2.4		1.4	5.3	11.9	22.8	1.6	3.1	2.1				
2.5.11.	1.69	5	5.20	3.1					21.3	3.9	7.8	27.4	6.9	2.7	3.0	11.1

TABLE 2.5.2. ^{103}Rh NMR Intensities in Nitric Acid/Sodium Nitrite

Figure . 2.5.12. Relative intensities of ^{103}Rh NMR spectra

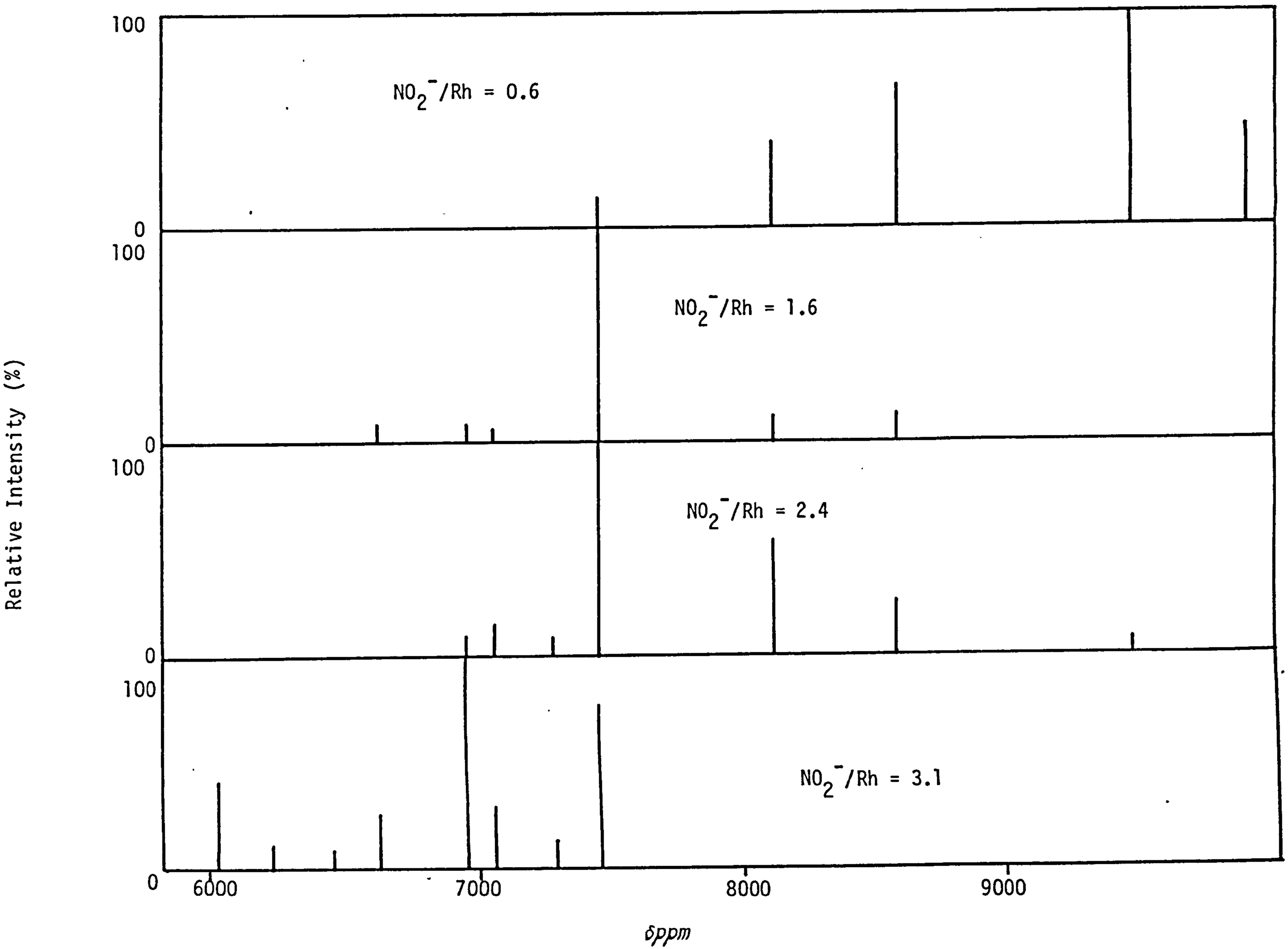

it was found that ^{103}Rh chemical shifts were very sensitive to temperature and added sodium nitrite, changing by up to 30ppm over the range of conditions used.

The resonances obtained from the above spectra have been assigned to the various rhodium nitrito species on the basis of the following observations:

(a) An increase in the ligand number, n, of the complex $\{Rh(H_2O)_{6-n}(NO_2)_n\}^{(3-n)+}$, from 0 to 6, produces a corresponding decrease in the electron density around the central metal ion, and causes the resonance for ^{103}Rh to shift to lower frequencies.

(b) The resonance for the cis isomer occurs at a lower frequency than the corresponding trans isomer (39).

(c) The resonance for the fac isomer occurs at a lower frequency than the corresponding mer isomer (39).

Clearly the resonance at δ9888 in Figure 2.5.8. must be due to the hexaaquo rhodium (III) ion, $\{Rh(H_2O)_6\}^{3+}$. The resonance at δ9457 is assigned to the pentaaquo nitrato rhodium (III) ion $\{Rh(H_2O)_5NO_3\}^{2+}$, athough it is unusual that, in this particular spectrum, this resonance has the largest intensity.

Figure 2.5.12. shows clearly the shift to lower frequencies as the concentration of nitrite ion in solution is increased. The resonances at the lowest frequencies, δ6008 and δ6211, must be due to the higher nitrito complexes, i.e. $\{Rh(NO_2)_6\}^{3-}$ and $\{Rh(H_2O)(NO_2)_5\}^{2-}$ respectively.

Similarly, the first resonance after δ9457, i.e. δ8578 must be due to the pentaaquonitritorhodium (III) ion, $\{Rh(H_2O)_5NO_2\}^{2+}$. This leaves the seven resonances between δ8097 and δ6432 to be assigned to the six cis/trans, fac/mer isomers. The extra resonance is believed to be due to a mixed nitrato/nitrito complex, i.e. $\{Rh(H_2O)_4NO_2NO_3\}^{+}$. In terms of frequency, the resonance for this complex would be expected to be lower than that for $\{Rh(H_2O)_5NO_2\}^{2+}$, (i.e. δ8578), but higher than $\{Rh(H_2O)_4(NO_2)_2\}^{2+}$, (i.e. δ7437). The first resonance of this group of seven, at δ8097 is thus assigned to $\{Rh(H_2O)_4NO_2NO_3\}^{+}$. The remaining resonances are assigned to the various cis/trans, fac/mer isomers as follows: δ7260 cis-$\{Rh(H_2O)_4(NO_2)_2\}^{+}$; δ7437 trans-$\{Rh(H_2O)_4(NO_2)_2\}^{+}$; δ6937 fac-$\{Rh(H_2O)_3(NO_2)_3\}$; δ7038 mer $\{Rh(H_2O)_3(NO_2)_3\}$; δ6432 cis-$\{Rh(H_2O)_2(NO_2)_4\}^{-}$;δ6606 trans-$\{Rh(H_2O)_2(NO_2)_4\}^{-}$. The final assignments are illustrated in Figure 2.5.13.

The concentration of acid in these solutions has a considerable influence on the resonances obtained. Figures 2.5.14. and 2.5.15. show the NMR spectra obtained for rhodium (III) sesquioxide in the presence of nitrite, (NO_2^{-}/Rh =1.6), at 8M nitric acid. The effect of the acid concentration can be seen when the spectra are compared with Figures 2.5.7. and 2.5.9. Again, for convenience the intensities are given in Table 2.5.3.

A high acid concentration is necessary to keep all the various rhodium species in solution. The only difference between Figures 2.5.9. and 2.5.14. is in the nitric acid concentration. At the higher acid concentration, Figure 2.5.14., the resonance due to the higher rhodium nitrito complexes are not observed. This is probably

Figure 2.5.13. Assignment of ^{103}Rh nuclear magnetic resonances

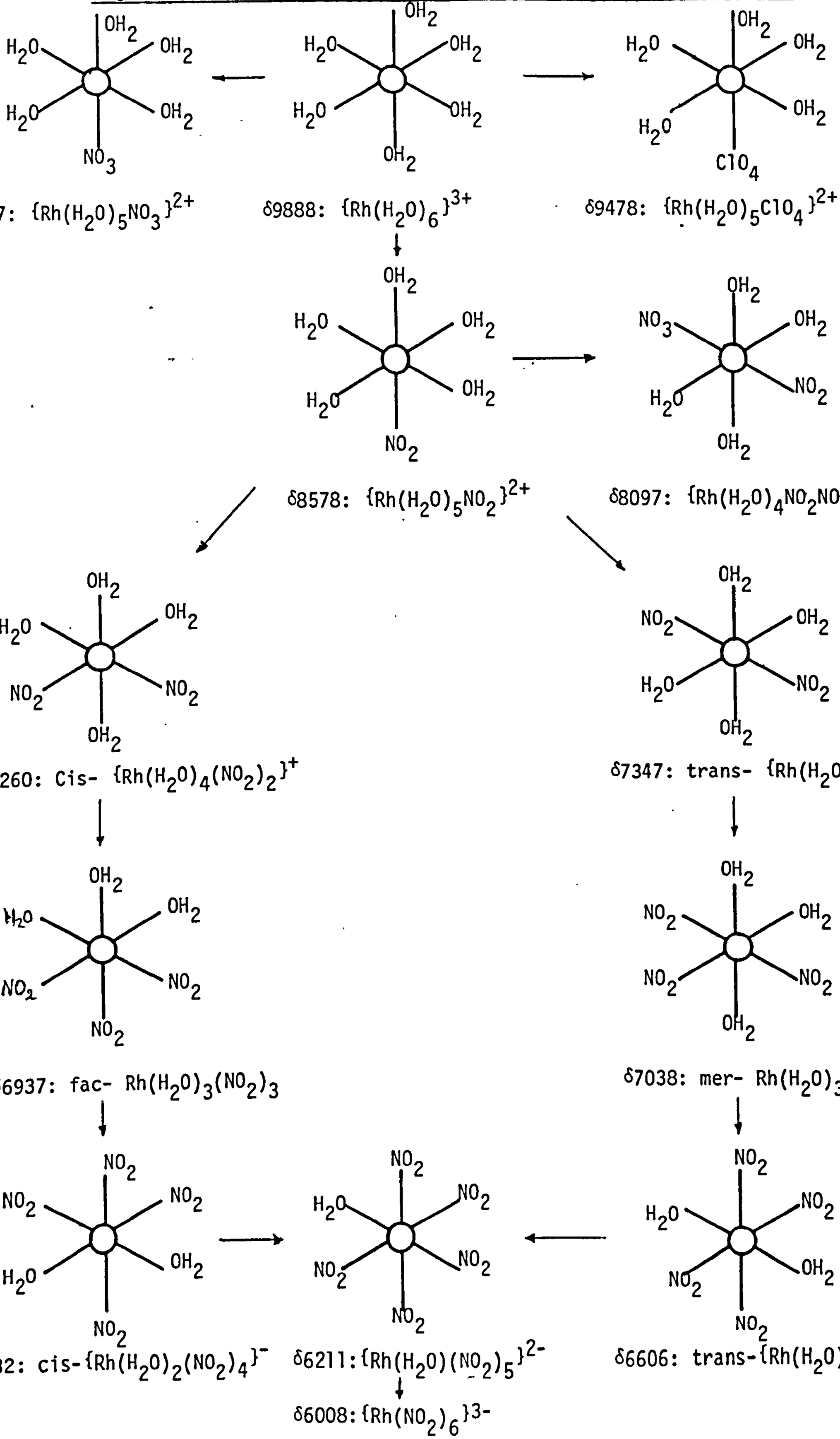

Figure 2.5.14. ^{103}Rh NMR spectrum of rhodium (III) sesquioxide (1.70M) in nitric acid (8M) and sodium nitrite (2.75M)

δppm	Intensity
9880	12.7
9447	18.3
8579	25.5
8092	23.1
7438	15.9

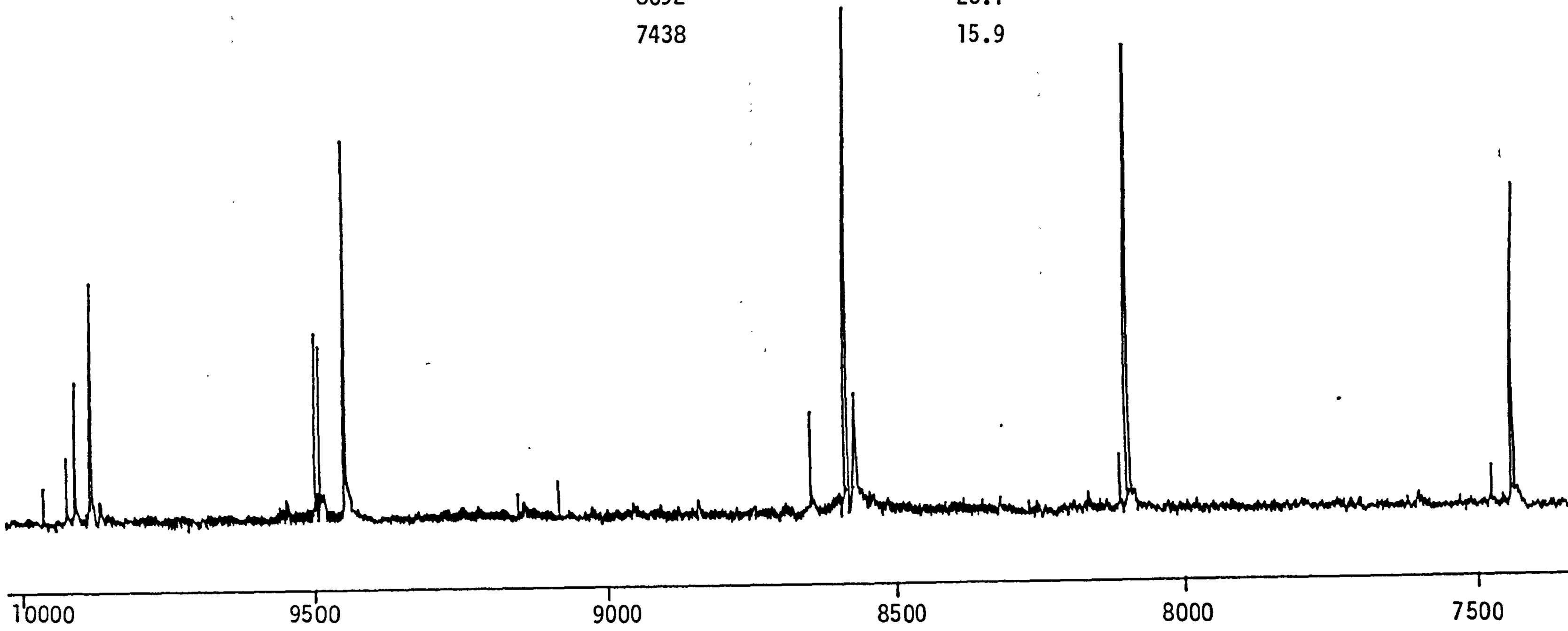

Figure 2.5.15. ^{103}Rh NMR spectrum of rhodium (III) sesquioxide (0.98M) in nitric acid (8M) and sodium nitrite (1.50M)

δppm	Intensity
9878	11.3
9443	18.8
8584	15.2
8092	16.2
7441	6.7

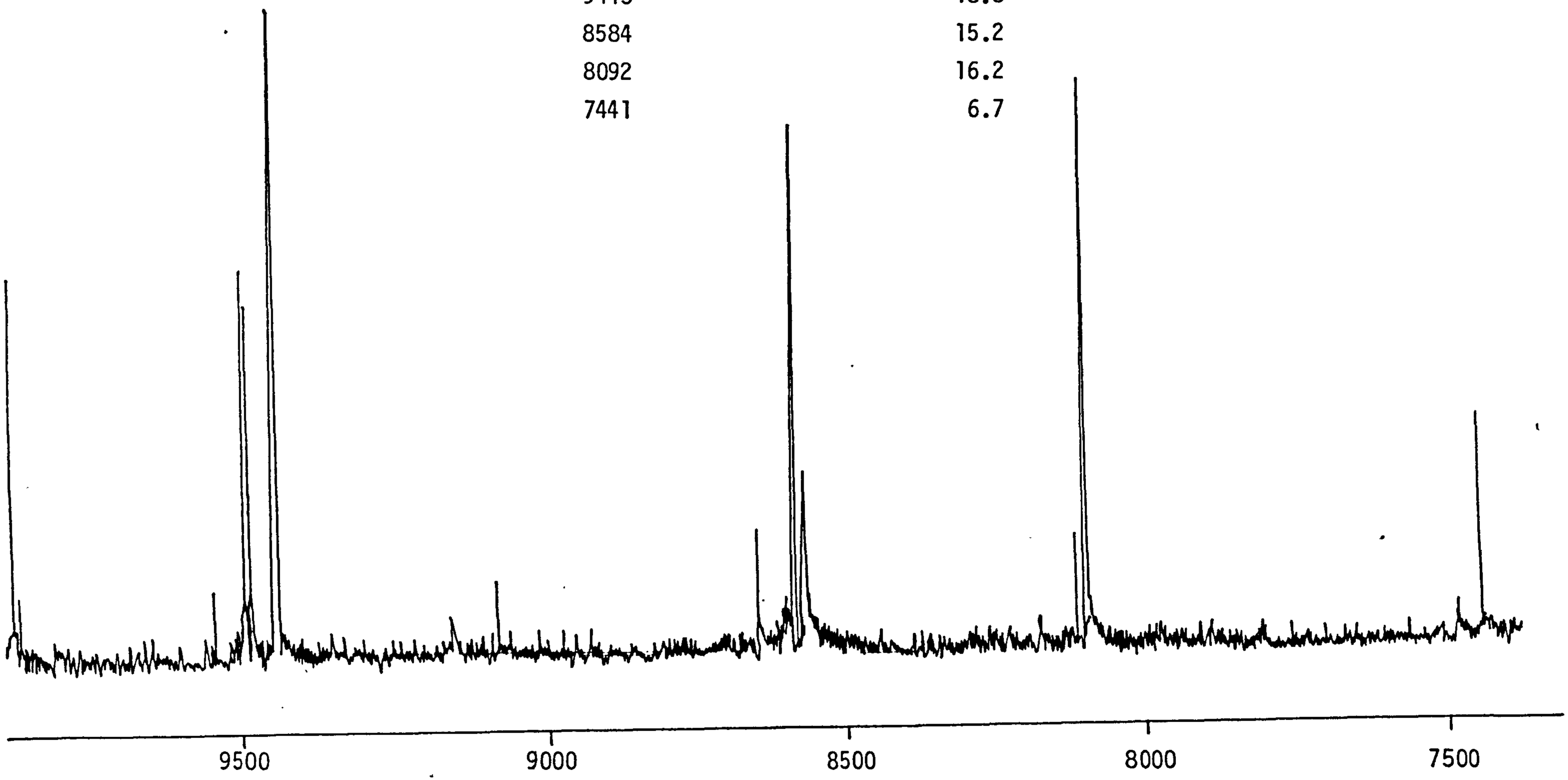

					Chemical Shift δppm											
Figure	(Rh)M	(HNO_3)M	($NaNO_2$)M	NO_2^-/Rh	9888	9457	8578	8097	7437	7260	7038	6937	6606	6432	6211	6008
2.5.7.	0.64	2	1.00	1.6			2.7		10.6							
2.5.9.	1.69	5	2.70	1.6			2.9	2.8	22.9		1.5	1.6	1.9			
2.5.11.	1.69	5	5.20	3.1					21.3	3.9	7.8	27.4	6.9	2.7	3.0	11.1
2.5.14.	1.70	8	2.75	1.6	12.7	18.3	25.5	23.1	15.9							
2.5.15.	0.98	8	1.50	1.5	11.3	18.8	15.2	16.2	6.7							
2.5.16.	0.70	1.25M HC104	1.00	1.4			4.8		15.0				1.1			
2.5.17.	1.69	5.0M HC104	5.00	3.1			11.2	2.1	24.9			1.1				

Table 2.5.3. : ^{103}Rh NMR intensities in nitric and perchloric acids with varying amounts of sodium nitrite

due to the removal of nitrite, which in aqueous solution will decompose according to (14):

$$3HNO_2 \rightarrow HNO_3 + H_2O + 2NO \quad \text{..... 2.8}$$

The possibility of the formation of rhodium nitrosyl complexes at the higher acid concentrations is discounted here, because there is no evidence in the literature to suggest the formation of such species in aqueous solution. Further, in the few inorganic rhodium nitrosyl species to have been isolated, the rhodium is present in a reduced state, -I or I, (1,162,163). For example, the compound $Rh(NO)_2Cl$ was prepared by Griffith et.al. (163) by passing nitric oxide at 60^oC over rhodium (I) dicarbonyl chloride for two days. The compound was reported to be unreactive and insoluble in water.

A comparison of Figures 2.5.7. (Rh = 0.64M) and 12.5.15 (Rh = 0.98M) shows the influence of the rhodium concentration. At the higher concentration, resonances at δ9883, δ9457 and δ8097 are observed in addition to those at δ8578 and δ7437 seen at the lower concentration. Clearly, when there are a number of rhodium complex species in solution, the actual concentration of rhodium has to be far greater than the normal detection limit of 25mg/ml, (0.24M).

Finally, Figures 2.5.16. and 2.5.17. show the influence of perchloric acid on the ^{103}Rh NMR spectra observed. In particular, Figures 2.5.11. and 2.5.17. bear comparison, since the only difference is the type of acid. Only one resonance is observed below δ7260 in perchloric acid, i.e. at δ6937 (intensity 1.1). In nitric acid this resonance is the

Figure 2.5.16. ^{103}Rh NMR spectrum of rhodium (III) sesquioxide (0.70M) in perchloric acid (1.25M) and sodium nitrite (1.00M)

δppm	Intensity
8594	4.7
7452	15.0
6625	1.1

Figure 2.5.17. ^{103}Rh NMR spectrum of rhodium (III) sesquioxide (1.69M) in perchloric acid (5.0M) and sodium nitrite (5.00M)

δppm	Intensity
8598	11.2
8080	2.1
7430	24.9
6931	1.1

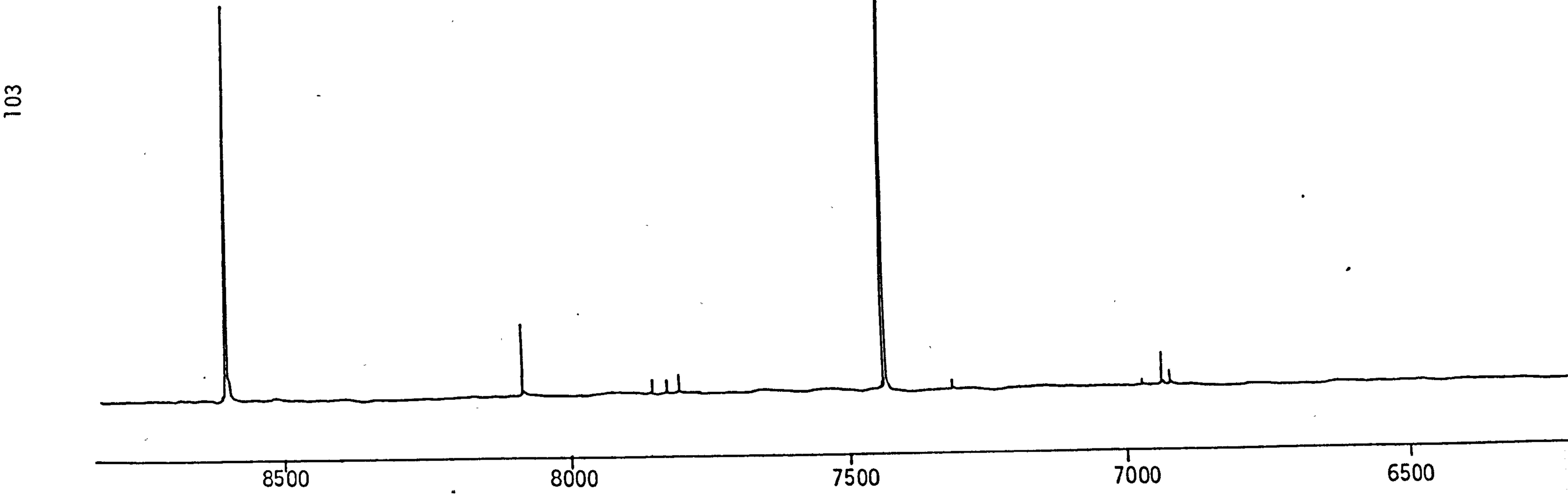

largest observed (intensity 27.4). Again, the lack of resonances for the higher nitrite complexes in perchloric acid is probably due to the removal of nitrite ions. Perchloric acid, being a much more powerful oxidising agent than nitric acid (14) will tend to remove nitrite by:

$$ClO_4^- + NO_2^- \rightleftarrows NO_3^- + ClO_3^- \quad \ldots\ldots\ldots\ldots\ldots\ldots\ldots\ldots\ldots\ldots 2.9$$

2.6. ELECTROCHEMICAL REDUCTION OF Rh(III) COMPLEXES AT THE DROPPING MERCURY ELECTRODE

Polarography can yield useful information about coordination compounds. In the case of reversible reduction processes in particular, the application of numerous mathematical methods can lead to the determination of a variety of parameters such as, number of electrons transferred during reduction, transference coefficients, stability coefficients, heterogeneous rate constants etc., all of which serve to provide an understanding of the mechanisms involved in the reduction process (164).

As already mentioned in Section 1.1.5., polarographic studies on rhodium (III) nitrate solutions have been limited. Scarano (48) observed two reduction waves for "rhodium nitrate" in potassium nitrate electrolyte, while in nitric acid only a single reduction wave was observed. Cozzi and Pantani (43) however, reported a single irreversible wave in 1M potassium nitrate with the half wave potential, $E_{\frac{1}{2}} = -0.012$ V.

Experimental details describing solution preparation and methods are given in Section 5.6.4.

2.6.1. Polarography of Rhodium (III) Nitrates

The polarogram of rhodium (III) sesquioxide in 0.1M perchloric acid and 0.9M sodium perchlorate, Figure 2.6.1., shows a single, well defined reduction wave. The current-potential data from the polarogram can be treated by application of the Heyrovsky -Ilkovic equation (164):

$$E = E_{\frac{1}{2}} - \frac{RT}{nF} \ln \frac{i}{i_d - i} \quad \text{..... 2.10}$$

where E = Electrode potential (V)

$E_{\frac{1}{2}}$ = Half-wave potential (V)

R = Gas constant

n = Number of electrons transferred in the reduction process

T = Temperature (K)

F = Faraday constant

i = Instantaneous current at E (μA)

i_d = Diffusion current (μA)

In effect, equation 2.10 describes the shape of a reversible polarographic wave. A plot of log $(i/i_d - i)$ Vs E will give a straight line of slope 2.303RT/nF and intercept $E_{\frac{1}{2}}$.

Current-potential data extracted from Figure 2.6.1. are displayed in Table 2.6.1. and presented graphically in Figure 2.6.2. Although the plot of log $(i/i_d - i)$ vs E is linear, the value of the function 2.303RT/nF is greater than 60mV, (4.97V), thus the polarographic reduction of rhodium in perchloric acid is an irreversible process. The value of $E_{\frac{1}{2}}$, as given by the intercept, is -0.363V, which is in good agreement with the value of -0.39V obtained by other workers (41,49).

Figure 2.6.1. Polarographic reduction of rhodium in 0.1M $HClO_4$/0.9M $NaClO_4$

$M_{Rh} = 1.37 \times 10^{-3}$ M

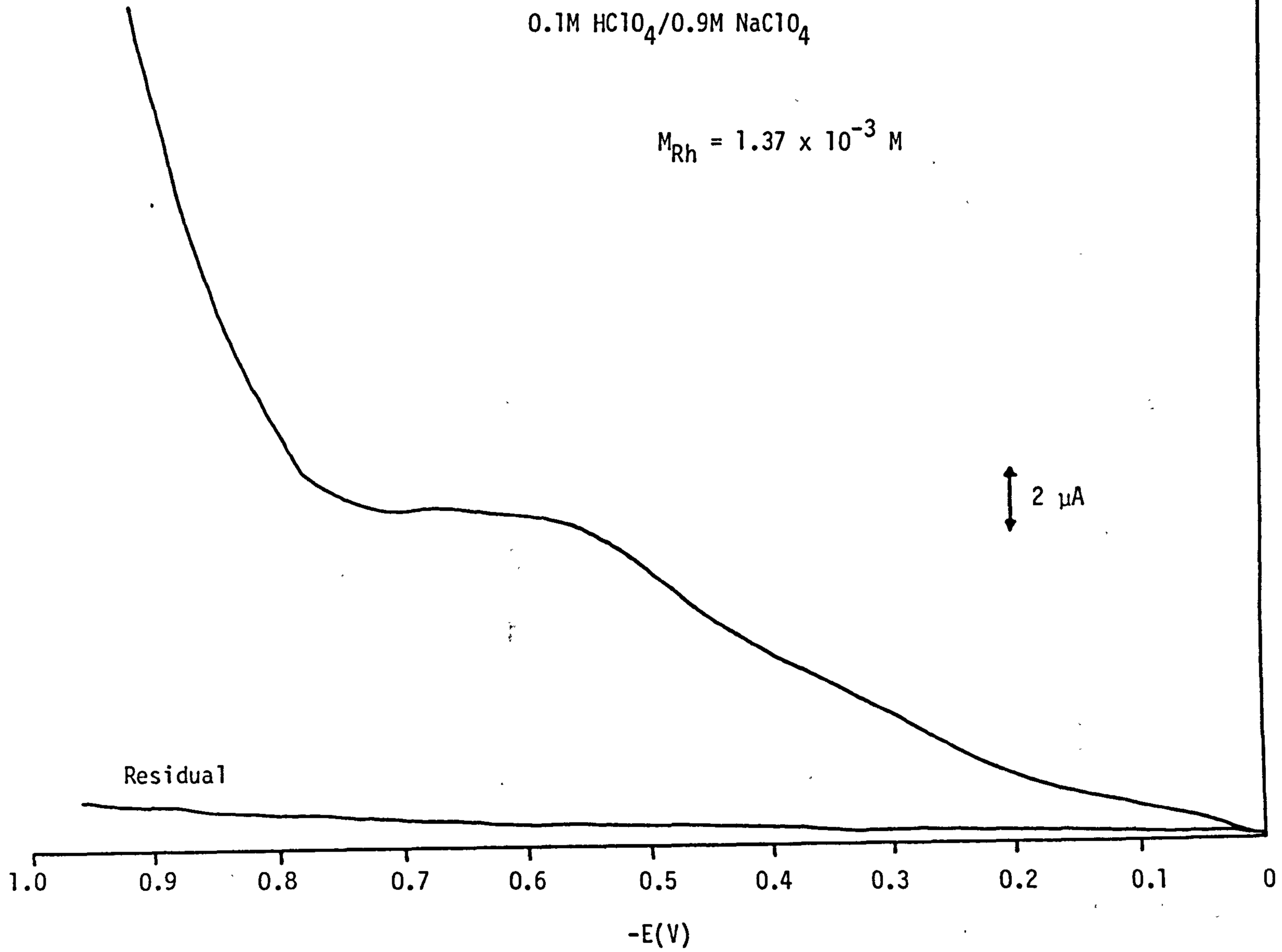

-E(V)	i(μA)	log i/i_d-i
0.05	0.35	-1.45
0.10	0.60	-1.20
0.15	1.00	-0.96
0.20	1.60	-0.73
0.25	2.60	-0.46
0.30	3.50	-0.28
0.35	4.70	-0.06
0.40	5.60	0.09
0.45	6.90	0.33
0.50	8.30	0.65
0.55	9.50	1.16

i_d = 10.15μA

Table 2.6.1. Current-potential data for the reduction of rhodium in 0.1M $HClO_4$/0.9M $NaClO_4$

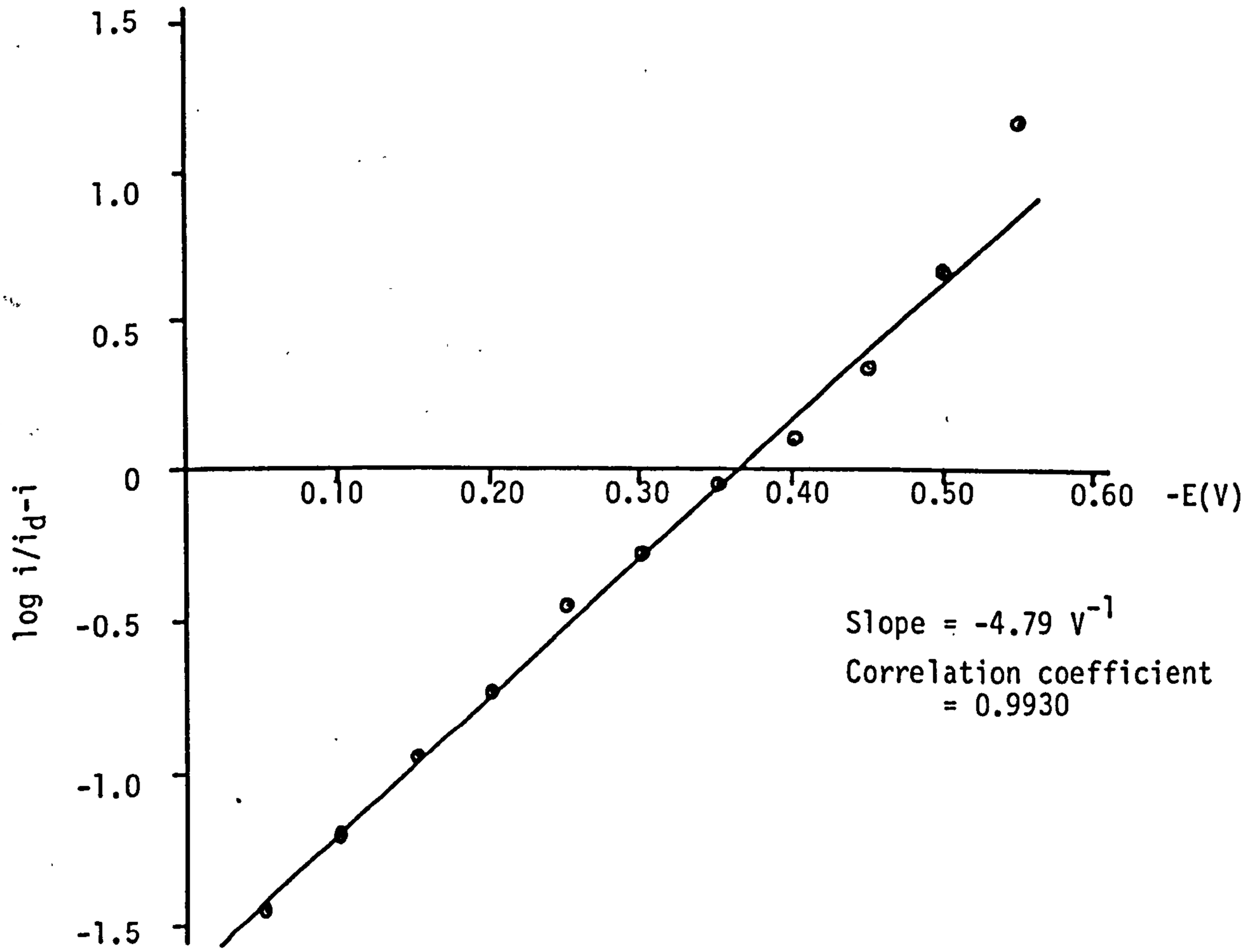

Figure 2.6.2. Plot of electrode potential against log i/i_d-i for the reduction of rhodium in 0.1M $HClO_4$/0.9M $NaClO_4$.

Although the value of n cannot be calculated from the plot of E vs log (i/i_d-i) in this case, it is possible to apply the Ilkovic equation (164) to determine n.

$$i_d = 607\ n\ D^{\frac{1}{2}}\ M^{2/3}\ t^{1/6}\ C \quad \ldots\ldots\ldots\ldots\ldots\ldots\ldots\ldots\ 2.11$$

where D = Diffusion coefficient, $cm^2.sec^{-1}$

M = Mercury flow rate, $mg.sec^{-1}$

t = Drop time, sec.

C = Concentration, mM

The diffusion coefficient, D, is normally obtained from conductance measurements by applying the Nernst equation (164). Conductivity data for rhodium compounds are scarce, but in the case of complex ions, the values of the corresponding cobalt complex ions can be used without any serious errors, since the mobility of such ions depends almost entirely on the relatively large volume of the coordinated groups, and D occurs as a square root in the Ilkovic equation. In the present case, the value of D is taken as 1.36×10^{-5} $cm^2.sec^{-1}$, this being the value obtained by Gaur and Goswami (165) for the cobalt aquo ion $\{Co(H_2O)_6\}^{2+}$ in sodium perchlorate. The electrode characteristic $M^{2/3}\,t^{1/6}$ was determined in the usual manner (section 5.6.4.) and found to be 1.74. Hence n from:

$$n = \frac{id}{607\ D^{\frac{1}{2}}\ M^{2/3}\ t^{1/6}\ C}$$

$$= \frac{10.15}{607 \times 3.69 \times 10^{-3} \times 1.74 \times 1.37}$$

$$= 1.90$$

The reduction of rhodium in 0.1M perchloric is therefore an irreversible two electron process:

$$Rh(H_2O)_6^{3+} + 2e^- \rightarrow Rh(H_2O)_6^{+} \quad \ldots\ldots\ldots\ldots\ldots\ldots\ldots\ldots\ 2.12$$

Polarograms of rhodium (III) sesquioxide in 0.1M nitric acid and 0.9M sodium nitrate are illustrated in Figures 2.6.3.-2.6.7. Current-potential data from these polarograms are given in Table 2.6.2., and the log $i/(i_d-i)$ vs E plots in Figure 2.6.8.

Two reduction waves are observed, the first of which has a half-wave potential of -0.235 ± 0.010 V and is irreversible. The dependence of the diffusion current (id) on the concentration of rhodium is illustrated in Figure 2.6.9. A linear relationship is observed, and it may be possible to apply this to the analytical determination of rhodium in nitrate solutions. The n values have again been determined by application of the Ilkovic equation, (equation 2.11), and are given in Table 2.6.3. It is seen that non-integral n values are obtained (mean n = 2.41).

The main difference between the polarographic reduction of rhodium in nitric and perchloric acids, is in the value of the half-wave potential $E_{\frac{1}{2}}$. In nitric acid the reduction occurs at a higher potential (-0.235 V) then in perchloric acid (-0.365V). In an extensive study of the reduction of hexamine cobaltic chloride, Laitinen et.al. (166) observed that the values of $E_{\frac{1}{2}}$ and i_d were dependent on the supporting electrolyte used. The authors interpreted these observations as being due to the formation of outer-sphere complexes with the anions of the supporting electrolyte. The direction in which the half-wave potential

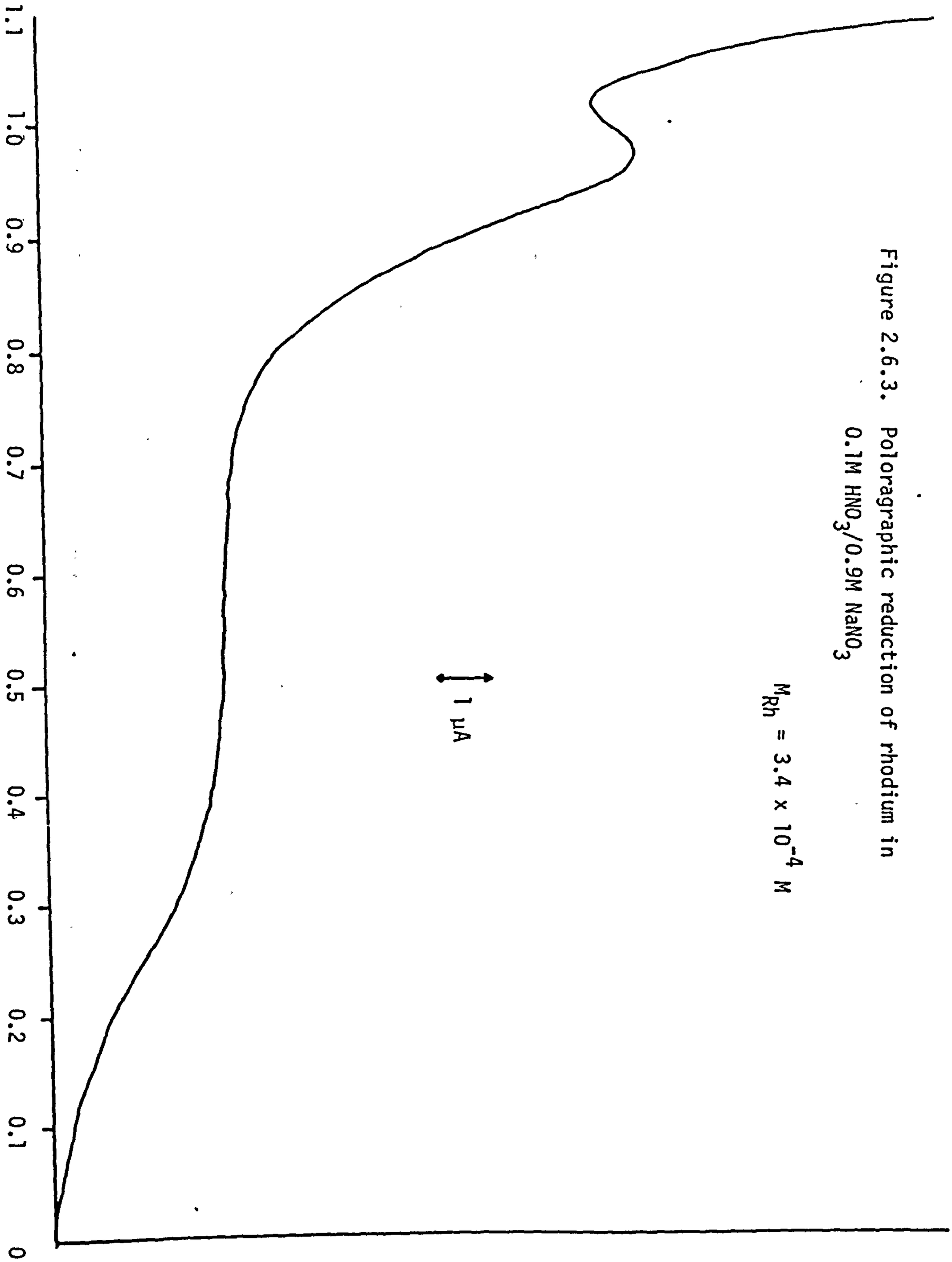

Figure 2.6.3. Polaragraphic reduction of rhodium in 0.1M HNO_3/0.9M $NaNO_3$

$M_{Rh} = 3.4 \times 10^{-4}$ M

Figure 2.6.4. Polarographic reduction of rhodium in 0.1M HNO_3/0.9M $NaNO_3$

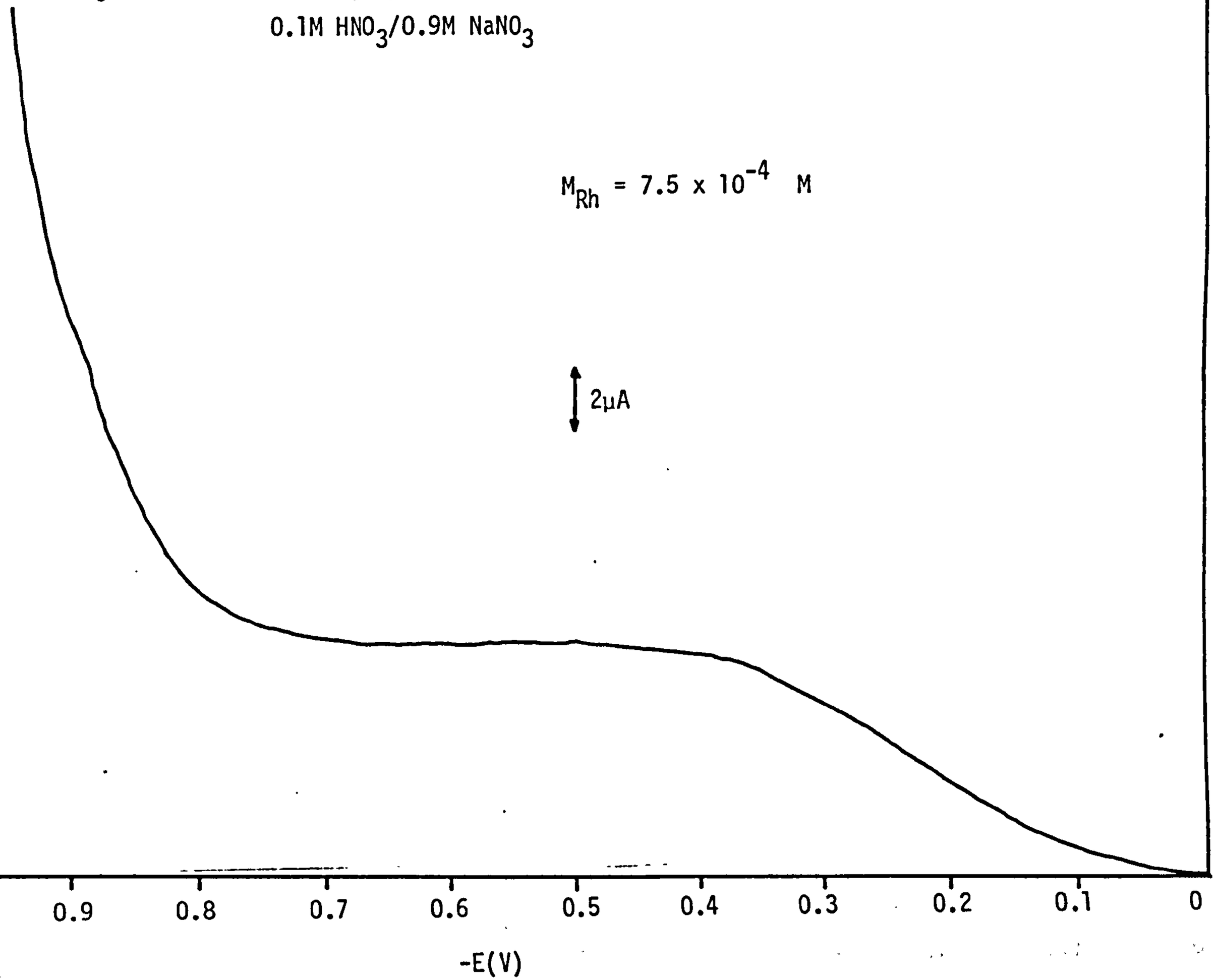

Figure 2.6.5. Polarographic reduction of rhodium in 0.1M HNO_3/0.9M $NaNO_3$

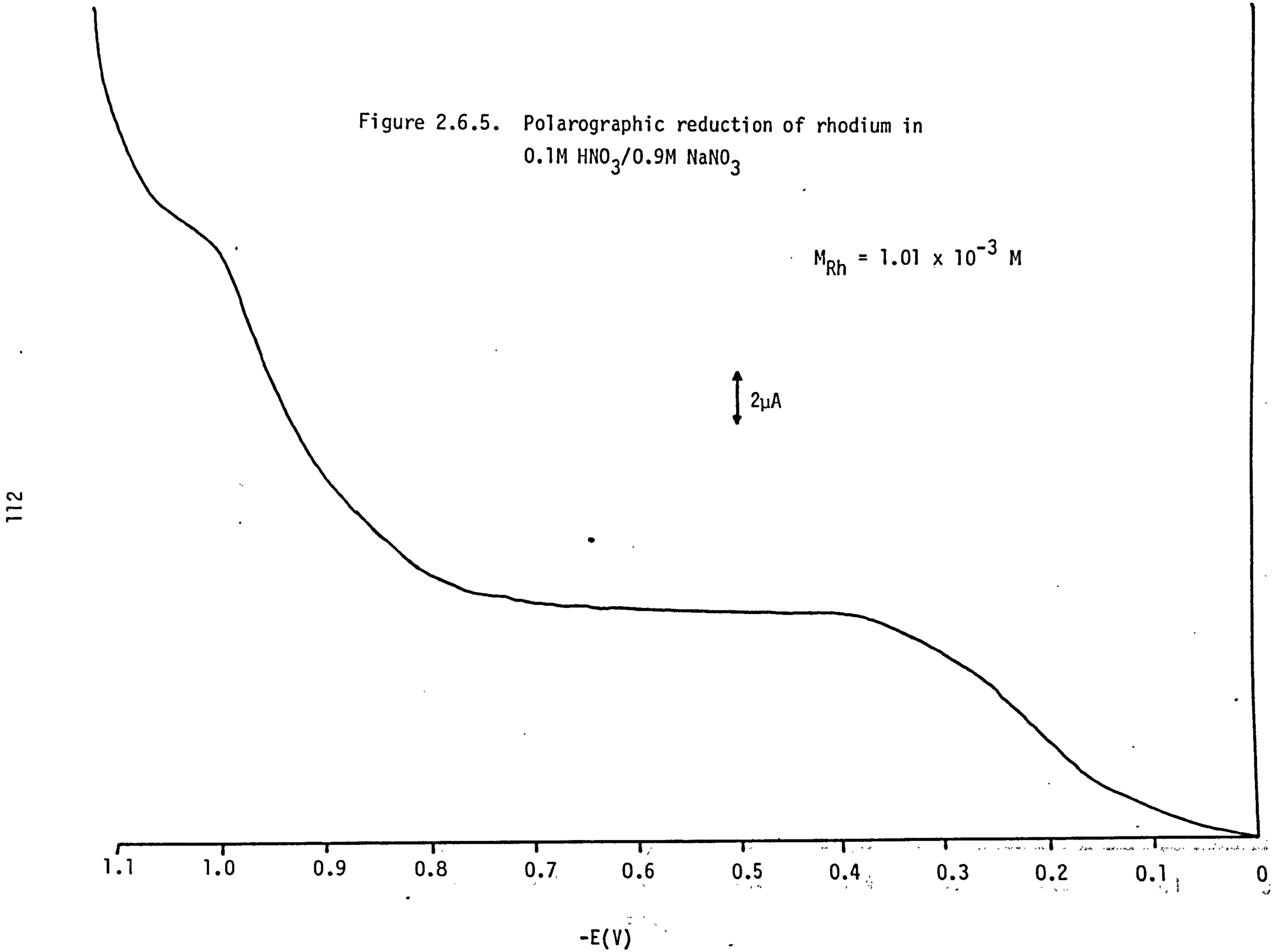

Figure 2.6.6. Polarographic reduction of rhodium in 0.1M HNO_3/0.9M $NaNO_3$

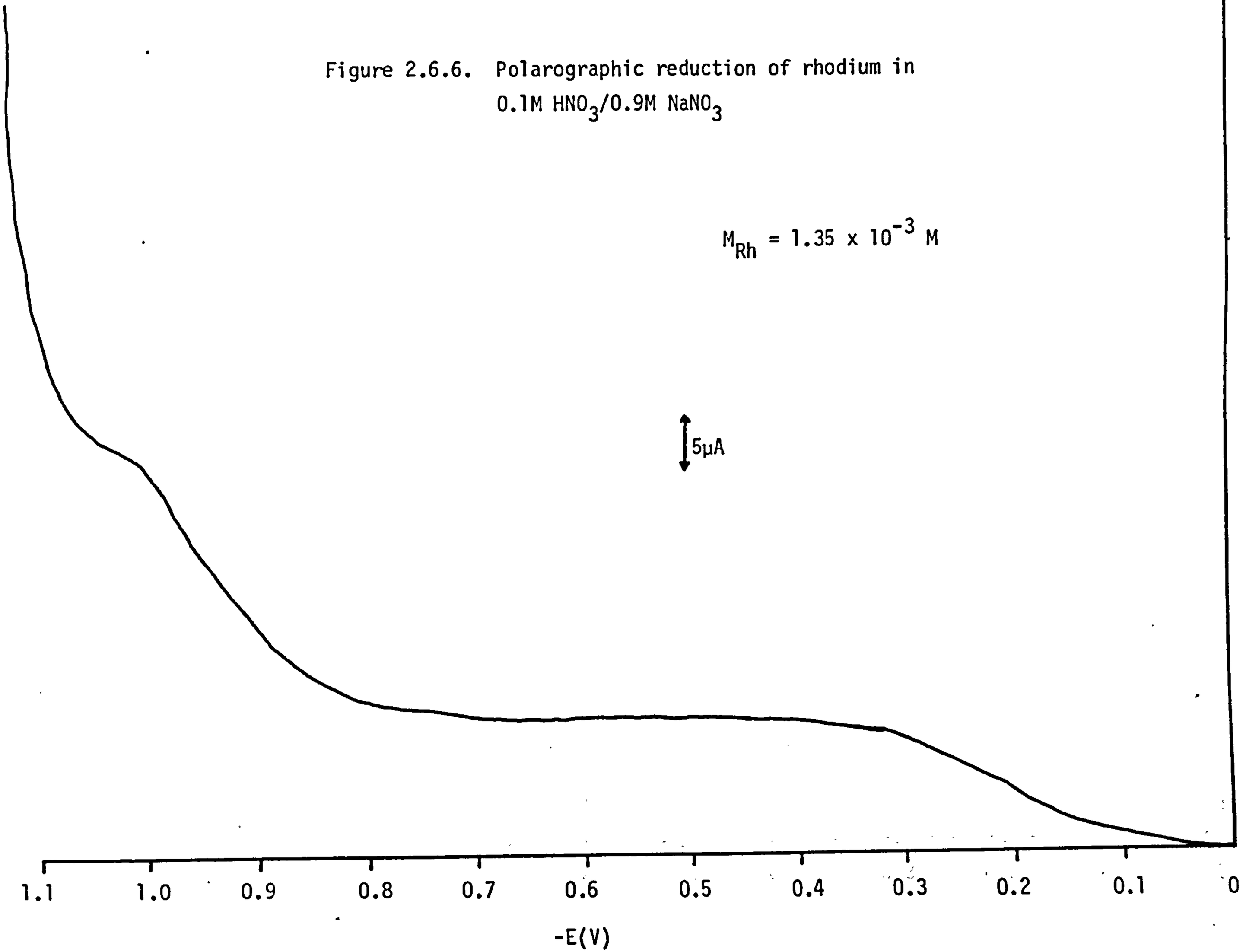

Figure 2.6.7. Polarographic reduction of rhodium in 0.1M HNO_3/0.9M $NaNO_3$

$M_{Rh} = 1.72 \times 10^{-3}$ M

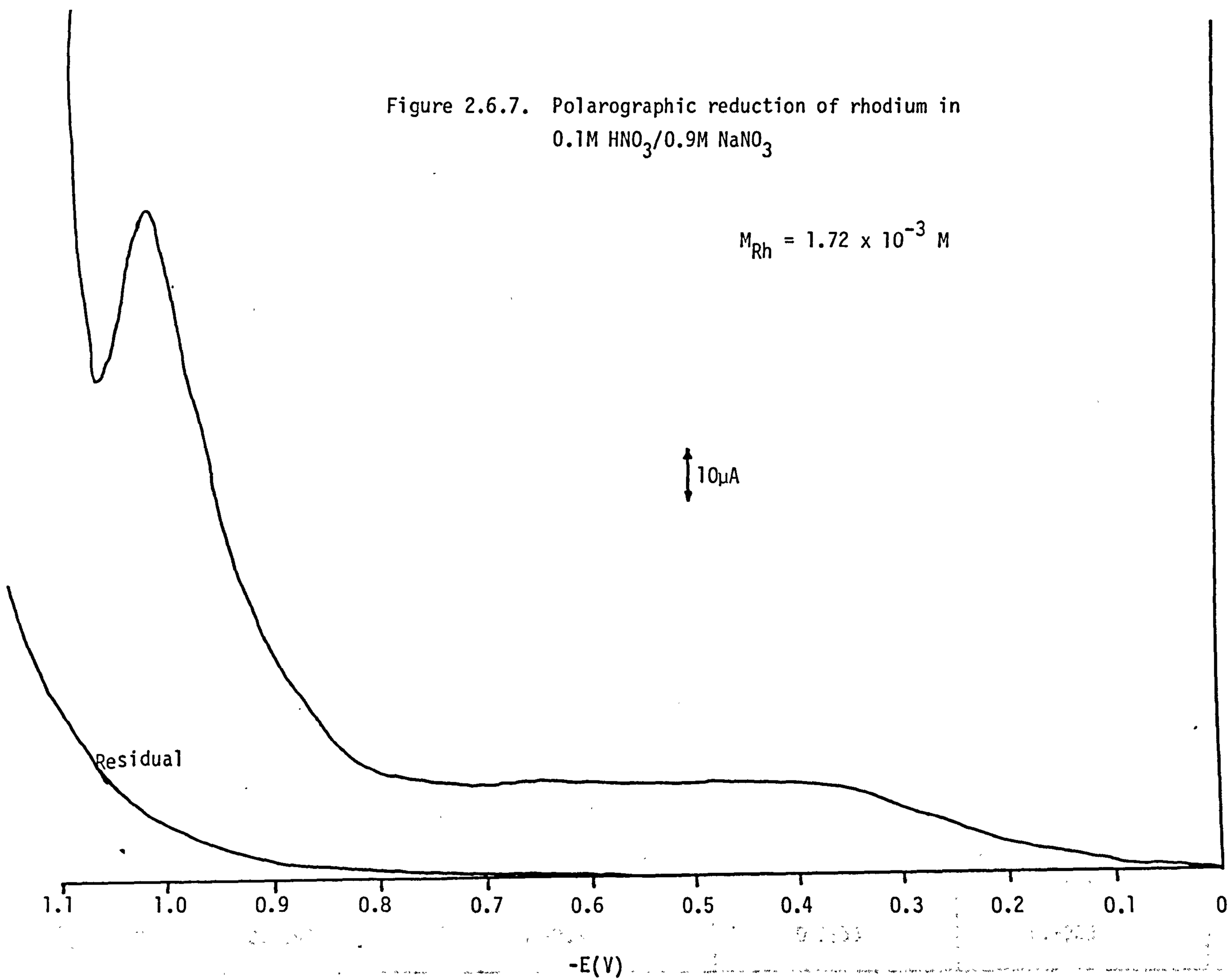

Table 2.6.2. Current-potential data for the reduction of rhodium(III) in 0.1M HNO_3/0.9M $NaNo_3$

	Fig. 2.6.3.		Fig. 2.6.4.		Fig. 2.6.5.		Fig. 2.6.6.		Fig. 2.6.7.	
E(V)	i	log i/i_d-i	i	log i/i_d-i	i	log i/i_d-i	i	log i/i_d-i	i	log i/i_d-i
0.05	0.19	-1.20	0.50	-1.13	0.25	-1.52	0.31	-1.60	0.63	-1.43
0.10	0.38	-0.88	1.00	-0.80	0.95	-0.91	1.25	-0.95	1.75	-0.95
0.15	0.68	-0.58	1.60	-0.55	2.00	-0.52	2.63	-0.57	3.38	-0.62
0.20	1.13	-0.28	2.75	-0.21	3.75	-0.11	5.00	-0.18	6.00	-0.28
0.25	1.75	0.08	4.20	0.15	5.50	0.25	7.88	0.23	9.38	0.07
0.30	2.25	0.37	5.40	0.48	7.00	0.64	10.00	0.60	12.88	0.46
0.35	2.69	0.71	6.38	0.89	8.00	1.12	11.38	1.01	15.88	1.03
0.40	3.00	1.14	7.00	1.55	8.50	1.93	12.25	1.69	16.88	1.53
0.45	3.12	1.50	7.10	1.85	8.55	2.23	12.38	2.01	17.25	2.12
0.50	3.19	2.03	-	-	-	-	-	-	-	-
Slope (V^{-1})	-6.98		-7.51		-9.18		-7.81		-8.56	
Correlation Coefficient	0.9969		0.9934		0.9953		0.9969		0.9946	

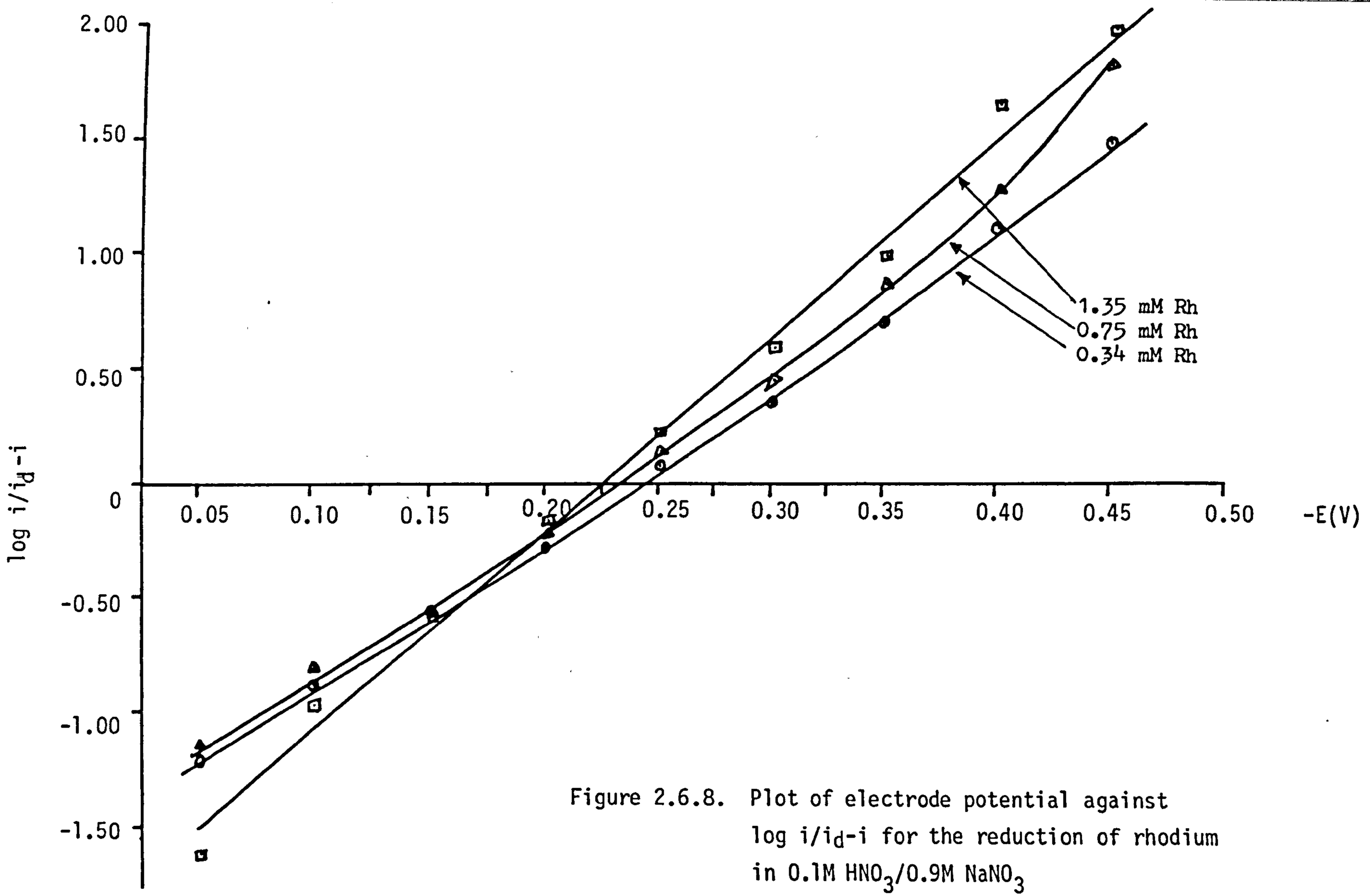

Figure 2.6.8. Plot of electrode potential against log i/i_d-i for the reduction of rhodium in 0.1M HNO_3/0.9M $NaNO_3$

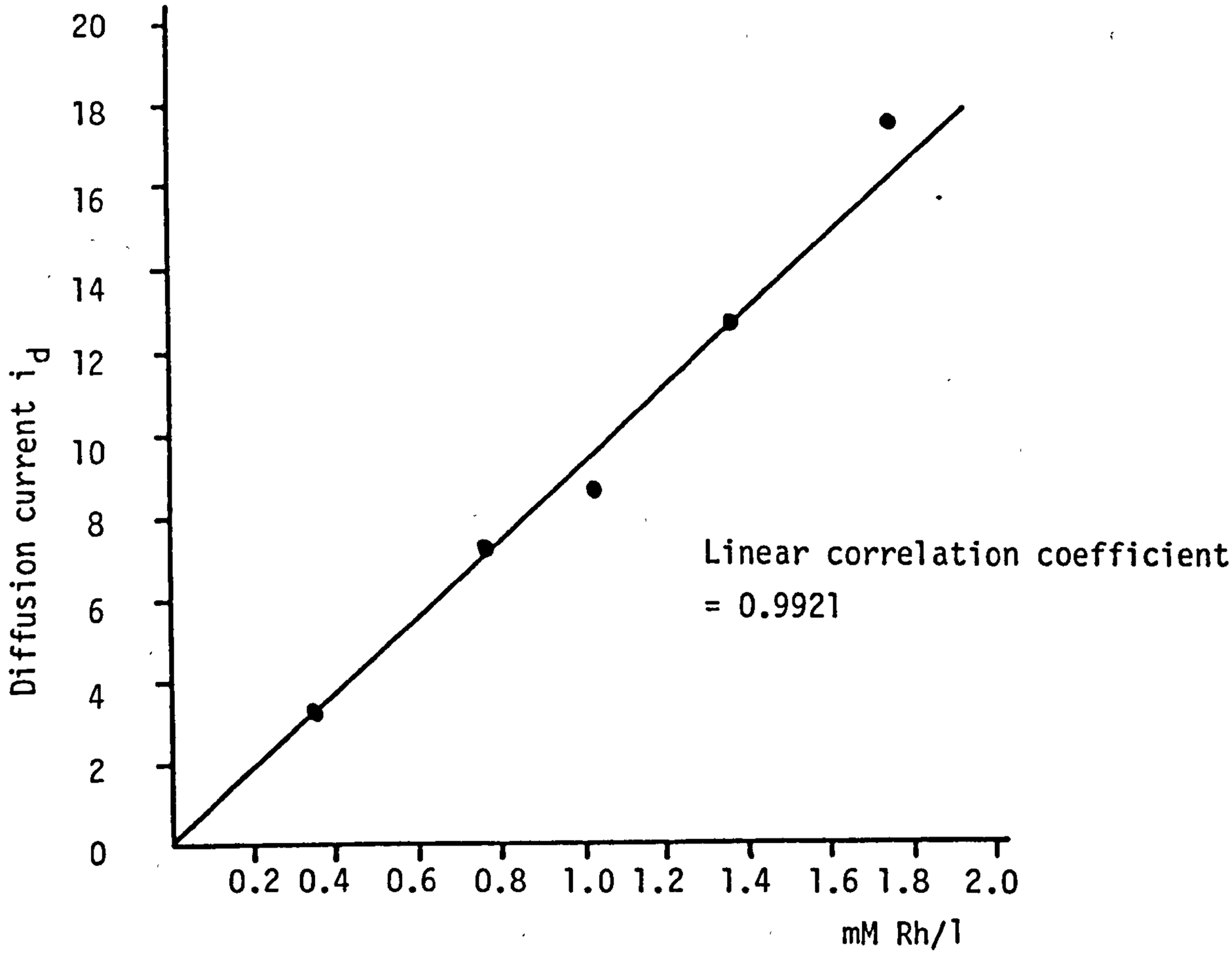

Figure 2.6.9 Dependence of the diffusion current id on the concentration of rhodium (mM/l)

Scan No	i_d (μA)	mMRh	n
1	3.22	0.34	2.43
2	7.20	0.75	2.46
3	8.60	1.01	2.18
4	12.50	1.35	2.37
5	17.38	1.72	2.59

Table 2.6.3. Number of electrons transferred (n) for the first reduction wave in nitric acid.

shifted was an indication of the coordinating power of the ligand, i.e. a shift to lower potentials indicates a stronger complexing ability and vice versa. In the present case the shift of $E_{\frac{1}{2}}$ to a higher potential in nitric acid may be attributed to outer-sphere rhodium (III) nitrato complexes, such as observed by ^{103}Rh NMR studies.

Analysis of the second reduction wave in nitric acid is difficult because of the accompanying reduction of the supporting electrolyte (see Figure 2.6.7.). Application of the Ilkovic equation proved unsuccessful, giving n values between 2.3 and 16.4. The half-wave potential was estimated graphically from the best of the curves (Figure 2.6.6.) and was found to be 0.94 ± 0.02V.

If it is assumed that the first reduction wave is a two electron process, then the second wave represents a further one electron reduction of $\{Rh(H_2O)_6\}^+$ to rhodium metal. In common with other transition metals, in particular the other platinum group metals (41) and technetium (167), the rhodium metal, probably present as an amalgam with mercury, will tend to catalyse the reduction of hydrogen ions in solution. In fact, the catalytic influence on the hydrogen discharge at the mercury electrode is more intense for rhodium than it is for platinum (41). This would account for the sharp rise in the current-potential curve for the second wave, which occurs at least 0.05V before the reduction of the supporting electrolyte (Figure 2.6.7).

2.6.2. Polarography of Rhodium (III) Nitrites

The effect of nitrite ion on the first reduction wave in 0.1M nitric acid and 0.9M sodium nitrite, is to shift the value of $E_{\frac{1}{2}}$ to a more

Figure 2.6.10. Polarographic reduction of rhodium in 0.1M HNO_3/0.9M $NaNO_2$

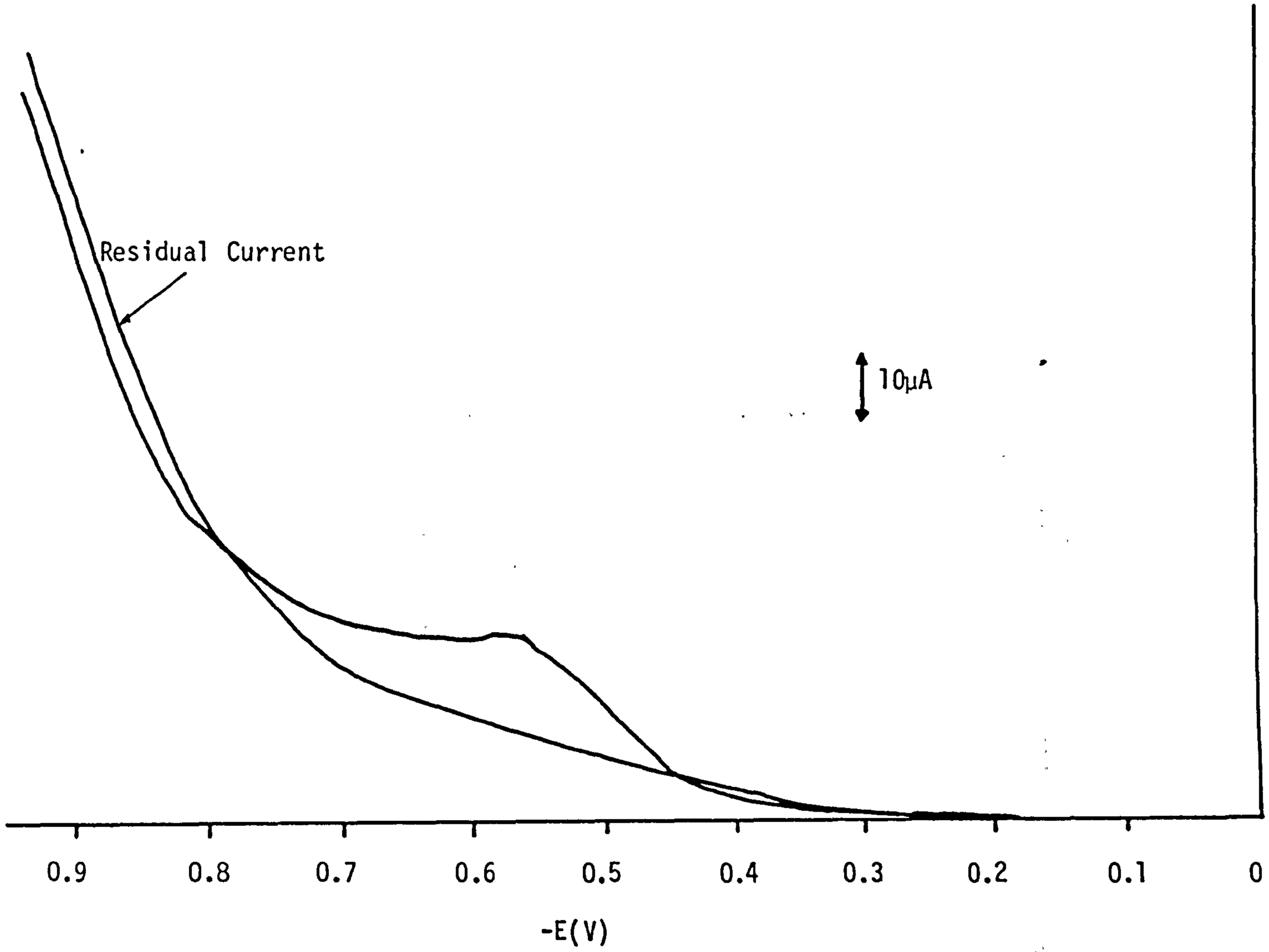

-E(V)	i(μA)	log i/i_d-i
0.45	1.25	-0.97
0.46	3.50	-0.43
0.47	5.00	-0.20
0.48	6.25	-0.03
0.49	8.75	0.31
0.50	9.50	0.43
0.51	10.00	0.52
0.52	11.75	0.97
0.53	12.50	1.40

i_d = 13μA at 0.55 V

Table 2.6.4. Current-potential data for the reduction of rhodium in 0.1M HNO_3/0.9M $NaNO_2$

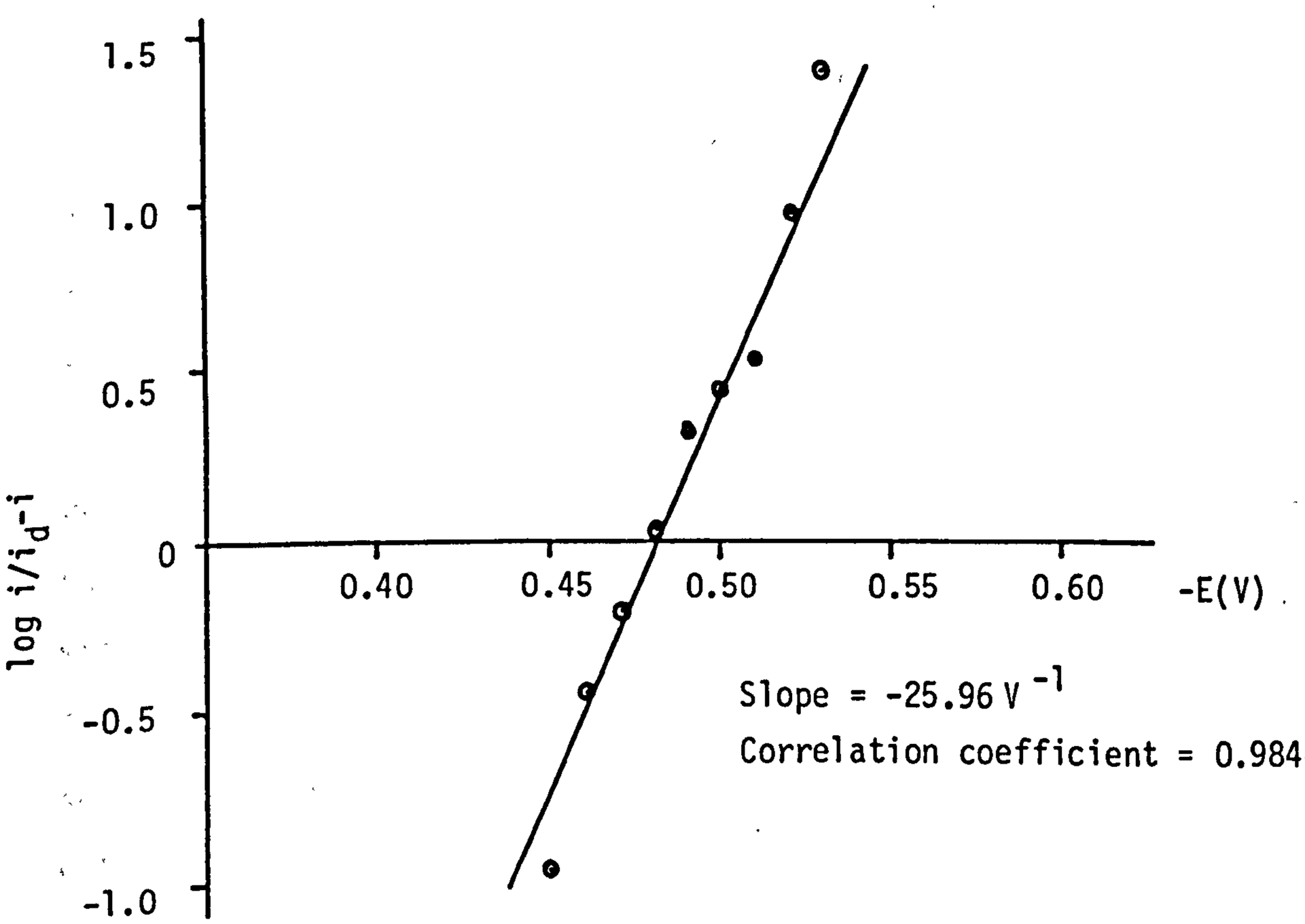

Figure 2.6.11. Plot of electrode potential against log i/i_d-i for the reduction of rhodium in 0.1M HNO_3/0.9M $NaNO_2$

negative potential. As can be seen from the polarogram recorded in Figure 2.6.10., the $E_{\frac{1}{2}}$ value has shifted from -0.235 V (for $\{Rh(H_2O)_6\}^{3+}$) to -0.48V. Application of the Heyrovsky-Ilkovic equation is made difficult because of the accompanying reduction, (the residual wave) of the supporting electrolyte. The main contribution of this residual current must be due to the reduction of nitrite ion, since the previous work (Figure 2.6.7) has shown that the reduction of the nitrate ion does not begin until a potential of -0.80V is reached. Nevertheless, the Heyrovsky-Ilkovic equation has been applied to the current-potential data taken from between -0.45V and -0.53V (Table 2.6.4.). The plot of $\log(i/i_d-i)$ vs E, Figure 2.6.11., gave a slope equal to 25.96V, indicating an irreversible reduction process.

The contribution of the residual electrolyte current to the overall reduction current can be reduced by increasing the rhodium concentration in solution, and also keeping the nitrite concentration in solution to below 0.1M. Figure 2.6.12. shows the polarogram obtained for rhodium (III) sesquioxide in 0.1M HNO_3/0.9M $NaNO_3$ supporting electrolyte, and varying concentrations of sodium nitrite (1-10mM).

Analysis of the polarogram obtained with the lowest concentration of sodium nitrite, i.e. 1mM, shows the reduction wave to be irreversible, with $E_{\frac{1}{2}}$ = -0.26V (Table 2.6.5., Figure 2.6.13). It is clear to see from Figure 2.6.12, that increasing nitrite concentration not only shifts $E_{\frac{1}{2}}$ to more negative potentials, indicating the presence in solution of several types of complex with a different number of nitrite ligands, but also produces a pronounced maximum on the reduction

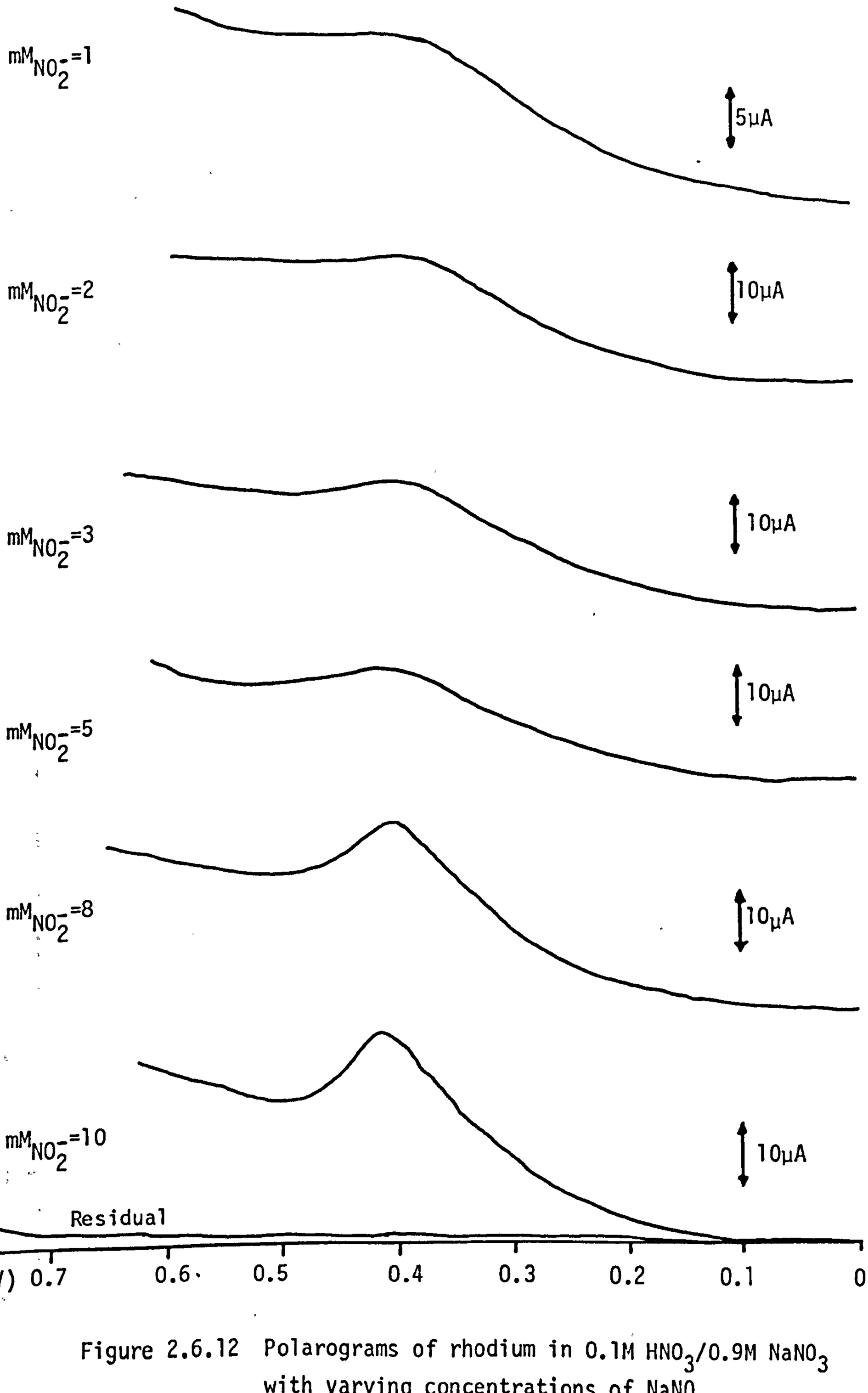

Figure 2.6.12 Polarograms of rhodium in 0.1M HNO_3/0.9M $NaNO_3$ with varying concentrations of $NaNO_2$

-E(V)	i(μA)	log i/i_d-i
0.05	0.63	-1.36
0.10	1.56	-0.93
0.15	2.50	-0.70
0.20	4.13	-0.42
0.25	6.75	-0.09
0.30	10.00	0.30
0.35	13.80	1.04
0.40	15.00	-
0.45	15.00	-

i_d = 15.00 μA

Table 2.6.5. Current-potential data for the reduction of rhodium in 0.1M HNO_3/0.9M $NaNO_3$, in the presence of 1mM $NaNO_2$.

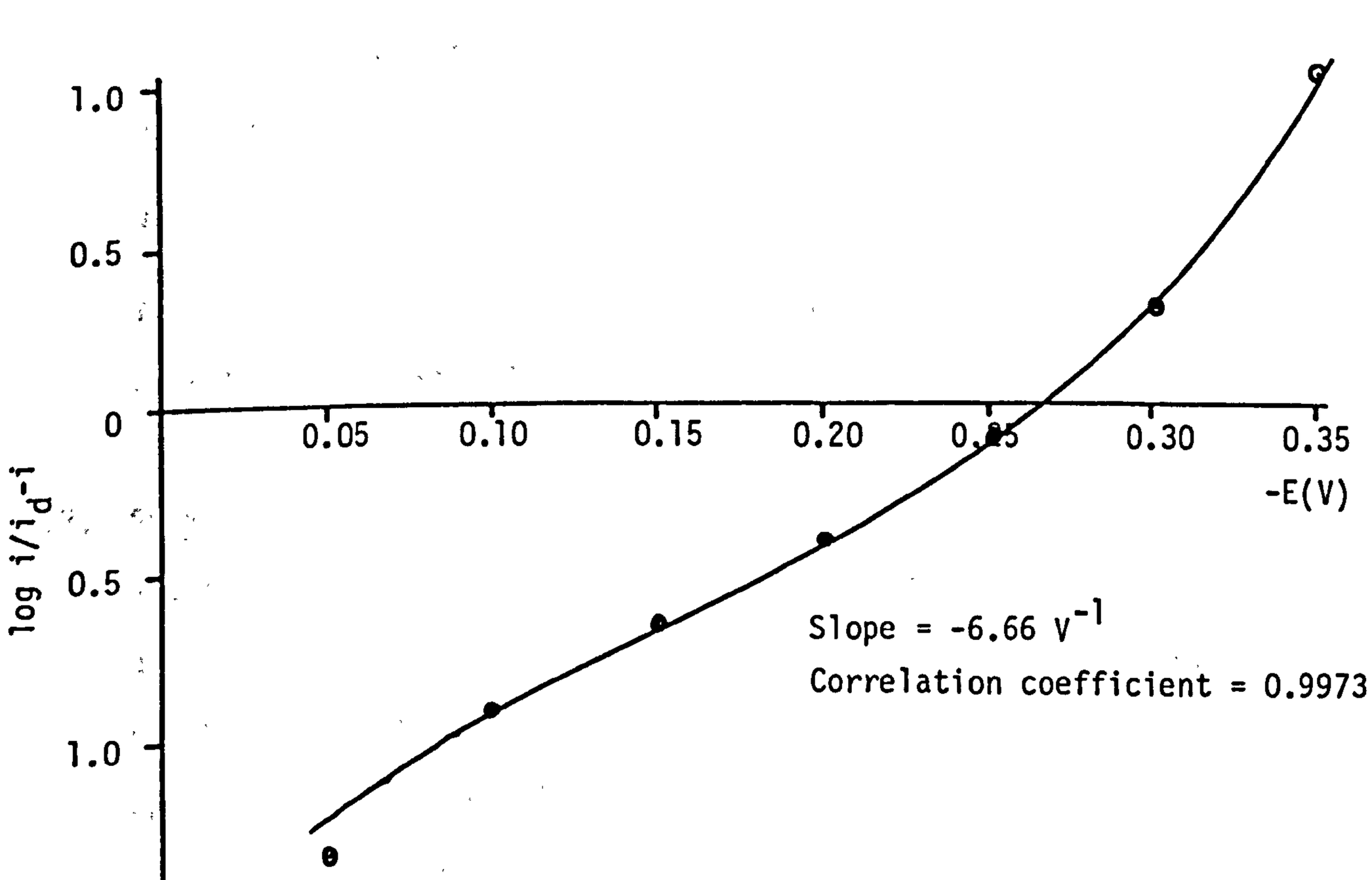

Figure 2.6.13. Plot of electrode potential against log i/i_d-i for the reduction of rhodium in 0.1M HNO_3 / 0.9M $NaNO_3$ and 1mM $NaNO_2$.

wave. These maxima could not be suppressed by further addition of Triton X-100 or gelatin. This makes it extremely difficult to estimate with any certainty the value of the diffusion current i_d. It is not clear why these maxima should appear at the higher nitrite concentrations. Heyrovsky and Ilkovic (168) have attributed such phenomena to an absorption of electroreducible species on the growing mercury drops, hence increasing the concentration of the reducible species above its true value in the bulk of the solution.

The polarographic data for rhodium is summarised in Table 2.6.6. From the values of $E_{\frac{1}{2}}$ it is possible to determine an order of complexation of the ligands for rhodium. Clearly, from this study as well as the previous work, the nitrate and perchlorate ions are seen to be essentially non-coordinating. The nitrite ion, by virtue of the shift in $E_{\frac{1}{2}}$ to more negative potentials, readily complexes with rhodium. The order of complexability then is:

$$NO_2^- > H_2O > NO_3^- \simeq ClO_4^-$$

This is exactly the order determined by Huheey (169) who considered only the field strengths of the ligands.

2.7. SUMMARY

The electrophoresis, electronic absorption measurements and ion-exchange experiments have shown that in nitric acid the predominant rhodium species is the hexaaquo rhodium (III) ion, $\{Rh(H_2O)_6\}^{3+}$. ^{103}Rh NMR spectroscopy has indicated the presence of the pentaaquonitrato rhodium (III) complex, $\{Rh(H_2O)_5NO_3\}^{2+}$, although both electrophoresis

Table 2.6.6. Summary of polarographic data for rhodium (III)

Substance	Supporting electrolyte	$E_{\frac{1}{2}}$(V SCE)	n	I	Remarks
Rh (III)	0.1M $HClO_4$, 0.9M Na ClO_4	-0.365	2	4.26	irr
Rh (III)	0.1M HNO_3, 0.9M $NaNO_3$	-0.235 (1st wave) -0.94 (2nd wave)	(2.4)	5.40	irr
Rh (III)	0.1M HNO_3, 0.9M $NaNO_3$ 10^{-3}M $NaNO_2$	-0.26			irr
Rh (III)	0.1M HNO_3, 0.9M $NaNO_2$	-0.48			irr

I = Diffusion current constant = $id/CM^{2/3}t^{1/6}$

and the ion-exchange experiments failed to show the presence of a second major species.

In the presence of nitrite ions, ^{103}Rh NMR spectroscopy has shown the existence of several complexes of the type $\{Rh(H_2O)_{6-n}(NO_2)_n\}^{(3-n)+}$, Table 2.7.1.

Polarography of rhodium (III) in nitric acid produced two irreversible reduction waves. The first wave, at $E_{\frac{1}{2}}$ -0.235V probably represents a two electron reduction of Rh(III) to Rh(I). This is followed by a second wave at $E_{\frac{1}{2}}$ -0.94V for the reduction of Rh(I) to Rh(0). The shifts in the half-wave potentials have also served to confirm that the nitrate and perchlorate ion are essentially non-coordinating, as far as rhodium (III) is concerned, but that the nitrite ion does form strong complexes with rhodium.

In conclusion, the rhodium speciation in stored highly active waste solutions (1-3M HNO_3), will range from $\{Rh(H_2O)_6\}^{3+}$, to a series of complexes of the type $\{Rh(H_2O)_{6-n}(NO_2)_n\}^{(3-n)+}$ depending on the nitrite concentration.

TABLE 2.7.1. ^{103}Rh Chemical Shifts for $\{Rh(H_2O)_{6-n}(NO_2)_n\}^{(3-n)+}$ in Nitric Acid

Species	(^{103}Rh)/ppm
$\{Rh(H_2O)_6\}^{3+}$	9888
$\{Rh(H_2O)_5NO_3\}^{2+}$	9457
$\{Rh(H_2O)_5(NO_2)\}^{2+}$	8578
$\{Rh(H_2O)_4NO_2NO_3\}^{+}$	8097
cis $\{Rh(H_2O)_4(NO_2)_2\}^{+}$	7260
trans $\{Rh(H_2O)_4(NO_2)_2\}^{+}$	7437
fac $\{Rh(H_2O)_3(NO_2)_3\}$	6937
mer $\{Rh(H_2O)_3(NO_2)_3\}$	7038
cis $\{Rh(H_2O)_2(NO_2)_4\}^{-}$	6432
trans $\{Rh(H_2O)_2(NO_2)_4\}^{-}$	6606
$\{Rh(H_2O)(NO_2)_5\}^{2-}$	6211
$\{Rh(NO_2)_6\}^{3-}$	6008

CHAPTER THREE

SOLVENT EXTRACTION OF RHODIUM

3.1. FOREWORD

Studies on the solvent extraction of rhodium from aqueous chloride media have been extensive, primarily because of the problems associated with isolating rhodium from the rest of the platinum group metals in their chloride concentrates. The solvent extraction behaviour of rhodium in aqueous nitrate media, however, is less established. Lunichkina and Renard (146) reported the extraction of rhodium by tri-n-octylamine and di-isoamyl methylphosphonate from an aqueous feed solution which was low in nitric acid concentration (0.1M), but high in added salt concentration (1-2M $Al(NO_3)_3$). Pohlandt (144) reported 20% maximum extraction of rhodium by octylaniline/DIBK from 2-14M nitric acid. Fritsch et.al. (171, 172) showed that rhodium could be extracted from 3-4M nitric acid, by organo-sulphides such as dibutyl or dioctyl sulphide, although equilibration times were long (3-4 hrs). The speciation studies in Chapter Two showed that the rhodium species present in nitric acid depends on the concentration of nitrite ion in solution. The obvious route for recovering rhodium is therefore to form the anionic nitrite complex and extract this with an amine. Beer et.al. (170) showed that this was possible by extracting the complex, $\{Rh(NO_2)_6\}^{3-}$ with tri-n-octylamine. However, the extraction only occurs at a pH of between 2-4 and would thus require the prior removal of a significant amount of the fission products before the nitric acid concentration could be reduced.

High level waste of composition given in Table 1.4.4. is stored in 1-3M nitric acid, in high integrity stainless steel tanks. Before reprocessing it would need to be adjusted to 6M nitric acid, to avoid sludge formation, and diluted to contain no more than 10g/l of fission products. The work presented in this chapter looks at the recovery of rhodium from such waste solutions, and outlines an integrated scheme for its isolation.

3.2. PRELIMINARY STUDIES

The aim of these preliminary studies was to discover a suitable reagent, or reagents which could extract rhodium from nitrate solutions with a distribution coefficient greater than 0.2. To allow a rapid assessment of a wide range of reagents, the well documented technique of reversed phase paper chromatography and the more standard shake-out tests were employed.

The aqueous acid concentration range investigated has been generally restricted to 0.1-6M HNO_3. A concentration of 6M HNO_3 is required to prevent sludge formation, while higher concentrations are not preferred because of corrosion problems. The lower limit of 0.1M HNO_3 was established since below this concentration of acid, rhodium forms numerous hydroxy species (34, 173) which could have complicated its solvent extraction behaviour.

The organic diluent preferred by the nuclear industry is odourless kerosene, and wherever possible, this diluent has been used to dissolve the various extractants investigated.

3.2.1. Reversed Phase Paper Chromatography

Reversed phase paper chromatography has been used by numerous workers to study the separation of metal ions from aqueous acid solutions (174-177). In this procedure, a strip of paper (e.g.Whatman No. 1 filter paper) was soaked in the organic phase, dried, and then spotted at the base with the rhodium containing aqueous phase. The paper strip was then placed in a chromatographic tank containing the aqueous mobile phase. On elution, the rhodium spot either remained on the base-line, indicating association with the organic phase and hence extraction, or was carried with the mobile phase, indicating weak or no association and hence no extraction. Full experimental details are given in Section 5.6.5.

Lunichkina and Renard (146) and Pohlandt (144) both reported on the extraction of rhodium from nitric acid by amines. Thus, a primary, secondary and tertiary amine were tested using reversed phase paper chromatography, together with chelating agents such as theonyltrifluoroacetone (HTTA), LIX 34 (8-alkylarylsulponamidoquinoline) and SME 418 (2-ethylhexyl phosphoric acid mono-2-ethylhexyl ester). The results are displayed in Figures 3.2.1. and 3.2.2. as R_f against $\{HNO_3\}$ plots,

$$\text{where } R_f = \frac{\text{Distance moved by Rh spot from the base-line}}{\text{Distance moved by the solvent front from the base-line}} \quad \ldots\ldots 3.0$$

Figures 3.2.1. and 3.2.2. reveal that at low nitric acid concentrations, all the rhodium is retained on the base-line, i.e. is strongly extracted by the reagent, while at higher nitric acid concentrations, only HTTA appears to partially extract rhodium. The possible extraction mechanism for this latter process is probably simply:

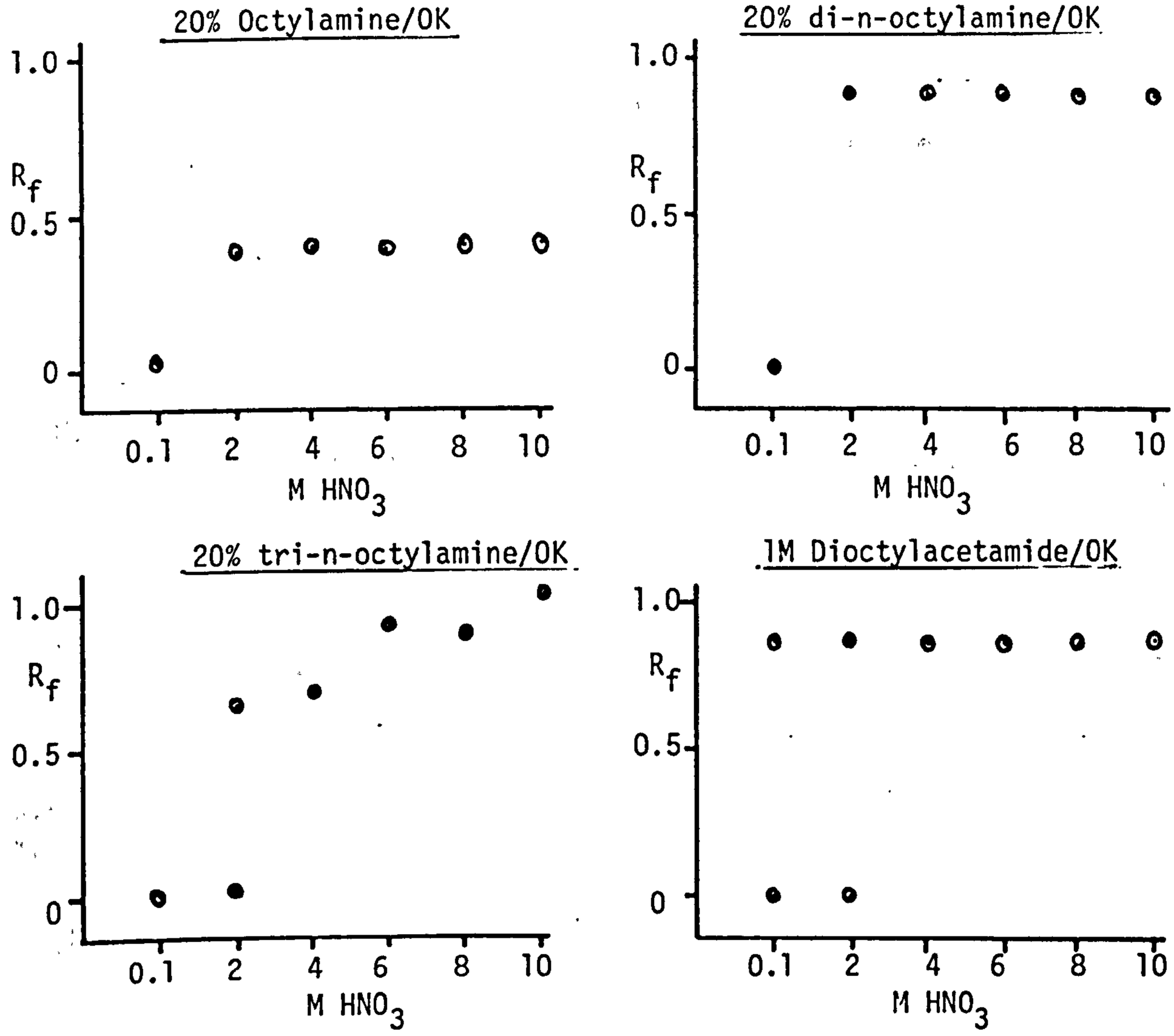

Figure 3.2.1. Reversed phase paper chromatographic plots of R_f against $\{HNO_3\}$

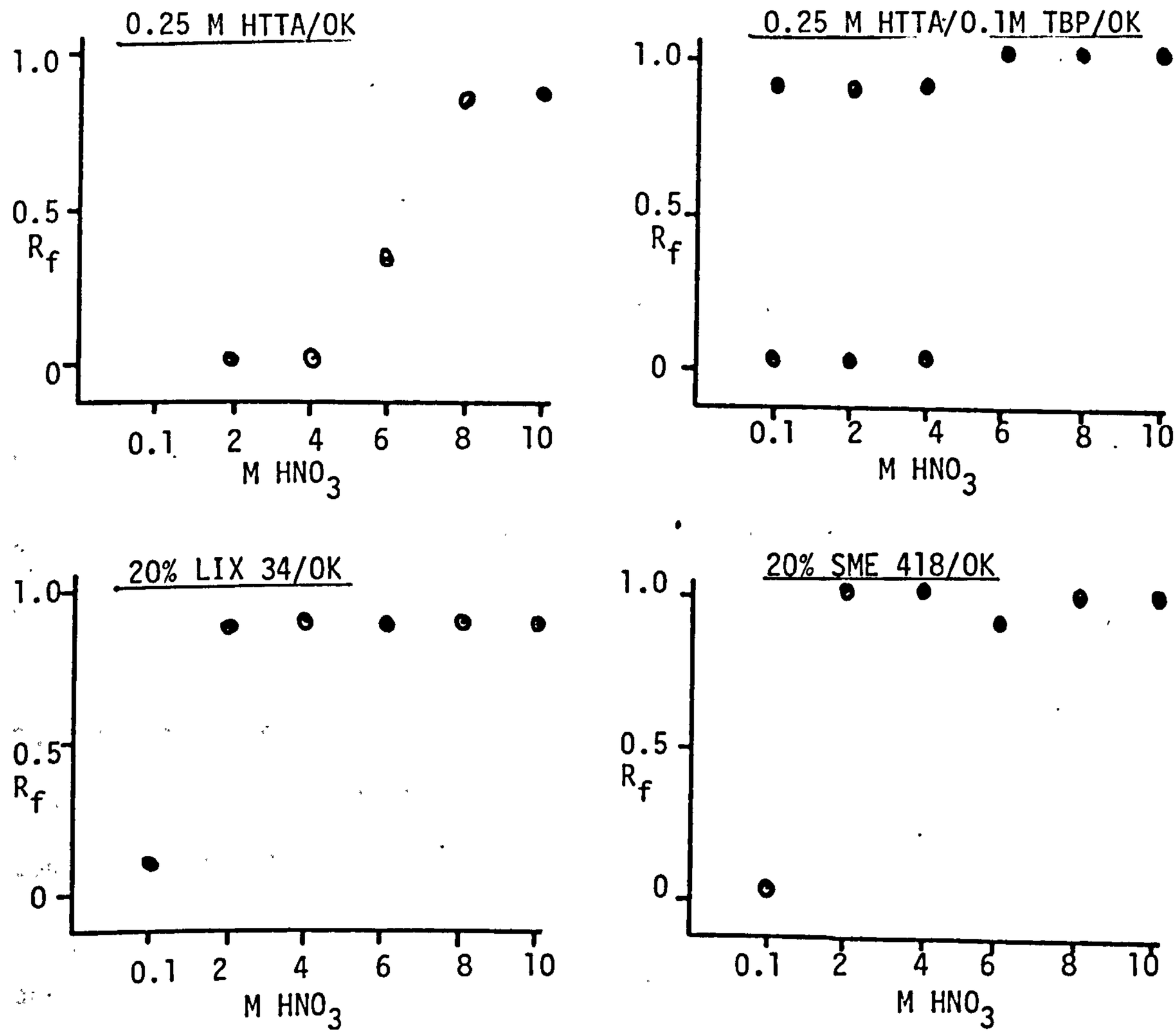

Figure 3.2.2. Reversed phase paper chromatographic plots of R_f against $\{HNO_3\}$

$$\{Rh(H_2O)_6\}^{3+} + \overline{3HL} = \overline{RhL_3} + 6H_2O + 3H^+ \quad \text{.....3.1}$$

The bar denotes the organic phase.

The partial extraction, at low nitric acid concentrations, by amines may be due to a rather unusual mechanism:

$$3NO_3^- + \{Rh(H_2O)_6\}^{3+} + \overline{nR_3N} = \overline{\{Rh(H_2O)_{6-n}(R_3N)_n\ (NO_3)_3\}} \quad \text{.....3.2}$$

At high nitric acid concentrations, the amine equilibrium below becomes prevalent:

$$\overline{R_3N} + HNO_3 = \overline{R_3NH^+NO_3^-} \quad \text{.....3.3}$$

and thus the amine can no longer replace the water molecules in the hexaaquo complex.

Subsequent shake-out tests (see section 3.2.2.), in which the amines and HTTA organic phases were equilibrated with equal volumes of rhodium containing aqueous phases showed no significant extraction of rhodium ($D_{Rh} < 0.01$). The reversed phase paper chromatography gave either an anomalous result, or a greater equilibration time was required. Generally, the literature has shown good agreement between reversed phase paper chromatography and subsequent shake-out tests (175, 176), although anomalies have been found. Elliott and Banks (177) found that U(VI) and Th(IV) were retained on the base-line, on paper impregnated with tri-n-octylphosphine sulphide (TOPS), when eluted with 5 or 7M HNO_3. In subsequent shake-out tests however, no extraction of U(VI) or Th(IV) was observed. No explanation for these results was offered, but it is quite probable that apart from the formation of complexes between the

metal ions and the impregnated reagents, the metal ions could also be strongly absorbed onto the chromatographic paper itself, and so be retained on the base-line.

Because of such anomalies, shake-out tests were preferred to reversed phase paper chromatography, as a general screening method for extraction studies.

3.2.2. Shake-out Tests

Shake-out tests were carried out by equilibrating equal volumes of organic and rhodium containing aqueous phases for 1 hour at room temperature. Aliquots of the aqueous phase were then taken for rhodium analysis. The results are displayed in Table 3.2.1.

None of the solvating type reagents, i.e. methyl isobutyl ketone (MIBK), tributylphosphate (TBP), tri-octylphosphine oxide (TOPO), butyl ether, or tetrabutyldiphosphinedisulphide (TBDPDS), showed any significant extraction of rhodium from the acid range studied. In the presence of tin (II) chloride/hydrochloric acid, however, MIBK did extract rhodium with $^{max}D_{Rh}$ = 0.45 (at 38.5^{o}C). Tri-butyl phosphine sulphide (TBPS) in odourless kerosene showed no extraction of rhodium, but in heptanol as diluent a $^{max}D_{Rh}$ of 0.3 was found. Tri-phenyl phosphine sulphide (TPPS) in odourless kerosene or heptanol as diluent showed no extraction for rhodium.

None of the chelating reagents, i.e. theonyltrifluoroacetone (HTTA), 2-thiotheonyltrifluoroacetone (2-HTTTA) or 2-mercaptobenzothiazole, showed any significant extraction of rhodium in the acid range studied.

Table 3.2.1. Preliminary shake-out tests

M_{Rh} = 0.001M, Equilibration time = 1hr, Temp. = 20°C, A/O = 1:1

Aqueous Phase	Organic Phase	Distribution Coefficient
0.1 - 4 M HNO_3	MIBK	< 0.01
0.1 - 5M HNO_3, 2MHCl, $SnCl_2$	MIBK	$^{max}D_{Rh}$ = 0.45 @ 38.5°C
0.1 - 8M HNO_3	Butylether	< 0.01
1-5M HNO_3	20% $^{v/}_{v}$ TBP/OK	< 0.01
0.1-4M HNO_3	20% $^{v/}_{v}$ TOPO/OK	< 0.01
0.1-4M HNO_3	20% $^{v/}_{v}$ TBPS/OK	< 0.01 @ 60°C
0.1-4M HNO_3	20% $^{v/}_{v}$ TBPS/Heptanol	$^{max}D_{Rh}$ = 0.3 @ 60°C
0.1-4M HNO_3	0.1M TPPS/OK	< 0.01 @ 60°C
0.1-4M HNO_3	0.1M TPPS/Heptanol	< 0.01 @ 60°C
0.1-1M HNO_3	0.1M TBDPDS/OK	< 0.01
2M HNO_3	1% $^{w/}_{v}$ Mercaptobenzo-thiazole/MIBK	< 0.01
0.1-1M HNO_3	0.25M HTTA/OK	< 0.01
0.1-1M HNO_3	0.25M 2-HTTTA/OK	< 0.01
0.1-1.5M HNO_3	10% $^{v/}_{v}$ H DEHP/OK	< 0.01
0.1-3M HNO_3	20% $^{v/}_{v}$ H DEHDTP/OK	< 0.01
0.1-1M HNO_3	10% $^{v/}_{v}$ HD/OK	0.16 in 1M HNO_3
1M HNO_3, 0.05-1.0M $NaNO_2$	10% $^{v/}_{v}$ Hostarex A327/OK	< 0.01
0.1M HNO_3, 0.1M $NaNO_2$	10% $^{v/}_{v}$ Hostarex A327/OK	0.18
0.1-2M HNO_3	20% $^{v/}_{v}$ TOA/OK	< 0.01
0.1-2M HNO_3	1M Dioctylacetamide/OK	< 0.01

Of the acidic extractants, only dinonylnaphthalene sulphonic acid (HD) showed significant extraction of rhodium (D_{Rh} = 0.16 in 1M HNO_3). Di-2-ethylhexyl phosphoric acid (HDEHP) and Di-2-ethylhexyl dithiophosphoric acid (HDEHDTP) did not extract rhodium from 0.1-3M nitric acid.

Of the amines tested, only Hostarex A327 (1:1 mixture of trioctyl and tridecyl amine) showed some extraction of rhodium (D_{Rh} = 0.18) from an aqueous solution of 0.1M HNO_3/0.1M $NaNO_2$. No significant extraction was observed at higher nitric acid concentrations.

3.3. EXTRACTION OF A RHODIUM-TIN COMPLEX BY MIBK

In hydrochloric acid, tin(II) chloride forms a red complex with rhodium which is believed to be (73):

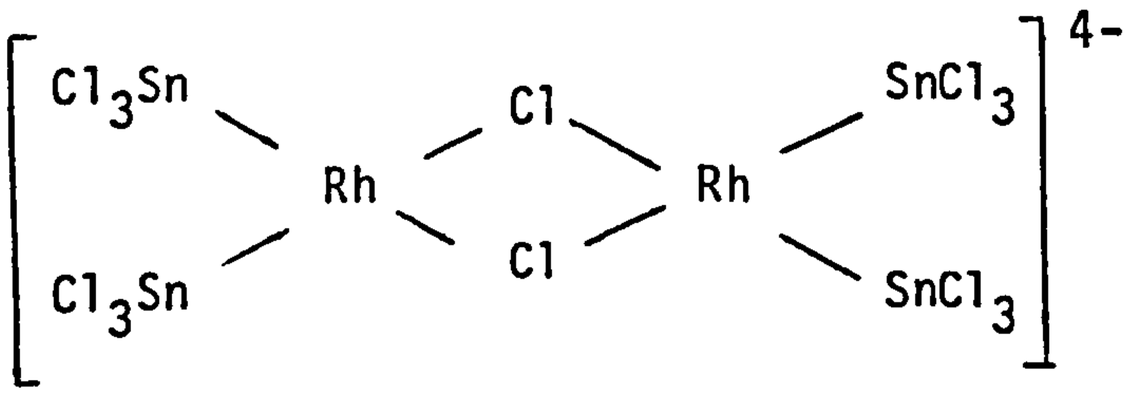

It is this complex that is the basis of an analytical method for determining rhodium (Section 5.2.1.). The complex is slow to form at room temperature, requiring at least twenty four hours, but on heating is quickly formed. The extraction of this complex from hydrochloric acid by trioctylamine has been investigated by Khattak and Magee (75). The authors suggest that the overall extraction may be represented as:

$$\overline{4R_3NHCT} + \{Rh_2Cl_2(SnCl_3)_4\}^{4-} = \overline{(R_3N)_4Rh_2Cl_2(SnCl_3)_4} + 4HCl \quad \text{.....3.4}$$

The rhodium-tin complex that forms in the presence of nitric and hydrochloric acids is not red but yellow, and can be extracted by MIBK.

The system was investigated to determine if the rhodium-tin complex would form in the absence of a large excess of chloride ions, and what the minimum required concentration of chloride ions would be. Experimental details are given under the appropriate sections in Chapter Five.

Figure 3.3.1. shows the distribution of rhodium between MIBK and an aqueous phase comprising 2M HNO_3, 1.25M HCl and 0.5M $SnCl_2$, as a function of equilibration time and temperature. The optimum conditions for maximum extraction are a long equilibration time (60 minutes), and a high temperature (>38^{o}C). The results further illustrate the slow substitution kinetics of rhodium (III) complexes (Section 1.1.2.)

The shake-out tests (Section 3.2.2.) have already shown that no rhodium is extracted by MIBK in the absence of $SnCl_2$/HCl. Figure 3.2.2. further shows, that the presence of $SnCl_2$/HCl, in high concentration, is required for significant extraction of rhodium. Attempts to form an extractable rhodium-tin complex using tin(II)nitrate (section 3.5.4.), and in the absence of chloride ions, were unsuccessful.

Figure 3.3.3. shows that maximum extraction is achieved when the nitric acid concentration is between 3-5M. Young et.al. (73) suggested that $SnCl_2$, in addition to functioning as a complexant, was required in excess to reduce Rh^{3+} to Rh^{+}. Increasing the nitric acid concentration beyond 5M clearly effects the efficiency with which the reduction occurs.

Figure 3.3.1. Extraction of rhodium by MIBK as a function of equilibration time and temperature

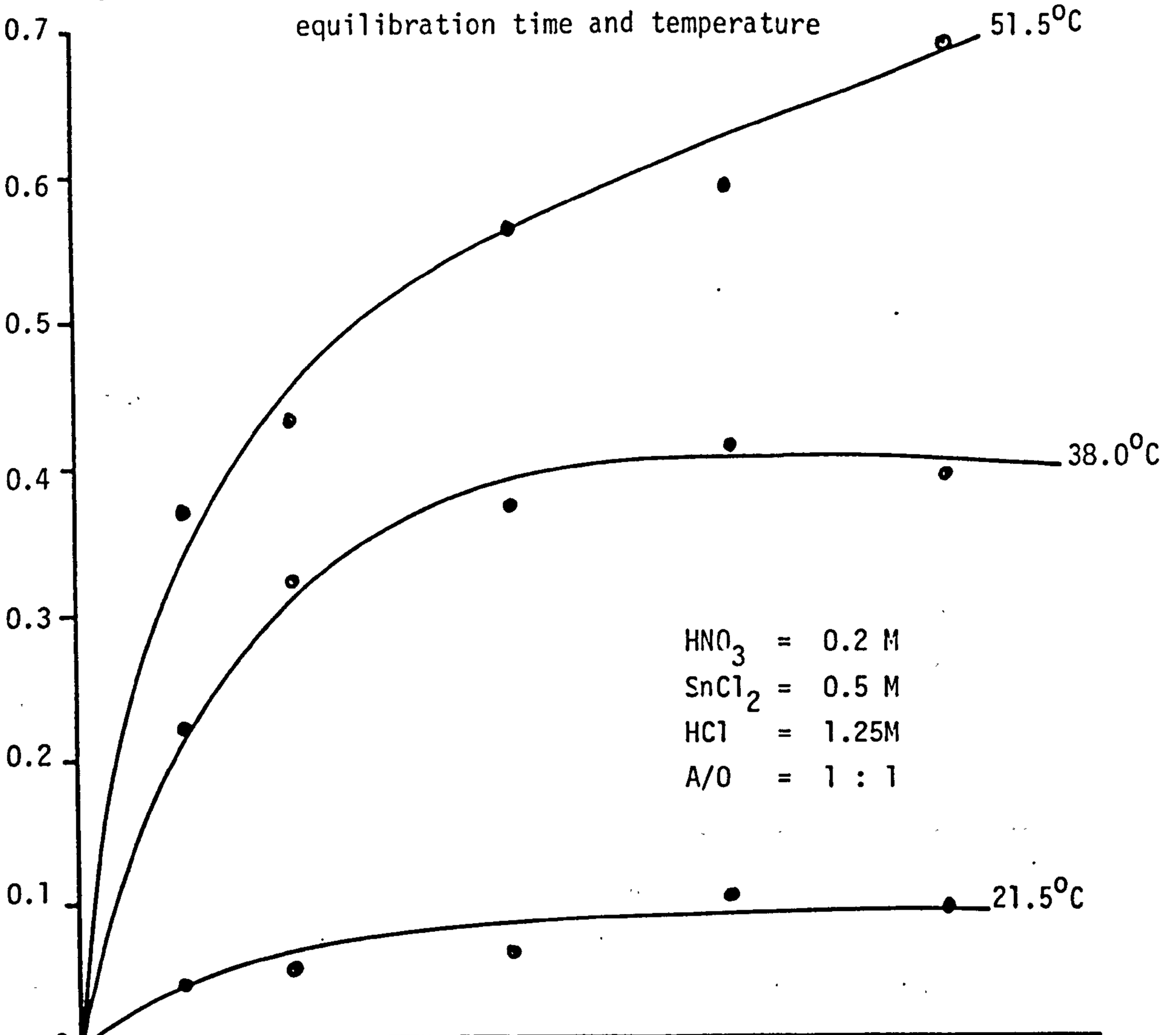

Figure 3.3.2. Extraction of rhodium by MIBK as a function of $SnCl_2$/HCl concentration

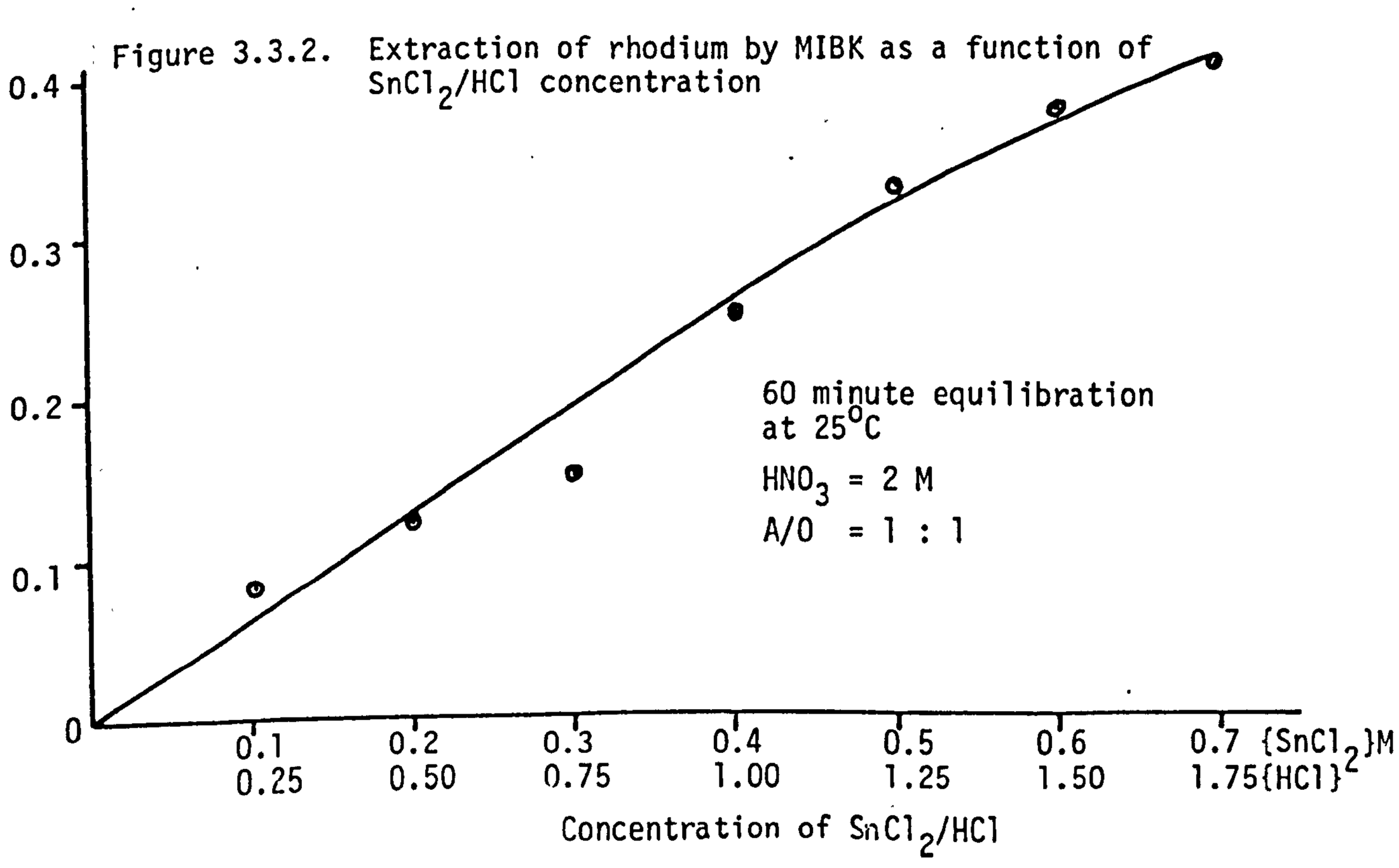

Figure 3.3.3. Extraction of rhodium by MIBK as a function of nitric acid concentration

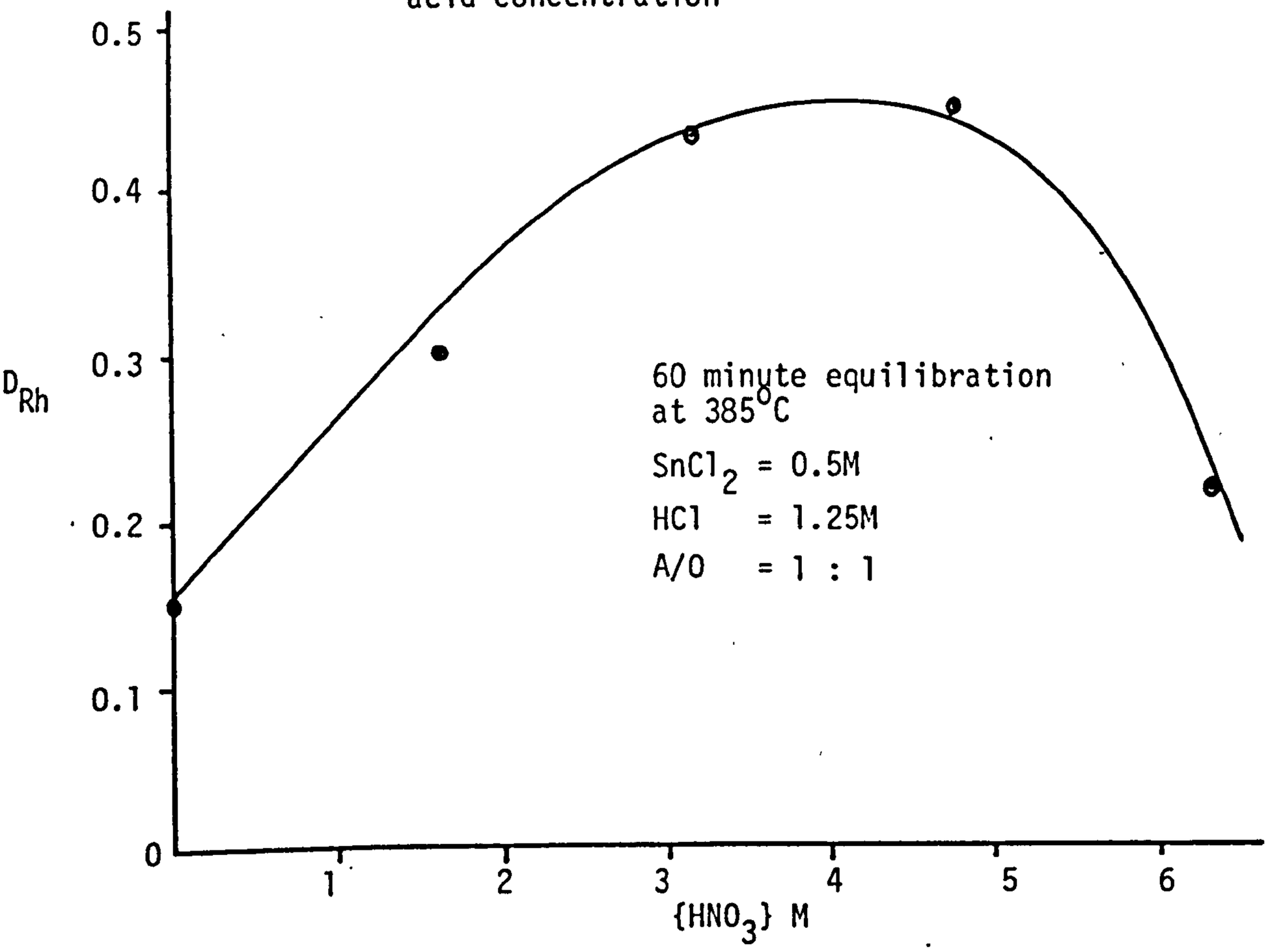

Figure 3.3.4. Extraction of rhodium by MIBK as a function of time and temperature

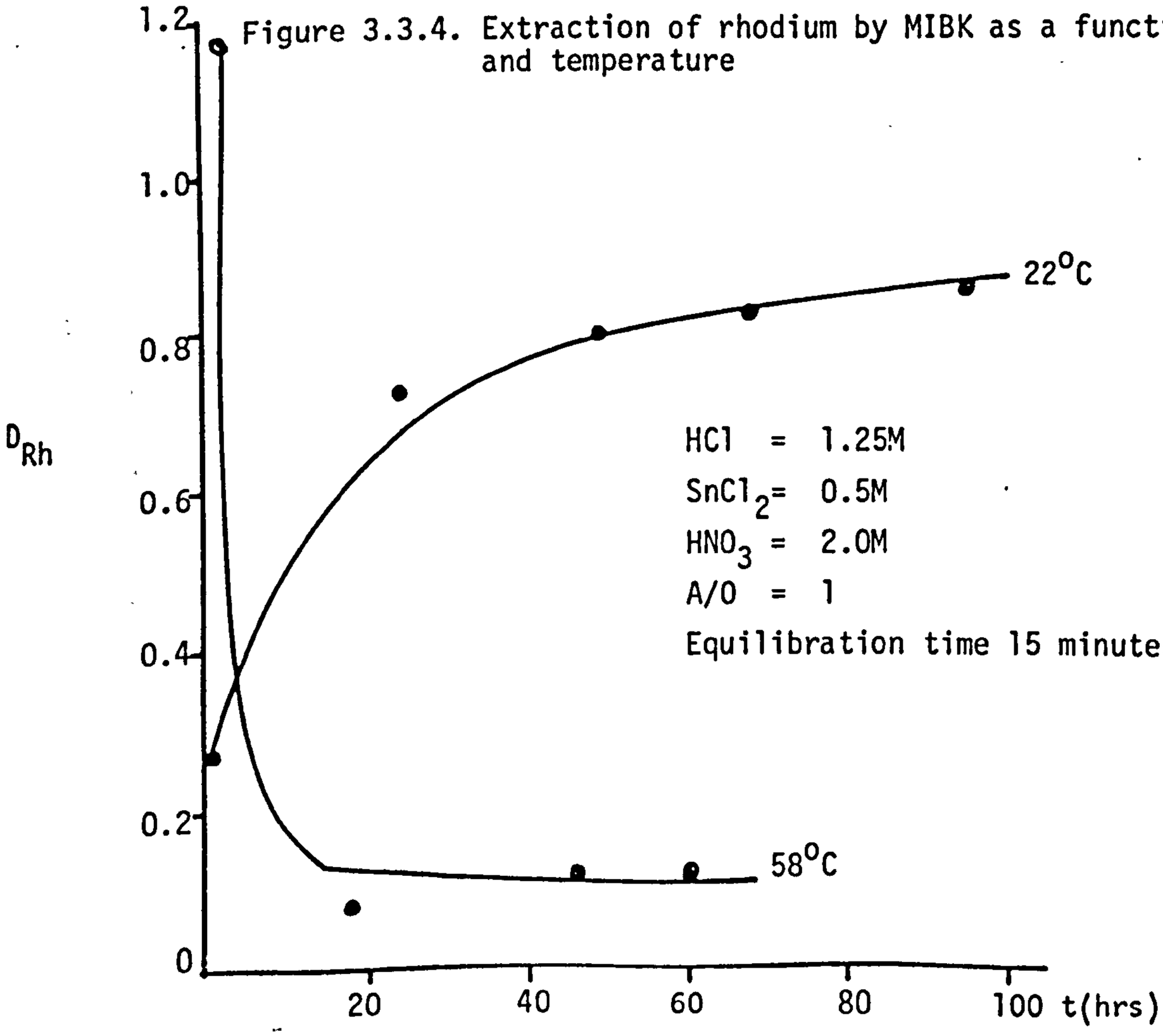

The stability of the extractable complex depends not only on the nitric acid concentration, but also on the temperature. Figure 3.3.4. shows the distribution of rhodium as a function of time (hours after the addition of $SnCl_2$/HCl) and temperature. At 22°C, the complex is slow to form, requiring more than 24 hours, but is stable for up to 90 hours, after the addition of $SnCl_2$/HCl. At the higher temperature (58°C), the complex forms within 30 minutes, but deteriorates with time. This is probably due to the oxidation of tin(II) to tin(IV) by nitric acid, which would occur more rapidly at the higher temperature, so removing the available tin(II) required for complexation with the rhodium species.

It is evident from these results that an extractable rhodium-tin complex cannot be formed in the absence of a large excess of chloride ions. The presence of chloride ions however, is unacceptable to the nuclear industry because of the associated corrosion problems. It is therefore unlikely that such a system would be considered for recovering rhodium from spent nuclear fuel.

3.4. EXTRACTION OF RHODIUM BY DINONYLNAPHTHALENE SULPHONIC ACID (HD)

3.4.1. Foreword

In 1958, Boyd and Linderbaum (178) demonstrated the close similarity between a solid cationic resin of the cross-linked polystyrene sulphonic acid type, and dinonylnaphthalene sulphonic acid (HD) dissolved in a non-polar diluent. Since then, the reagent has been shown to extract various metal ions by a simple cation exchange mechanism (179-184), i.e:

$$M^{z+} + \overline{n(HD)_m} = \overline{MH_{nm-z}D_{nm}} + zH^+ \quad \text{.....3.5}$$

HD is prepared commercially by alkylating naphthalene with tripropylene and then sulphonating this to yield the acid (185). Although a mixture of many isomers is produced, the predominant structure contains highly branched Cq chains at the 2,6 positions on the naphthalene ring (186, 187), Figure 3.4.1. In non-polar organic diluents, HD forms inverted micelles, analogous to sulphonate micelles in aqueous systems, but with the sulphonate groups turned inward (185).

Since the major rhodium cation in nitric acid is the hexaaquo ion, the extraction of this complex by HD micelles may prove to be a promising system for recovering rhodium from spent nuclear fuel.

3.4.2. $\{H^+\}$ and $\{HD\}$ Dependence on the Extraction of Rhodium from Nitric Acid

If the extraction of rhodium $\{M^{z+}\}$ by HD is represented by the equilibrium reaction given in equation 3.5, then the equilibrium constant K, is given by:

$$K = \frac{a_{\overline{MH_{nm-z}D_{nm}}}\, a_{H^+}^2}{a_{M^{z+}}\, a_{\overline{(HD)_m}}^n} \quad \text{.....3.6}$$

where a denotes activities of the various species in solution. Assuming activities remain constant, then concentration terms can be used, i.e.:

$$K = \frac{\{\overline{MH_{nm-z}D_{nm}}\}\ \{H^+\}^z}{\{M^{z+}\}\ \{\overline{(HD)_m}\}^n} \quad \text{.....3.7}$$

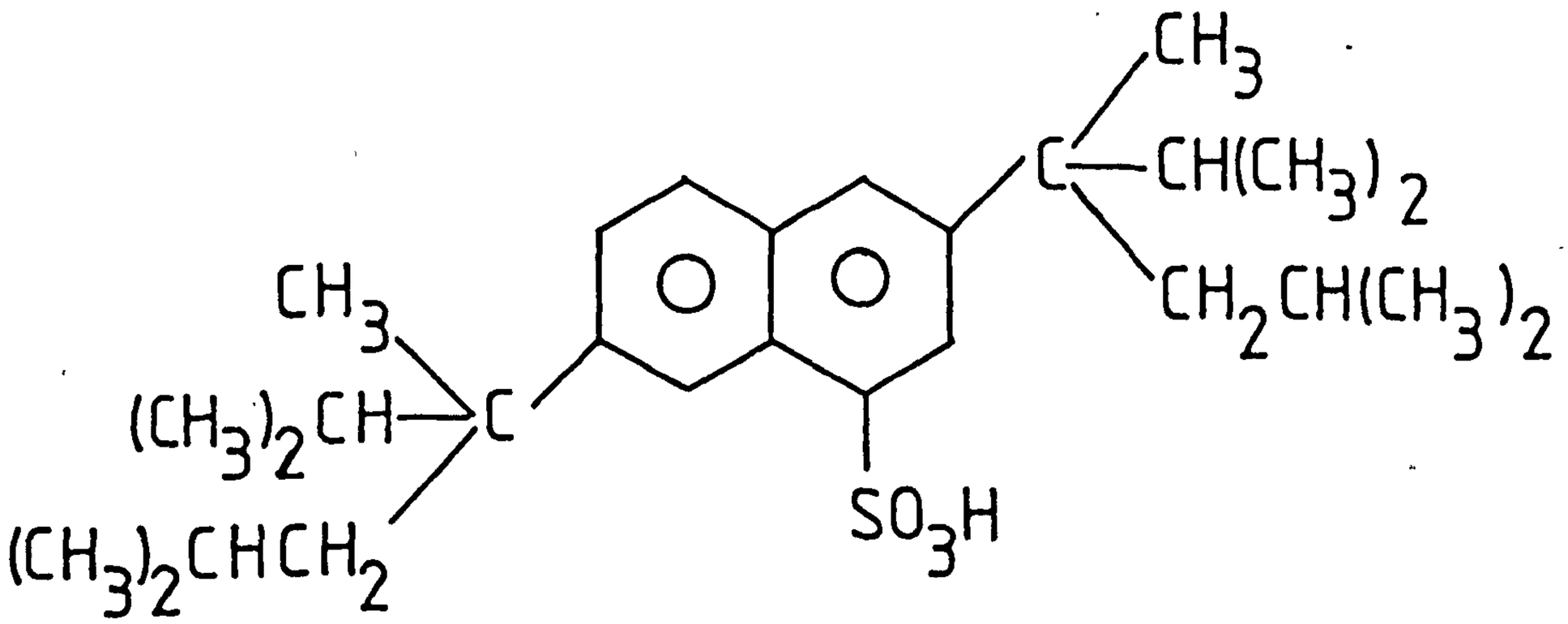

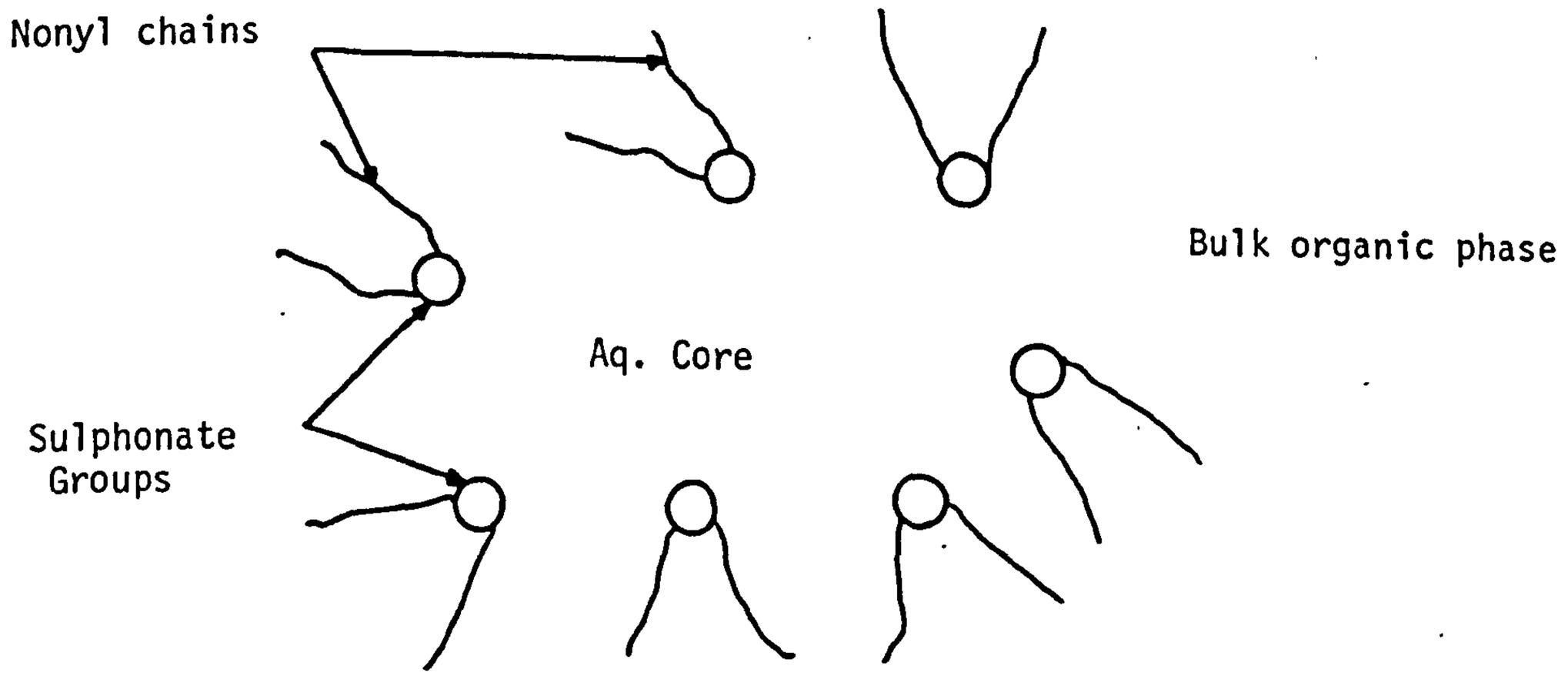

Figure 3.4.1. Dinonylnaphthalene sulphonic acid

Since the distribution coefficient D,

$$= \frac{\{\overline{MH_{nm-z}\ D_{nm}}\}}{\{M^{z+}\}} \qquad \ldots\ldots 3.8$$

then combining equations 3.7 and 3.8 gives:

$$D = K \frac{\overline{\{(HD)_m\}^n}}{\{H^+\}^z} \qquad \ldots\ldots 3.9$$

Therefore,

$$\log D = \log K - z \log \{H^+\} + n \log \{(HD)_m\} \ldots\ldots 3.10$$

Hence a plot of log D against log $\{H^+\}$ and log $\{(HD)_m\}$ should yield straight lines of slope -z and n respectively.

Figures 3.4.2. and 3.4.3. show the dependence of the equilibrium hydrogen ion and HD concentrations on the extraction of rhodium from nitric acid. It is seen that the distribution of rhodium between HD in odourless kerosene and aqueous nitric acid is a function of the inverse third power of the hydrogen ion concentration, and varies with the first power of the formal concentration of HD in the organic phase. The extraction of rhodium by HD can therefore, accurately be represented by the equilibrium reaction given in equation 3.5.

3.4.3. Temperature Dependency and Thermodynamic Parameters

Choppin and Markovits (188) reported the thermodynamic functions for the extraction of some actinides by the sodium salt of dinonylnaphthalene sulphonic acid, NaD. More recently, Danesi et.al. (182, 183) and Raieh and Aly (189) reported the thermodynamic functions for the extraction of trivalent lanthanides and actinides by HD, in order to

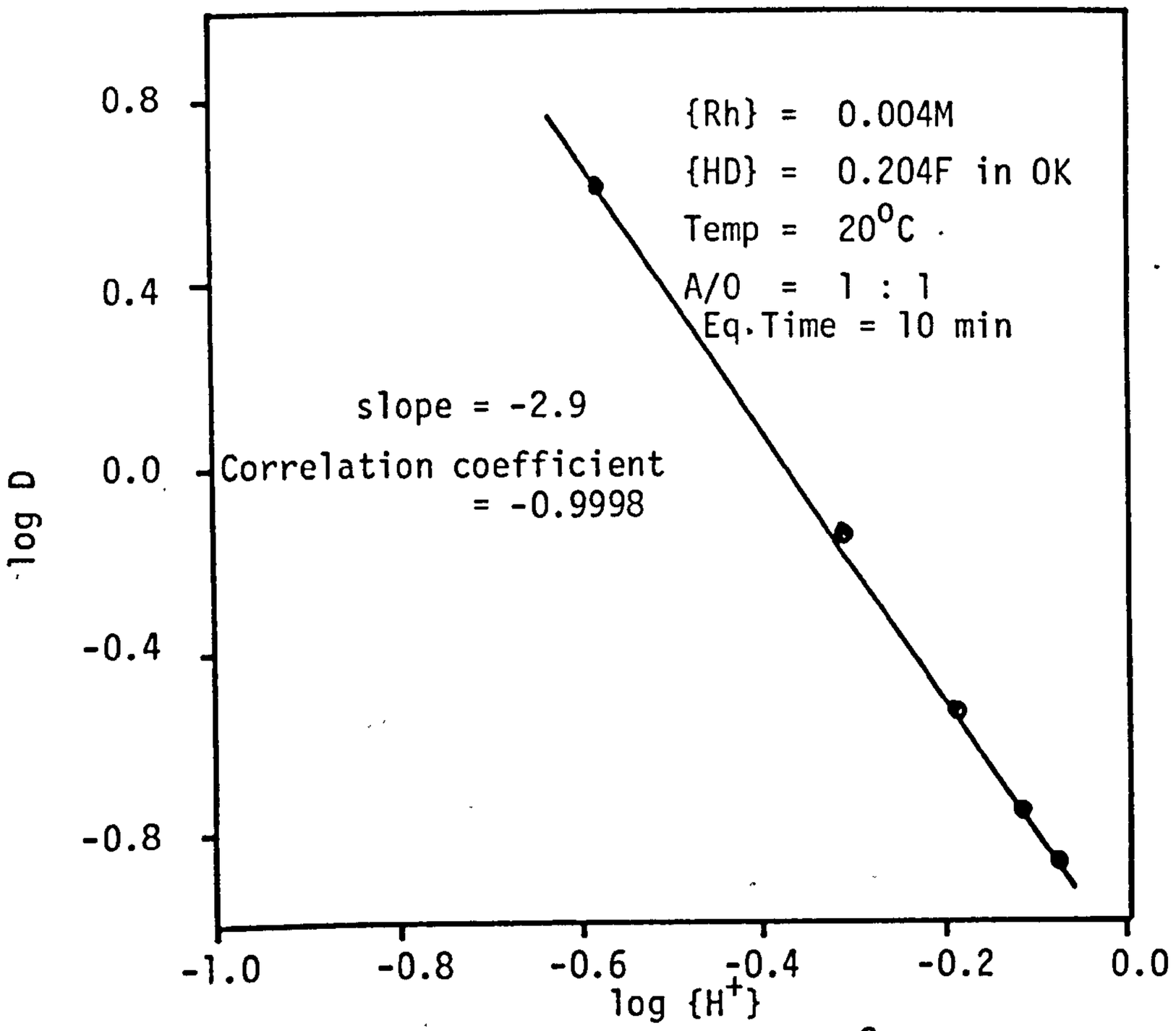

Figure 3.4.2. Distribution of $\{Rh(H_2O)_6\}^{3+}$ as a function of equilibrium acid concentration

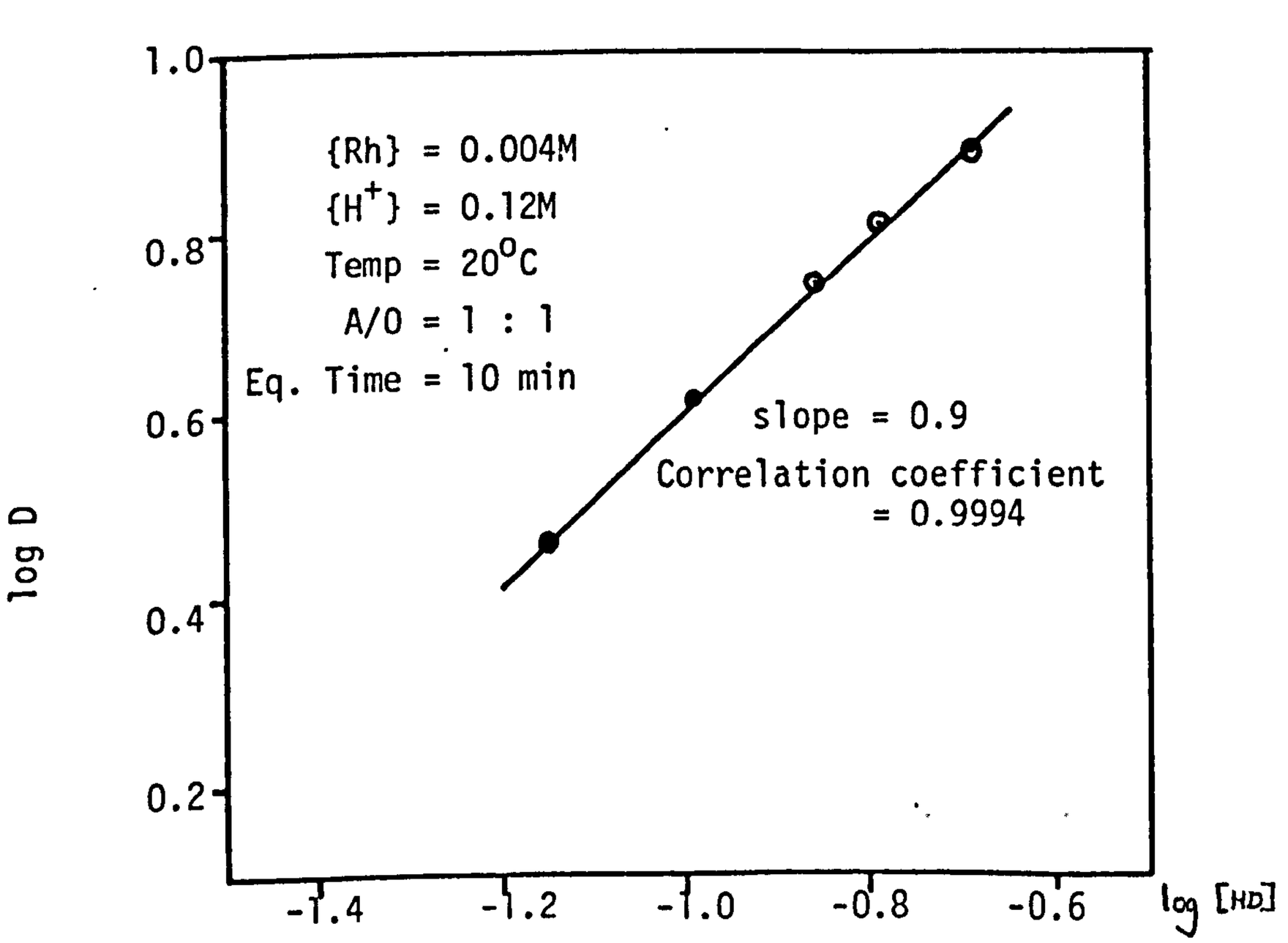

Figure 3.4.3. Distribution of $\{Rh(H_2O)_6\}^{3+}$ as a function of HD concentration in odourless kerosene

obtain a complete thermodynamic picture of the extractant's ion-exchange selectivity.

The thermodynamic parameters for the extraction of $\{Rh(H_2O)_6\}^{3+}$ by HD were determined by measuring the distribution of tracer concentrations of rhodium (^{105}Rh), between 1M nitric acid and varying concentrations of HD, at different temperatures. Experimental details are given in sections 5.5.4. and 5.6.6.

Figure 3.4.4. shows the HD and temperature dependency for the extraction of rhodium from 1M nitric acid. Slopes close to one further confirms the equilibrium reaction represented by equation 3.5.

In wet organic diluents, HD aggregates to form inverted micelles (114, 188, 190), according to the equilibrium:

$$m(HD) = (HD)_m \quad \ldots\ldots 3.11.$$

The relationship between the polymerised extractant concentration, $\{(HD)_m\}$, the monomer concentration {HD} and the analytically measured concentration C_{HD}, is given by (183, 189)

$$C_{HD} = \{HD\} + m\{(HD)_m\} \quad \ldots\ldots 3.12$$

$$\text{Therefore } \{(HD)_m\} = \frac{C_{HD} - \{HD\}}{m} \quad \ldots\ldots 3.13$$

when the extent of polymerisation is very pronounced,

$$C_{HD} = m\{(HD)_m\} \quad \ldots\ldots 3.14$$

Substituting equation 3.13 into equation 3.10 gives:

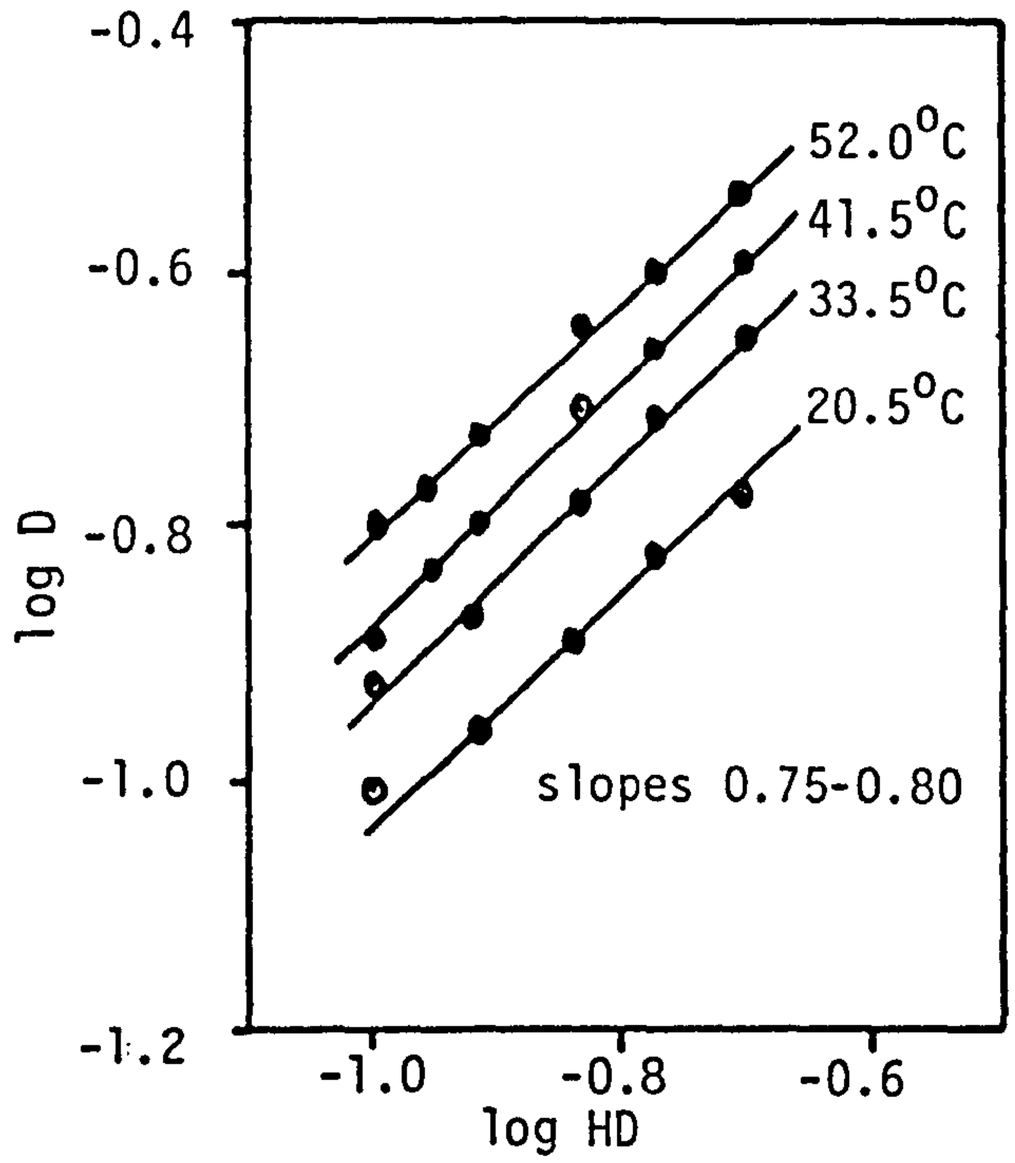

{Rh} = 10^{-4}M
{HNO_3}= 1.0M
A/O = 1 : 1
Eq. Time = 10 min

Figure 3.4.4. HD and temperature dependency for the extraction of $\{Rh(H_2O)_6\}^{3+}$ from 1M HNO_3

Diluent	Method	m	Ref.
Toluene	Interfacial tension	6	191
Toluene	Distribution	8	191
Nitrobenzene	Distribution	8	191
n-Dodecane	Distribution	7	190
n-Heptane	Distribution	7	181
Benzene	Cryoscopy	2.6	191
n-Heptane	Distribution	20	191
n-Heptane	Vapour pressure	10	188
Chlorobenzene	Distribution	15	183
Dichloro benzene	Distribution	15	183

Table 3.4.1. The aggregation number, m, of HD micelles (191)

$$\log D = \log K - z \log \{H^+\} + n \log (C_{HD} - \{HD\}/m) \quad \ldots\ldots\ldots\ldots\ldots 3.15$$

hence:

$$\log D = \log K - z \log \{H^+\} + n \log m - n \log (C_{HD} - \{HD\}) \quad \ldots\ldots 3.16$$

Data taken from Figure 3.4.4. can be treated by applying equation 3.16. Slopes close to one show that the relationship between the analytical extractant concentration, C_{HD} and the polymerised extractant concentration, $\{(HD)_m\}$ holds, i.e. n=1. The aggregation number, m varies between 2 and 20, depending on the diluent used, Table 3.4.1. A value of m=7, determined by Van Dalen (190) for HD in dodecane, is assumed for HD in odourless kerosene. Values of log K, determined by application of equation 3.16 are collected in Table 3.4.2. The thermodynamic functions have been calculated by application of the Gibbs-Helmholtz equation (192),

$$\Delta G = \Delta H - T\Delta S \quad \ldots\ldots\ldots\ldots\ldots 3.17$$

where ΔG is the Gibb's free energy, ΔH the enthalpy variation and ΔS the entropy variation. ΔG is also given by the Gibb's equation:

$$\Delta G = -2.303\ RT \log K \quad \ldots\ldots\ldots\ldots\ldots 3.18$$

where R is the gas constant and T the temperature (K). Combining equations 3.17 and 3.18 gives:

$$-2.303\ RT \log K = \Delta H - T\Delta S \quad \ldots\ldots\ldots\ldots\ldots 3.19$$

and

$$\log K = \frac{-\Delta H}{2.303\ RT} + \frac{\Delta S}{2.303\ R} \quad \ldots\ldots\ldots\ldots\ldots 3.20$$

A plot of log K against 1/T should yield a straight line of slope $-\Delta H/2.303R$ and intercept $\Delta S/2.303R$. A typical log K - 1/T plot is displayed in Figure 3.4.5., and the linear correlation coefficients, slopes and intercepts are collected in Table 3.4.2. The mean values of ΔH and ΔS, derived from the slopes and intercepts are:

$\Delta H = 13.81\ kJmol^{-1}$

$\Delta S = 62.50\ J.K^{-1}.mol^{-1}$

At $25^{o}C$, the ΔG value, calculated by applying equation 3.17 is -4.81 $kJmol^{-1}$.

The enthalpy and entropy changes for the extraction of other metal ions by NaD and HD are collected in Tables 3.4.3. and 3.4.4. respectively. The enthalpy values are endothermic, hence the spontaneity of the extraction reaction is due to the relatively large entropy changes.

The lower values for the entropy change when the extraction reaction involves HD may be related to the increased solvent structuring in the aqueous phase as the hydrogen ions replace the metal cations. Further, as the metal cations replace hydrogen ions in HD, the aggregation number increases. The increased ordering caused by polymer formation would lead to a decrease in the entropy change (188).

3.4.4. Effect of Diverse Metal Ions on the Extraction of Rhodium by HD

From previous work (182, 184, 189, 196) it is clear that HD will extract a whole series of metal cations from aqueous solution. Morris

Figure 3.4.5. Plot of log K against 1/T ($X10^{-3}$)

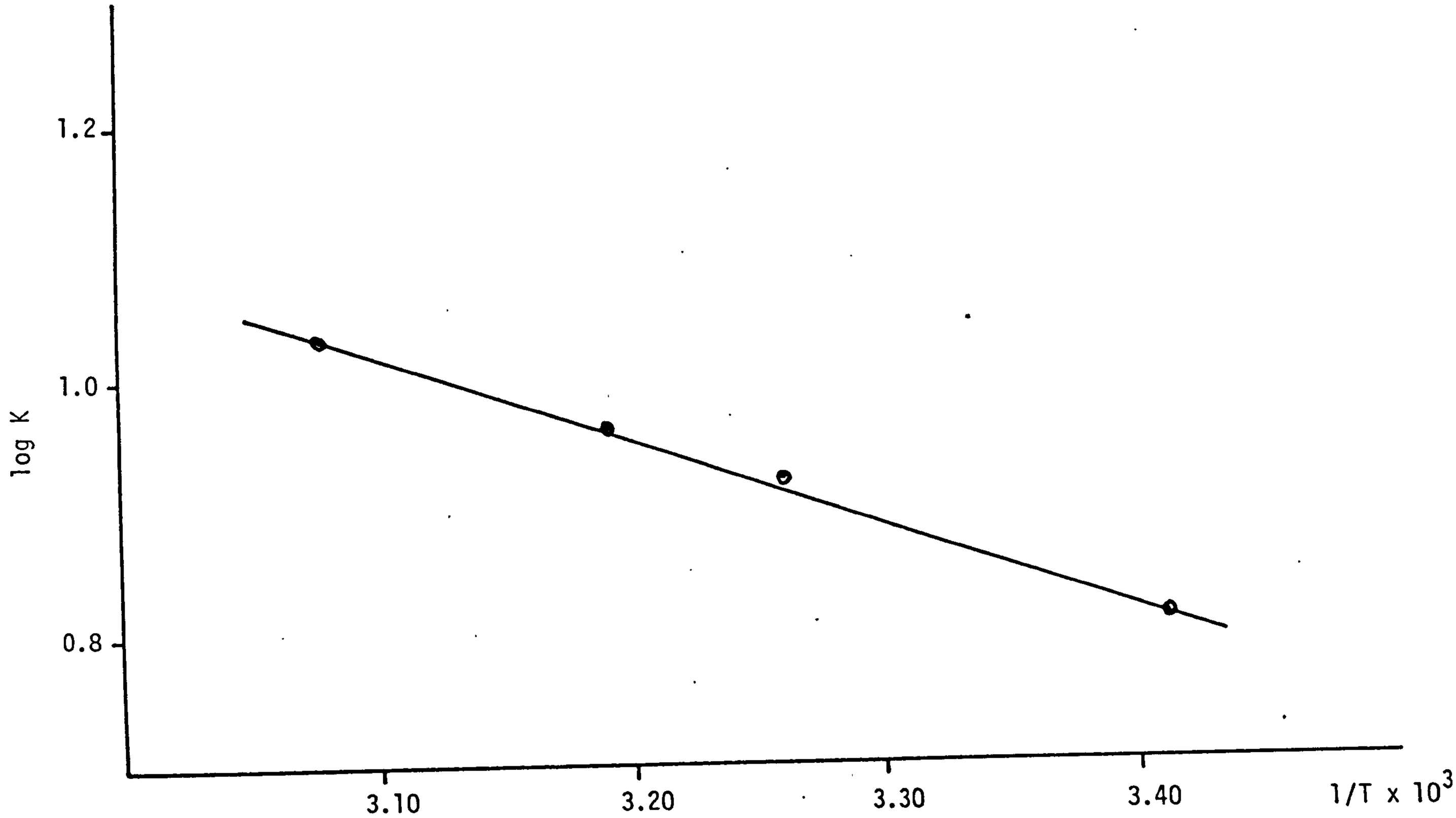

Table 3.4.2. Gibbs-Helmholtz plots for determining ΔH and ΔS

		{HD} F				
	log K	0.195	0.164	0.146	0.121	0.096
Temp (K)	$1/T \times 10^{-3}$					
293.5	3.41	0.78	0.81	0.80	0.80	0.83
306.5	3.26	0.91	0.92	0.91	0.89	0.95
314.5	3.18	0.97	0.97	0.98	0.96	0.98
325.0	3.08	1.03	1.03	1.05	1.03	1.07
Correlation coefficient		-0.9963	-0.9986	-0.9994	-0.9973	-0.9935
Slope		-764.1	-668.0	-764.5	-703.6	-706.6
Intercept		3.39	3.09	3.41	3.19	3.24
ΔH		14.63	12.79	14.64	13.47	13.53
ΔS		64.91	59.16	65.29	61.08	62.04

$$\Delta H = 13.81 \pm 1.02 \text{ Kjmol}^{-1}$$

$$\Delta S = 62.50 \pm 3.34 \text{ jK}^{-1}\text{mol}^{-1}$$

Metal Ion	$-\Delta G$ kJmol^{-1}	ΔH kJmol^{-1}	ΔS J.K^{-1}.mol^{-1}	Ref.
Am(III)	18.81	24.24	146.3	188
Cm(III)	18.81	18.81	125.4	188
Bk(III)	17.85	14.96	108.7	188
Cf(III)	19.44	26.96	154.7	188
Ce(III)	17.14	12.87	96.1	188
Eu(III)	18.39	9.61	91.9	188
Eu(III)	11.79	3.38	50.2	193

Table 3.4.3. Thermodynamic parameters for the extraction reaction at 25^{o}C with NaD in heptane

Metal Ion	$-\Delta G$ kJmol^{-1}	ΔH kJmol^{-1}	ΔS J.K^{-1}.mol^{-1}	Ref
Am(III)	17.51	4.93	75.2	188, 194
Cm(III)	17.10	4.43	72.3	188, 194
Cf(III)	17.77	5.14	76.9	188, 194
Ce(III)	8.78	3.76	41.8	182
Eu(III)	8.36	3.76	41.8	182
Gd(III)	8.36	4.60	41.8	182
Cr(III)	6.73	4.97	41.8	195
Rh(III)*	4.81	13.81	62.50	-

*In odourless kerosene

Table 3.4.4. Thermodynamic parameters for the extraction reaction at 25^{o}C with HD in toluene.

(196) and White et.al. (184) showed that HD in heptane would extract zinc, scandium, cobalt and manganese from perchloric acid, all according to the equilibrium reaction given in equation 3.5, and with small separation factors, e.g. $D_{Zn}/D_{Co} \simeq 10$. For this study, it was important to determine the separation factors of rhodium from the rest of the high level waste, and in particular from caesium and strontium.

The distribution of caesium, strontium, silver, ruthenium, rhodium, technetium and promethium between HD/OK and the aqueous phase was measured as a function of nitric acid concentration. Details of solution preparation and isotope counting procedures are given in the appropriate experimental sections. The results are presented as log D against log $\{H^+\}$ plots in Figure 3.4.6. As can be seen, HD extracts all the metal ions investigated to some extent. The exception is technetium, the distribution coefficient of which was less than 0.001 throughout the acid range studied. In the mild oxidising media provided by 0.1-1M nitric acid, technetium is probably present as pertechnetate, TcO_4^-, and therefore not extractable by HD.

The slopes of the log D - log $\{H^+\}$ plots, Table 3.4.5., particularly in the region between 0.6-1.0M HNO_3, give the charge on the metal ion, and further confirms the validity of the extraction equilibrium given by equation 3.5. The exceptions are ruthenium and promethium. The ruthenium speciation in nitric acid is complex, and it is known that a whole series of ruthenium - nitrosyl, - nitro and - nitrato complexes are formed (197). The slope of the log D - log $\{H^+\}$ plot for ruthenium

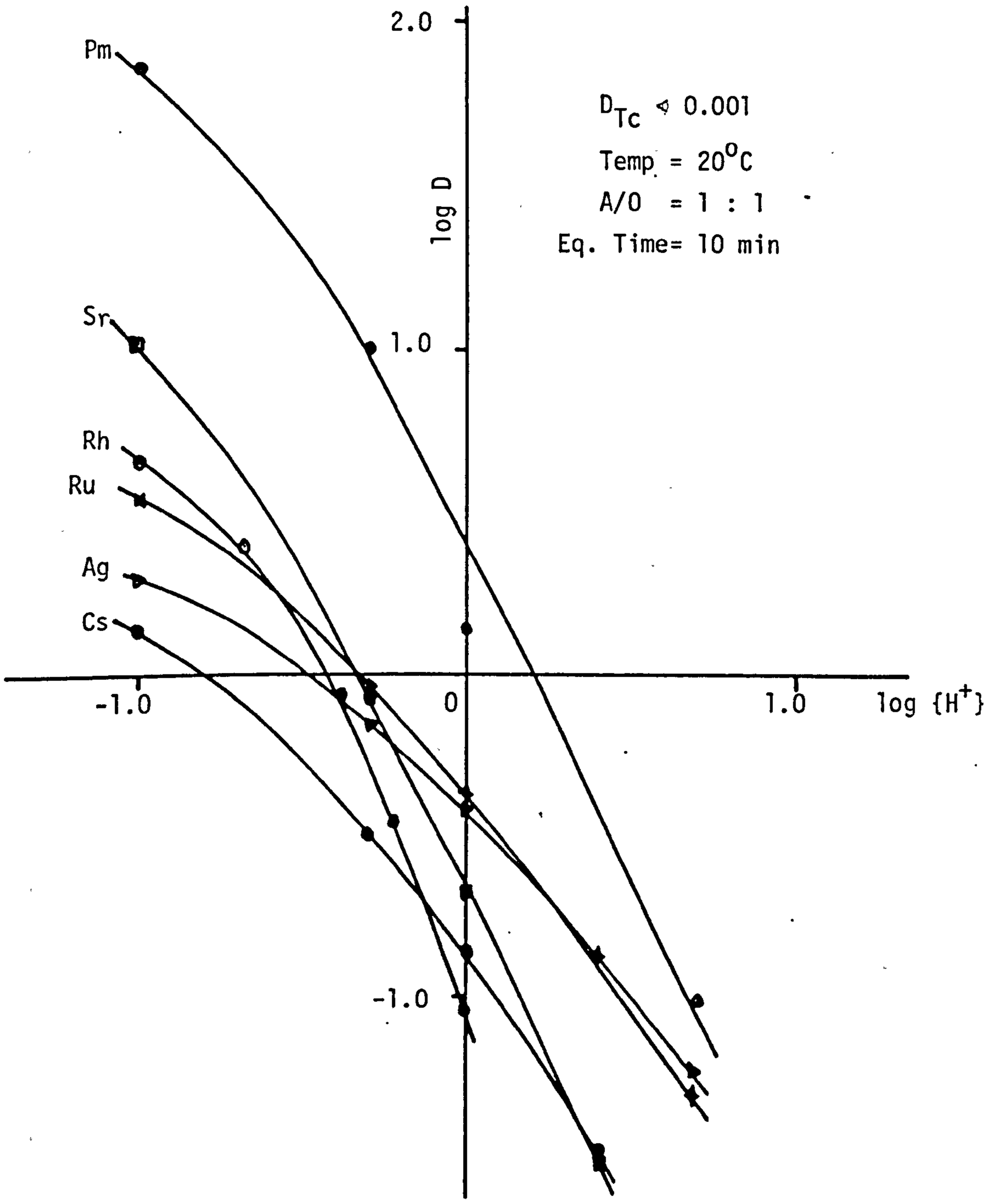

Figure 3.4.6. Log D against log $\{H^+\}$ plots for the extraction of Cs, Sr, Ag, Ru, Rh and Pm from nitric acid by 0.1 F HD/OK.

Metal Ion	log D against log $\{H^+\}$ plot	
	Slope	Correlation Coefficient
Cs (I)	-1.1	-0.9865
Sr (II)	-2.0	-0.9961
Ag (I)	-0.9	-0.9898
Ru (IV or IV)	-1.1	-0.9934
Rh (III)	-2.7	-0.9968
Pm (III)	-1.9	-0.9786

Table 3.4.5. Slopes and Correlation Coefficients for the plots of log D against log $\{H^+\}$ for Cs, Sr, Ag, Ru, Rh and Pm

	HNO_3 (M)					
	1.0	0.63	0.40	0.25	0.15	0.10
D_{Rh}/D_{Cs}	0.68	1.38	2.36	3.90	3.31	3.31
D_{Rh}/D_{Sr}	0.43	0.60	1.27	0.69	0.59	0.46
D_{Rh}/D_{Ru}	0.21	0.46	0.84	1.42	1.23	0.91
D_{Rh}/D_{Ag}	0.24	0.56	1.10	1.66	2.63	2.95
D_{Rh}/D_{Pm}	0.04	0.05	0.07	0.07	0.07	0.07

Table 3.4.6. Separation factors for rhodium from Cs, Sr, Ru, Ag and Pm.

thus represents a net contribution from all extractable cationic species. For promethium, the slope of -1.9 may represent the formation in nitric acid of a divalent cation, e.g. $\{Pm(H_2O)_5NO_3\}^{2+}$ (14).

In the low acid region, between 0.1-0.6M HNO_3, there is slight curvature in the log D-log $\{H^+\}$ plots. This is probably due to the formation of hydroxy species, which occurs for most metal ions when the acid concentration approaches 0.1M (14).

The distribution for rhodium approaches a maximum at a pH of between 2-2.5, before falling with increasing pH, Figure 3.4.7. The initial increase in the extraction of $\{Rh(H_2O)_6\}^{3+}$ is of course due to the decrease in hydrogen ion concentration of the aqueous phase. The decrease in extraction beyond pH 3can be attributed to the precipitation of rhodium sesquioxide, which in nitric acid begins at pH 3(198).

The separation factors determined for rhodium between 0.1 and 1.0M HNO_3, Figure 3.4.6. are collected in Table 3.4.6. The low values obtained show that HD is a non-specific extractant. The separation factors, particularly of rhodium from caesium and strontium, reach a maximum between 0.2 and 0.4M HNO_3. This may allow a separation to be affected using a multi-stage counter-current process.

3.4.5. Effect of Nitrite Ion on the Extraction of Rhodium by HD

One of the by-products of nitric acid radiolysis is nitrite ion (100-102). It has already been shown, by ^{103}Rh NMR spectroscopy, that in the presence of nitrite, a whole series of rhodium (III) nitrito species,

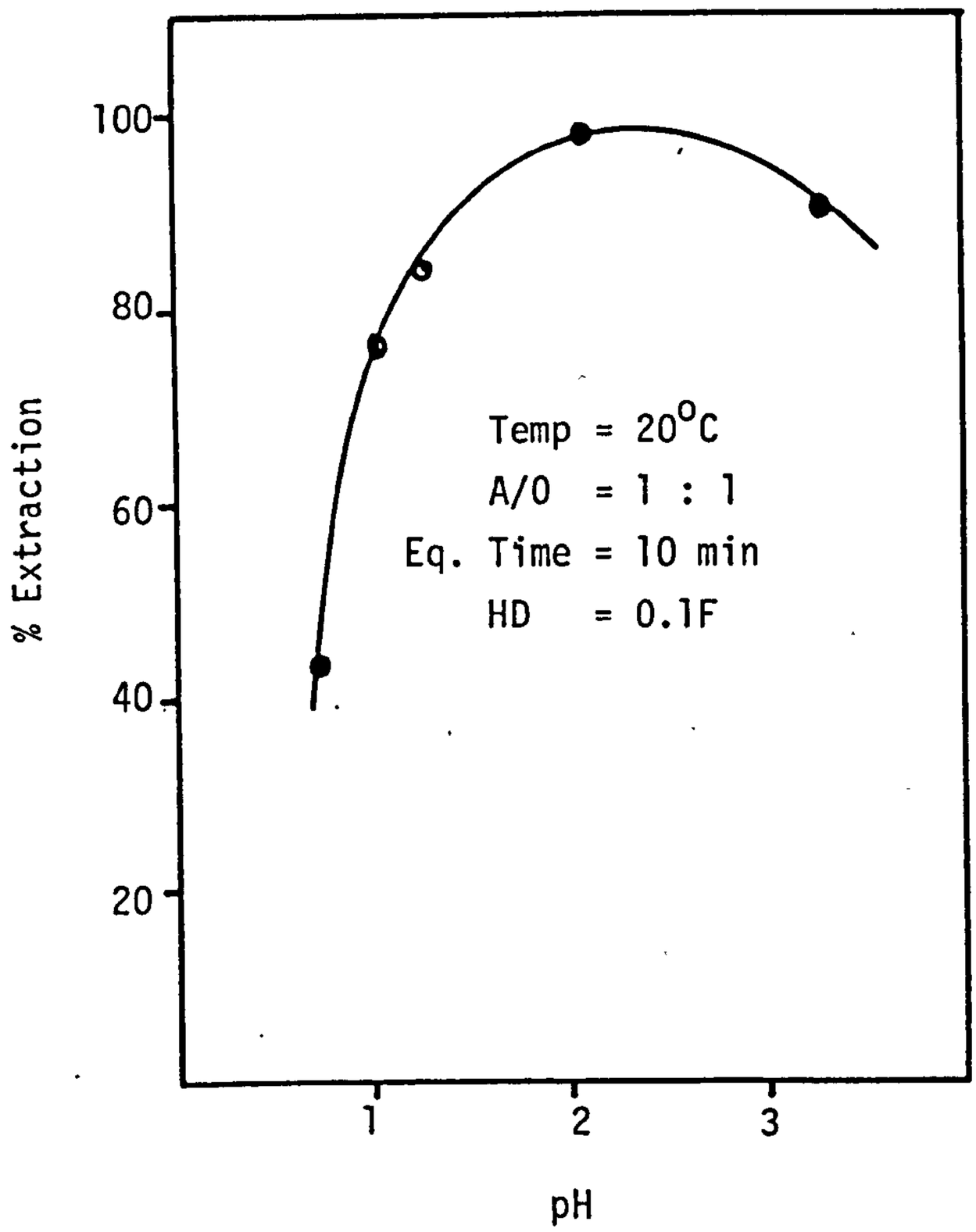

Figure 3.4.7. Distribution of $\{Rh(H_2O)_6\}^{3+}$ between nitric acid and HD/OK at low pH's.

of the type $\{Rh(H_2O)_{6-n}(NO_2)_n\}^{(3-n)+}$ would exist. The effect of such complexation on the distribution of rhodium between nitric acid and HD is therefore an important consideration.

Figure 3.4.8. shows the effect of added sodium nitrite on the extraction of rhodium by HD, from various concentrations of nitric acid. It is seen that even a small excess of nitrite ion over rhodium (x10), is sufficient to bring the distribution ratio of rhodium to zero. This is due to the formation of neutral and anionic rhodium (III) nitrito complexes i.e. $Rh(H_2O)_3(NO_2)_3$, $\{Rh(H_2O)_2(NO_2)_4\}^-$, $\{Rh(H_2O)(NO_2)_5\}^{2-}$ and $\{Rh(NO_2)_6\}^{3-}$, which are not extracted by HD.

The maximum distribution of rhodium is obtained between a nitrite : rhodium ratio of 0.5 and 1.0, and the most pronounced maxima are observed at the lower nitric acid concentrations. The reasons for the maxima are not clear. At a nitrite : rhodium ratio of between 0.5 - 1.0, there would exist in aqueous solution not only the hexaaquo ion, $\{Rh(H_2O)_6\}^{3+}$, but also other cationic species such as $\{Rh(H_2O)_5NO_2\}^{2+}$ and $\{Rh(H_2O)_4(NO_2)_2\}^+$. The increased extraction suggests that D_{Rh} for the divalent species in particular, is greater than D_{Rh} for the hexaaquo ion. This, however, is surprising since on purely electrostatic grounds, the extraction of $\{Rh(H_2O)_5(NO_2)\}^{2+}$ would be expected to be considerably less than that of $\{Rh(H_2O)_6\}^{3+}$.

4.5.1. Stability Constants of the Rhodium (III) Nitrite System

Because HD behaves as a liquid cation exchanger, it is possible to apply the method of Fronaeus (114, 199) to determine the stability

Figure 3.4.8. Extraction of rhodium as a function of $\{NO_2^-\}$

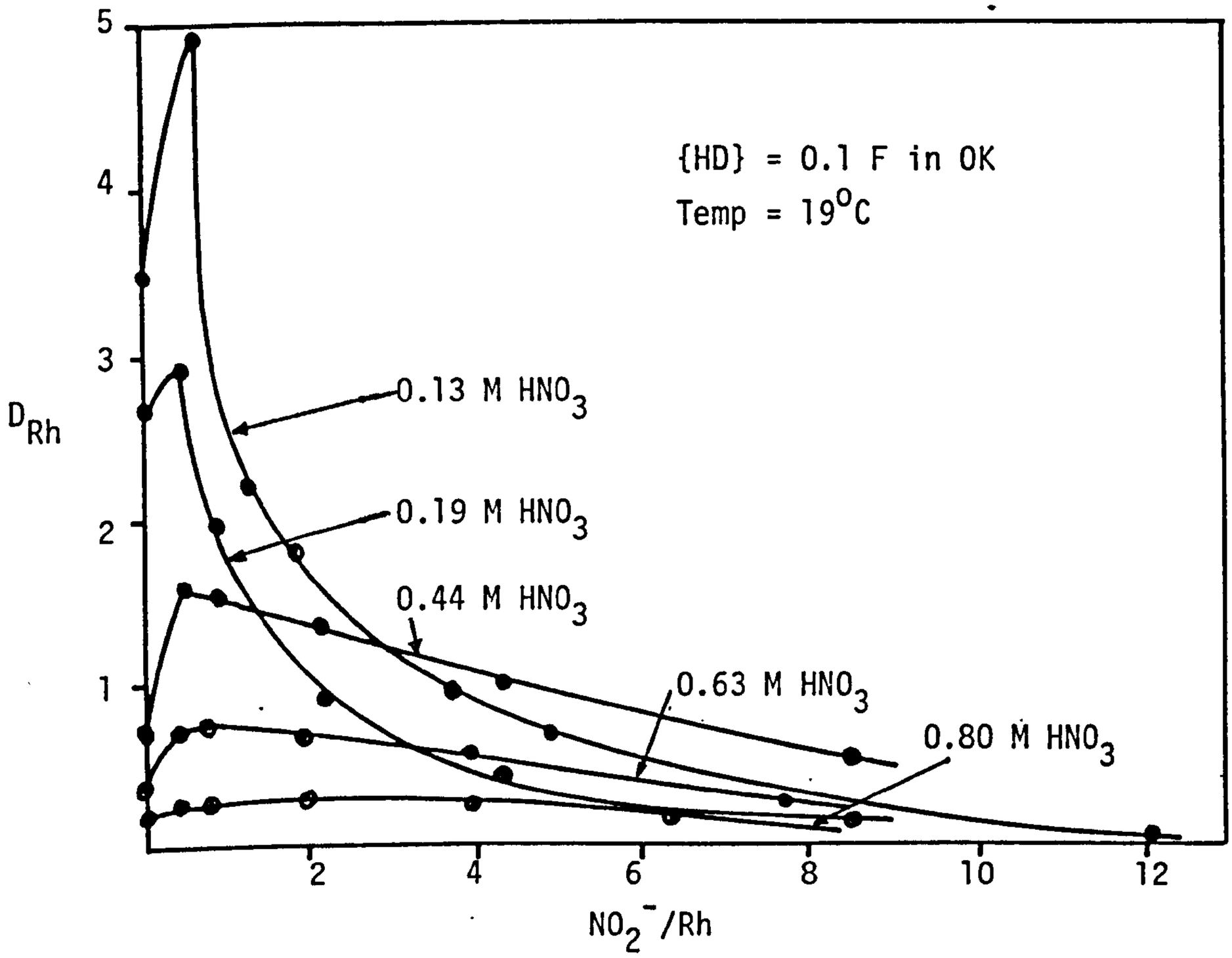

constants of the rhodium (III) nitrite system. The method has been applied to determine the stability constants of indium and nickel halides using ion-exchange resins (200, 201), but is also applicable to systems where HD is used (184, 196, 202).

In the absence and presence of nitrite ion in the aqueous phase, the distribution coefficients may be written (114):

$$D_o = \frac{\overline{\{Rh\}}}{\{Rh^{3+}\}} \quad \text{.....3.21}$$

$$\text{and } D = \frac{\overline{\{Rh\}}}{\{Rh^{3+}\}+\{RhNO_2^{2+}\}+\{Rh(NO_2)_2^{+}\}+} \quad \text{.....3.22}$$

respectively, omitting coextracted water. Dividing equation 3.21 by 3.22 and introducing the stability constant β_j, where $\beta_j = \{Rh(NO_2)^{(3-j)+}\}/\{Rh^{3+}\}\{NO_2^-\}^j$, one obtains:

$$D_0/D = 1 + \beta_1\{NO_2^-\} + \beta_2\{NO_2^-\}^2 \ldots\ldots + \beta_N\{NO_2^-\}^N \quad \ldots\ldots 3.23$$

On the basis of equation 3.23, a function F, can now be defined (114):

$$F = (D_0 D^{-1} - 1)\{NO_2^-\}^{-1} \quad \text{.....3.24}$$

A plot of F against $\{NO_2^-\}$ should yield a straight line parallel to the abscissa if $\{Rh(H_2O)_5NO_2\}^{2+}$ is the only complex species formed in aqueous solution. The plot should be a straight line of positive slope if $\{Rh(H_2O)_4(NO_2)_2\}^{+}$ is also present, and the existence of higher complexes should yield a curve that is concave upwards (202).

Figure 3.4.9. shows the distribution of rhodium between 0.2F HD/OK and 0.38M nitric acid as a function of the initial nitrite ion concentration in the aqueous phase. As expected, the distribution ratio decreases with increasing nitrite ion concentration. The maximum distribution is not however observed, since the concentration of nitrite is always in excess of the rhodium concentration in solution.

The F function of equation 3.24 has been determined from the data presented in Figure 3.4.9., and plotted against the nitrite ion concentration, Figure 3.4.10. The curve is concave upwards, confirming the existence in solution of the higher rhodium (III) nitrite complexes. To determine the first two stability constants, it is necessary to extrapolate the curve to $\{NO_2^-\} = 0$, to obtain F_o (114), where:

$$F_o = \lim_{\{NO_2^-\}\to 0} F = \lim_{\{NO_2^-\}\to 0} \frac{(\beta_1 - D_1/D_o) + (\beta_2 - D_2/D_o)\{NO_2^-\} + \ldots}{1 + (D_1/D_o)\{NO_2^-\} + (D_2/D_o)\{NO_2^-\}^2 + \ldots} = \beta_1 - D_1/D_o \quad \ldots.3.25$$

and D_1 and D_2 represent the distribution ratios for $\{Rh(H_2O)_5NO_2\}^{2+}$ and $\{Rh(H_2O)_4(NO_2)_2\}^{+}$ respectively. Having found F_o, another function, G, can now be calculated (114, 202):

$$G = \{(D_o/D)(F_o\{NO_2^-\} - 1) + 1\}\{NO_2^-\}^{-2} \quad \ldots\ldots\ldots\ldots\ldots\ldots\ldots\ldots\ldots\ldots\ldots\ldots 3.26$$

A plot of G against $\{NO_2^-\}$, Figure 3.4.10. is also concave upwards, and on extrapolation gives G_o where:

$$G_o = \lim_{\{NO_2^-\}\to 0} G = \beta_1(\beta_1 - D_1/D_o) - \beta_2 \quad \ldots\ldots\ldots\ldots\ldots\ldots\ldots\ldots\ldots\ldots\ldots\ldots 3.27$$

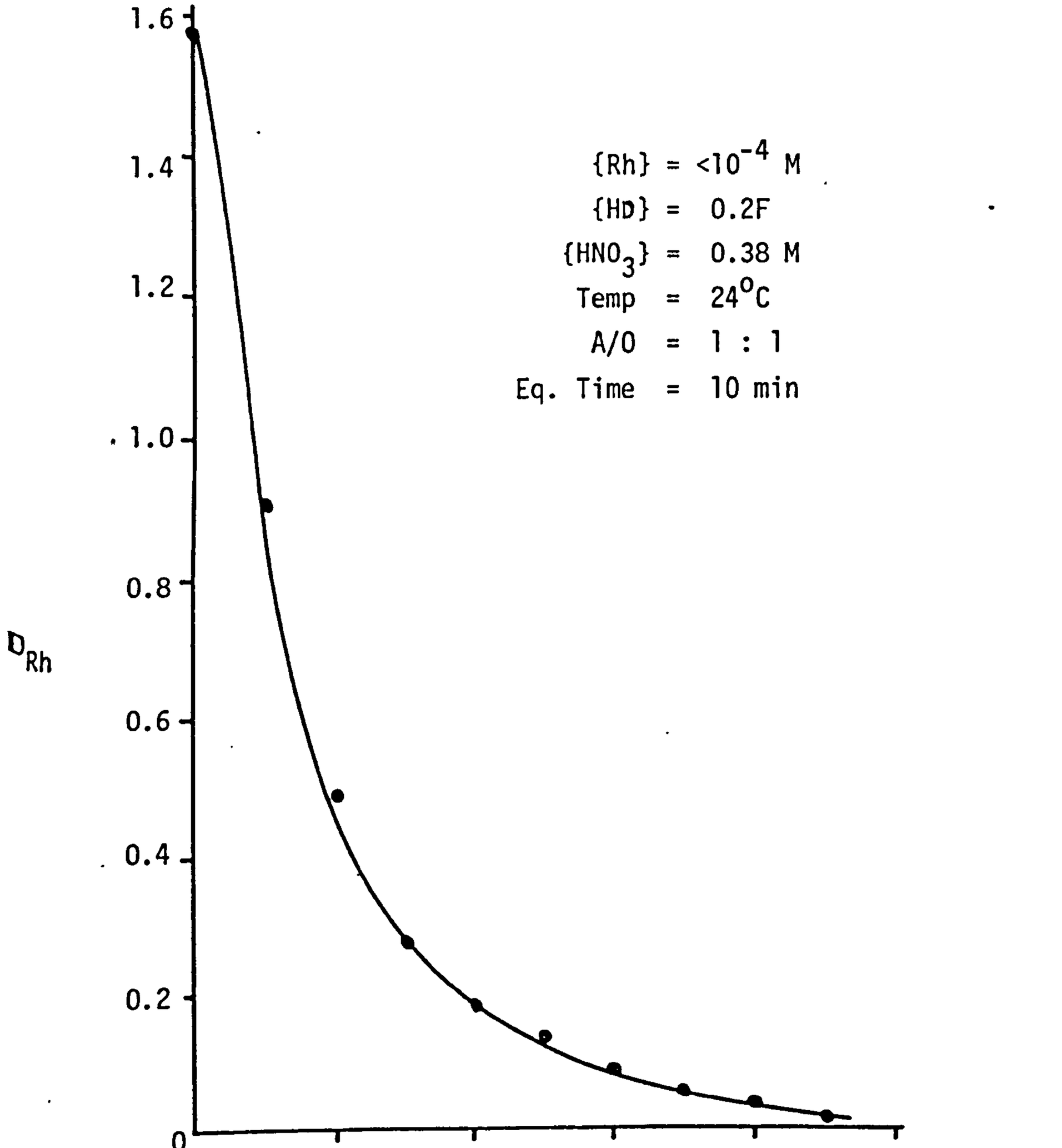

{Rh} = $<10^{-4}$ M
{HD} = 0.2F
$\{HNO_3\}$ = 0.38 M
Temp = 24°C
A/O = 1 : 1
Eq. Time = 10 min

Figure 3.4.9. Distribution of rhodium between nitric acid and HD/OK as a function of nitrite ion concentration.

Figure 3.4.10. Plot of functions F and G against nitrite ion concentration

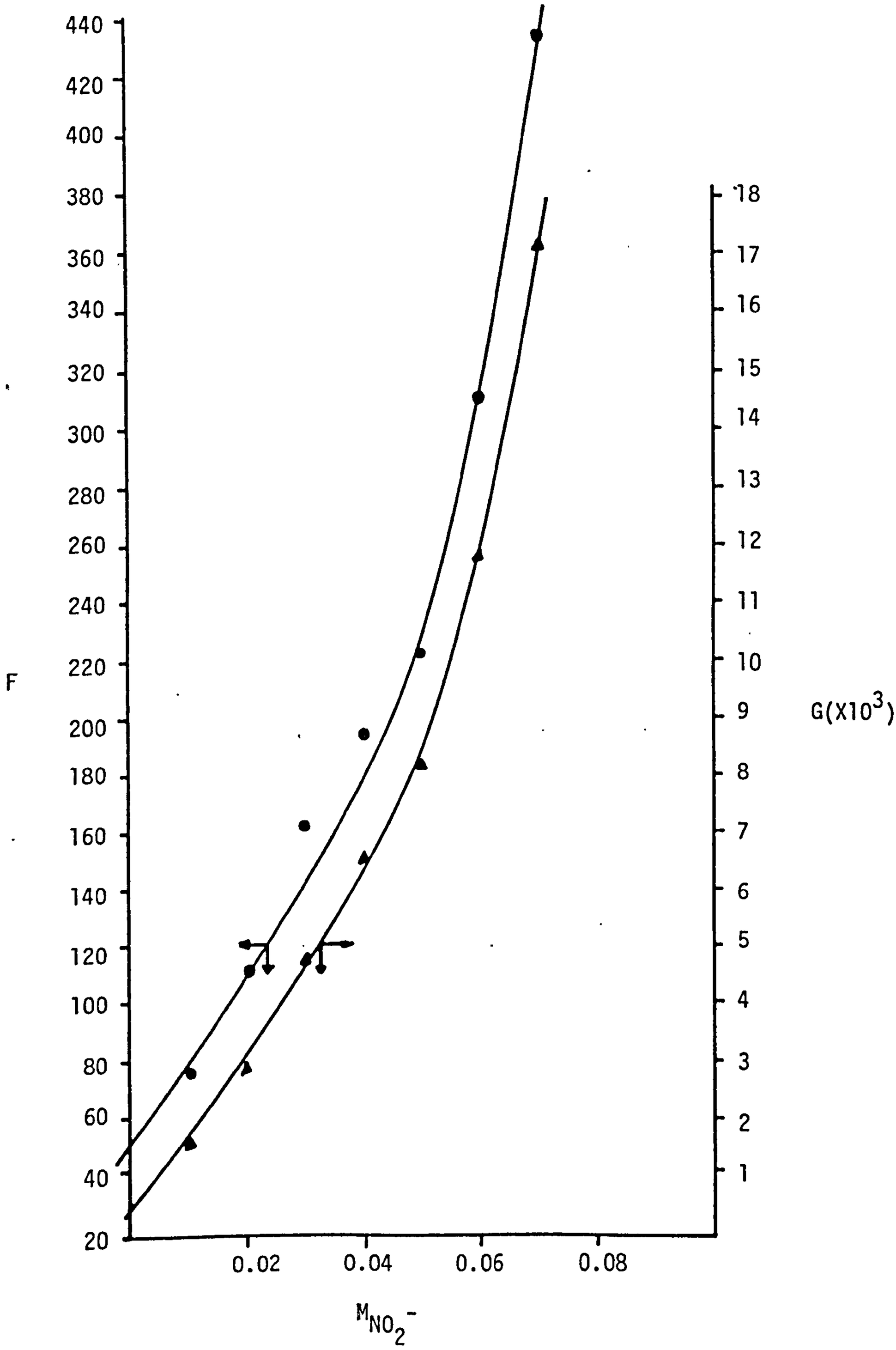

Finally, a plot of the function $(G-G_0)/\{NO_2^-\}$ against $(F-F_0)/\{NO_2^-\}$ should yield a straight line of slope = β_1, provided that $D_n = 0$ for $n > 2$ (114). The values of the various functions calculated are given in Table 3.4.7., and Figure 3.4.11. shows the plot of $(G-G_0)/\{NO_2^-\}$ against $(F-F_0)/\{NO_2^-\}$. The slope of the curve, which is equal to β_1 is found to be 41. The value of β_2 is determined by substituting β_1 into equation 3.27. A value of 1682 for β_2 was determined.

Further values of the stability constants are normally obtained using computer methods, since the large number of graphical extrapolations involved in the Fronaeus method give rise to considerable errors, particularly for β_j where $j>2$. The values of β_1 and β_2 obtained in the present case, nevertheless serve as a good first approximation, and also illustrates the ease with which the rhodium (III) nitrite complexes are formed.

3.4.6. Interfacial Behaviour and Diluent Effects of HD

One of the problems of using HD as an extractant is its tendency for emulsion formation. This is a direct consequence of the surfactant properties of HD. It is well-known that in wet organic diluents, HD forms inverted micelles, even at very low HD concentration (178, 188). Osseo-Asare and Keeney (203) and Chiarizia et.al. (191) determined the critical micelle concentration (CMC) of HD in hexane and toluene respectively. They showed that in these diluents, the HD micelles form when the concentration of HD is as low as 10^{-6}M.

$M_{NO_2^-}$	D_{Rh}	F	$G(x10^3)$	$(G-G_o)/\{NO_2^-\}$ $(x10^3)$	$(F-F_o)/\{NO_2^-\}$ $(x10^3)$
0.00	1.57	-	-	-	-
0.01	0.90	75	1.6	115	2.30
0.02	0.49	110	2.8	118	2.90
0.03	0.27	161	4.7	142	3.63
0.04	0.18	193	6.5	151	3.53
0.05	0.13	222	8.1	153	3.40
0.06	0.08	310	11.8	189	4.30
0.07	0.05	434	17.1	238	5.46
0.08	0.03	642	26.0	319	7.38
0.09	0.01	1733	71.5	789	18.68

$(F_o=52)$ $(G_o=450)$

Table 3.4.7. Parameters for the Determination of Stability Constants

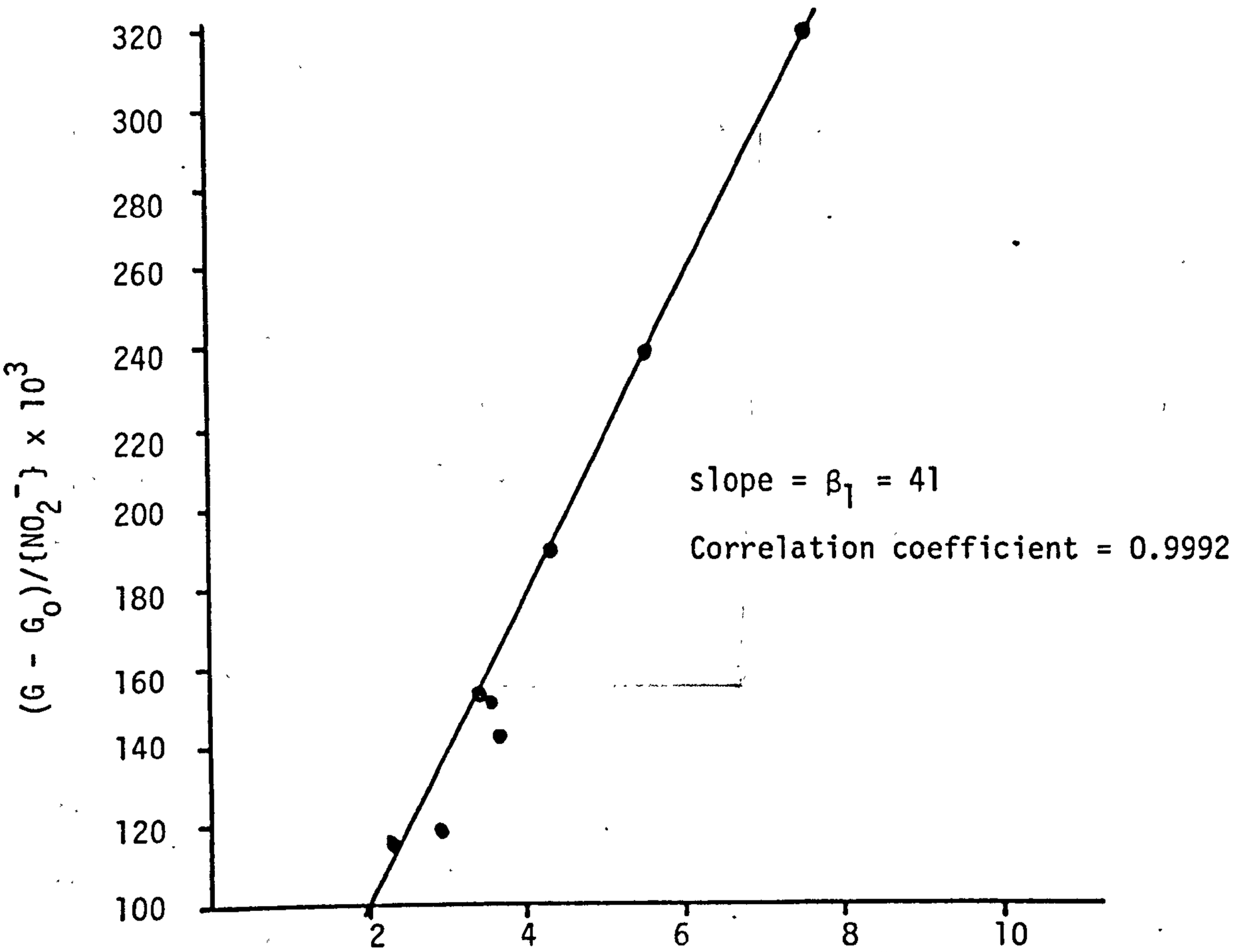

Figure 3.4.11. Plot of $(G - G_o)/\{NO_2^-\}$ against $(F - F_o)/\{NO_2^-\}$

The CMC of HD in odourless kerosene was determined by measuring the interfacial tension between solutions of HD/OK and 0.1M nitric acid (Section 5.6.7.). Figure 3.4.12. shows the plot of interfacial tension against the log of the concentration of HD. The curve may be divided into three parts. In the low concentration region ($<10^{-6}$M) there is negligible change in interfacial tension with varying HD concentration. Between 10^{-6} and 10^{-5} M HD, the interfacial tension falls dramatically, before the final part of the curve is reached ($>10^{-5}$M). The onset of the third region marks the CMC, or the point at which the sulphonate groups aggregate in the bulk organic solution.

It is the ability of HD micelles to retain adsorbed water at its core, that leads to emulsion formation. A consequence of this is that on mixing the organic and aqueous phases, the settling time, i.e. the time required for the two phases to completely separate, is long. Table 3.4.8. shows the settling times, estimated visually, on equilibrating equal volumes (4 mls) of organic and aqueous phases for two minutes at room temperature. It is observed that the settling time increases with increasing concentration of HD in the organic phase, and decreases with increasing nitric acid concentration in the aqueous phase. The most pronounced effect is observed at 0.1M nitric acid, and increasing concentration of HD. Clearly, at the higher HD concentrations there are more micelles in solution to accommodate adsorbed water and consequently the settling times are very long (>1200 sec.). These long settling times are unacceptable for continuous mixer-settler operation. However, when the mixed phases are centrifuged at 2000 rpm

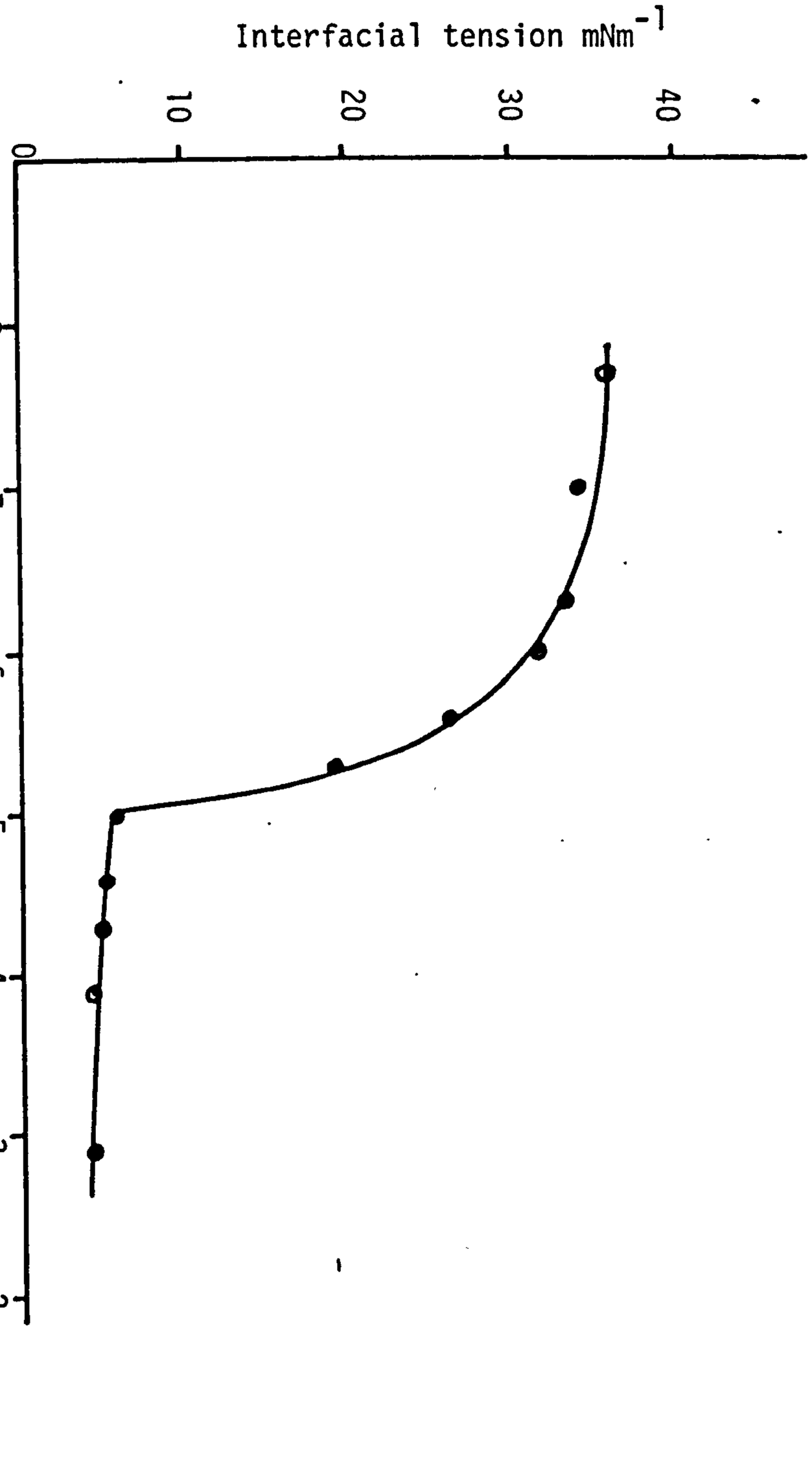

Figure 3.4.12. Plot of interfacial tension against log {HD}

	{HD} /OK			
HNO_3 (M)	0.01 F	0.10 F	0.20 F	0.20F HD + 0.15 M HDEHDTP
0.1	128	>1200	>1200	200
0.5	95	170	435	200
1.0	98	130	225	180
2.0	82	105	110	135

Table 3.4.8. Settling times (secs)

Organic Phase	Settling Time (secs)	%E
Toluene	107	42.4
Carbon tetrachloride	117	42.4
Hexanol	73	Not Extracted
Dodecane	116	48.0
Odourless kerosene	180	47.5

Initial $\{HNO_3\}$ = 0.25 M HD = 0.1 F

Table 3.4.9. Effect of diluent on the extraction of $\{Rh(H_2O)_6\}^{3+}$ by HD

for one minute, a clean separation is achieved. Thus the use of HD at low nitric acid concentrations could be possible if a centrifugal contactor was used instead of a mixer-settler (103).

Van Dalen and Gerritsma (204) noted that the extraction of cerium and americium by HD could be enhanced by the addition of di-(2-ethylhexyl) phosphoric acid, HDEHP. They further noted that the emulsion forming capacity of HD was greatly reduced by the addition of HDEHP. This latter effect was due to the formation of inclusion compounds, wherein the HDEHP replaced adsorbed water in the core of the HD micelles. In the present study, the sulphur analogue of HDEHP, i.e. di-(2-ethylhexyl) dithiophosphoric acid, (HDEHTP) was used as the additive to see whether an enhancement in the extraction of $\{Rh(H_2O)_6\}^{3+}$, or a decrease in the emulsion forming tendency of HD was observed. In fact, a mixture of HD and HDEHDTP (0.2F and 0.15M respectively in OK), showed no enhancement in the extraction of $\{Rh(H_2O)_6\}^{3+}$ from 0.1M nitric acid, even at long equilibration times (1 hour) and high temperatures (50^{o}C). However, as the last column of Tables 3.4.8. shows, a decrease in the settling time was observed, allowing this extraction system to be operated on a continuous mixer-settler, if required.

The influence of the diluent on the extraction of $\{Rh(H_2O)_6\}^{3+}$ by HD is illustrated in Table 3.4.9. As expected, there is no significant difference in the percent extraction of $\{Rh(H_2O)_6\}^{3+}$ when either dodecane or odourless kerosene is used as the diluent. Although these are the preferred diluents of the nuclear industry, toluene or carbon tetrachloride, which show a slight decrease in the percent

extraction of rhodium could also be used. No extraction however, was observed when hexanol, which shows the lowest settling time, was used as the diluent. This was probably due to the breakdown of the HD micelles which occurs when diluents of high dielectric constants are used (183, 188). This would prevent the extraction of $\{Rh(H_2O)_6\}^{3+}$ into the core of the micelles. Chiarizia et.al. (183) showed that the extraction of europium by HD decreased when the dielectric constant of the diluent (toluene/nitrobenzene) increased. The equilibrium between the monomer and polymerised concentrations of HD, equation 3.11, thus shifts towards the left with increasing dielectric constant of the diluent.

3.4.7. Radiolysis of the Organic Phase

Of prime importance when considering any new extractant for the nuclear industry is the stability of the reagent towards radiation. In particular, it is important to understand the effect that the radiolysis products have on the distribution of rhodium between the organic and aqueous phases.

Samples of HD, obtained from King Industries Ltd., (purified according to Section 5.4.5.), and Pfaltz and Bauer (used as received), were sealed in glass ampoules and subjected to radiation doses of between 0-1000 MRads in the cooling pond at AERE Harwell. The distribution of $\{Rh(H_2O)_6\}^{3+}$ between nitric acid and the radiolysed samples was then determined. The results are displayed in Tables 3.4.10. and 3.4.11., and for Pfaltz and Bauer HD, are presented graphically in Figure 3.4.13.

	Dose M Rads			
	0	100	250	1000
{HD} F	0.068	0.056	-	0.002
D_{Rh}, 0.31 M HNO_3	0.97	0.51	-	0.06

Table 3.4.10. Effect of radiation on the distribution of rhodium between nitric acid and King Industries HD/OK.

	Dose M Rads			
	0	100	250	1000
{HD} F	0.105	0.081	0.053	0.015
D_{Rh}, 0.35 M HNO_3	1.19	1.05	0.67	0.18

Table 3.4.11. Effect of radiation on the distribution of rhodium between nitric acid and Pfaltz and Bauer HD/OK.

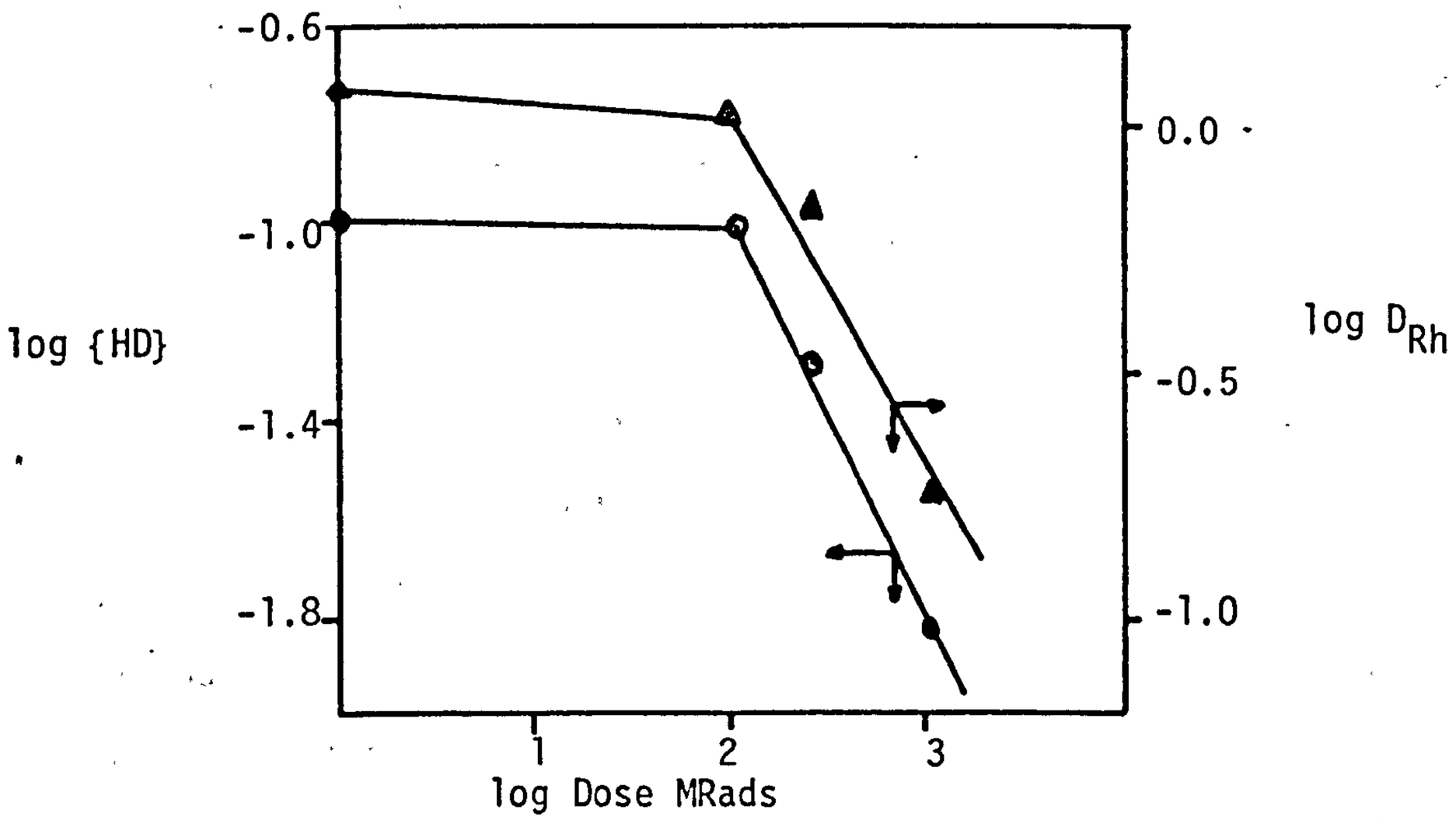

Figure 3.4.13. Effect of radiation dose on the acidic character of HD (Pflatz and Bauer) and the distribution ratio of rhodium

Figure 3.4.14. Equilibration Time for the Extraction of $\{Rh(H_2O)_6\}^{3+}$ from Nitric Acid by HD/OK.

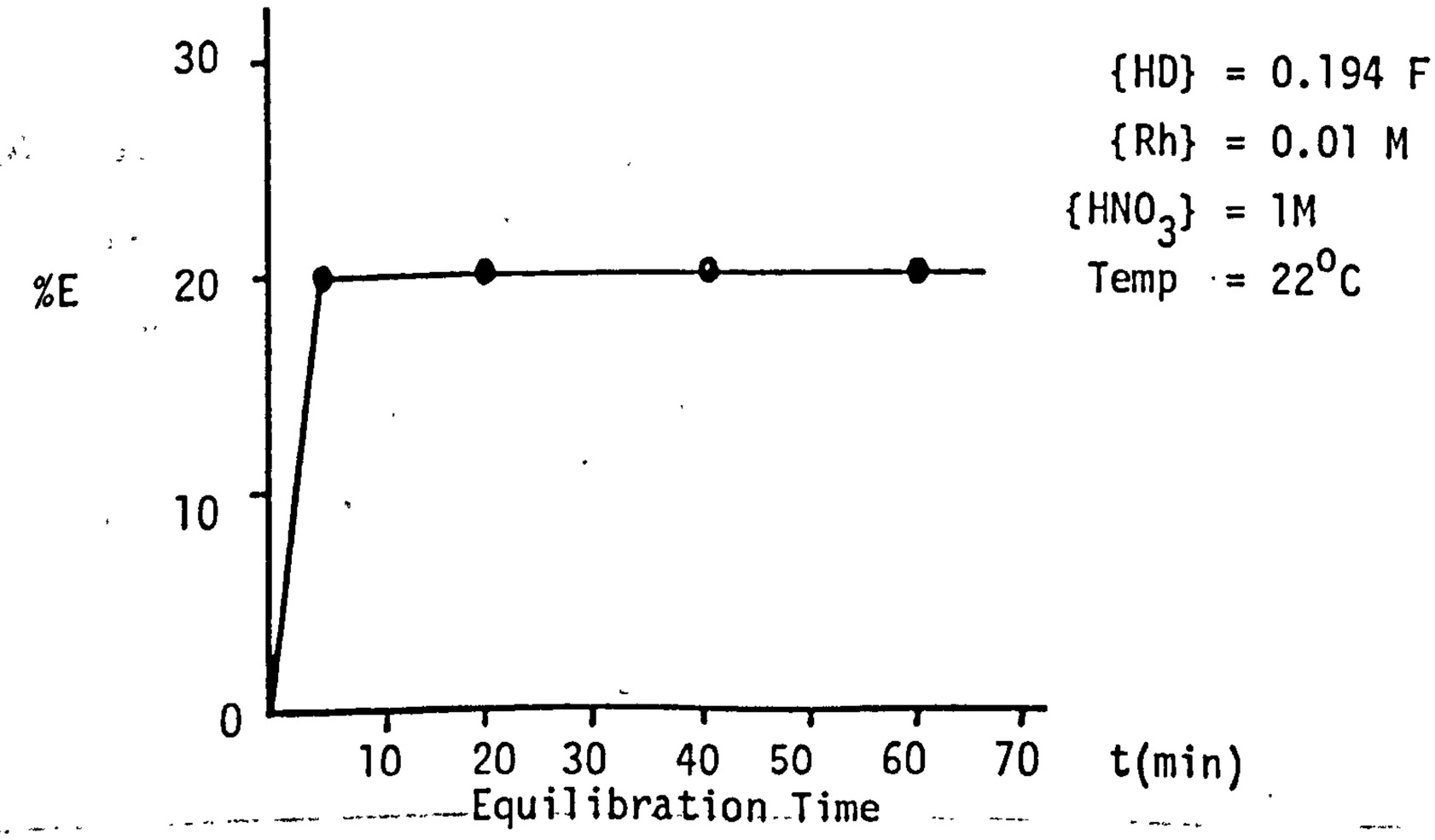

It is seen that in both cases, the concentration of HD, as determined by measuring the hydrogen ion concentration of the organic phase, decreases with increasing radiation dose. The distribution coefficient for rhodium also decreases with increasing radiation dose. Figure 3.4.13. shows that HD is quite stable to radiation up to a dose of 100 M Rads. Above this, there is a sharp decrease in the acidic character of the extractant leading to a drop in the distribution ratio for rhodium. One would expect that with high radiation doses, either the naphthalene SO_3H bond breaks, giving sulphuric acid, or the SO_3-H bond breaks, giving hydrogen gas (205). The fact that the acidic character of the extractant decreases, and that a gaseous product was present in the samples that received the higher radiation doses, suggests the latter. In particular, at the higher radiation dose (1000 M Rads), the effect on the nonyl hydrocarbon chains would be that both C-C and C-H bonds are broken, giving rise to dimerization, formation of H_2, and fragmentation (205).

The stability of HD towards radiation then, is analogous to that of the solid ion-exchange resins, which are stable to doses of between 250-300 M Rads (96).

3.4.8. Distribution Isotherms

Previous work on the extraction of metal ions by HD (188-191), has shown that equilibration between the organic and aqueous phase is attained rapidly (<10 minutes). As Figure 3.4.14. shows, the equilibration time for the distribution of rhodium between nitric

acid and HD/OK is less than five minutes, and is therefore ideal for mixer-settler operation. This rapid equilibration suggests that the rhodium species extracted is in fact the hexaaquo ion, $\{Rh(H_2O)_6\}^{3+}$ and not the dehydrated ion Rh^{3+}. The extraction equlibrium is thus more accurately represented as:

$$\{Rh(H_2O)_6\}^{3+} + \overline{n(HD)_m} = \overline{Rh(H_2O)_6H_{nm-3}D_{nm}} + 3H^+ \quad \ldots\ldots\ldots\ldots\ldots\ldots 3.28$$

rather than by equation 3.5.

To determine how many mixer-settler stages are required for complete recovery of rhodium from the aqueous phase, it is necessary to construct distribution isotherms (103, 206). This is done by determining the distribution of rhodium between nitric acid and HD/OK at various organic to aqueous phase ratios (see Section 5.6.6.). Figure 3.4.15. shows the distribution isotherms for the extraction of rhodium by HD/OK from 0.1-1.0M nitric acid. As expected, the distribution isotherms confirm the low loading of rhodium obtained at the higher acid concentrations. High organic loadings can however be obtained at very low (0.1M) acid concentrations. The distribution isotherm for 0.101M nitric acid has been used to construct the McCabe-Thiele diagram (206) shown in Figure 3.4.16. With an aqueous feed containing 1.3 g/l rhodium in 0.101M nitric acid, and an aqueous : organic flow rate of 1:1, five mixer-settler stages would be required to recover approximately 90% of the rhodium. The number of stages can be reduced to three, if the system is operated at a higher temperature, as shown by the distribution isotherms in Figure 3.4.17.

Figure 3.4.15. Distribution isotherms for the extraction of $\{Rh(H_2O)_6\}^{3+}$ by HD

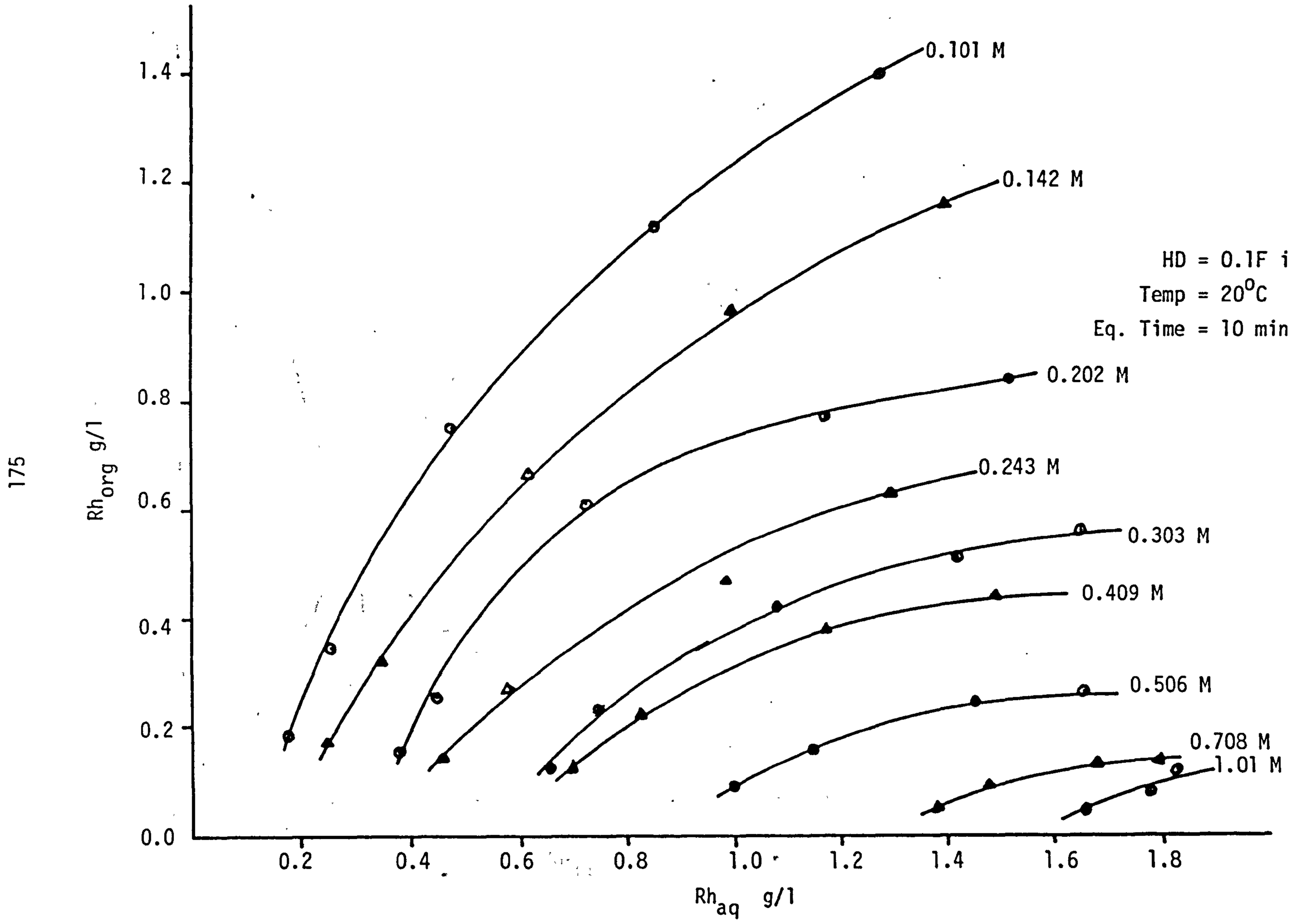

Figure 3.4.16. Distribution isotherm for the extraction of $\{Rh(H_2O)_6\}^{3+}$ by HD

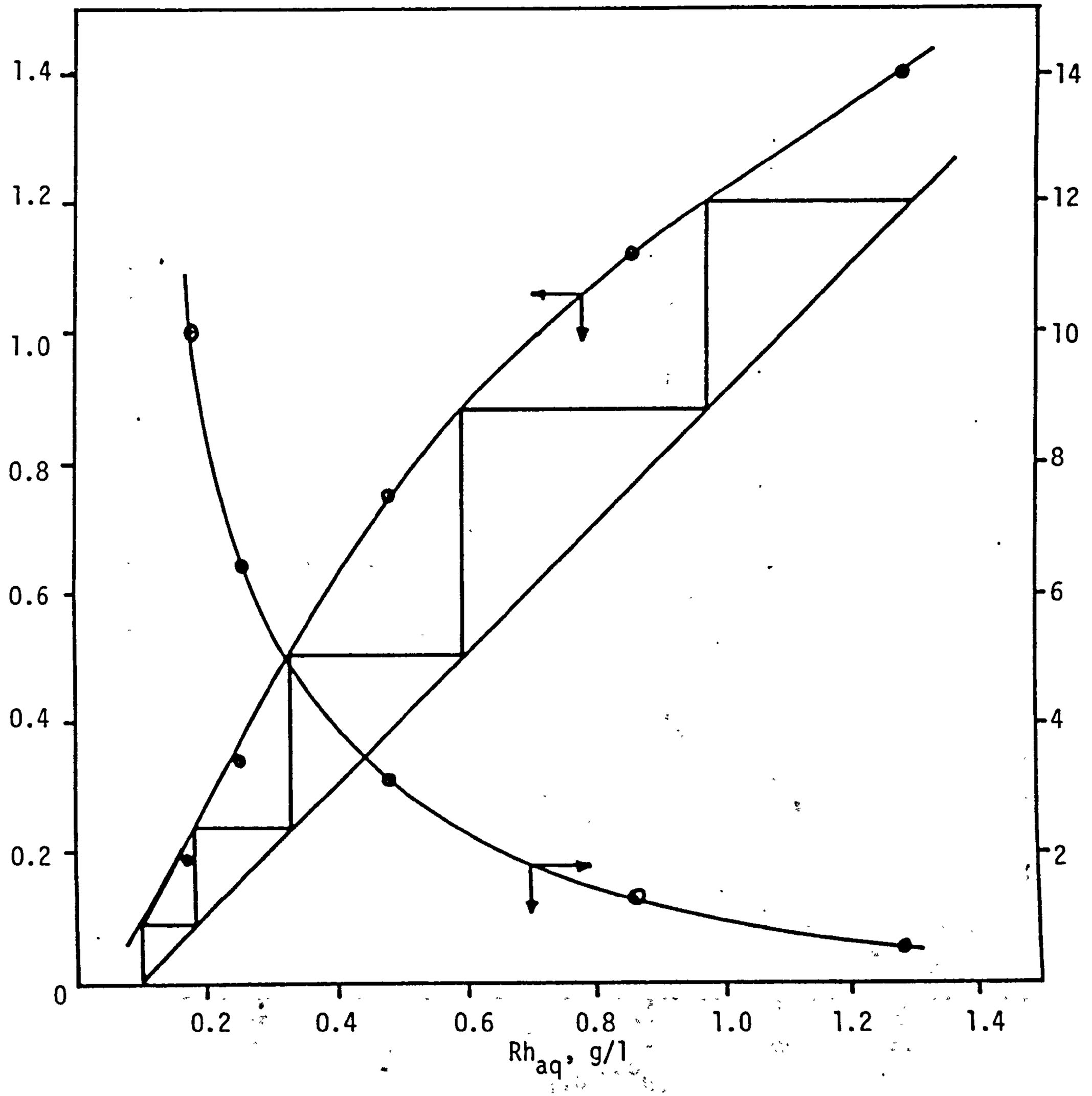

HD = 0.1 F in OK
$\{HNO_3\}_{ini}$ = 0.101 M
Temp = $20^{o}C$
Eq. Time = 10 min

-5 stages of extraction will recover (1.3-0.12)/1.3≃90% Rh

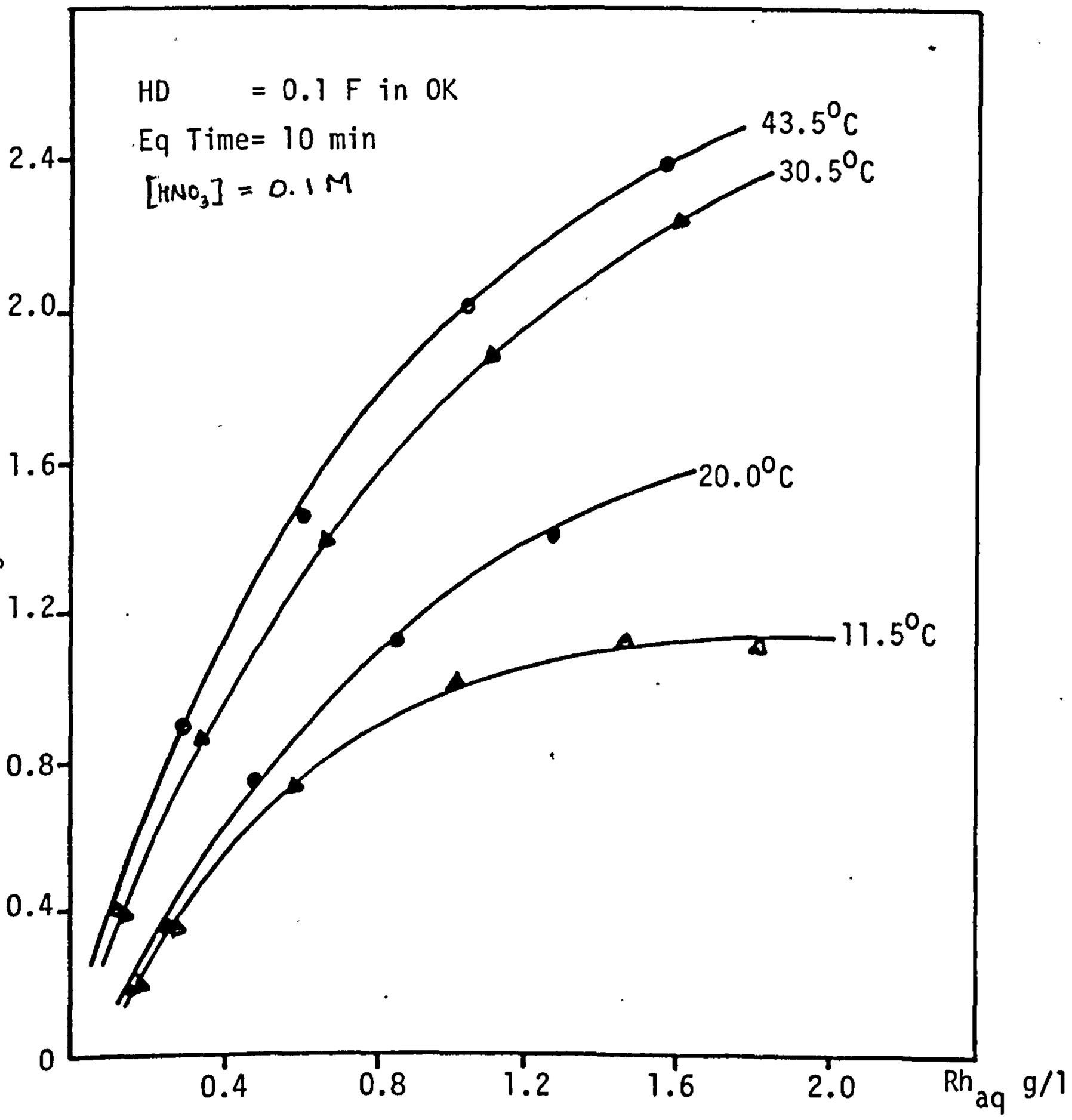

Figure 3.4.17. Distribution isotherms for the extraction of $\{Rh(H_2O)_6\}^{3+}$ by HD/OK at different temperatures.

Backwashing with 2 or 3M nitric acid is sufficient to recover $\{Rh(H_2O)_6\}^{3+}$ from the organic phase, Figure 3.4.18. Strip data taken from Figure 3.4.18. is displayed in Table 3.4.12., and shows that the maximum recovery of rhodium is best achieved at low organic: aqueous ratios.

A solution of 2M nitrite/0.1M nitric acid can also be used to strip the loaded organic phase. As Figure 3.4.19. shows, a single stage extraction is sufficient to recover 96% of the $\{Rh(H_2O)_6\}^{3+}$ complex from an organic feed solution containing 3g/l rhodium and an aqueous : organic flow rate of 4:1.

The equilibration time for stripping with 2M $NaNO_2$/0.1M HNO_3 is rapid, Figure 3.4.20, with 90% of the $\{Rh(H_2O)_6\}^{3+}$ being recovered after a ten minute equilibration. A similar equilibration time is observed for 2M nitric acid, however, there is no gradual increase in the percent rhodium stripped, with increasing equilibration time, as is observed with 2M $NaNO_2$/0.1M HNO_3. In the case of 2M $NaNO_2$/0.1M HNO_3, there are two competing equilibrations, i.e:

$$\overline{Rh(H_2O)_6H_{nm-3}D_{nm}} + 3H^+(\text{or } Na^+) = \{Rh(H_2O)_6\}^{3+} + \overline{n(H,NaD)}_m \quad \ldots\ldots\ldots 3.29$$

and

$$\{Rh(H_2O)_6\}^{3+} + 6NO_2^- = \{Rh(NO_2)_6\}^{3-} + 6H_2O \quad \ldots\ldots\ldots 3.30$$

The formation of $\{Rh(NO_2)_6\}^{3-}$ only occurs after a long equilibration time, and would cause the equilibrium reaction of equation 3.29 to shift to the right.

Figure 3.4.19. Strip isotherm for $\{Rh(H_2O)_6\}^{3+}$ into 2M $NaNO_2$/0.1 M HNO_3

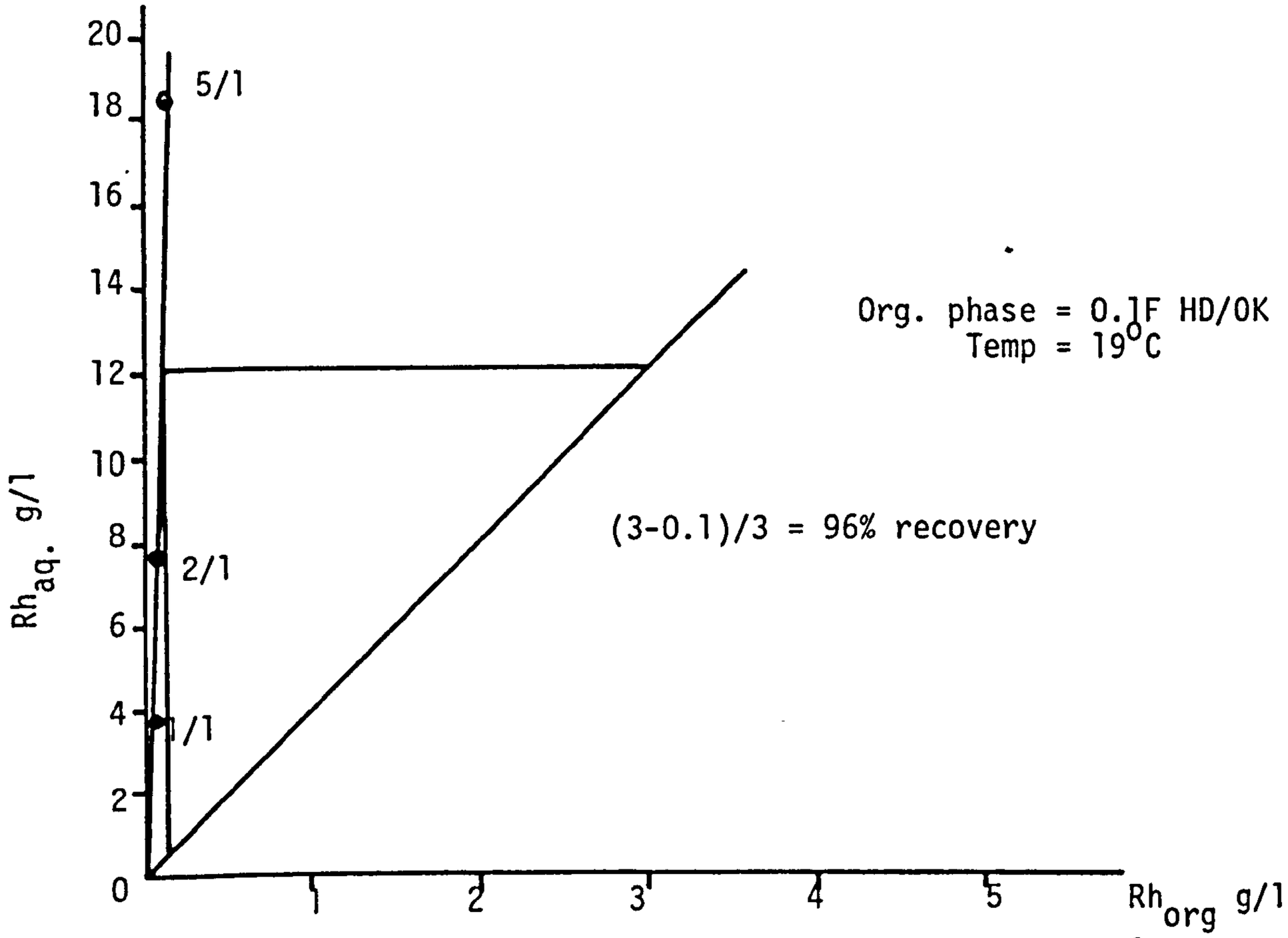

Figure 3.4.20. Equilibration time for stripping $\{Rh(H_2O)_6\}^{3+}$ into 2M HNO_3 and 2 M $NaNO_2$/0.1 M HNO_3

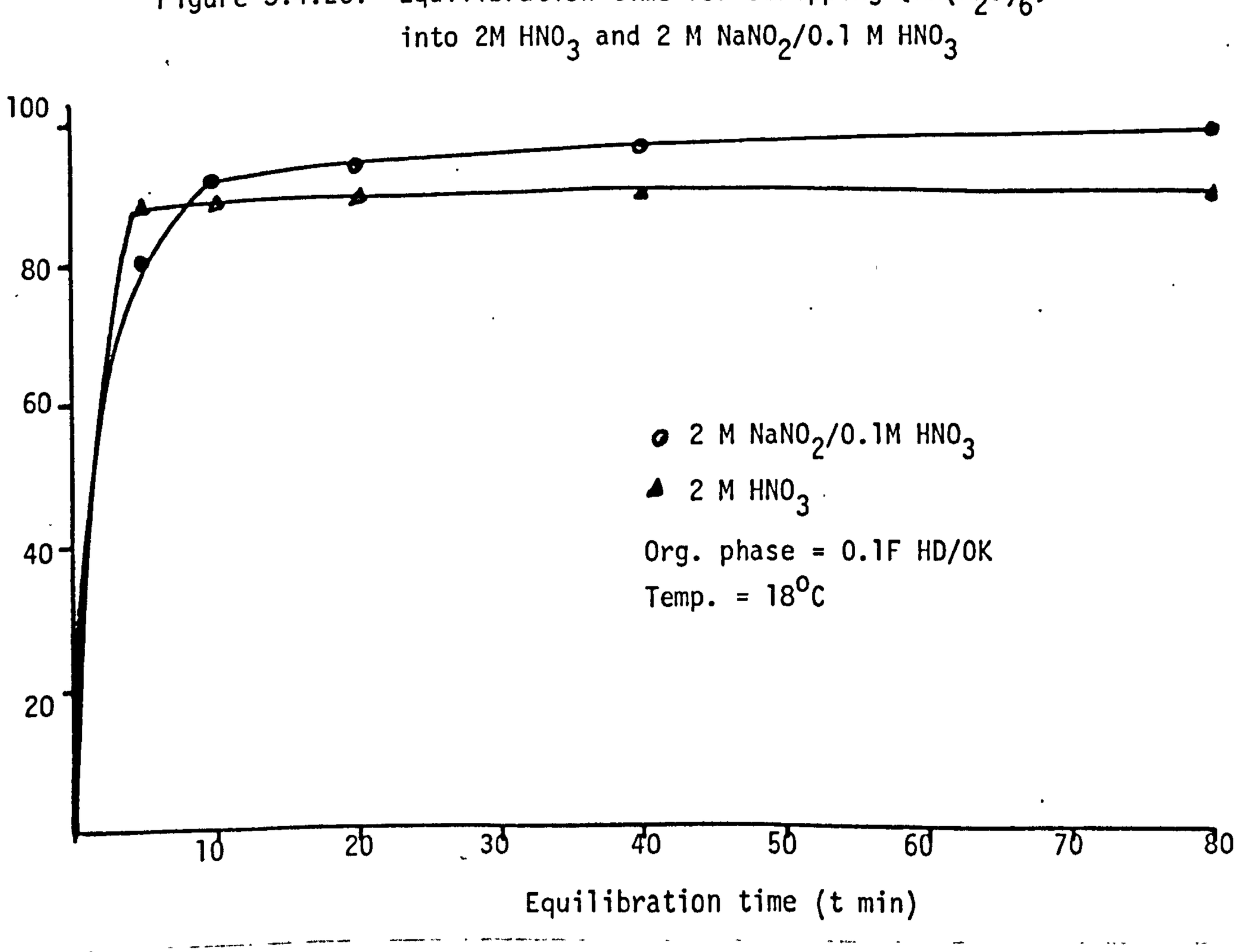

3.5. EXTRACTION OF RHODIUM BY ORGANO-PHOSPHINE SULPHIDES

Thermodynamically, the platinum group metals form their most stable complexes with ligands containing the heavier donor atoms, i.e. soft or class b centres (11, 147, 148). Thus gold, silver and palladium in hydrochloric or nitric acid readily form extractable complexes with organic sulphides (207-210). Lewis et.al. (129) showed that rhodium could be extracted by diheptyl or dioctyl sulphoxide from 5-7M HCl, although equilibration times were long (30-40 minutes). Fritsch et.al. (171) used the precursors of the sulphoxides, i.e. dibutyl and dioctyl sulphide to show the extraction of rhodium from 3-4M HNO_3, although again, equilibration times were long (4-5 hours).

It is appropriate here to consider the solvent extraction of rhodium by the sulphur analogues of organo-phosphine oxides. These reagents may show an improved extraction for rhodium, and in view of the long equilibration times, might also be more resistant to high levels of radiation than the corresponding butyl or octyl sulphides. For the extraction of rhodium from nitric acid, the following organo-phosphine sulphides were considered : tri-phenylphosphine sulphide, tri-n-butyl-phosphine sulphide and N, N', N" - tri-n-hexyl phosphorothioic triamide, Figure 3.5.1.

3.5.1. Nitric Acid Dependency

Triphenyl phosphine sulphide (TPPS) could not be dissolved in odourless kerosene. N, N', N" - tri-n-hexylphosphorothioic triamide (THPS) did dissolve in odourless kerosene, and tri-n-butyl phosphine sulphide

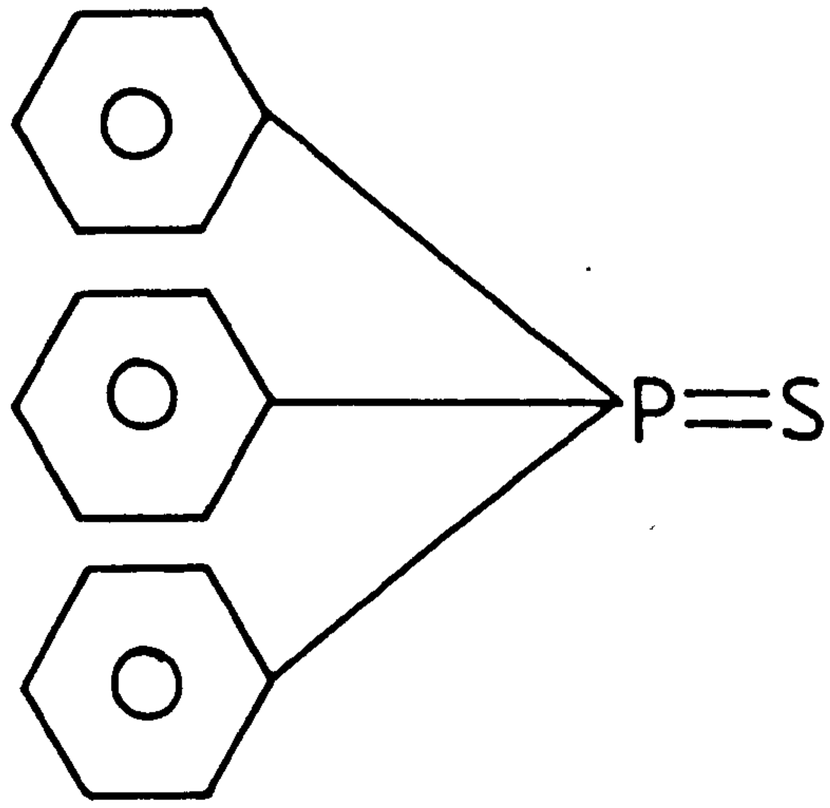

Triphenylphosphine sulphide

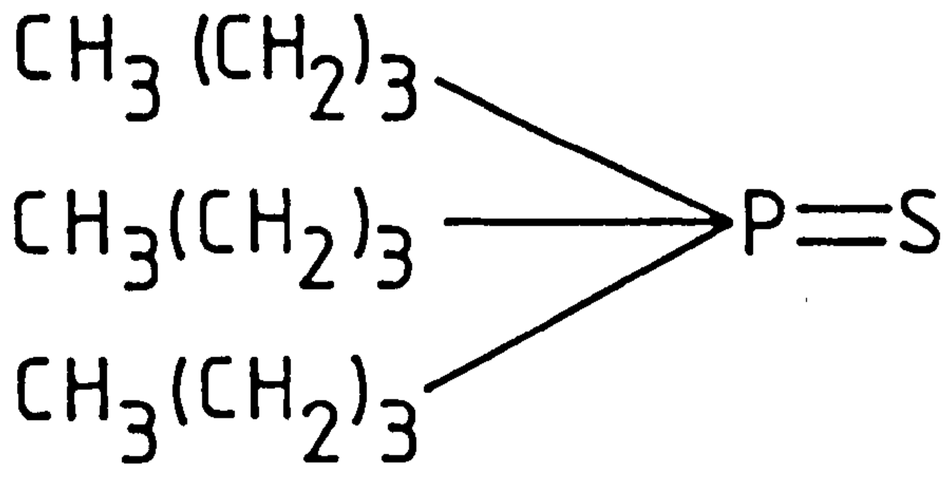

Tri-n-butylphosphine sulphide (TBPS)

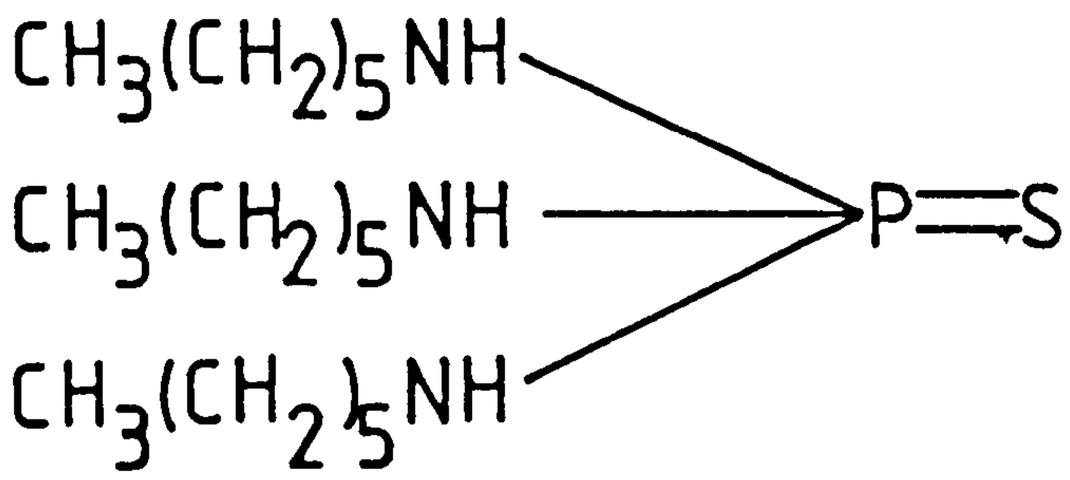

N, N', N" tri-n-hexylphosphrothioic triamide (THPS)

Figure 3.5.1. Orgnophosphine sulphides

(TBPS) was miscible, but neither reagent showed any extraction of rhodium from 0.1-4M nitric acid after a three hour equilibration at $60^{o}C$.

The choice of diluent appears to be significant. The sulphides readily dissolve in diluents which have a labile hydrogen, e.g. long-chain alcohols,and chloroform (211). Fritsch et.al. (171) also recommended the use of long-chain alcohols,suggesting that in other solvents, the oxidation of the sulphides to sulphoxides is favoured. All of the above reagents, except TPPS, when dissolved in heptanol extract rhodium from nitric acid.

Figure 3.5.2. shows the nitric acid dependency on the extraction of rhodium by TBPS and THPS in heptanol. TPPS in heptanol showed no extraction of rhodium ($D_{Rh} < 0.01$) between 0.1-8M nitric acid. The maximum distribution coefficient is observed to be at approximately 1M HNO_3 for TBPS and 2M HNO_3 for THPS. The decrease in D_{Rh} at the higher acid concentrations is probably due to the increased extraction of nitric acid, which may be represented as:

$$H^{+} + NO_3^{-} + \overline{mTHPS} = \overline{HNO_3\ mTHPS} \quad \text{.....3.31}$$

The order for the extraction of rhodium from nitric acid is therefore THPS>TBPS>TPPS. This order can be rationalised in terms of the polarisation of the P=S band. The solvating power of the extractant is due to the ionic character, or shift from P=S to P^{+}-S^{-}. This

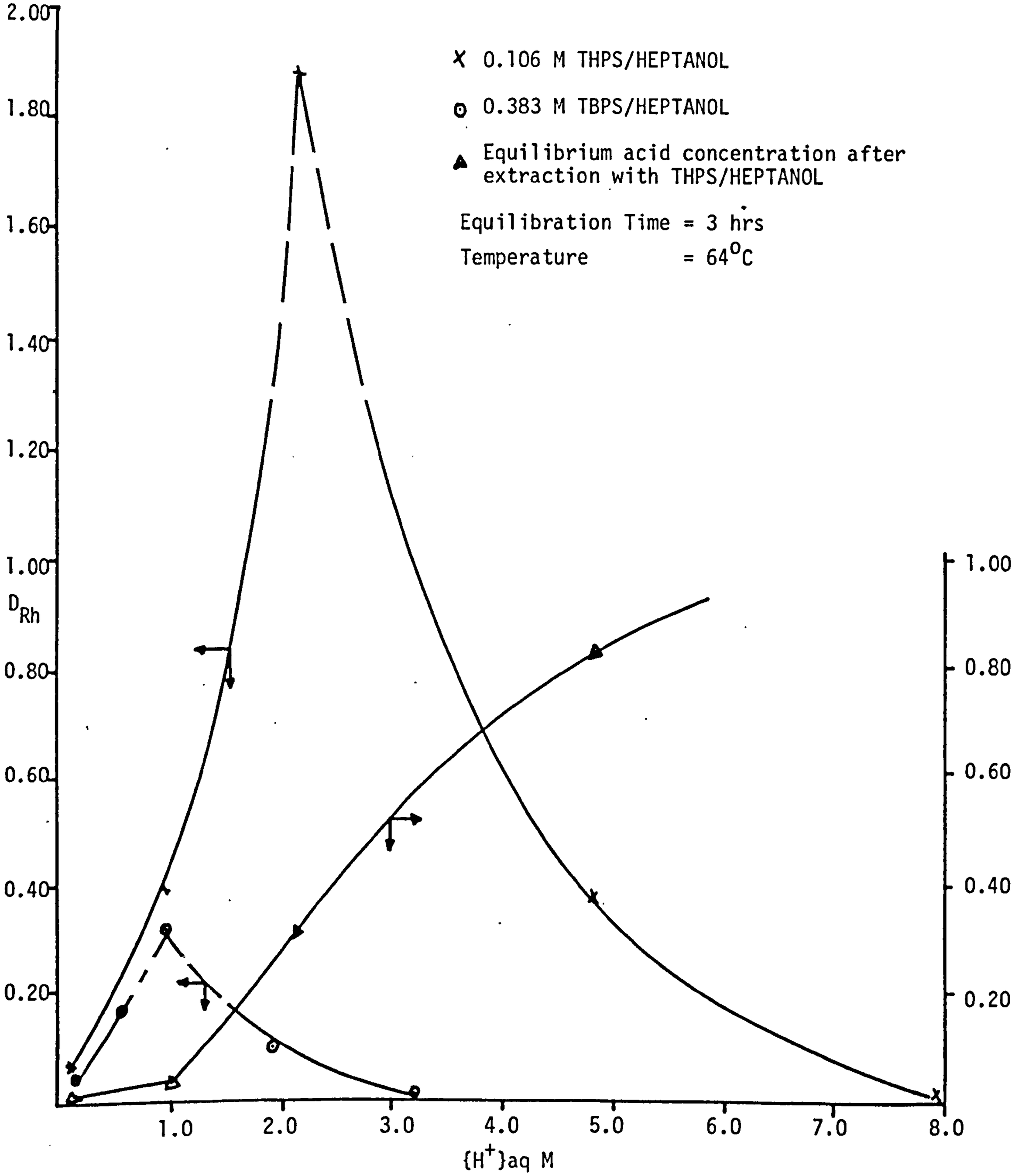

Figure 3.5.2. Hydrogen ion dependency for the extraction of Rh by TBPS and THPS

shift is most pronounced for THPS, where three pairs of lone electrons on the nitrogens are able to contribute to the P=S bond. With TPPS, the three benzene rings, which are electron withdrawing, will greatly reduce the ionic character of the P=S bond. TBPS provides an intermediate case between these two extremes.

3.5.2. {THPS} Dependency on the Extraction of Rhodium from Nitric Acid

The distribution ratio for the extraction of rhodium from nitric acid increases with increasing reagent concentration. Figure 3.5.3. shows the dependence of log D_{Rh} on the log of the THPS concentration. If the mechanism for extraction is simply one of solvation, then the extraction reaction may be represented as:

$$Rh^{3+} + 3NO_3^- + \overline{mTHPS} = \overline{Rh(NO_3)_3.mTHPS} \quad \ldots\ldots 3.32$$

omitting coextracted water.

Hence,

$$K = \frac{\{\overline{Rh(NO_3)_3.mTHPS}\}}{\{Rh^{3+}\}\{NO_3^-\}^3\{\overline{THPS}\}^m} \quad \ldots\ldots 3.33$$

and

$$K = \frac{D_{Rh}}{\{NO_3^-\}^3\{\overline{THPS}\}^m} \quad \ldots\ldots 3.34$$

therefore

$$\log D_{Rh} = \log K + 3 \log \{NO_3^-\} + m \log \{THPS\} \quad \ldots\ldots 3.35$$

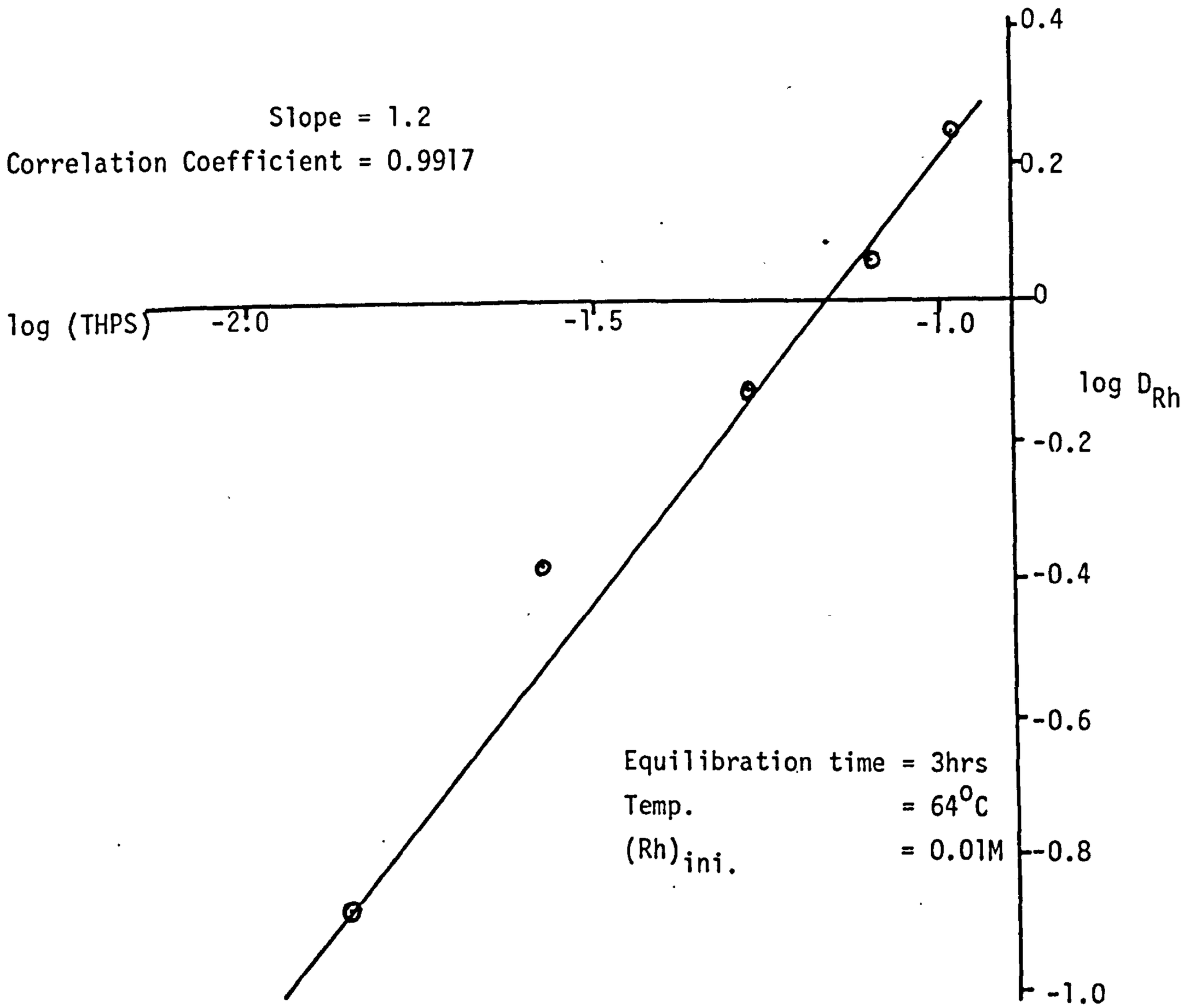

Figure 3.5.3. Dependence of D_{Rh} on the THPS Concentration

Thus a plot of log D_{Rh} against log {THPS} should yield a straight line of slope m, and against log $\{NO_3^-\}$, a straight line of slope 3.

The slope of Figure 3.5.3. is found to be 1.2, the value of m is therefore taken as 1. Figure 3.5.4. shows the plot of log D_{Rh} against log of the equilibrium nitrate ion concentration. The slope of the straight line is 2.9. The extraction of rhodium by THPS thus appears to proceed according to the equilibrium reaction given in equation 3.32.

Figure 3.4.8. showed the effect of nitrite ion on the extraction of rhodium by HD/OK. The results indicated that the formation of the divalent species, $\{Rh(H_2O)_5NO_2\}^{2+}$ enhanced the extraction of rhodium. A similar plot for the extraction of rhodium by THPS is shown in Figure 3.5.5. In this case however, no $^{max}D_{Rh}$ is observed, and the distribution ratio of rhodium would appear to be independent of the nitrite ion concentration. However, when a large excess of nitrite ion was present in solution ($NO_2^-/Rh = 20$) distribution ratios in excess of 50 were obtained, showing essentially quantitative extraction of rhodium. Under these circumstances, the predominant rhodium species would be $\{Rh(NO_2)_6\}^{3-}$ and the extraction reaction may proceed according to:

$$3H^+ + \{Rh(NO_2)_6\}^{3-} + \overline{mTHPS} = \overline{H_3\{Rh(NO_2)_6\}.mTHPS} \quad \ldots\ldots\ldots\ldots\ldots\ldots \quad 3.36$$

3.5.3. Temperature Dependency and Thermodynamic Parameters

Significant extraction of rhodium from nitric acid only occurs at elevated temperatures ($\sim 60^oC$). As Figure 3.5.6. shows, the distribution

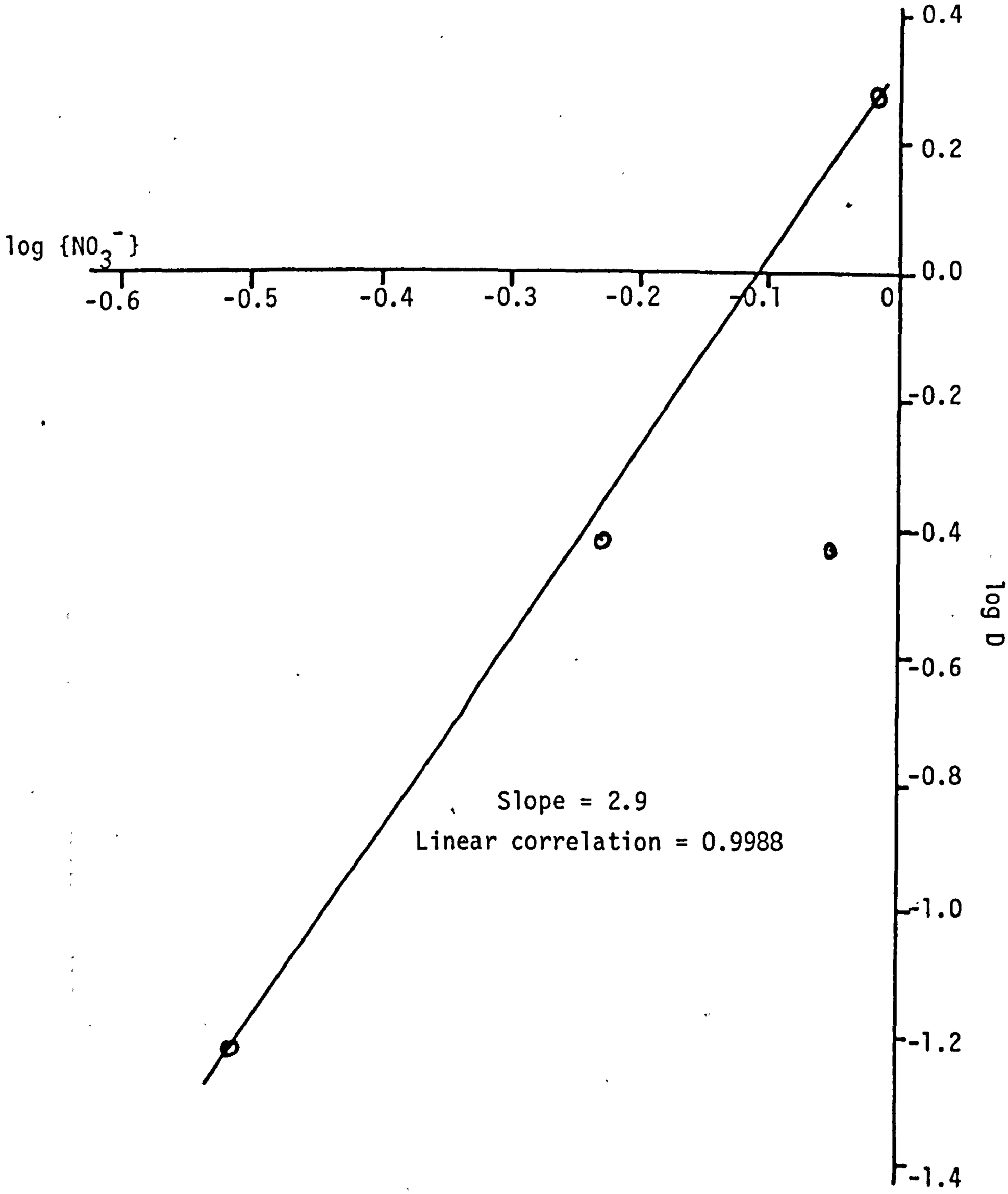

Figure 3.5.4. Dependence of D_{Rh} on the equilibrium nitrate ion concentration.

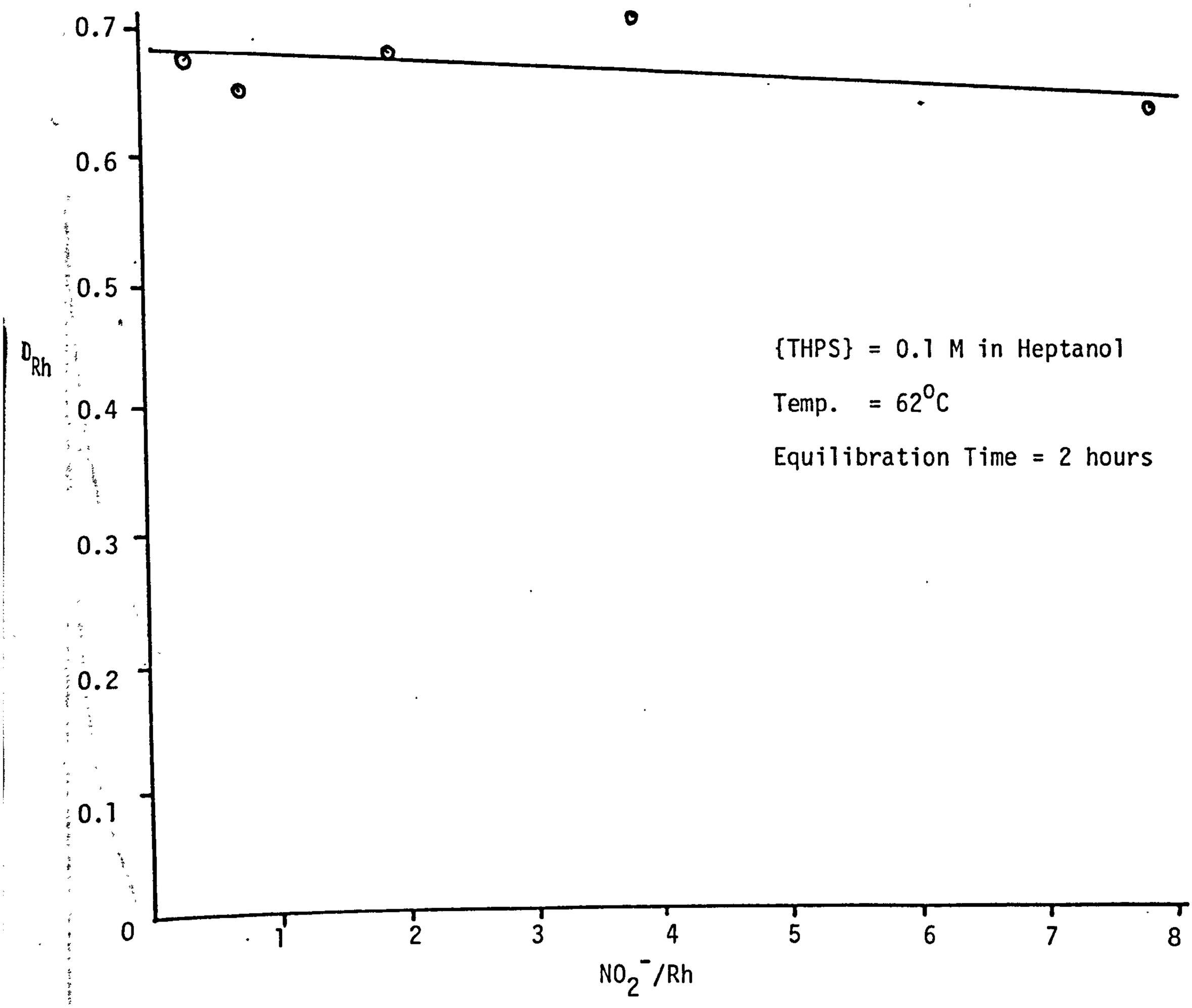

Figure 3.5.5. Dependence of D_{Rh} on the nitrite ion concentration

Figure 3.5.6. Dependence of D_{Rh} on temperature (^{o}C)

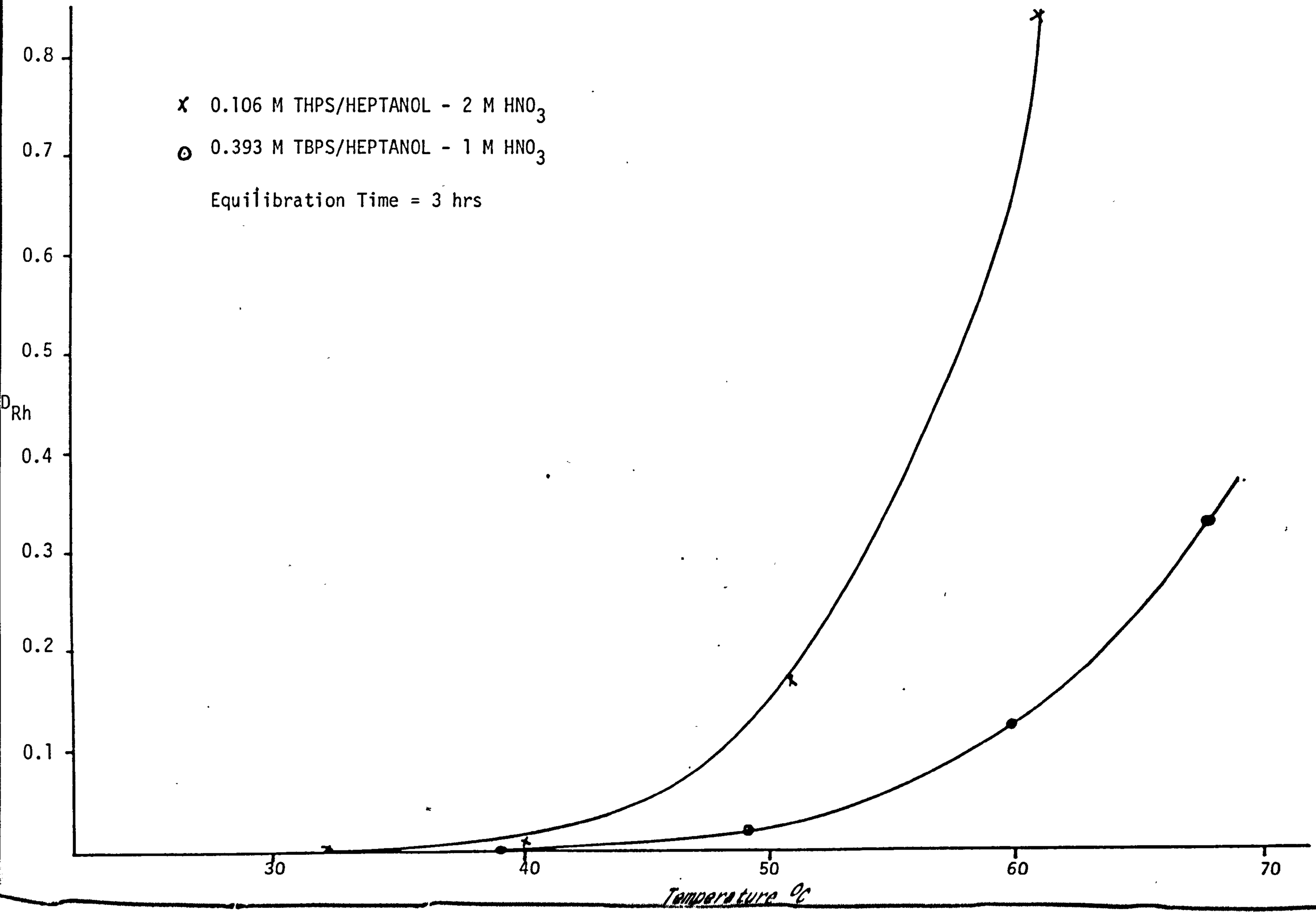

ratio for rhodium below $40^{o}C$ is insignificant.

Figure 3.5.7. shows the log D_{Rh} against 1/T plots from which the thermodynamic functions ΔG, ΔH and ΔS have been determined by application of the Gibbs-Helmholtz (equation 3.17) and Gibbs (equation 3.18) equations. The values are shown in Table 3.5.1.

	ΔH ($kJmol^{-1}$)	ΔS ($J.K^{-1}.mol^{-1}$)	ΔG ($kJmol^{-1}$)
TBPS/Heptanol	140.3	402.7	20.3
THPS/Heptanol	188.5	564.5	20.3

Table 3.5.1. Thermodynamic functions ($25^{o}C$) for the extraction of rhodium by TBPS and THPS in heptanol.

The positive ΔG values show that the extraction process does not proceed spontaneously. This is further confirmed by the long equilibration times required for the extraction, Figure 3.5.8.

Contributions to the values of ΔH and ΔS come from a combination of the following:

(a) a positive enthalpy variation ($\Delta H>0$) as a result of the breakage of ion-water bonds and, a positive entropy variation ($\Delta S>0$) due to the increase in randomness of the system, and,

(b) a negative enthalpy variation ($\Delta H<0$) as a consequence of new bond formation between Rh^{3+}, NO_3^- and THPS/TBPS, and a negative entropy variation ($\Delta S<0$) due to the increase in order caused by new bond formation.

Figure 3.5.7. Plot of log D against $^{1}/T$

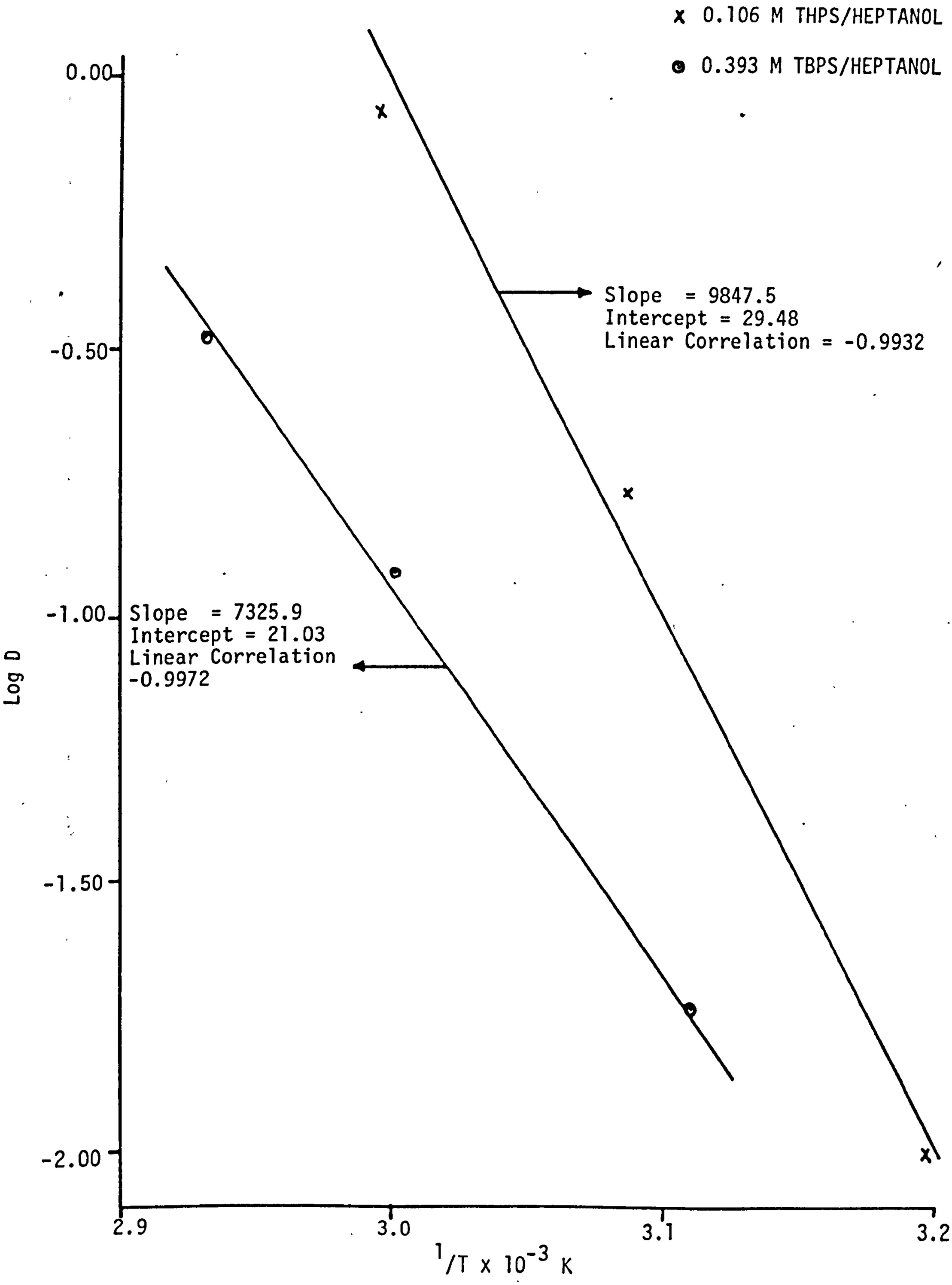

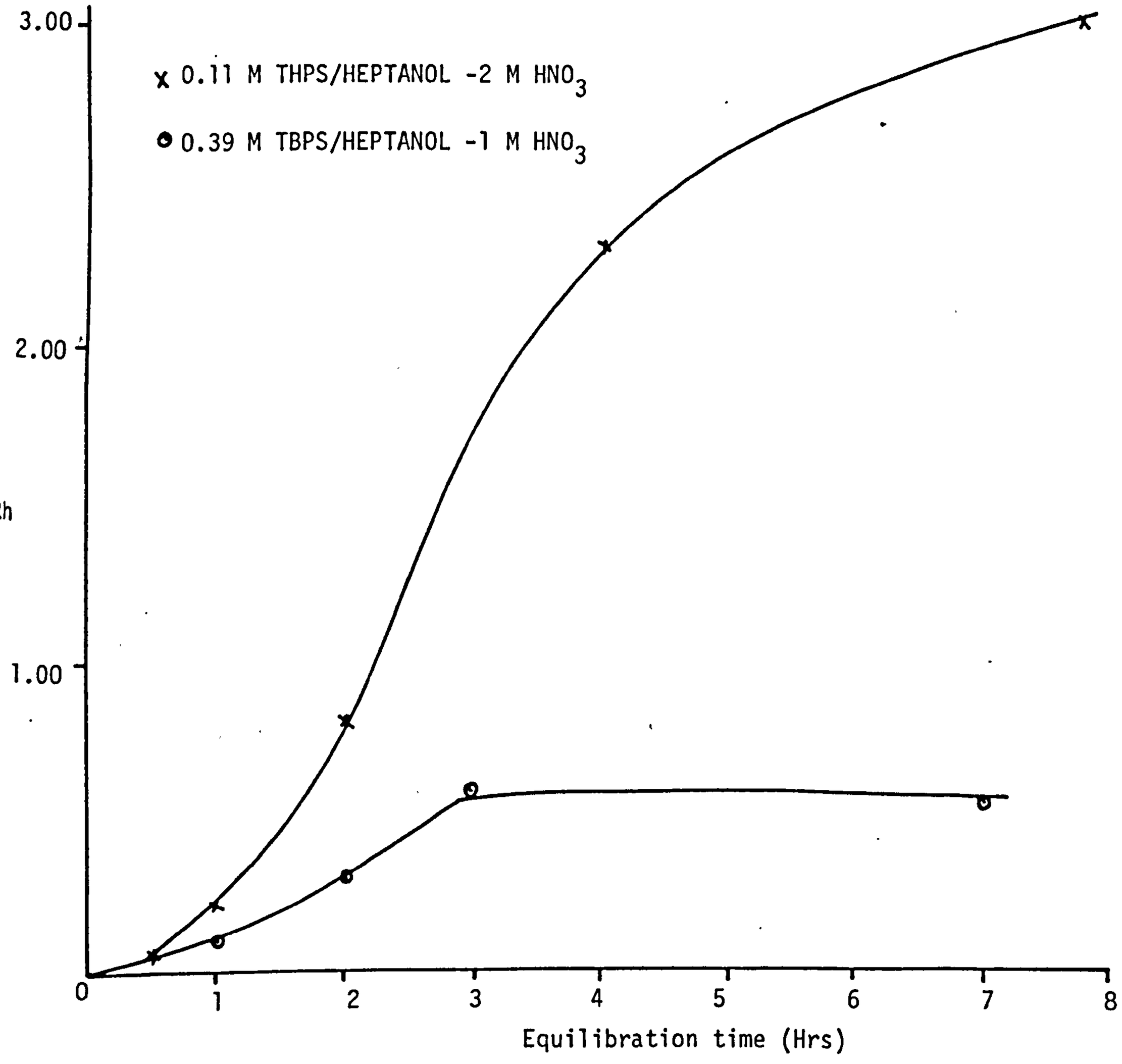

Figure 3.5.8. Dependence of D_{Rh} on equilibration time (Hrs)

The fact that large positive values of ΔH and ΔS are obtained, suggests that the contribution to ΔH and ΔS by new bond formation is very small, or insignificant.

3.6. INTEGRATED SCHEME FOR THE RECOVERY OF RHODIUM FROM HLW

It is clear from the above studies, that none of the extractants considered can be applied directly to recovering rhodium from the type of feed solutions used for extracting uranium and plutonium. The rhodium-tin complex extracted by MIBK only forms in the presence of chloride, and is therefore unacceptable as far as the nuclear industry is concerned. Of the organo-phosphine sulphides, THPS would appear to be the most promising. The advantages are that the extraction takes place from a relatively high nitric acid concentration (2M), and the extractant would be reasonably selective, only silver (I), ruthenium (II-IV), palladium (II) and possibly technetium (VII) would be coextracted (211). The major disadvantage is the long equilibration time, making the system unsuitable for mixer-settler operation.

Rhodium could be recovered in the form $\{Rh(NO_2)_6\}^{3-}$, by extraction with amines as suggested by Beer et.al. (170). Amines, however, are not favoured by the nuclear industry because of the problems of third phase formation (213). Although this can be avoided by the use of suitable additives, a three-component system is nevertheless undesirable.

Extraction of rhodium by dinonylnaphthalene sulphonic acid (HD), can be effected in 0.1-1M nitric acid. By close control of the nitrite ion

concentration in solution, the maximum distribution ratios shown in Figure 3.4.8. can be achieved. The major problem however, is one of selectivity. In particular, the lanthanides and actinides would have to be removed before a multi-stage counter current extraction is applied to recover the rhodium. The role of HD in any scheme for recovering rhodium is therefore a secondary one, applicable only after the majority of other elements present in HLW have been removed.

One of the most promising schemes for fractionating HLW has been investigated by Svantesson et.al. (214, 215), and their work has progressed to the pilot plant scale (216). The flowsheet for this process is displayed in Figure 3.6.1. In the first extraction cycle, di-(2-ethylhexyl) phosphoric acid (HDEHP) acts as a solvating extractant, removing Zr, Nb, In, Mo, Pa, U, Np and Pu from the aqueous phase. In the second extraction cycle, TBP not only removes Pd, Ru and Tc, but also extracts nitric acid, thus reducing the aqueous acid concentration from 6M HNO_3 to approximately 0.1M HNO_3. This is followed by a second HDEHP cycle, in which the extractant removes Am, Cm, Bk, Cf and the lanthanides, either by solvation or cation exchange. Since neither HDEHP or TBP extracts rhodium the aqueous raffinate after the second HDEHP cycle comprises primarily of caesium, strontium, rhodium and residual waste, in approximately 0.1M HNO_3.

In considering the extraction of rhodium from this raffinate by HD, it is important to determine the decontamination factors for caesium and strontium in particular. Figure 3.6.2. shows the effect of caesium and

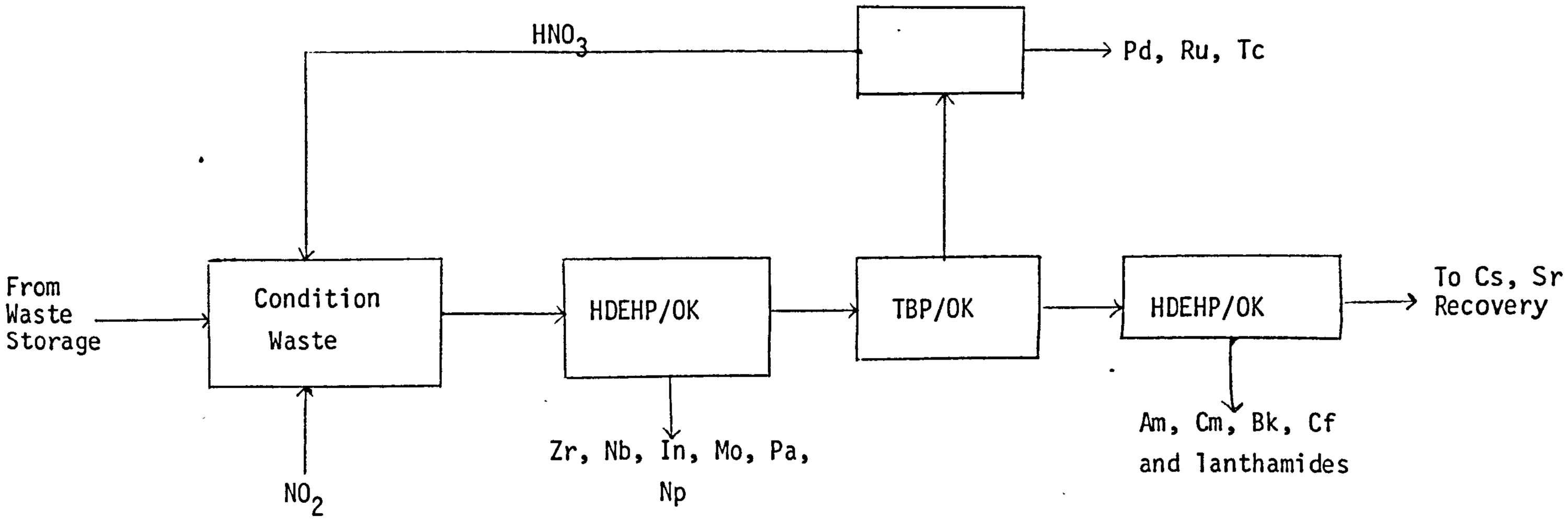

Figure 3.6.1. Flowsheet for fractionating HLW (214, 215)

strontium on the extraction of rhodium by HD. It is seen that the distribution of rhodium is much more sensitive to the presence of strontium than caesium. In the flowsheet illustrated by Figure 3.6.1., the rhodium is present as the hexanitrite anion, $\{Rh(NO_2)_6\}^{3-}$. Strontium could be removed by HD prior to the destruction of nitrite ion, and a second HD cycle, for recovering rhodium.

A simulate waste solution comprising caesium, strontium and rhodium in concentrations ten times that found in HLW (i.e. 8.1, 2.6 and 1.5 g/l respectively), was prepared in 0.1M HNO_3. On a single extraction with an equal volume of 0.1F HD/OK, separation factors of 1.2 (Rh/Sr) and 2.7 (Rh/Cs) were obtained. The results of stripping this loaded organic phase with 2M $NaNO_2$/0.1M HNO_3 are displayed in Table 3.6.1. The results show that it may be possible to strip caesium and strontium preferentially if low organic : aqueous flow rates are employed.

The distribution of rhodium between nitric acid and HD/OK was also followed by γ-counting of the isotope ^{105}Rh (section 5.6.6.). Thus aqueous solutions of caesium, strontium, and rhodium in concentrations close to those found in HLW could be studied. Figure 3.6.3. shows the effect of nitrite ion on the distribution of caesium, strontium and rhodium (0.85, 0.26 and 0.39 g/l respectively), from 0.3M HNO_3. It is observed that the distribution ratios for caesium and strontium are independent of the nitrite ion concentration, whilst for rhodium a maximum is observed at $\{NO_2^-\}/\{Rh\} \simeq 1$. Again a separation of the three components may be possible by removing strontium at high nitrite

	Sr		Cs		Rh	
O/A	D	% stripped	D	% stripped	D	% stripped
10/1	6.20	13.8	5.20	16.13	4.16	19.35
5/1	2.30	30.3	1.66	37.6	5.74	14.80
2/1	0.63	61.3	0.44	69.5	5.90	14.50

Table 3.6.1. Strip data for a mixture of Cs, Sr and Rh into 2M $NaNO_2$/0.1 M HNO_3

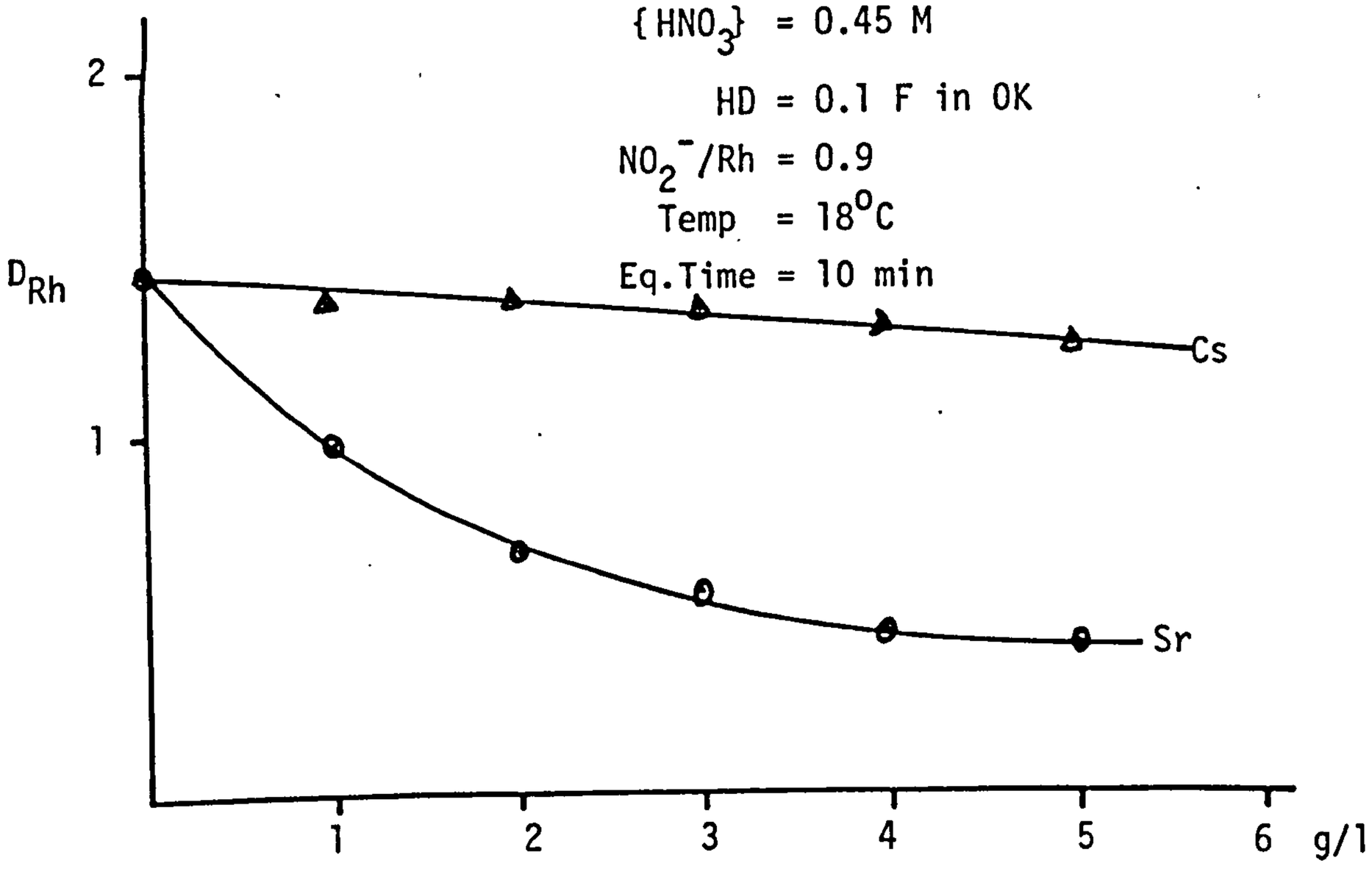

Figure 3.6.2. Effect of the presence of Cs and Sr on the distribution of rhodium between nitric acid and HD/OK.

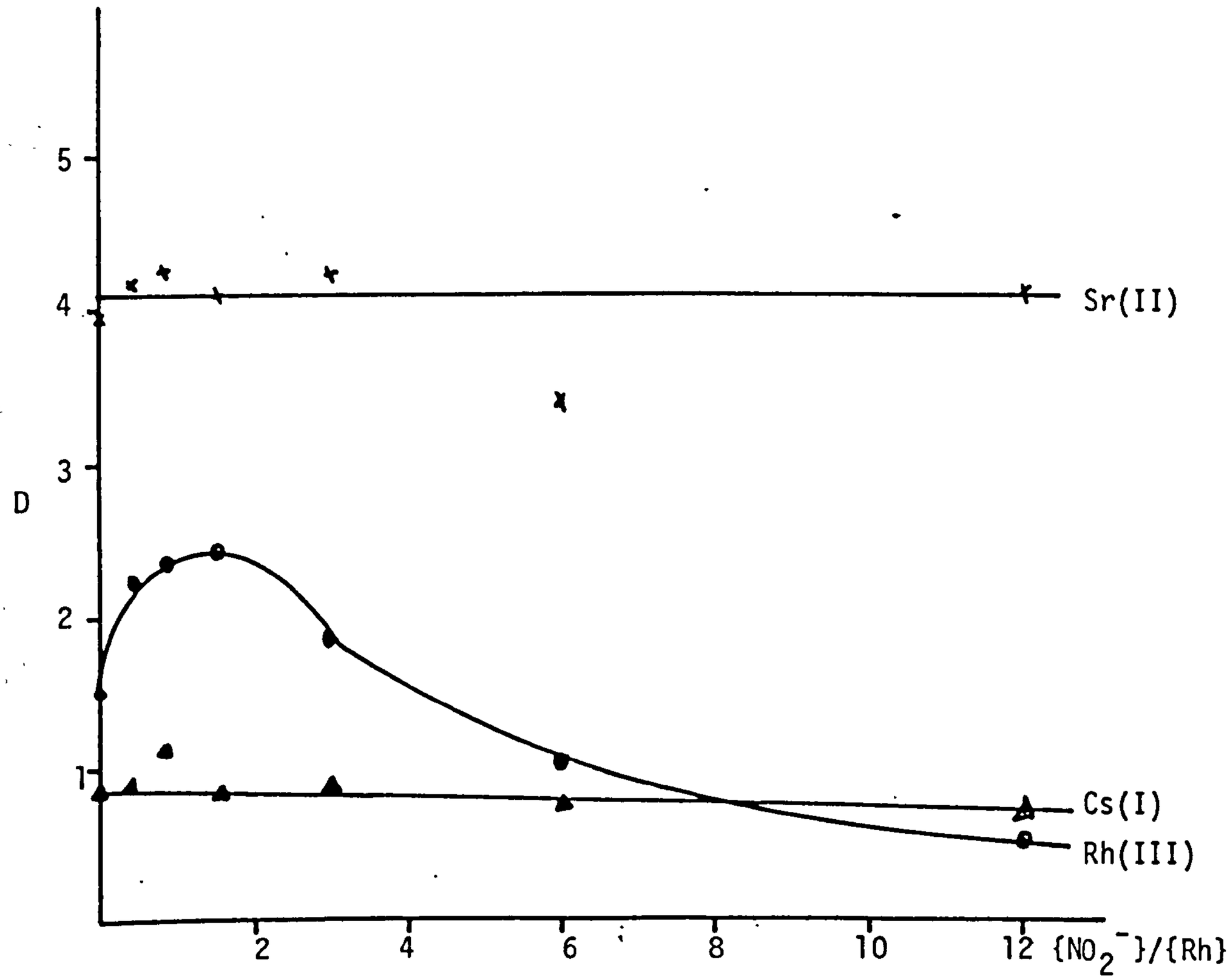

Figure 3.6.3. Effect of nitrite ion on the distribution of Cs, Sr and Rh between 0.3 M HNO_3 and 0.1 F HD/OK.

ion concentration, and then separating rhodium from caesium by suitable adjustment of the nitrite ion concentration.

The overall usefulness of HD for recovering rhodium was tested by determining the separation factors for rhodium, from caesium and strontium, from a simulate HLW solution. The HLW solution was prepared as outlined in Section 5.5.5., and contained 10g/l fission products in 6M HNO_3 and 0.2M $NaNO_2$. The distribution ratios for rhodium were determined by γ-counting ^{105}Rh (Section 5.2.4), and for caesium and strontium by atomic absorption analysis (Section 5.2.5.). Preliminary experiments showed that three TBP (50%^{v}/v) cycles at an organic : aqueous ratio of 5:1 would be required to reduce the acid concentration from 6M HNO_3 to 0.1M HNO_3.

The first five extraction cycles involving HDEHP and TBP are shown in Figure 3.6.4. It is observed that for the first HDEHP cycle, D_{Rh} is less than 0.01. The following three TBP cycles reduce the acid concentration to 0.02M. There is some extraction of rhodium by TBP, but this is not significant in view of the large O/A ratios employed. The final HDEHP cycle again shows no extraction of rhodium ($D_{Rh} < 0.01$).

The aqueous raffinate can now be treated in the following manner, Figure 3.6.5. Caesium and strontium can be removed by extraction with HD. Since the rhodium at this stage would be present as $\{Rh(NO_2)_6\}^{3-}$, it would not be extracted by HD, and this is confirmed by the low distribution ratio obtained ($D_{Rh} = 0.03$). The distribution ratios for caesium and strontium are 0.69 and 1.48 respectively. This would allow more than 98% of strontium and 90% of caesium to be removed after a five-stage

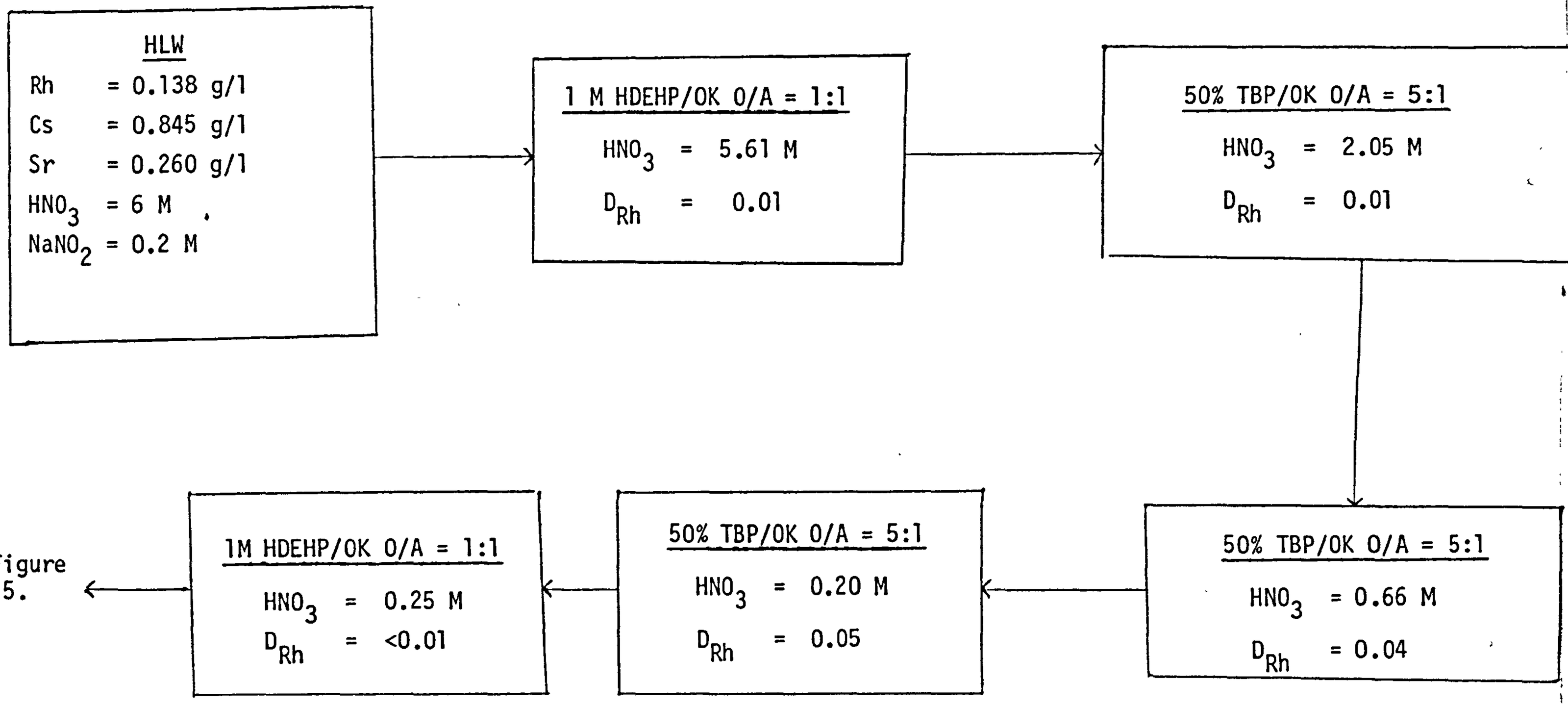

Equilibration time = 5 minutes
Temperature = 26.5°C

Figure 3.6.4. Flowsheet for recovering rhodium from HLW

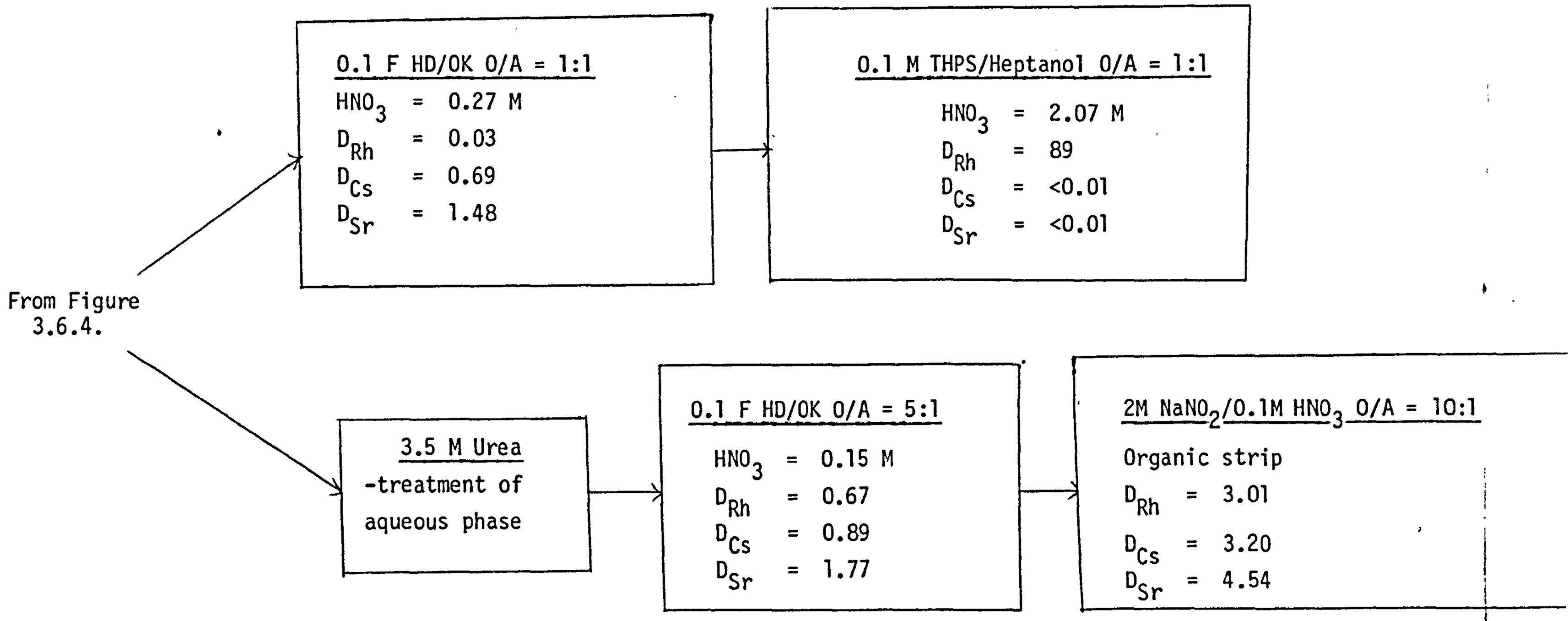

Equilibration time = 5 minutes (Except for THPS, Eq. time = 2 hrs).

Temperature = 26.5°C (60°C for THPS)

Figure 3.6.5. Flowsheet for recovering rhodium from HLW

mixer-settler run at an organic : aqueous ratio of 1:1, Table 3.6.2.

Having removed caesium and strontium, the radioactivity associated with the aqueous raffinate will have been considerably reduced. Thus the aqueous phase could be treated in a separate contactor with THPS/heptanol to recover rhodium. As Figure 3.6.5. shows, the distribution ratio is high (D_{Rh} = 89), and consequently the decontamination factors, from caesium and strontium are also high (>8000).

Mixer-settler stage	{Sr} g/l	% Sr remaining	{Cs} g/l	% Cs remaining
0	0.260	-	0.845	-
1	0.105	40.32	0.500	59.2
2	0.042	16.3	0.296	35.0
3	0.017	6.6	0.175	20.7
4	0.007	2.6	0.104	12.3
5	0.003	1.1	0.061	7.2

Table 3.6.2. Recovery of Cs(I) and Sr(II) after a five-stage mixer-settler run.

An alternative route to treating the aqueous raffinate after the final HDEHP cycle, is to destroy nitrite ion, thus converting the rhodium to the hexaaquo form, and then to extract with HD/OK. Thiourea, urea or sulphamic acid could be used to destroy nitrite (217), by the following reactions:

$$CS(NH_2)_2 + HNO_2 = N_2 + HSCN + 2H_2O \quad \ldots\ldots\ldots\ldots\ldots\ldots\ldots\ldots\ldots\ldots \quad 3.37$$

$$CO(NH_2)_2 + 2HNO_2 = 2N_2 + CO_2 + 3H_2O \quad \ldots\ldots\ldots\ldots\ldots\ldots\ldots\ldots \quad 3.38$$

$$HO.SO_2.NH_2 + HNO_2 = N_2 + H_2SO_4 + H_2O \quad \ldots\ldots\ldots\ldots\ldots\ldots\ldots\ldots \quad 3.39$$

Urea is preferred since the reaction products are easily removed, and would not interfere in subsequent extraction cycles. Thiourea and sulphamic acid both give rise to reaction products which would form anionic rhodium (III) complexes, e.g. $\{Rh(SCN)_6\}^{3-}$ and $\{Rh_2O(SO_4)_7\}^{10-}$ which would not be extracted by HD.

Urea was added directly to the aqueous raffinate, after the final HDEHP cycle, to give a 3.5M solution. This solution was boiled for fifteen minutes to ensure complete destruction of nitrite. As the flowsheet in Figure 3.6.5. shows, on extraction with HD/OK, distribution ratios of $D_{Rh} = 0.7$, $D_{Sr} = 1.8$ and $D_{Cs} = 0.9$ are obtained, and consequently the separation factors are small. Although theoretically a separation of the three components could be affected, in practical terms, mixer-settler operation would not be possible. The large number of equilibrium stages required, could however be accommodated if a packed column is used instead of a mixer-settler. A similar problem is encountered if the organic phase is stripped with 2M $NaNO_2$/0.1M HNO_3, Figure 3.6.5.

CHAPTER FOUR

CONCLUSIONS AND FURTHER WORK

4.1. RHODIUM SPECIATION IN NITRIC ACID

Electrophoresis, electronic absorption measurements and the cation exchange experiments have shown that the predominant rhodium species in nitric acid is the hexaaquo ion, $\{Rh(H_2O)_6\}^{3+}$. None of these techniques confirms the presence of the pentaaquonitratorhodate (III) ion, $\{Rh(H_2O)_5NO_3\}^{2+}$, suggestive therefore that this particular ion is indeed a minor constituent in aqueous nitrate media. The ^{103}Rh NMR spectroscopic studies have shown the presence, in a wide range of nitric acid containing solutions, of both the $\{Rh(H_2O)_6\}^{3+}$ and $\{Rh(H_2O)_5NO_3\}^{2+}$ Ions. In the presence of nitrite ions, all the rhodium (III) nitrite complexes of the general formula $\{Rh(H_2O)_{6-n}(NO_2)_n\}^{(3-n)+}$ have been identified by ^{103}Rh NMR spectroscopy. Subject to the constraints of sensitivity, it is clear that this particular technique affords the best method for a qualitative study of rhodium species in nitric acid. Further confirmation that the nitrate ion, like the perchlorate ion, is essentially non-coordinating to rhodium is provided by the shifts in the polarographic half-wave potentials of rhodium containing nitrate, nitrite and perchlorate solutions (Section 2.6).

The rhodium species in stored highly active waste solutions will range from the hexaaquorhodium (III) ion to complexes of the type $\{Rh(H_2O)_{6-n}(NO_2)_n\}^{(3-n)+}$, depending on the nitrite ion concentration. If the latter greatly exceeds that of rhodium in solution, then the

predominant species will be $\{Rh(NO_2)_6\}^{3-}$. There exists the possibility that such anionic complexes of rhodium may be adsorbed onto the inorganic particulate matter that is present in HLW. For example, it is well known that zirconium readily hydrolyses, even in very acidic solutions, to give species such as $\{Zr_3(OH)_4\}^{2+}$ and $\{Zr_4(OH)_8\}^{8+}$ which are able to function as inorganic anion exchangers (14). Polymeric forms of zirconium phosphate, $Zr(HPO_4)_2.nH_2O$ may also be formed during Purex processing. These behave as cationic exchangers and may adsorb rhodium cationic species such as the hexaaquo ion (149). If these zirconium complexes constitute a significant portion of the particulate matter, and if they function as ion exchangers, then these possibilities cannot be overlooked. Further investigation in this area is required, and if indeed the rhodium species are adsorbed onto the particulate matter, a simpler route to their recovery may be possible.

4.2. SOLVENT EXTRACTION OF RHODIUM

As an overall screening method, shake-out tests, as recommended by Ritcey and Ashbrook (103), are to be preferred to reversed phase paper chromatography. Although more time consuming, they nevertheless avoid the spurious results sometimes obtained with the latter technique.

The recovery of rhodium, by the formation of an extractable rhodium-tin complex is not a practical proposition because of the need to maintain a relatively large concentration of chloride ions. As Figures 3.3.1. - 3.3.3. show, the optimum nitric acid concentration when using a 0.5M $SnCl_2$/1.25 M HCl solution is between 3-5M, and equilibration times are

long (>60 min.). Although this system would be unacceptable to the nuclear industry, it may be of use to processors in the precious metals industry. For example, the chlorostannous complexes of other precious metals have been identified e.g. $\{RuCl_2(SnCl_3)_2\}^-$, $\{Ir_2Cl_6(SnCl_3)_4\}^{4-}$ (1), and Khattak and Magee (75) have shown that the corresponding complexes of platinum and palladium can be extracted by amines. Further investigations into the solvent extraction behaviour of these complexes are required, as this may lead to an alternative scheme to recover platinum metals from their chloride concentrates.

In the absence of nitrite ion, the extraction studies of section 3.4 have shown that it is possible to recover $\{Rh(H_2O)_6\}^{3+}$ by extraction with HD/OK. Significant extraction only occurs at low acid concentrations (0.1M), thus requiring the prior removal of nitric acid (by TBP) from HLW. Further, the removal from HLW of lanthanides and actinides, by extraction with HDEHP, would leave an aqueous raffinate comprising essentially of caesium, strontium and rhodium. From this aqueous raffinate, the recovery of $\{Rh(H_2O)_6\}^{3+}$ by HD could be accomplished by the use of multi-stage counter current processes. The efficiency with which the rhodium extraction occurs could also be improved by the close control of the nitrite ion concentration, such that the $\{Rh(H_2O)_5NO_2\}^{2+}$ complex predominates.

The studies of Danesi et.al. (182, 183) and Raieh and Aly (189), show that the distribution ratios for the extraction of trivalent lanthanides and actinides by HD are at least an order of magnitude higher than for

rhodium from one molar acid solutions. An alternative scheme for fractionating HLW is thus possible, wherein HD replaces HDEHP for extracting lanthanides and actinides, Figure 4.2.1.

In the first extraction cycle, TBP removes uranium, plutonium, palladium, technetium and ruthenium. The nitric acid concentration is also reduced to approximately one molar. In the second cycle, extraction which HD will remove lanthanides and actinides, leaving an aqueous raffinate of rhodium and residual waste (mainly caesium and strontium). After adjustment of the nitric acid concentration, to two molar, extraction with THPS will recover rhodium, leaving caesium and strontium in the waste stream. Alternatively, after the removal of nitrite ion, further extraction with HD using multi-stage counter current processes could fractionate rhodium, caesium and strontium from the remaining aqueous raffinate. Further studies on this flowsheet, and the one illustrated in Figures 3.6.4. and 3.6.5. are required. In particular, bench scale mixer-settler trials on simulate HLW solutions are required to assess the suitability of using a three or four component extraction system in a continuous process.

Selective extraction of rhodium from nitric acid can be achieved by equilibration with a whole series of organo-phosphine sulphides (Section 3.5). In particular, those phosphine sulphides which contain electron donating groups able to contribute to the polarisability of the P=S bond would appear to be the most promising. Thus a diphosphinedisulphide tetraamide such as:

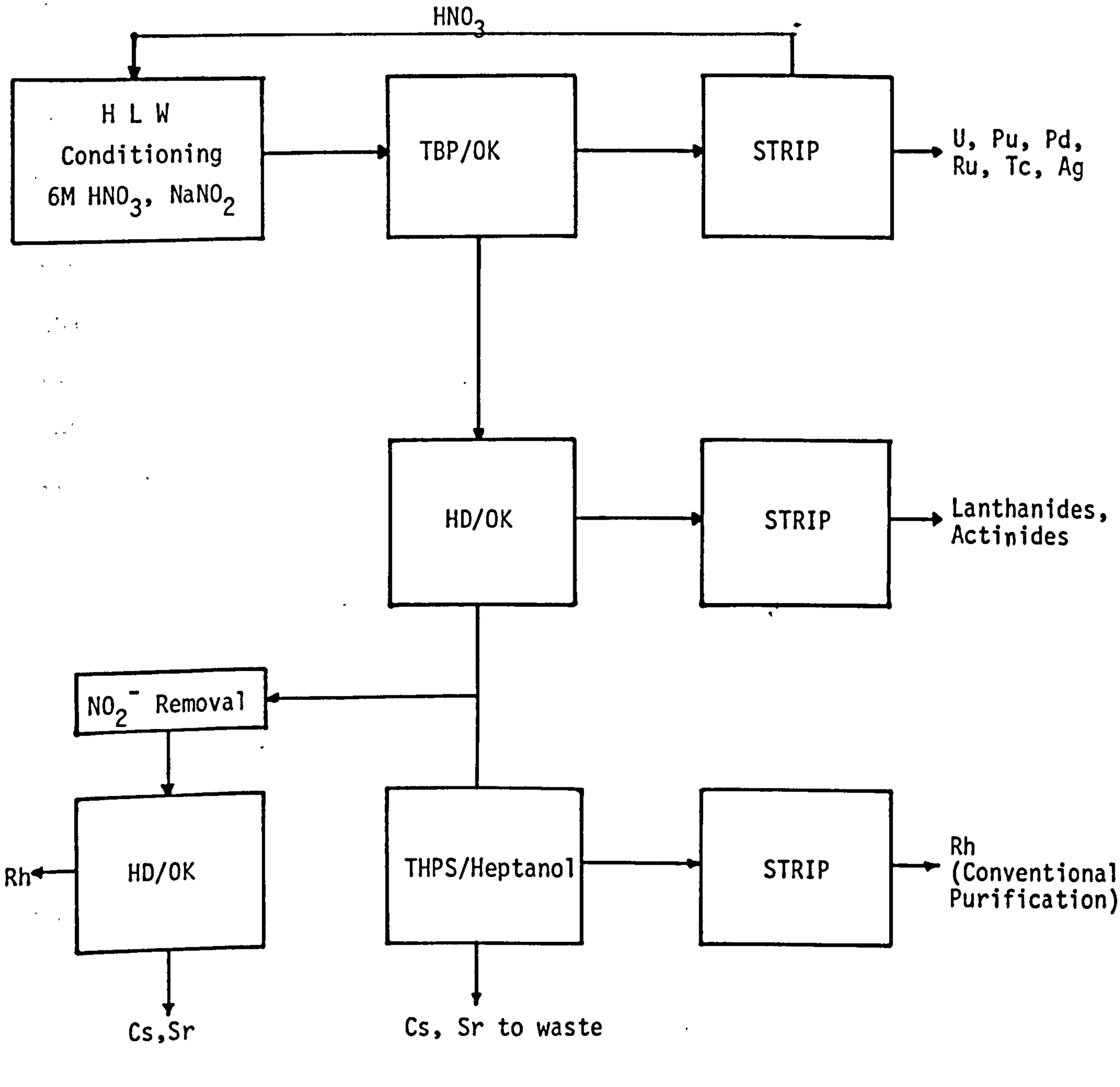

Figure 4.2.1. Fractionation of HLW

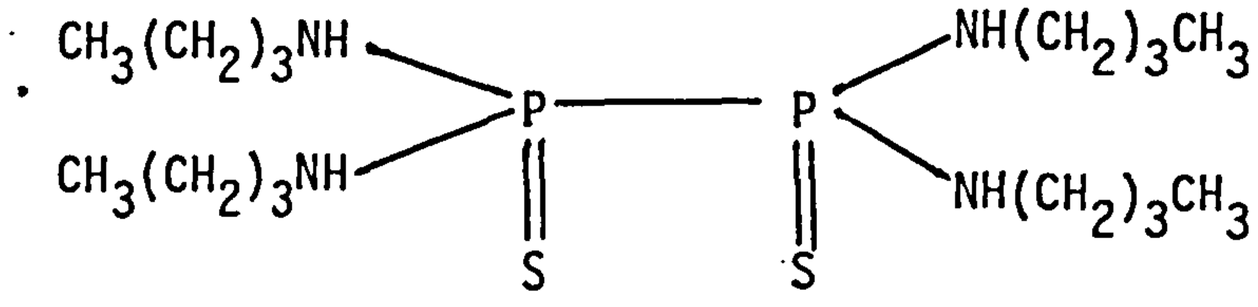

may show a greater extraction for rhodium than THPS. The main advantages of such a system are that it would be reasonably selective, only palladium, ruthenium, silver and technetium would be expected to co-extract, and that the extraction could take place from 1-2 M nitric acid. The main disadvantage however, is the long equilibration times involved. Thus the stability of such reagents to radiation is of prime importance and requires further investigation.

CHAPTER FIVE

EXPERIMENTAL

5.1. FOREWORD

In this chapter are described, with appropriate details, the experimental procedures used in obtaining the data presented in chapters two and three. Some preliminary results are also included.

Where available, analytical grade reagents were used. A list of these chemicals is given in Table 5.1.1.

5.2. ANALYTICAL METHODS

5.2.1. Analytical Determination of Rhodium

A stock standard solution of rhodium was prepared, for calibration purposes, by dissolving a known weight (0.3854 gm) of ammonium hexachlororhodate in doubly distilled water, and diluting to 100 mls in a volumetric flask. This stock solution was standardised gravimetrically in the following manner (54, 55). An aliquot of the stock solution (25 ml) was diluted to 200 mls, acidified with hydrochloric acid and then treated with 10 mls of 1.4% $^{W}/v$ thiobarbituric acid in 95% ethanol. The solution was boiled for two hours to precipitate the rhodium-thiobarbituric acid complex, which was filtered, washed with water, ignited in a weighing boat, reduced in hydrogen, cooled in nitrogen and weighed. Calibration standards, for analysing rhodium by colorimetric procedures, were prepared from this stock solution.

Table 5.1.1. List of Chemicals

Reagent	Supplier
Acetic acid	Fisons
Acetic anhydride	Fisons
Ammonium hexachlororhodate	Johnson Matthey
Ammonium Molybdate	BDH
Barium nitrate	Fisons
Butyl ether	Fisons
Cadmium nitrate	BDH
Caesium nitrate	BDH
Carbon tetrachloride	Fisons
Cerium nitrate	Fisons
Deutrated water	BDH
Diethyl ether	Fisons
Dinonylnaphthalene sulphonic acid	Pflatz and Bauer, King Industries
Dioctylamine	Aldrich
Dowex-1 anion exchange resin	Fluka
Dowex 50W-X8 cation exchange resin	Fluka
Ethanol	Fisons
Ethylene diamine tetraacetic acid	Fisons
2-Ethylhexanol	Fisons
Fiso Fluoro 2	Fisons
Hydrochloric acid	Fisons
Heptanol	Fisons
Hexylamine	Aldrich
Hostarex A327	Hoechst AG
Lanthanum nitrate	Fisons
Mercaptobenzo thiazole	Aldrich
Methanol	Fisons
Methyl isobutyl ketone	Fisons

Table 5.1.1. continued

Reagent	Supplier
Methyl orange	Fisons
Neodynium oxide	BDH
Neutral alumina	Fisons
Nitric acid	Fisons
Odourless kerosene	AERE Harwell, Shell
Perchloric acid	Fisons
Phosphorous pentasulphide	Aldrich
Potassium hexanitritorhodate	Johnson Matthey
Potassium hydrogen phthalate	Fisons
Potassium hydroxide	Fisons
Potassium nitrite	Fisons
Potassium permanganate	Fisons
Praseodymium oxide	BDH
Palladium nitrate	Johnson Matthey
Rhodium nitrate	Fluka
Rhodium trichloride	Johnson Matthey
Rubidium chloride	Fisons
Ruthenium trichloride	Johnson Matthey
Samarium oxide	Johnson Matthey
Silver nitrate	Fisons
Sodium acetate	Fisons
Sodium chloride	Fisons
Sodium hydroxide	East Anglia Chemicals
Sodium hypochlorite	Fisons
Sodium nitrate	Fisons
Sodium sulphate	Fisons
Stannous chloride	Fisons
Stannous oxide	Fisons
Strontium nitrate	Fisons
Sulphur	Fisons

Table 5.1.1. continued

Reagent	Supplier
Tetrabutyl ammonium hydroxide	Fisons
Tetrabutyldiphosphinedisulphide	Alfa
Theonyltrifluoroacetone	Fluka
Thiobarbituric acid	Aldrich
Thiophosphoryl chloride	Aldrich
2-Thiotheonyltrifluoroacetone	Fluka
Thorium nitrate	Fisons
Titron X-100	Fisons
Toluene	Fisons
Tributylphosphate	Aldrich
Tributylphosphine	Aldrich
Trioctylamine	Aldrich
Trioctylphosphine oxide	BDH
Triphenylphosphine sulphide	Aldrich
Uranyl nitrate	Fisons
Xylenol orange	Fisons
Ytterium chloride	Hopkin & Williams
Zirconium nitrate	BDH
Radioisotopes: ^{105}Rh, ^{137}Cs, ^{85}Sr, ^{110m}Ag, ^{106}Ru, ^{99m}Tc, ^{147}Pm.	Amersham International

Two colorimetric methods were used in analysing rhodium solutions. In the hypochlorite method (218), acetate buffer (10 mls of 0.8 M CH_3COOH/ 2.4 M CH_3 COONa) was mixed with sodium hypochlorite (50 mls of a 5% solution). An aliquot of the rhodium sample solution was then added, and the mixture made up to 100 mls. After one hour the transmittance of the solution was measured at 665 nm relative to a blank solution made up in a similar manner. Absorption measurements were carried out on a Cecil model CE 5095 absorption spectrophotometer using matched 1 cm^2 silica cells. A typical calibration plot is shown in Figure 5.2.1.

The majority of rhodium sample solutions for analysis were determined by the tin(II) chloride method (74). Concentrated hydrochloric acid (10 ml) was added to the sample solution, followed by 10 mls of a freshly prepared tin(II) chloride solution (1 M $SnCl_2$/2.5 M HCl). The mixture was diluted to 60 mls with water and boiled gently for thirty minutes. After cooling to room temperature, a further 10 mls of tin(II) chloride solution was added before dilution to 100 mls. The absorbance of the red colour so obtained was measured relative to a similarly prepared blank solution at 475 nm (Cecil model CE 5095 or Pye-Unicam model SP-8100 absorption spectrophotometer). The calibration plot in Figure 5.2.2., shows that the method is sensitive to the presence of nitrate ion. This however, is easily removed by treating the rhodium sample solution to repeated evaporations with concentrated hydrochloric acid, before carrying out the analysis procedure. If interference from the nitrate ion still persisted, the rhodium sample solution was repeatedly fumed to a small volume with a mixture of hydrochloric acid, sodium chloride (5 mg) and perchloric acid (CAUTION).

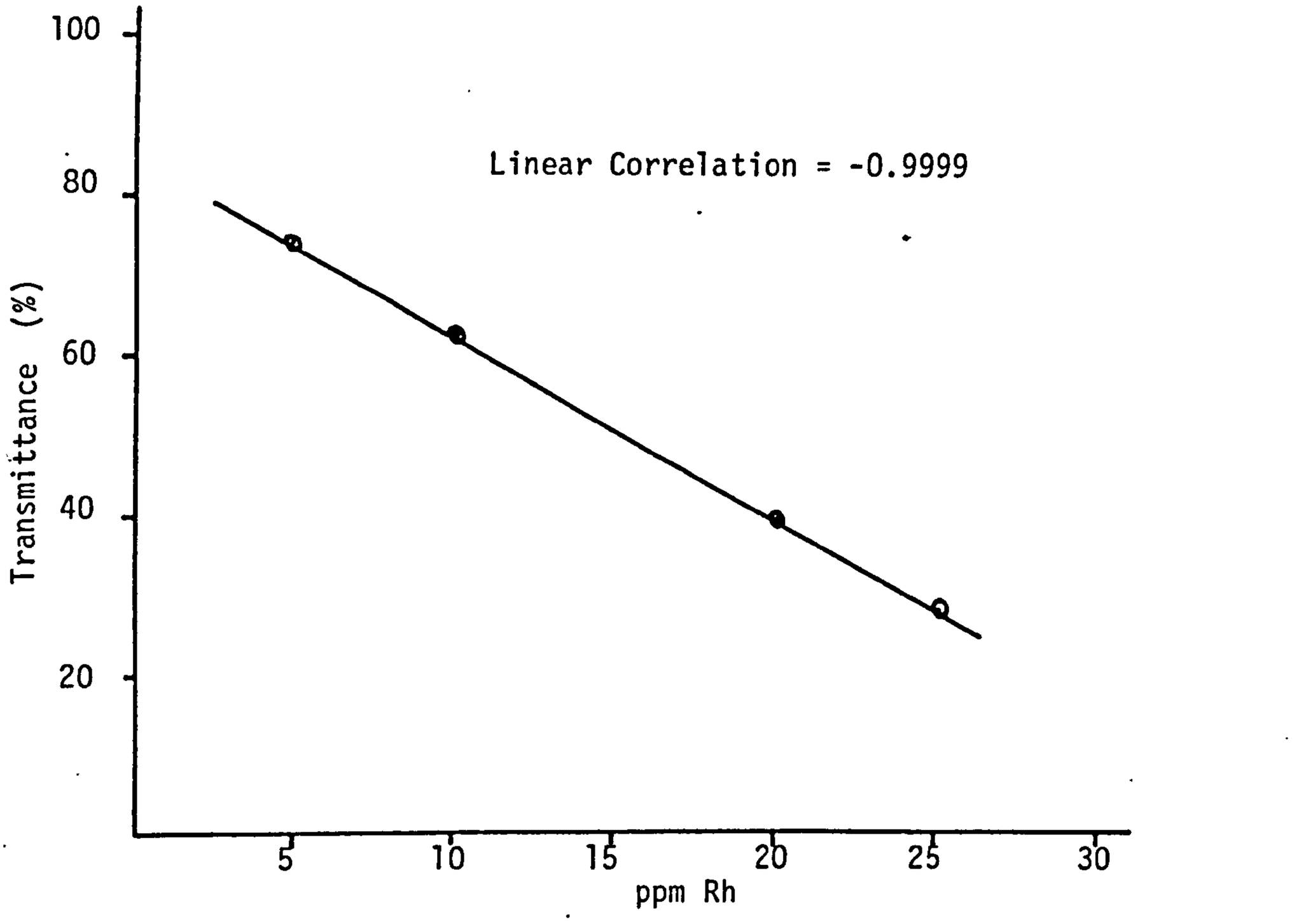

Figure 5.2.1. Calibration plot for determining rhodium by the hypochlorite method

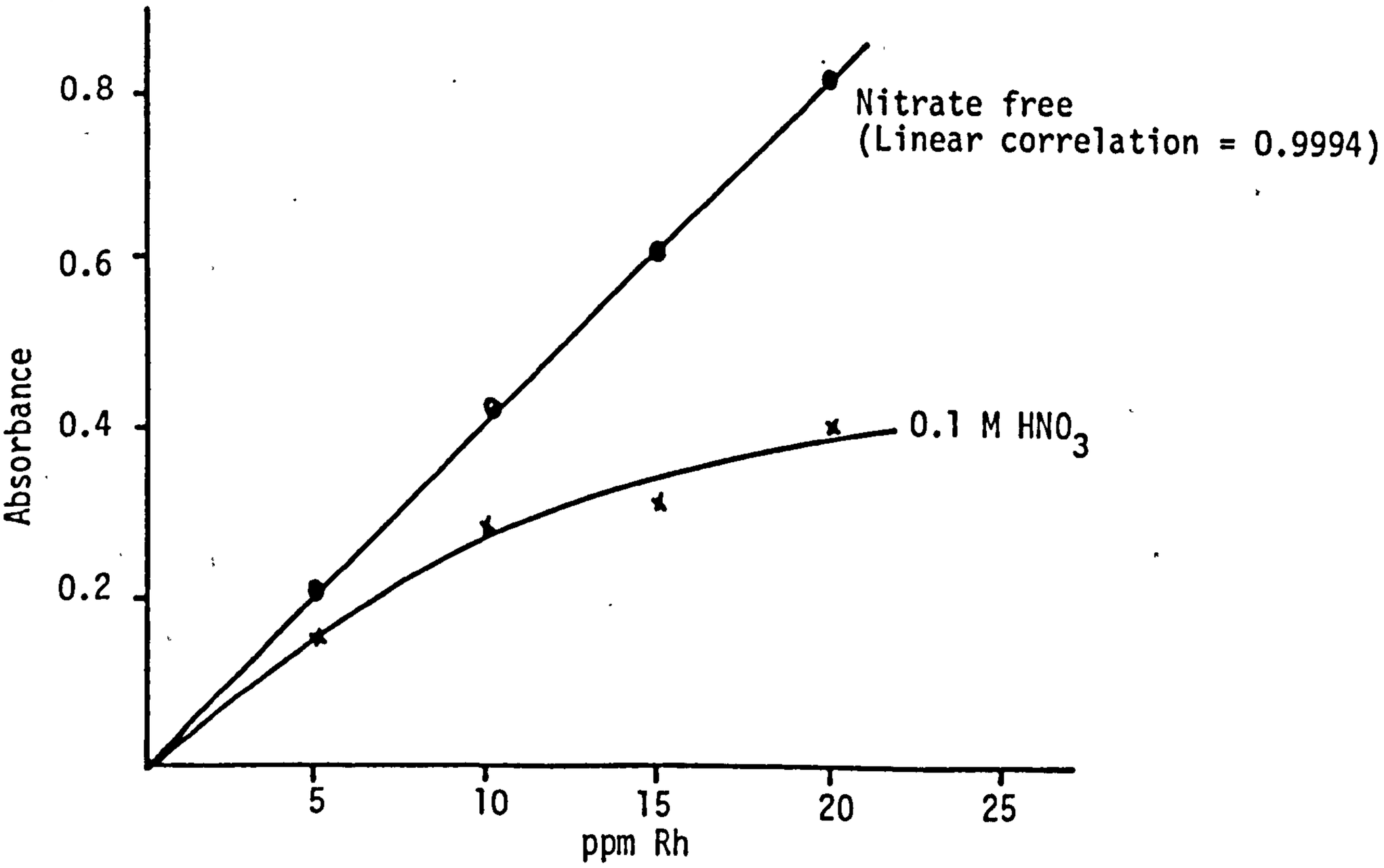

Figure 5.2.2. Calibration plot for determining rhodium by the tin(II) chloride method.

Organic samples for rhodium analysis were digested with a mixture of nitric and perchloric acids (CAUTION), prior to analysis.

5.2.2. Volumetric Methods for $\{H^+\}$, $\{NO_2^-\}$ and $\{Th^{4+}\}$

Hydrogen ion concentration was determined by titration with standard sodium hydroxide (against potassium hydrogen phthalate), using methyl orange indicator (219).

Nitrite ion concentration was determined by titration with standard potassium permanganate at 40^oC (219).

Thorium ion concentrations in aqueous solutions were determined by titration with standard (0.02 M) EDTA using xylenol orange indicator (219).

5.2.3. Potentiometric Methods for $\{NO_3^-\}$ and $\{H^+\}$

A nitrate ion-selective electrode (EDT Research) used in conjunction with a calomel electrode, and linked to a Philips model PW 4909 millivolt meter, was used to determine nitrate ion concentration in aqueous solutions. Standard solutions were prepared using analytical grade sodium nitrate, and a typical calibration plot is shown in Figure 5.2.3.

A combined glass/calomel micro-electrode (Corning) linked to a Corning model 140 pH meter was used to measure aqueous hydrogen ion concentrations. The electrode was calibrated by measuring the pH of a standard 0.1 M hydrochloric acid solution.

The concentration of stock solutions of HD and HDEHDTP in odourless kerosene were determined by non-aqueous potentiometric titration with

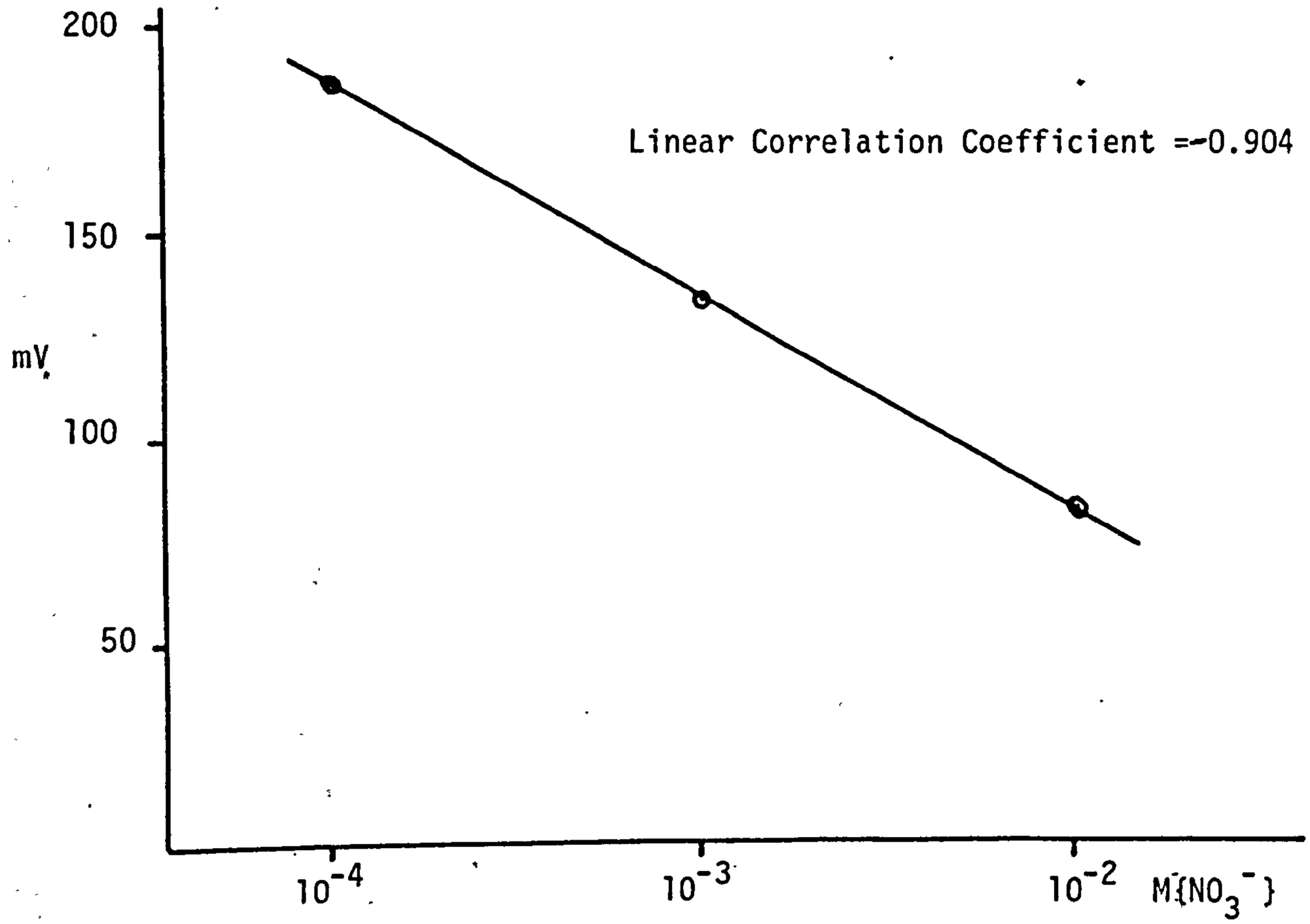

Figure 5.2.3. Calibration plot for determining the nitrate ion concentration

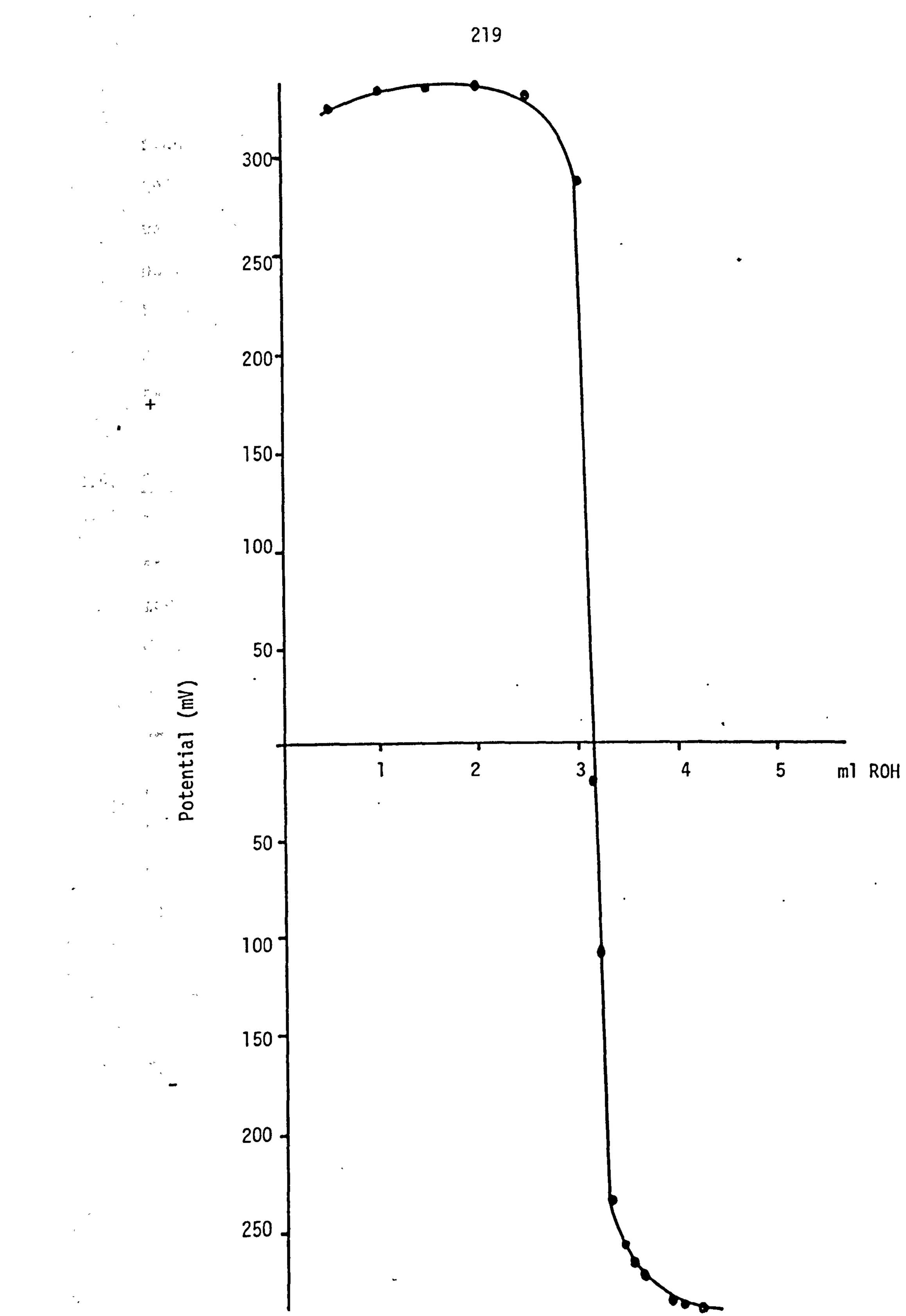

Figure 5.2.4. Titration of HD/OK with 0.1 M t-butyl ammonium hydroxide (ROH)

standard 0.1 N t-butylammonium hydroxide in a 1:1 mixture of toluene/methanol. In a typical titration, an aliquot of HD or HDEHDTP would be diluted to approximately 40 mls with 1:1 toluene/methanol. The potential of the solution after each addition of 0.1 N t-butylammonium hydroxide is recorded (combined glass electrode linked to a Philips model PW 4909 millivolt meter), and from the titration curve so obtained, Figure 5.2.4., the equivalence point is determined.

5.2.4. Radiometric Methods

Table 5.2.1. lists the radionuclides that were used as tracers for the several elements. The radionuclides ^{105}Rh, ^{137}Cs, ^{85}Sr, ^{110m}Ag, ^{106}Ru and ^{99m}Tc were counted directly in liquid aliquots using a Ge(Li) detector linked to a Canberra series 80 multichannel analyser, or with a well type NaI(Tl) scintillation counter (Philips model PW 4800 gamma counter).

Element	Nuclide	Half-life	Decay modes Radiations, Energies (MeV)
Rhodium	^{105}Rh	35.5 hr	β^-0.6; δ0.319, 0.306
Caesium	^{137}Cs	30.1 yr	β^-0.5; 1.7; many γ
Strontium	^{85}Sr	64.9 d	γ0.514
Silver	^{110m}Ag	250.4 d	β^-0.09; δ0.658 - 0.937
Ruthenium	^{106}Ru	368 d	β^-0.04 (to 30s ^{106}Rh β^-3.61; γ0.512, 0.622)
Technetium	^{99m}Tc	6.0 hr	γ0.14
Promethium	^{147}Pm	2.62 yr	β^-0.2

Table 5.2.1. List of Radionuclides

^{147}Pm was determined by liquid scintillation counting using an LKB model 1215 Rackbeta liquid scintillation counter and Fiso Fluor 2 aqueous scintillant.

Solutions of ^{85}Sr, ^{106}Ru, ^{147}Pm and ^{99m}Tc were treated to repeated evaporations with nitric acid before being made up to standard volume. The preparation of solutions containing ^{105}Rh is described in Section 5.5.4.

5.2.5. Analysis of Caesium and Strontium

Caesium and strontium were determined by atomic absorption analysis, by the Analytical Services Section of the Chemical Technology Division of AERE Harwell.

5.2.6. Elemental C, H, N and S Analysis

Elemental C, H, N and S analysis was carried out by the Microanalytical Services Department of Manchester University.

5.3. INORGANIC PREPARATIONS

5.3.1. Hydrated Rhodium (III) Sesquioxide ($Rh_2O_3.xH_2O$)

Rhodium sesquioxide was prepared by the addition of small quantities of sodium hydroxide to a warm solution (50^oC) of rhodium trichloride in distilled water (220). On appearance of the lemon-yellow precipitate, the pH of the solution was adjusted to 7, and the solution boiled for five minutes to coagulate the precipitate (23). After cooling,the solution was filtered, and the precipitate washed with copious quantities of distilled water until a spot test on the filtrate showed it to be free of chloride ions ($AgNO_3$ test). To ensure that all chloride ions

were removed, the rhodium sesquioxide was dissolved in 0.5 M perchloric acid and the preciptation procedure repeated. The final precipitate of $Rh_2O_3.xH_2O$ was dried under vacuum.

5.3.2. Potassium Hexanitratorhodate (III), $K_3\{Rh(NO_3)_6\}$

$K_3\{Rh(NO_3)_6\}$ was prepared by the method of Shubochkin et.al. (27, 28). Six grams of potassium hexanitritorhodate, $K_3\{Rh(NO_2)_6\}$ was added slowly to concentrated nitric acid (50 mls) in a 150 ml conical flask. The flask was placed in an oil bath, and the acid solution heated to boiling for 3 hrs. Nitric acid lost by evaporation during this time was replaced by periodic addition. Finally, all the nitric acid was evaporated, and a yellow/brown product was obtained. This was dried to constant weight in a drying oven at 105^oC. Analysis of this product showed it to contain 17.1% Rh (cf. 17.4% for $K_3\{Rh(NO_3)_6\}$).

5.3.3. Potassium Hexanitritorhodate (III), $K_3\{Rh(NO_2)_6\}$

$K_3\{Rh(NO_2)_6\}$ was prepared by the addition of potassium nitrite to a hot acidified (pH 1) solution of rhodium trichloride in water (1, 220). After the colour of the solution had changed from red to yellow, the solution was boiled for one hour. On cooling a creamy white precipitate of $K_3\{Rh(NO_2)_6\}$ was obtained. This was washed with water and dried under vacuum.

5.3.4. Tin(II) Nitrate, $Sn(NO_3)_2$

Tin (II) nitrate was prepared by the slow addition of tin oxide (6 gm) to 5 M HNO_3 (20 ml), in a 100 ml round bottom flask under a flowing nitrogen atmosphere (221, 222). The resulting mixture was

filtered to remove any insoluble material, and the solution of tin(II) nitrate was used immediately for the required experiment.

5.4. ORGANIC PREPARATIONS

5.4.1. N, N-Dioctylacetamide

N, N-Dioctylacetamide was prepared by reacting equal molar concentrations of acetic anhydride (5 gm, 50 mM) and di-octylamine (12 gm, 50 mM) overnight, in the presence of diethyl ether (142).

$$(CH_3CO)_2O + (CH_3(CH_2)_7)_2NH = (CH_3(CH_2)_7)_2NCOCH_3 + CH_3COOH \quad \ldots\ldots\ldots\ldots 5.1$$

The reaction mixture was then treated with several portions of sodium bicarbonate, to neutralise the acetic acid formed, followed by washing with 3M HCl to remove unreacted amine. The organic phase was washed with water, and emulsified water was removed by the addition of anhydrous sodium sulphate. After decantation, the ether was evaporated. N, N-Dioctylacetamide was obtained as a clear, slightly yellowish liquid, which was shown by gas chromatography to be free of amine impurities.

5.4.2. Di-2-ethylhexyldithiophosphoric Acid (HDEHDTP)

HDEHDTP was prepared by the slow addition of phosphrous pentasulphide (92 gm, 0.42 M) to 2-ethylhexanol (215 gm, 1.65 M), in a 500 ml round bottom flask.

$$8ROH + 2P_2S_5 = 4(RO)_2PSSH + 2H_2S \quad \ldots\ldots\ldots\ldots 5.2.$$

The resulting mixture was refluxed for 1.5 hrs at 85^oC (223, 224). After cooling, the reaction mixture was filtered to remove any insoluble residue. The HDEHDTP solution was assayed for hydrogen ion concentration (Section 5.2.3.), and showed 91% conversion to the acid product.

5.4.3. Tri-n-butylphosphine Sulphide (TBPS)

TBPS was prepared by the direct addition of small quantities of sulphur to tri-n-butylphosphine (100 gm, 0.5M) in a 250 ml round bottom flask and a flowing nitrogen atmosphere (223, 225). Gentle heating was required to dissolve the sulphur, when a slightly yellowish solution was obtained, the reaction mixture was allowed to cool, before being filtered to remove undissolved sulphur. The last traces of sulphur were removed by passing the solution through a column packed with chromatographic grade neutral alumina (177).

Calculated (found) percentages for $(C_{12}H_{27})P \rightarrow S$: C, 61.5 (61.2); H, 11.5 (11.8); S, 13.7 (14.4).

5.4.4. N,N',N'' - Tri-n-hexylphosphorothioictriamide (THPS)

THPS was prepared by the slow addition of thiophosphoryl chloride (25 gm, 0.15 M) to hexylamine (90 gm, 0.90 M) in a 250 ml round bottom flask at $5^{o}C$ (211, 223, 226).

$$3CH_3(CH_2)_5NH_2 + PSCl_3 = (CH_3(CH_2)_5NH)_3PS + 3HCl \quad \text{.....5.3}$$

The resulting mixture was refluxed for six hours on a steam bath, cooled, washed free of amine hydrochloride, and recrystallised three times from absolute ethanol. THPS was obtained as white needle-like crystals in 40% yield.

Calculated (found) percentages for $(C_{18}H_{42}N_3)P \rightarrow S$; C, 59.5 (59.4); H, 11.6 (11.4); N, 11.6 (11.7). Mpt., $51^{o}C$ (cf. lit. 50-$51^{o}C$ (211)).

5.4.5. Purification of Dinonylnaphthalene Sulphonic Acid (HD)

HD was donated by K & K-Greeff Chemicals Ltd., Croydon and King Industries Inc., Norwalk, Connecticut. The chemical was dissolved either in butyl cellusolve (Nacure 1051) or odourless kerosene (Synex DN-052/Norpar 12). Research grade HD was also obtained from Pflatz and Bauer.

In all cases, the HD was purified by the following anion exchange method (227). The HD solution (25 ml) in butyl cellusolve or odourless kerosene, was diluted to 75 mls with absolute ethanol, and loaded onto a column containing 25 gms of anion exchange resin (Fluka Dowex-1), previously converted to the hydroxyl form. The column was then washed with absolute ethanol until a clear eluate was obtained. In this way, all neutral impurities were removed. HD was then eluted with a 1M solution of hydrochloric acid in absolute ethanol. The eluate was evaporated to a solid mass at 50°C, under vacuum, on a rotary evaporator. The final product was repeatedly, washed, first with small portions of water, and then absolute ethanol, followed each time by evaporation at 50°C under vacuum. Finally, the product was dissolved in the required diluent and assayed potentiometrically (5.2.3.).

5.5. SOLUTION PREPARATIONS

5.5.1. Preparation of Solutions Containing the Hexaaquorhodium (III) Ion

A perchloric acid solution containing the hexaaquorhodium (III) ion was prepared by dissolving rhodium (III) sesquioxide (200 mg) in 10 ml of 72% perchloric acid. The resulting solution was evaporated to a small volume (~3 mls) on a hot-plate (CAUTION!) This procedure was repeated several times, before diluting to 40 mls with water. The solution was

then boiled for ten minutes, before being cooled and made up to 50 mls. A clear yellow solution was obtained (15-17).

5.5.2. "Rhodium Nitrate" Solutions

In all cases, the following standard procedure was used to produce "rhodium nitrate" solutions. Rhodium (III) sesquioxide was dissolved in the minimum required concentrated nitric acid, and evaporated to near dryness on a hot-plate. The evaporation was repeated several times, after which the residue was dissolved in 0.1 M nitric acid and boiled for ten minutes. The resulting solution was then made up to volume with the required strength nitric acid.

5.5.3. Solutions for ^{103}Rh NMR Spectroscopy

Solutions for ^{103}Rh NMR spectroscopy were prepared to contain approximately 175 mg/ml or rhodium. In a typical procedure, the required amount of rhodium (III) sesquioxide was dissolved in 1 ml of 10 M nitric acid, (to give a final 5 M acid solution), with gentle heating. This was followed by the addition of 0.5 ml of D_2O and the required amount of sodium nitrite. After dissolution of the sodium nitrite, the solution was made up to 2ml with D_2O.

5.5.4. Preparation of Solutions Containing ^{105}Rh

Rhodium-105 ($t_{\frac{1}{2}}$ = 35.5 hr) is produced by thermal neutron irradiation of ruthenium, the formation sequence being $^{104}Ru\ (n,\gamma)\ ^{105}Ru \xrightarrow[4.4hr]{\beta^-} {}^{105}Rh$. The isotope (500 μCi) was purchased from Amersham International plc, who irradiated 0.1 gm of ruthernium powder in the DIDO reactor at AERE Harwell (5 hr irradiation at thermal neutron flux of 7.19×10^{12} $ncm^{-2}s^{-1}$).

^{105}Rh was isolated from ruthenium by the chemical separation method of Morris and Khan (228). The irradiated ruthenium powder was mixed with powdered potassium hydroxide (3 gm) in a 250 ml beaker. Carbon tetrachloride (40 mls) and water (30 mls) were added to the mixture, and chlorine gas bubbled through the solution until all the ruthernium has been dissolved and oxidised to the tetraoxide, RuO_4. The mixture was transferred to a 100 ml separating funnel, and the organic phase discarded. The aqueous phase was washed with 4 x 40 ml portions of carbon tetrachloride, before being acidified with hydrochloric acid. After the addition of 5 mg of rhodium carrier (5 mg/ml, $RhCl_3/H_2O$), the pH of the solution was adjusted to 7, and the solution heated gently to coagulate the precipitate of rhodium sesquioxide, which was cooled, centrifuged, and washed with copious quantities of water, before being converted to "rhodium nitrate" solutions by the procedure given in Section 5.5.2.

5.5.5. Preparation of Simulate High Level Waste (HLW)

Synthetic HLW solutions were prepared from stock solutions which were 50-100 times the concentration found in HLW (214, 215). Most single elements were dissolved as their nitrates or oxides in 6 M HNO_3, concentrated HNO_3 or water. Where chlorides were used, these solutions were treated with a slight excess of silver nitrate to precipitate AgCl, which was filtered and discarded. Aliquots of the stock solutions were mixed, treated with sodium nitrite, and made up to volume to give HLW of composition shown in Table 5.5.1.

Element	g/l	wt. added chemical (in 50 mls)	ml stock required to make 100 ml HLW
Rb	0.127	0.4509 gm $RbCl$/6 M HNO_3	2
Sr	0.260	1.5703 gm $Sr(NO_3)_2$/6 M HNO_3	2
Y	0.172	1.4624 gm $YCL_3.6H_2O$/6 M HNO_3	2
Zr	1.276	5.9429 gm $Zr(NO_3)_4$/6 M HNO_3	4
Mo	1.198	18.3614 gm $(NH_4)_6Mo_7O_{24}.4H_2O/H_2O$	0.6
Ru	0.786	0.9297 gm $RuCl_3$/6 M HNO_3	8
Rh	0.138	$Rh_2O_3.5H_2O$/6916ppm stock	2
Pd	0.439	0.6878 gm $Pd(NO_3)_2.2H_2O$/6 M HNO_3	8
Ag	0.024	0.0957 gm Ag NO_3/6 M HNO_3	2
Cd	0.020	0.1360 gm $Cd(NO_3)_2.4H_2O$/6 M HNO_3	2
Cs	0.845	3.0962 gm Cs NO_3/6 M HNO_3	2
Ba	0.609	2.9024 gm $Ba(NO_3)_2/H_2O$	2
La	0.428	1.6649 gm $La(NO_3)_3.6H_2O$/6 M HNO_3	4
Ce	0.806	3.2356 gm $Ce(NO_3)_3.6H_2O$/6 M HNO_3	4
Pr	0.414	1.7856 gm Pr_6O_{11}/conc.HNO_3 dil.6 M	1.4
Nd	1.374	2.0038 gm Nd_2O_3/conc. HNO_3 dil.6 M	4
Sm	0.281	0.2035 gm Sm_2O_3/conc. HNO_3 dil.6 M	8
U	0.256	1.3476 gm $UO_2(NO_3)_2.6H_2O$/6 M HNO_3	2

Table 5.5.1. Synthetic HLW Solution

5.6. EXPERIMENTAL METHODS

5.6.1. Electronic Absorption Measurements

Electronic absorption measurements were carried out on a Cecil model CE5095 or Pye Unicam model SP-8100 spectrophotometers using matched $1cm^2$ silica cells.

5.6.2. Electrophoresis

Electrophoretograms were recorded on strips (22 x 3 cm) of Whatman No. 1 filter paper, using a Vokam model 400 electrophoresis tank and power pack. The rhodium complex bands were developed by spraying the electrophoretogram with a solution of 1 M $SnCl_2$/2.5 M HCl. On drying under an infra-red lamp, the presence of rhodium was indicated by the appearance of yellow bands.

5.6.3. Ion Exchange: Charge per Metal Atom

An ion exchange column (0.7 cm internal diameter, 30 cm long) with a frit capable of holding 400 mesh cation exchange resin (Dowex 50W-X8) was used. Solutions of rhodium sesquioxide in nitric acid (200 ml 0.1 M HNO_3, 0.006 M Rh) were equilibrated with 3-5 gm of resin, (previously washed with 1 M HNO_3, water and air dried) by stirring for thirty minutes before being loaded onto the column. The elutriant, Th $(NO_3)_4$/0.1 M HNO_3, was fed into the column via a peristaltic pump, the flow rate being maintained at 0.85 ml/min.

Two-ml fractions of the rhodium band were collected as they eluted from the column. Analysis of the hydrogen ion (5.2.3.) and rhodium

ion (5.2.1.) concentrations, and application of equation 2.2 enabled the calculation of the charge per metal atom.

5.6.3.1. Capacity of Dowex 50W - X8 Cation Exchange Resin

The capacity of Dowex 50W - X8 cation exchange resin was determined by equilibrating 10 gm of air dried resin with 50 mls of 4 M NaCl for 6 hours. Ten ml aliquots of the solution were then titrated against standard 1 M NaOH, to determine hydrogen ion concentration. The capacity of the resin is given by the mg of H^+ equivalent to 1 gm of resin. For Dowex 50W - X8, a value of 1.98 meq/gm was determined.

5.6.3.2. Ion Exchange: Charge per Species

Rhodium containing fractions (0.2 mls) from experiment 5.6.3. were used in the charge per species determinations. To these fractions, 60 mls of 1 M HNO_3 and 3 gm of Dowex 50W - X8 resin were added. The mixture was equilibrated for six hours. After allowing the resin to settle, a 10 ml aliquot of the supernatant was withdrawn for rhodium analysis. Water (50 mls) was added to the remaining solution, and the pH determined. The solution was subjected to a further six hour equilibration, after which a 20 ml aliquot of the supernatant was removed for rhodium analysis. The value of the charge per species was calculated by applying equation 2.7.

5.6.4. Polarography

Polarograms were recorded on a Metrohm model 626 Polarecord using an E505 polarographic cell. Rhodium containing solutions for polarography

were prepared as outlined in Section 5.5.2. Solutions which contained nitrite ion were left to equilibrate for two weeks, at room temperature, before being used. All solutions were deaerated in oxygen-free nitrogen for fifteen minutes, and contained 2 drops of a 0.2% solution of Titron X-100. Reduction potentials are referenced to the saturated calomel electrode at $25^{o}C$.

The height of the mercury head was maintained at 20 cm from the capillary end. The flow rate of Hg, mgs^{-1} was determined by weighing the mercury collected over three half-minute timed intervals. A value of 2.30 mgs^{-1} was determined.

5.6.5. Reversed Phase Paper Chromatography

Strips (2.5 x 15 cm) of Whatman No. 1 filter paper were soaked in the required organic solvent, and then placed on absorbent paper to remove excess solvent. After air drying, the strips were spotted, at the base, with the rhodium containing solution (10µl). After a one hour equilibration at room temperature, the strips were placed in chromatographic tanks which contained the eluting solvent (nitric acid). After elution, the chromatograms were developed by spraying the paper strips with a solution of 1 M $SnCl_2$/2.5 M HCl. The presence of rhodium was indicated by the appearance of bright yellow bands. R_f values were calculated by applying equation 3.0.

5.6.6. Distribution Measurements

Organic and aqueous phases were equilibrated in 10 or 20 ml glass vials, or in 100 ml conical flasks (with screw tops), depending on the volume of solution taken. Equilibrations were carried out using a Griffin flask shaker, or a thermostated (± 2°C) water bath (Heto, Denmark).

The concentration of rhodium in the organic phase was assumed to be the difference in the concentrations of the initial and equilibrated aqueous phases, i.e:

$$\{Rh\}_o = \{Rh\}_{a,ini.} - \{Rh\}_{a,eq.} \quad \ldots\ldots\ldots\ldots\ldots\ldots\ldots\ldots \quad 5.4.$$

where o and a represent organic and aqueous phases respectively. Analysis of rhodium in the organic phases (Section 5.2.1.) showed this assumption to be valid, and material balance was better than 98%.

The concentration distribution ratio, D_c is easily determined from

$$D_c = \frac{\text{Conc. solute in organic phase}}{\text{Conc. solute in aqueous phase}} = \frac{\{Rh\}_o}{\{Rh\}_a} \quad \ldots\ldots\ldots\ldots\ldots\ldots \quad 5.5$$

Since concentration is in grams of solute per volume of solvent, it follows that:

$$D_c = \frac{(\text{moles Rh})_o/V_o}{(\text{moles Rh})_a/V_a} = \frac{(\text{moles Rh})_o\ V_a}{(\text{moles Rh})_a\ V_o} \quad \ldots\ldots\ldots\ldots\ldots\ldots\ldots\ldots \quad 5.6$$

where V_o and V_a are the volumes of the organic and aqueous phases respectively.

The mass distribution ratio, D_m, is the ratio of the amounts of solute in the two phases:

$$D_m = \frac{(\text{moles Rh})_o}{(\text{moles Rh})_a} \quad \ldots\ldots 5.7$$

Thus the relationship between D_c and D_m is given by:

$$D_c = D_m \frac{V_o}{V_a} \quad \ldots\ldots 5.8$$

Where radioistopes were used, the concentration distribution ratio, D_c, could be obtained directly by counting equal volumes of organic and aqueous phases, i.e.

$$D_c = \frac{\text{Counts per ml of organic phase}}{\text{Counts per ml of aqueous phase}} \quad \ldots\ldots 5.9$$

5.6.7. Interfacial Tension Measurements

The interfacial surface tension, between an aqueous phase of 0.1 M nitric acid and an organic phase of varying concentrations of HD in odourless kerosene, was determined by the Du Nouy ring method (229). A Du Nouy tensiometer (Cambridge Instruments) and a platinum ring (radius = 0.67 cm) were used for the measurements. Before each measurement, the ring was cleared by exposing it to the colourless flame of a microburner.

The interfacial surface tension (α, Nm^{-1}) is given by:

$$\alpha = \frac{W_o}{4\pi R} F \quad \ldots\ldots 5.10$$

where W_o is a measure of the maximum force, or pull on the ring (N), R is the radius of the ring (m) and F is a correction factor which accounts for the complex shape of the liquid suspended from the ring (230).

Appendix I

The Nuclear Overhauser Effect (NOE)

One of the important ways in which magnetic nuclei relax from their upper to their lower energy levels is through a dipolar spin-spin interaction with another magnetic nucleus. This process takes place through space, and its efficiency is inversly proportional to the sixth power of the internuclear distance involved (231).

Consider two magnetic nuclei A and B, which are in sufficiently close proximity to influence each others relaxation times. If the nucleus A is observed while the nucleus B is simultaneously irradiated, the relaxation process in nucleus A becomes more efficient because nucleus B, which is undergoing rapid up and down transitions, becomes effectively a rotating magnetic field. This results in a perturbation of the usual Boltzmann distribution of nuclei A towards the lower state and increases up to 50% the intensity of the signal due to A. This enhancement of intensity is known as the NOE. Under normal circumstances the value of the NOE lies between 1 (no effect) and a maximum value given by (38),

$$NOE_{max} = 1 + \frac{\gamma_s}{2\gamma_I} \quad \ldots\ldots\ldots\ldots\ldots\ldots\ldots\ldots\ldots\ldots\ldots\ldots \quad 1$$

where γ_s is the magnetogyric ratio of species s (irradiated) and γ_I is the magnetogyric ratio of nucleus I (observed). Thus for the system

$^{103}Rh-\{^{1}H\}$ (the irradiated nucleus is placed in curly brackets after the observed nucleus),

$$NOE_{max} = 1 + \frac{26.7510 \times 10^{7}}{2(-0.8420 \times 10^{7})}$$

$$= -14.88$$

The negative sign indicates that there will be a diminution in the integrated peak intensity.

APPENDIX II

SOLVENT EXTRACTION GLOSSARY

DECONTAMINATION FACTOR: the ratio of the proportion of contaminant to the main solute in a feed before treatment to that after treatment by an extraction process or stage.

DILUENT: the liquid or homogeneous mixture of liquids in which extractant(s) may be dissolved together with modifiers to form the organic phase.

DISTRIBUTION RATIO (CONCENTRATION): the ratio of the concentration of a solute in the organic phase to that in the aqueous phase.

DISTRIBUTION RATIO (MASS): the ratio of the total mass of a solute in the organic phase to that in the aqueous phase.

DISTRIBUTION ISOTHERM: the graphical or algebraic representation of the relationship between the concentrations of a solute in the organic phase and the corresponding concentrations in the aqueous phase at equilibrium at a given temperature. Alternatives in common are equilibrium line and (where appropriate) extraction isotherm, scrubbing isotherm, stripping isotherm.

EXTRACTANT: the active substance(s) in the organic phase primarily responsible for the transfer of a solute from the aqueous phase.

EXTRACTION: the operation of transferring a solute from one (liquid) phase to another.

EXTRACTION EQUILIBRIUM CONSTANT: the equilibrium constant of a specified extraction reaction expressed in terms of thermodynamic activities of the reacting species.

FRACTION EXTRACTED: the fraction of the total quantity of a solute extracted (usually by the organic phase) under specified conditions.

LIGAND: any atom, ion or molecule capable of functioning as a donor partner in one or more coordinating bonds.

LIQUID-LIQUID EXTRACTION: the process of transferring a solute from one liquid phase to another immiscible or partially miscible liquid in contact with the first.

LOAD (Verb): to transfer solute from a feed to another liquid phase.

MODIFIER: a substance dissolved in an organic phase to improve its properties, e.g. extractant solubility, interfacial properties.

OPERATING LINE: a graphical representation of the mass balance relationship across an extraction process or stage.

PARTITION COEFFICIENT: the ratio of the concentration of a solute in a single definite chemical form in the organic phase to that of the same form in the aqueous phase at equilibrium. This term is used as a

synonym for distribution coefficient, distribution ratio.

PHASE RATIO: the ratio of the quantity of the organic phase to that of the aqueous phase.

RAFFINATE: the aqueous phase after extraction of some specified solute(s).

SALTING OUT: improvement of the extraction of a solute as a result of the addition of specific electrolytes to the aqueous phse.

SCRUBBING: the selective removal of contaminating solutes (impurities) from an extract containing these and the main extractable solute (usually) by treatment with a fresh aqueous phase.

SEPARATION FACTOR: the ratio of the two respective distribution ratios of two solutes measured under the same conditions.

SOLVENT: the term applied to the whole usually composite, initial organic phase which may consist of a homogeneous mixture of extractant(s) and diluent and/or modifier.

STRIPPING: the process of removing a particular solute from a loaded solvent or extract.

SYNERGISM: a. term describing the cooperative effect of two (or more) extractants whereby the distribution ratio for the combination is greater than the sum of the distribution ratios (measured under comparable conditions) for individual extractants.

REFERENCES

1. W. P. Griffith, The Chemistry of the Rarer Platinum Metals (Os, Ru, Ir and Rh), Interscience Publishers Inc., 1967.

2. W. H. Wollaston, Phil. Trans., 94, 419, 1804; Nicholsons Journal of the Arts and Natural Philosophy, 10, 34, 1805.

3. V. M. Goldschmidt, Geochemistry, Oxford University Press, Oxford, 1954.

4. K. Turner, Chemistry and Industry, 551, 1980.

5. C. Johnson and R.H. Atkinson, Trans. Inst. Chem. Eng., 15, 131, 1937.

6. F. S. Clements, The Industrial Chemist, 345, 1962.

7. R.J. Dowsing, Metals and Materials, 32, 1980.

8. T.J. Walsh and E.A. Hausman in Treatise on Analytical Chemistry, Eds. I.M. Kolthoff and P.J. Elving, Part II, 8, 379, 1963.

9. L. R. P. Reavill and P. Charlesworth, Proc. Int. Conf. Solvt. Extrn., Paper 80-93, Liege, Belgium, 1980.

10. P. Charlesworth, Platinum Mets. Rev., 25, 106, 1981.

11. M. J. Cleare, P. Charlesworth and D. J. Bryson, J. Chem. Tech. Biotechnol., 29, 210, 1979.

12. J. E. Barnes and J. D. Edwards, Chem. Ind., 5, 151, 1982.

13. J. R. Thornback, AERE Harwell, Report SPS-SAR-43, 1980.

14. K.F. Purcell and J. C. Kotz, Inorganic Chemistry, Holt-Saunders Publishers, 1977; F.A. Cotton and G. Wilkinson, Advanced Inorganic Chemistry, Interscience Publishers Inc., 1967.

15. C.K. Jørgensen, Acta. Chem. Scand.,10, 500, 1956.

16. S.K. Shukla and M. Lederer, J. Less-Common Mets., 1, 202, 1959.

17. G. H. Ayres and J. S. Forrester, J. Inorg. Nucl. Chem., 3, 365, 1957.

18. W. Plumb and G. M. Harris, Inorg. Chem., 3, 542, 1964.

19. E. Blasius and W. Preetz, Z. Anorg. Allg. Chem., 335, 1, 1965.

20. W. C. Wolsey, C. A. Reynolds and J. Kleinberg, Inorg. Chem., 2, 463, 1963.

21. K. E. Hyde, H. Kelm and D. A. Palmer, Inorg. Chem., 17, 1647, 1978.

22. W. Robb and G. M. Harris, J.Am. Chem. Soc., 87, 4472, 1965.

23. Gmelins Handbuch Der Anorganischen Chemie, System No. 64, Rh, 1938.

24. M. Lederer, J. Chromatog., 1, 279, 1958.

25. S. K. Shukla, Annales de Chemie., 1383, 1961.

26. C. Claus, Bull. Acad. Petersburg, 2, 187, 1860.

27. L. K. Shubochkin, M. A. Golubnichaya and E. F. Shubochkina, Russ. J.Inorg. Chem., 18, 1735, 1973.

28. L. K. Shubochkin, V. I. Nefedov, E. F. Shubochkina, M. A. Golubniichaya and L. D. Sorokina, Russ. J. Inorg. Chem., 17, 1496, 1972.

29. P. B. Critchlow and S. D. Robinson, Coord. Chem. Rev., 25, 69, 1978.

30. B. O. Field and C. J. Hardy, Quart. Rev., 18, 361, 1964.

31. C. C. Addison and D. Sutton, Prog. Inorg. Chem., 8, 195, 1967.

32. V. Casellato and P. A. Vigato, Coord. Chem. Rev., 36, 183, 1981.

33. C. C. Addison, N. Logan, S. C. Wallwork, Quart. Rev., 25, 289, 1971.

34. J. S. Forrester and G. H. Ayres, J. Phys. Chem., 63, 1979, 1959.

35. A. M. Kristjanson and M. Lederer, J. Less -Common Mets., 1, 245, 1959.

36. S. K. Shukla and M. Lederer, J. Less-Common Mets., 1, 255, 1959.

37. H. L Friedman, J. Chem. Phys., 21, 318, 1953.

38. R. K. Harris and B.E. Mann, NMR and the Periodic Table, Academic Press, 1978.

39. B. E. Mann and C. Spencer, Inorg. Chimica. Acta., 65, L57, 1982.

40. B. E. Mann and C. Spencer, Inorg. Chimica. Acta., 76, L65, 1983.

41. J. F. Llopis and I. M. Tordesillas, Encyclopedia of the Electrochemistry of the Elements, Vol.6, Ed. A. J. Bard, 1976, Marcel Dekker.

42. G. Van Loon and J. A. Page, Talanta, 12, 227, 1965.

43. D. Cossi and F. Pantani, J. Inorg. Nucl. Chem., 8, 385, 1958.

44. R. D. Gillard, J. A. Osborn and G. Wilkinson, J. Chem. Soc., 4105, 1965.

45. F. Pantani, J. Electroanal. Chem., 5, 40, 1963.

46. W. H. Douglas and R. J. Magee, J. Electroanal. Chem., 5, 171, 1963.

47. J. B. Willis, J. Am. Chem. Soc., 66, 1067, 944 .

48. E. Scarano, Atti. Acc. Naz. Lincei, Classe Sci. Fis. Mat. e Nat., 14, 428, 1953.

49. A. Wagnerova, Coll. Czech. Chem. Comm., 26, 2076, 1961.

50. D. Cozzi and F. Patani, J. Electroanal. Chem., 2, 72, 1961.

51. J. Korkisch, Modern Methods for the separation of the Rarer Metal Ions, Pergamon Press, 1969.

52. F. E. Beamish, The Analytical Chemistry of the Noble Metals, Pergamon Press, 1966.

53. F. E. Beamish and J. C. Van Loon, Recent Advances in the Analytical Chemistry of the Noble Metals, Pergamon Press, 1972.

54. J. E. Currah, W. A. E. McBryde, A. J. Cruikshank and F. E. Beamish, Ind. Eng. Chem., Anal. Ed., 18, 120, 1946.

55. C. Duval, P. Champ and P. Fauconnier, Analytica. Chimica. Acta., 12, 138, 1955.

56. R. L. Haines and D. E. Ryan, Can. J. Res., 27B, 72, 1949.

57. E. Jackson, Analyst, 84, 106, 1959.

58. W. J. Allan and F. E. Beamish, Anal. Chem., 22, 451, 1950.

59. F. E. Beamish, Talanta, 12, 789, 1965.

60. J. R. Deily, At. Abs. Newsletter, 6, 65, 1967.

61. A. Strasheim and G. J. Wessels, Appl. Spectroscopy, 17, 65, 1963.

62. M. M. Schnepfe and F. S. Grimaldi, Talanta, 16, 591, 1969.

63. J. M. Scarborough, Anal. Chem., 41, 250, 1969.

64. R. C. Mallett, D. C. G. Pearton, E. J. Ring and T. W. Steele, Talanta, 19, 181, 1972.

65. M. G. Atwell and J. Y. Hebert, Appl. Spectroscopy, 23, 480, 1969.

66. A. Diamantatos, Analytica. Chimica. Acta., 131, 53, 1981.

67. C. O. T. Lee, M.Sc. diss., 1981, Chelsea College, University of London, England.

68. G. G. Tertipis and F. E. Beamish, Anal. Chem., 34, 623, 1962.

69. A. V. Rangnekar and S. M. Khopkar, Bull. Chem. Soc. Jap., 39, 2169, 1966.

70. E. B. Sandell, Colorimetric Determination of Traces of Metals, Interscience Publishers, 1959.

71. A. G. Davis, G. Wilkinson and J. F. Young, J. Am. Chem. Soc., 85, 1692, 1963.

72. W. A. E. McBryde and J. H. Yoe, Anal. Chem., 20, 1094, 1948.

73. J. F. Young, R. D. Gillard and G. Wilkinson, J. Chem. Soc., 5176, 1964.

74. G. H. Ayres, B. L. Tuffly and J. S. Forrester, Anal. Chem., 27 1742, 1955.

75. M. A. Khattak and R. J. Magee, Analytica. Chimica. Acta., 45 297, 1969.

76. J. O. Karttunen and H. B. Evans, Anal. Chem., 32, 917, 1960.

77. R. B. Chenley, R. G. Osmond and S. G. Perry, Report AERE C/R 1870, UKAEA, 1956.

78. R. D. Gardner and A. D. Hues, Anal. Chem., 31, 1488, 1959.

79. M. E. Smith, Anal. Chem., 30, 912, 1958.

80. E. L. Steele and W. W. Meinke, Analytica. Chimica. Acta., 26, 269, 1962.

81. C. E. Miller, Report No. ORNL - 2715, 1959.

82. J. C. Armstrong and G. R. Choppin, Radiochemistry of Rhodium, Nuclear Science Series, NAS-NS-3008 (Rev), USAEC, 1965.

83. J. V. Holder, Radiochim. Acta., 25, 171, 1978.

84. J. O. Elomeke and M. F. Todd, ORNL-2127, 1958.

85. S. Soentono, Ph.D. thesis, University of Salford, England, 1979.

86. G. R. Howells, T. G. Hughes and K. Saddington, Prog. Nucl. Energy, 3, 151, 1961.

87. H. A. C. McKay and R. K. Webster, Chemistry and Industry, 731, 1977.

88. I. L. Jenkins, Hydrometallurgy, 4, 1, 1979.

89. G. R. Choppin and J. Rydberg, Nuclear Chemistry Theory and Applications, Pergamon Press, 1980.

90. F. R. Bruce, Prog. Nucl. Energy, 1, 130, 1956.

91. J. Rydberg, J. Inorg. Nucl. Chem., 5, 79, 1957.

92. J. R. Thornback, AERE-R9908, UKAEA, 1980.

93. J. O. Elomeke and M. F. Todd, ORNL-2127, 1958.

94. L. L. Clark, F. P. Roberts, J. C. Sheppard and J. D. Kaser, BNWL-1690, 1970.

95. D. E. Deonigi, R. W. McKee and D. R. Haffner, BNWL-716, 1968.

96. J. H. Miles, AERE Harwell, Private Communication.

97. T. Rigg and W. Wild, Prog. Nucl. Energy, 2, 320, 1958.

98. A. M. Rochon, Z. Nowak and Z. P. Zagorski, Radiochem. Radioanal. Lett., 27, 1, 1976.

99. I. L. Jenkins and A. G. Wain, Rep. Prog. Appl. Chem., 57, 301, 1972.

100. R. G. Sowden, Trans. Faraday Soc., 55, 2084, 1959.

101. M. Daniels, J. Phys. Chem., 73, 3710, 1969.

102. H. E. Zittel, Prog. Nucl. Chem., 10, 395, 1970.

103. G. M. Ritcey and A. W. Ashbrook, Solvent Extraction, Part II, Elsevier Publishing Co., 1979.

104. W. P. Babbington, Scientific American, 235, 30, 1976.

105. M. Lederer, Nature, 162, 776, 1948.

106. F. H. Burstall, G. R. Davies, R. P. Linstead and R. A. Wells, J. Chem . Soc., 516, 1950.

107. D. B. Rees-Evans, W. Ryan and R. A. Wells, Analyst, 83, 356, 1958.

108. S. T. Payne, Analyst, 85, 698, 1960.

109. J. Korkisch, Modern Methods for the Separation of the Rarer Metal Ions, Pergamon Press, 1969.

110. C. Pohlandt and T. W. Steele, Talanta, 19, 839, 1972.

111. S. Przeszlakowski and A. Flieger, Talanta, 28, 557, 1981.

112. P. C. Stevenson, A. A. Franke, R. Borg and W. Neruik, J. Am. Chem. Soc., 75, 4876, 1953.

113. F. W. E. Strelow, R. Pethemeyer and C. J. C. Bothma, Anal. Chem., 37, 106, 1965.

114. Y. Marcus and A. S. Kertes, Ion Exchange and Solvent Extraction of Metal Complexes, Wiley-Interscience Publishers, 1969.

115. C. H. Eshelman, J. Dyer and J. Armentor, Analytica. Chimica. Acta., 32, 411, 1965.

116. J. R. Stokely and W. D. Jacobs, Anal. Chem., 35, 149, 1963.

117. M. Lindner, USAEC, Rept. UCRL-4377.

118. T. Kato, Bull. Chem. Soc. Jap., 37, 1453, 1964.

119. D. E. Ryan, Analyst, 76, 167, 1951.

120. D. E. Ryan, Can. J. Chem., 39, 2389, 1961.

121. A. Diamantatos, Analytica. Chimica. Acta., 66, 147, 1973.

122. A. Diamantatos and A.A. Verbeck, Analytica. Chimica. Acta., 91, 287, 1977.

123. M. A. Khan and D. F. C. Morris, J. Less-Common Mets., 13, 53, 1967.

124. H. Bode, Z. Analyst. Chem., 144, 165, 1955.

125. H. Irving and H. S. Rossotti, Analyst, 80, 245, 1955.

126. K. Beyermann, Z. Analyt. Chem., 200, 183, 1964.

127. G. H. Faye and W. R. Inman, Anal. Chem., 35, 985, 1963.

128. T. Ishimori, Y. Kobayashi and Y. Usuba, Bull. Chem. Soc. Jap., 41, 1458, 1968.

129. P. A. Lewis, D. F. C. Morris, E. L. Short and D. N. Waters, J. Less-Common Mets., 45, 193, 1976.

130. E. W. Berg and W. L. Senn, Analytica. Chimica. Acta., 19, 109, 1958.

131. R. B. Wilson and W. D. Jacobs, Anal. Chem., 33, 1650, 1961.

132. A. T. Casey, Proc. Int. Conf. Solvt. Extrn., 327, 1966.

133. F. Pantani and G. Piccardi, Analytica. Chimica. Acta., 22, 231, 1960.

134. J. Forsythe, R. Magee and C. Wilson, Talanta, 3, 324, 1950; ibid., 3, 330, 1950.

135. F. E. Beamish, Talanta, 14, 991, 1967.

136. E. W. Berg, I. R. Saunders, Analytica. Chimica. Acta., 38, 377, 1967.

137. E. W. Berg and E. Y. Lau, Analytica. Chimica. Acta., 27, 248, 1962..

138. L. M. Gindin, Ion Exchange and Solvent Extraction, 8, 311, 1981.

139. W. Maeck and G. Booman, Anal. Chem., 33, 1775, 1961.

140. G. A. Kanert and A. Chow, Analytica. Chimica. Acta., 69, 355, 1974.

141. A. M. Orlov, Y. S. Shorikov, N. N. Chalissova, I. V. Kunaeva, I. P. Ryzhova, T. A. Fomina and M. I. Yuzko, Proc. Int. Solvt. Extrn. Conf., Paper 80-151, 1980.

142. C. Pohlandt and J. S. Fritz, Talanta, 26, 395, 1979.

143. N. V. Fedorenko and T. I. Ivanova, Russ. J. Inorg. Chem., 10, 387, 1965.

144. C. Pohlandt, Talanta, 26, 199, 1979.

145. L. M. Gindin, Proc. Int. Solvt. Ext. Conf., p433, 1966.

146. K. P. Lunichkina and E. V. Renard, Soviet Radiochem., 16, 269, 1974.

147. S. Arhland, J. Chatt and N. R. Davies, Quart. Rev. Chem. Soc., 12, 265, 1958.

148. R. G. Pearson, J. Am. Chem. Soc., 85, 3533, 1963.

149. V. Kourim and O. Vojtech, Atomic Energy Rev., 12, 215, 1974.

150. J. H. Goode, ORNL-5015.

151. D. R. O'Boyle, F. L. Brown and J. E. Sanecki, J. Nucl. Mat., 29, 27, 1969.

152. J. I. Bramman, R. M. Sharpe, D. Thom and G. Yates, J. Nucl. Mat., 25, 1968, 201.

153. Exxon Nuclear Co., XN-FR-ER-2, 1978.

154. F. J. Smith and H. F. McDuffie, Sep. Sci. Tech., 16, 1071, 1981.

155. R. H. Moore, US Patent 3,848,048, 1974.

156. J. V. Panesko, ARH-911, 1968.

157. J. V. Panesko, ARH-733, 1968.

158. J. V. Panesko, ARH-1082, 1972.

159. D. J. Shaw, Electrophoresis, Academic, 1969.

160. R. E. Connick and H. H. Cady, J. Am. Chem. Soc., 79, 4242, 1957; ibid., 80, 2645, 1958.

161. J. Burgess, Metal Ions in Solution, Ellis Horwood Ltd., Publishers, 1978.

162. J. C. Bailar, H. J. Emelevs, R. Nyholm and A. F. Trotman-Dickenson, Comprehensive Inorganic Chemistry, 3, 1249, 1973, Pergamon Press.

163. W. P. Griffith, J. Lewis and G. Wilkinson, J. Chem. Soc., 1775, 1959.

164. D. R. Crow, Polorography of Metal Complexes, Academic Press, 1969.

165. J. N. Gaur and N. K. Goswani, Electrochimica. Acta., 15, 519, 1970.

166. H. A. Laitinen, J. C. Bailar, H. F. Holtzclaw and J. V. Quagliano, J. Am. Chem. Soc., 70, 2999, 1948.

167. N. M. Patel, M.Sc. Dissertation, Chelsea College, University of London, 1981.

168. I. M. Kolthoff and J. J. Lingane, Polarography, Vols. 1&2, 1952, 2nd ed., Interscience, NY.

169. J. E. Huheey, Inorganic Chemistry, Harper and Row Publishers, 1975.

170. M. Beer, B. Gorski and L. Russ, East German Patent DD205,620, (Cl. BO/D11/04), 4/1/84, Appl. 240, 849.

171. E. Fritsch, B. Gorski and M. Beer, Int. Solvt. Extrn. Conf., p.199, 1983, Colorado, USA.

172. E. Fritsch. M. Beer and B. Gorski, East German Patent DD 205, 619, (Cl. B01D11/00), 4/1/84, Appl. 240, 989.

173. Gmelins Handbuch Der Anorgamischen Chemie, Rh supplement, 1984.

174. M. Lederer and C. Majani, Chromatogr. Rev., 12, 299, 1970.

175. A. S. Kertes and A. H. I. Ben-Bassat, J. Chromatogr., 1, 489, 1958.

176. S. Przeszlakowski, Chromatogr. Rev., 15, 29, 1971.

177. D. E. Elliott and C. V. Banks, Analytica. Chimica. Acta., 33, 237, 1965.

178. E. Hogfeldt, Ion Exchange and Solvent Extraction, J. Marinsky Ed., Marcel Dekker Inc., NY, 1966.

179. A. Van Dalen, K. W. Gerritsma and J. Wijkstron, J. Colloid Interface. Sci., 48, 122, 1974.

180. A. Van Dalen, K. W. Gerritsma and J. Wijkstra, J. Colloid Interface Sci., 48, 127, 1974.

181. D. F. C. Morris, J. Colloid Interface. Sci., 51, 52, 1975.

182. P. R. Danesi, R. Chiarizia, M. A. Raieh and G. Scibona, J. Inorg. Nucl. Chem., 37, 1495, 1975.

183. R. Chiarizia, P. R. Danesi, M. A. Raieh and G. Scibona, J. Inorg. Nucl. Chem., 37,1495, 1975.

184. J. M. White, P. Tang and N. C. Li, J. Inorg. Nucl. Chem., 14, 255, 1960.

185. L. V. Gallacher, Proc. Int. Symp. Soln. Behav., Surfactants, 2, 791, 1980.

186. G. G. David, D. F. C. Morris and E. L. Short, J. Colloid Interface. Sci., 82, 226, 1981.

187. D. F. C. Morris and E. L. Short, Electrochimica Acta., 29, 1083, 1984.

188. G. Y. Markovits and G. R. Choppin, Solvent Extraction with Sulphonic Acids, Vol. 3, J. A. Marinsky and Y. Marcus (Eds.), Marcel Dekker Publishers, 1973.

189. M. A. Raieh and H. F. Aly, J. Radioanal. Chem., 57, 17, 1980.

190. A. Van Dalen, RCN 141, 1971.

191. R. Chiarizia, P. R. Danesi, G. Dalessandro and B. Scuppa, J. Inorg. Nucl. Chem., 38, 1367, 1976.

192. W. J. Moore, Physical Chemistry, 4th Ed., Longmans, 1966.

193. G. R. Choppin and W. F. Strazik, Inorg. Chem., 4, 1250, 1965.

194. M. A. Raieh, N. Zakareia and M. F. Aly, J. Radioanal. Chem., 52, 285, 1979.

195. D. F. C. Morris and S. D. Hammond, Electrochimica Acta., 13, 545, 1968.

196. D. F. C. Morris, Chemistry and Industry, 624, 1973.

197. P. G. M. Brown, J. M. Fletcher, C. J. Hardy, J. Kennedy, D. Scargill, A. G. Nain and J. L. Woodhead, Proc. 2nd Int. Conf. Peaceful Uses At. Eng. 17, 118, 1958.

198. R. C. Fay and T. S. Piper, J. Am. Chem. Soc., 84, 2303, 1962.

199. S. Fronaeus, Techniques of Inorganic Chemistry, H. B. Jonassen and A. Weissberger Eds., 1, 1, 1963.

200. B. G. F. Careleson and H. Irving, J. Chem. Soc., 4390, 1954.

201. D. F. C. Morris, G. L. Reed, E. L. Short, D. N. Slater and D. N. Waters, J. Inorg. Nucl. Chem., 27, 377, 1965.

202. D. F. C. Morris, D. T. Anderson, S. L. Waters and G. L. Reed, Electrochimica Acta., 14, 643, 1969.

203. K. Osseo-Asare and M. E. Keeney, Metall. Trans., 11B, 63, 1980.

204. A. Van Dalen and K. W. Gerritsma, Proc. Int. Solvt. Ext. Conf., p.1096, 1971.

205. J. H. Miles, AERE Harwell, Private Communication.

206. G. M. Ritcey and A. W. Ashbrook, Solvent Extraction, Part I, Elsevier Publishing Co., 1984.

207. T. H. Handley and J. A. Dean, Anal. Chem., 34, 1312, 1962.

208. R. H. Zucal, J. A. Dean and T. H. Handley, Anal. Chem., 35, 988, 1963.

209. T. H. Handley, Nucl. Sci. Eng., 16, 440, 1963.

210. R. Titonssi, S. Lours and C. Musikas, European Patent No. 8014238, 26/6/80.

211. T. H. Handley, Anal. Chem., 36, 2467, 1964.

212. T. H. Handley, Talanta, 12, 893, 1965.

213. E. S. Lane, A. Pilbeam and J. M. Fletcher, AERE R.4440, Part I, 1965.

214. I. Svantesson, I. Hagstrom, G. Persson and J. O. Liljenzin, J. Inorg. Nucl. Chem., 41, 383, 1979.

215. I. Svantesson, G. Persson, I. Hagstrom and J. O. Liljenzin, J. Inorg. Nucl. Chem., 42, 1037, 1980.

216. J. R. Thornback, Loughborough University of Technology, Private Communication.

217. A. I. V^{o}gel, Macro and Semimicro Qualitative Inorganic Analysis, p.338, 4th ed, 1965, Longmans.

218. G. H. Ayres and F. Young, Anal. Chem., 24, 165, 1952.

219. A. I. Vogel, A Textbook of Quantitative Inorganic Analysis, 3rd. ed., 1966, Longmans.

220. G. Brauer, Handbook of Preparative Inorganic Chemistry, Vol. 2, p.1588, 1965, Academic, NY.

221. Gmelins Handbuch Der Anorganischon Chemie, System No. 46, Tin, p. 366, 1971.

222. J. D. Donaldson and W. Moser, J. Chem. Soc., 1996, 1961.

223. G. M. Kosolapoff, Organic Phosphrous Compounds, 1950, John Wiley, NY.

224. J. G. McNab, N. V. Hakala and J. P. McDermott, Chem. Ab. 45, 7785e, 1951.

225. R. B. Hitchcock, J. A. Dean and T. H. Handley, Anal. Chem., 35, 254, 1963.

226. L. F. Audrieth and A. D. F. Toy, J. Am. Chem. Soc., 64, 1553, 1942.

227. P. R. Danesi, R. Chiarizia and G. Scibona, J. Inorg. Nucl. Chem., 35, 3926, 1973.

228. D. F. C. Morris and M. A. Khan, Radiochimica. Acta., 6, 110, 1966.

229. J. T. Davies and E. K. Rideal, Interfacial Phenomena, Academic Press, 1961.

230. W. D. Harkins and H. F. Jordan, J. Am. Chem. Soc., 52, 1751, 1930.

231. H. H. Bauer, G. D. Christian and J. E. O'Relilly, Instrumental Analysis, 2nd ed., p.354, 1978, Allyn and Bacon Inc., Boston.